REINFORCED CONCRETE DEEP BEAMS WITH WEB OPENINGS

by

GRAHAM RICHARD SHARP, B.Sc.

A thesis submitted to the University of Nottingham for the degree of Doctor of Philosophy

Department of Civil Engineering,
University of Nottingham

October 1977

PAGE NUMBERING AS FOUND IN THE ORIGINAL THESIS

ACKNOWLEDGMENTS

The Author is most sincerely grateful to Professor R.C. Coates of Nottingham University and Dr.F.K. Kong of Cambridge University for their supervision of the research work and for their much valued encouragement and advice.

The experiments were carried out in the Department of Civil Engineering, University of Nottingham, and the Author is grateful to Messrs. J. Barlow, J. Ellis, and other members of staff in the Structures Laboratory for their co-operation and assistance.

Sincere thanks are due to Mrs. Ruth Shawcross for the typing of this thesis; to Mr.I. Conway for his valuable help with the preparation of the drawings; and to Mr.J.C. Kaern, a visiting research student to Cambridge from the Technical University of Denmark, for the numerical checking of some of the calculations.

The final draft of this thesis was prepared in Cambridge in June and July 1977. Sincere thanks are due to Professor J. Heyman for extending the facilities of the University Engineering Department, Cambridge, to the Author during this period; sincere thanks are also due to Allott and Lomax, Consulting Engineers, for leave of absence to enable the Author to complete the thesis in Cambridge.

The research reported in this thesis was supported by the Science Research Council.

SYNOPSIS

The design of reinforced concrete deep beams is not yet covered by the current British Code CP110:1972. Some provisions are given in the CEB-FIP Recommendations (1970) and the ACI318-71 Building Code, and the new (1977) CIRIA design guide contains more comprehensive guidance including a number of recommendations for the design of deep beams with web openings.

This thesis is concerned with the general behaviour in shear of single-span reinforced concrete deep beams and in particular the effects of web openings on their ultimate strength and serviceability.

The test specimens comprised seventy-five lightweight and sixteen normal weight reinforced concrete deep beams with span/depth ratios ranging from one to two. The effects of a varied range of web openings on deflections , crack widths, cracking loads, failure modes, and ultimate shear strengths were studied, and the influence of web reinforcement was investigated.

The exact analysis of reinforced concrete deep beams with web openings presents formidable problems. However, the ultimate shear strengths of such beams can be predicted with reasonable accuracy using a simple structural idealization, which was derived from the results of the test programme. A simple design method is explained and design hints are given.

The procedures currently used by practising engineers

for the design of deep beams are outlined and discussed, and a more detailed review of the new CIRIA guide is presented. Design examples are given to illustrate the use of the various methods.

In all the current procedures, the design assumptions regarding the anchorage requirements of the longitudinal tension reinforcement are necessarily conservative. Appendix 1 describes the details of nine tests carried out to provide information on the effects of various amounts of end anchorage on the strength and crack control of deep beams. In Appendix 2 details are given of three tests carried out to investigate the behaviour of deep beams under repeated loading conditions.

TABLE OF CONTENTS

	Page
Acknowledgments	i
Synopsis	ii
List of Tables and Figures	viii
Symbols and Units of Measurement	xiii
CHAPTER 1 INTRODUCTION AND BACKGROUND	
1.1 Introduction	1
1.2 Background	3
1.2.1 Elastic analysis	3
1.2.2 Deep beam tests	3
1.2.2.1 de Paiva and Siess's tests	4
1.2.2.2 Leonhardt and Walther's tests	7
1.2.2.3 Crist's tests	9
1.2.2.4 Nottingham-Cambridge tests	12
CHAPTER 2 THE DESIGN OF R.C. DEEP BEAMS IN CURRENT PRACTICE	
2.1 Introduction	17
2.2 Outlines of current design methods	17
2.2.1 CEB-FIP Recommendations	17
2.2.2 ACI Building Code	21
2.2.3 Portland Cement Association	25
2.3 General comments	28
CHAPTER 3 THE EXPERIMENTAL PROGRAMME	
3.1 Introduction	31
3.2 Materials	33
3.2.1 Cement	33
3.2.2 Lightweight aggregates	33

3.2.3 Normal weight aggregates 34
3.2.4 Reinforcement 34
3.3 Concrete mixes 35
3.3.1 Lightweight concrete 35
3.3.2 Normal weight concrete 35
3.4 Beam manufacture 36
3.4.1 Formwork 36
3.4.2 Reinforcement fabrication 37
3.4.3 Casting and curing 38
3.5 Control specimens 39
3.6 Testing 40
3.6.1 Test equipment 40
3.6.2 Test preparation 41
3.6.3 Test procedures 42

CHAPTER 4 LIGHTWEIGHT CONCRETE DEEP BEAMS WITH WEB OPENINGS: PILOT STUDY

4.1 Test programme 44
4.2 Test results 45
4.2.1 Crack patterns and modes of failure 45
4.2.2 Crack widths and deflection 48
4.2.3 Ultimate loads 50
4.3 General comments 53

CHAPTER 5 LIGHTWEIGHT CONCRETE DEEP BEAMS WITH WEB OPENINGS: FURTHER TESTS

5.1 Introduction 56
5.2 Test programme 57
5.3 Test results 59
5.3.1 Crack patterns and modes of failure 59

Page

5.3.2 Crack widths and deflection 63

5.3.3 Ultimate loads 66

CHAPTER 6 NORMAL WEIGHT CONCRETE DEEP BEAMS WITH WEB OPENINGS

6.1 Introduction 72

6.2 Test programme 73

6.3 Test results 74

6.3.1 Crack patterns and modes of failure 74

6.3.2 Crack widths and deflection 75

6.3.3 Ultimate loads 77

CHAPTER 7 A STRUCTURAL IDEALIZATION FOR DEEP BEAMS WITH WEB OPENINGS

7.1 The structural idealization 81

7.2 General discussion 88

CHAPTER 8 A PROPOSED METHOD FOR THE DESIGN OF DEEP BEAMS WITH WEB OPENINGS

8.1 Introduction 91

8.2 Proposed design equations for shear 91

8.3 Design hints 94

8.4 Design example 96

CHAPTER 9 A CRITICAL REVIEW OF THE CIRIA DESIGN GUIDE FOR DEEP BEAMS

9.1 Introduction 100

9.2 CIRIA design method: solid top-loaded deep beams 101

9.3 Comparison of design loads with test results 113

9.4 CIRIA Guide: Provisions for deep beams with holes 114

Page

CHAPTER 10 CONCLUSIONS AND SUGGESTIONS FOR FURTHER RESEARCH

10.1 Conclusions 119

10.2 Suggestions for further research 120

APPENDIX 1 ANCHORAGE OF TENSION REINFORCEMENT IN LIGHTWEIGHT CONCRETE DEEP BEAMS

A1.1 Introduction and background 122

A1.2 Test programme 123

A1.3 Test results 125

A1.3.1 Deflection control 125

A1.3.2 Crack control 125

A1.3.3 Crack patterns and modes of failure 126

A1.3.4 Ultimate loads 127

A1.4 General comments 127

APPENDIX 2 SHEAR STRENGTH OF LIGHTWEIGHT DEEP BEAMS SUBJECTED TO REPEATED LOADS

A2.1 Introduction and background 130

A2.2 Test programme 131

A2.2.1 Test specimens 131

A2.2.2 Testing 132

A2.3 Test results 132

A2.3.1 Deflections and crack widths 132

A2.3.2 Crack patterns and modes of failure 133

A2.3.3 Ultimate loads 134

A2.4 Summary 135

REFERENCES 136

LIST OF TABLES AND FIGURES

All full page tables and diagrams appear at the end of the text, in groups as listed below.

		Page
CHAPTER 1		
Figure 1.1	Effect of inclined cracking on steel and concrete strains	145
Figure 1.2	Leonhardt and Walther: Reinforcement arrangement	146
Figure 1.3	Meanings of symbols	147
Figure 1.4	Comparison of computed and measured ultimate loads	148
Figure 1.5	Nottingham tests: Details of web reinforcement	149
CHAPTER 2		
Figure 2.1	Reinforcement pattern: CEB-FIP Recommendations	150
Figure 2.2	Deep beam in design examples	151
Figure 2.3	Beam designed to CEB-FIP Recommendations	152
Figure 2.4	Beam designed to ACI Building Code	152
Figure 2.5	PCA's Design chart	153
Figure 2.6	Beam designed to PCA design guide	153
CHAPTER 3		
Table 3.1	Sieve analysis of Lytag aggregates	154
Table 3.2	Sieve analysis of Hoveringham gravel aggregates	155
Table 3.3	Tensile properties of reinforcements	156
Figure 3.1	Load v. extension diagrams for reinforcement	157
Figure 3.2	The loading apparatus: general arrangement	158
Figure 3.3	The loading apparatus: detail at the supports	159

Page

CHAPTER 4

Table 4.1 Properties of test beams (Pilot tests; lightweight concrete) 160

Table 4.2 Measured ultimate loads (Pilot tests; lightweight concrete) 161

Figure 4.1 Dimensions and reinforcement details (Pilot tests; lightweight concrete) 162

Figure 4.2 Opening reference numbers: applicable to beams in Table 4.1 163

Figure 4.3 Typical crack patterns at failure 164

Figure 4.4 Typical sequence in which the cracks appeared 166

Figure 4.5 Typical failure modes of deep beams with web openings 167

Figure 4.6 Maximum crack widths 168

Figure 4.7 Development ofcracking in Beam M-0.4/4 170

Figure 4.8 Development of cracking in Beam 0-0.4/4 171

Figure 4.9 Average crack widths 172

Figure 4.10 Central deflections 174

Figure 4.11 Load transmission paths 176

Figure 4.12 Explanation of symbols 177

CHAPTER 5

Table 5.1 Properties of test beams (Further tests; lightweight concrete) 178

Table 5.2 Measured ultimate loads (Further tests; lightweight concrete) 180

Figure 5.1 Dimensions and reinforcement details (Further tests; lightweight concrete) 181

Figure 5.2 Opening reference nos: applicable to lightweight beams in Table 5.1 and normal weight beams in Table 6.1 182

Figure 5.3 Four point loading - for beams W1(A) W3(A), W4(A) and W7(A) 183

		Page
Figure 5.4	Typical crack patterns at failure	184
Figure 5.5	Maximum crack widths	189
Figure 5.6	Central deflections	191
Figure 5.7	Ultimate strengths of deep beams with web openings	193
Figure 5.8	Beam W6-0.3/4 after failure	194
Figure 5.9	Beam W7-0.3/4 after failure	195
Figure 5.10	Beam W5-0.3/4 after failure	196
CHAPTER 6		
Table 6.1	Properties of the normal weight test beams	197
Table 6.2	Measured ultimate loads of the normal weight beams	198
Table 6.3	Comparison of the ultimate strength of normal weight and lightweight test specimens	199
Figure 6.1	Dimensions and reinforcement details of the normal weight concrete beams	200
Figure 6.2	Crack patterns at failure of the normal weight beams	201
Figure 6.3	Maximum crack widths	203
Figure 6.4	Central deflections	204
CHAPTER 7		
Table 7.1	Measured and computed ultimate loads	205
Figure 7.1	The structural idealization	209
Figure 7.2	Explanation of symbols	210
Figure 7.3	Properties and dimensions of Beam W3-0.3/4	211
Figure 7.4	Comparison of computed and measured ultimate loads	212
CHAPTER 8		
Figure 8.1	Design equations: geometrical notation	213

Page

Figure 8.2 Design example: geometry and loading 214

Figure 8.3 Design example: main steel and web steel details 215

CHAPTER 9

Table 9.1 Comparison of computed design loads 216

Figure 9.1 Basic dimensions of deep beams:CIRIA Guide 217

Figure 9.2 Meanings of symbols: CIRIA Guide 217

Figure 9.3 CIRIA design tables 218

Figure 9.4 Beam designed to CIRIA Guide 219

Figure 9.5 Assessment of hole admissibility: CIRIA Guide 220

Figure 9.6 CIRIA Guide condition of admissibility applied to test specimens 221

Figure 9.7 System of notional deep beams around an opening: CIRIA Guide 222

Figure 9.8 Principal stresses: CIRIA Guide 222

Figure 9.9 Reinforcement around openings: CIRIA Guide 223

APPENDIX 1

Table A1.1 Properties of test beams 224

Table A1.2 Ultimate loads 225

Figure A1.1 Singh's test specimens 226

Figure A1.2 Dimensions and reinforcement details of the present test specimens 226

Figure A1.3 Central deflection curves 227

Figure A1.4 Maximum crack widths 228

Figure A1.5 Crack patterns at failure 229

APPENDIX 2

Table A2.1 Properties of test specimens 230

Table A2.2 Measured and computed loads 231

Page

Figure A2.1	General arrangement and details of web reinforcement	232
Figure A2.2	Central deflections	233
Figure A2.3	Maximum diagonal crack widths	233
Figure A2.4	Comparison of Singh's and present test results: central deflections	234
Figure A2.5	Crack patterns at failure	235

SYMBOLS AND UNITS OF MEASUREMENT

A	area of an individual web bar (for the purpose of Eqns.(1.9), (4.1), (4.2), (7.1), (7.2), (7.3), (8.1) and (8.2), the main longitudinal bars are also regarded as web bars)
A_s	area of main longitudinal reinforcement
A_h	area of horizontal web reinforcement
A_v	area of vertical web reinforcement
A_w	area of web reinforcement
A_r	used in Eqn.(9.4), see symbol A
a_1, a_2	coefficients defining the dimensions of an opening (Figures 4.2 and 5.2)
a_v	distance between the line of action of the load and the face of the supporting member
b	width (breadth) of beam section
C	length of support measured in the direction of the span of the beam
C_1	empirical coefficient in Eqns.(1.9), (4.1), (4.2), (7.1), (7.2)and (7.3) (for normal weight concrete, C_1 = 1.40; for lightweight concrete, C_1 = 1.35 where the cylinder-splitting strength f_t is determined in accordance with ASTM Standard C330, C_1 = 1.0 where f_t is determined in accordance with BS 1881)
C_2	empirical coefficient in Eqn.(1.9), (4.1), (4.2), (7.1) and (7.3) (for deformed bars, C_2 = 300 N/mm^2; for plain round bars, C_2 = 130 N/mm^2)

C_1^*	empirical coefficient in Eqns.(8.1) and (8.2) (for normal weight concrete $C_1^* = 0.44$; for lightweight concrete $C_1^* = 0.36$)
C_2^*	empirical coefficient in Eqns.(8.1) and (8.2) (for deformed bars $C_2^* = 195$ N/mm^2; for plain round bars $C_2^* = 97.5$ N/mm^2)
D	over-all depth of beam (Figs.4.1, 5.1, 6.1)
d	effective depth of beam, measured to centroid of A_s
f_c'	characteristic (or specified) cylinder compressive strength of concrete
f_{cu}	characteristic cube strength of concrete
f_t	characteristic cylinder splitting strength of concrete
f_y	characteristic (or specified) yield strength of reinforcement
f_s	allowable tensile stress in reinforcement
h_a	effective height of beam (Fig.9.1)
k_s	shear stress modifying factor
k_1, k_2, k_1', k_2'	coefficients defining the position of an opening (Figs.4.2, 5.2, 7.1)
L	simple span of beam (Figs.4.1, 5.1, 6.1)
l	effective span (Fig.9.1); in Chapter 2.2.2, l = clear distance between faces of supports

l_o	clear distance between faces of supports (Fig.9.1)
M	design bending moment
M_u	design bending moment at critical section (Eqn.2.4)
"	"
P_s	modified P_s according to de Paiva and Siess
P_s'	$= 2\ v_s\ bD$
P_t	steel ratio used in Laupa, Siess and Newmark's formula (page 6)
P	main steel ratio A_s/bd
P_{web}	web steel ratio = ratio of volume of web steel to that of the concrete in the beam
P_{ms}, P_{wh}, P_{wv}	modified percentage of main steel; horizontal web steel; vertical web steel (Fig.9.3)
Q_{ult}	ultimate shear strength ($Q_{ult} = W_2/2$)
s	spacing of web reinforcement, measured in a vertical direction for horizontal reinforcement and in a horizontal direction for vertical and inclined reinforcement
s_h	spacing of horizontal web reinforcement
s_v	spacing of vertical web reinforcement
T	total tensile force resisted by A_s
V	design shear force
V_c	shear capacity of a beam (Eqn.9.6)

V_u	design shear force at critical section (Eqn.2.4)
v	allowable shear stress (Eqn.2.9)
v_c	ultimate concrete shear stress; in Eqn.(2.4) v_c = nominal shear stress carried by the concrete
v_u	limiting concrete shear stress; in Eqn.(2.2), v_u = nominal shear stress at critical section.
v_s	nominal shear stress in Laupa, Siess and Newmark's formula
v_{max}, v_x, v_{ms} v_{wh}, v_{wv}	concrete shear stress parameters and steel shear stress parameters (Fig.9.3 and Eqn.9.6)
W	total load on beam
W_o	measured ultimate load of solid beam (Table 4.2)
W_1	measured ultimate load
W_2	ultimate load computed from Eqn.(7.2) (Table 7.1 and Fig.7.4); in Fig.(1.4) W_2 = ultimate load computed from Eqn.(1.9)
W_4 through W_7	computed design loads (Chapter 9.3, Table 9.1)
w	uniformly distributed load, axial load per unit length
x	clear-shear-span distance (Figs.4.1, 5.1, 6.1)
x_e	effective clear-shear-span (Eqn.9.2)

y	depth at which a typical bar intersects the potential critical diagonal crack in a solid deep beam, which is approximately the line joining the loading and reaction points
y_1	depth at which a typical bar intersects a potential critical diagonal crack in a deep beam with openings, idealized as the line EA or CB in Fig.(7.2)
y_r	used in Eqn.(9.4), see symbol y
z	lever arm
α	angle of intersection between a typical bar and the potential critical diagonal crack described in the definition of y above
α_o	angle of inclination of reinforcement to horizontal (Eqn.1.2)
α_1	angle of intersection between a typical bar and a potential critical diagonal crack in a deep beam with openings, idealized as the line EA or CB in Fig.(7.2)
β	a characteristic ratio (Eqns.2.6 and 2.7)
$\beta_1, \beta_2, \beta_3$	constants (Eqn.9.6)
γ_f	partial safety factor for loading
γ_m	partial safety factor for materials
ε	a characteristic ratio (Eqns.2.6 and 2.7)
θ_r	angle between reinforcement and diagonal crack (Eqn.9.4)
λ	empirical coefficient, equal to 1.5 for web bars and 1.0 for main bars

λ_1, λ_2	constants (Eqn.9.4)
ϕ, ϕ'	angles defining the directions of the potential critical diagonal cracks (lines EA and CB in Fig.7.2); in Chapter 2.2.2 ϕ = capacity reduction factor (Eqn.2.2)

UNITS OF MEASUREMENT

The SI system of measurement is used throughout this thesis, unless otherwise stated.

C H A P T E R O N E

INTRODUCTION AND BACKGROUND

1.1 INTRODUCTION

1.2 BACKGROUND

1.2.1 ELASTIC ANALYSIS

1.2.2 DEEP BEAM TESTS

1.2.2.1 de Paiva and Siess's tests.

1.2.2.2 Leonhardt and Walther's tests.

1.2.2.3 Crist's tests.

1.2.2.4 Nottingham - Cambridge tests.

C H A P T E R O N E

INTRODUCTION AND BACKGROUND

1.1 INTRODUCTION

At a Mechanics Colloquium [1] given at the University of Cambridge, it became clear that the strength and behaviour of reinforced concrete deep beams, and, in particular, the strength and behaviour of deep beams with web openings, were topics that recurred in design [2]. Often, it may be found necessary to provide openings for services or for access but the practical design of deep beams with web openings is not yet covered by any of the major codes of practice: such as CP110[3] in the U.K.; the ACI Building Code [4] in the U.S.A.; and the CEB-FIP Recommendations [5] in Europe. Indeed, the British code CP110:1972, as yet, provides little guidance on the design of deep beams.

It is only during the last decade or so that research in reinforced concrete deep beams has been carried out on a practical scale [6,7]. In 1970, the Comité Européen du Béton (CEB) and Fédération Internationale de la Précontrainte (FIP) first included provisions for solid deep beams in their International Recommendations [5]. In 1971, the ACI Building Code for the first time included recommendations for solid deep beams. These two documents, together with the Portland Cement Association's widely known Concrete Information ST66[8] and the Construction Industry Research and Information Association's recently published CIRIA design guide [9] (1977), form the major design guides currently available in the U.K.

Deep beams are becoming increasingly employed in modern construction and have useful applications in a variety of structures. In modern building construction for example, in department stores, hotels, buildings housing a theatre, municipal buildings and so on, it is often desired to have the lower floors entirely free of columns. Here, instead of heavy frame construction, the use of Vierendeel trusses in concrete or even structural steel trusses, it may be simpler to utilise the external and partition walls as deep beams to span across the column free space and carry the building above them. Other uses of deep beams may be found in cooling-water pumphouses for power stations; in foundation engineering, where a deep beam may be provided to distribute column loads into the foundation; and in bunkers and silos, where the walls may act as deep beams spanning between column supports.

At the University of Nottingham several research projects [10-12] on reinforced concrete deep beams have been reported. These projects, which were carried out on deep beams without web openings, have shown that their post-cracking behaviour is so complex that, at least for some time yet, design procedures must be based on tests. Since recent surveys [9-12] of the literature have shown that little information and experimental data are available on reinforced concrete deep beams with web openings, an experimental study, which concentrated on the effects of web openings, was carried out.

In this chapter, as a background to the present investigation, a review of selected previous investigations on reinforced concrete deep beams is presented.

1.2 BACKGROUND

1.2.1 ELASTIC ANALYSIS

A substantial library of work is available, covering the behaviour of deep beams in terms of elastic linear analysis [13-21]. The pioneering work in this field was done by Dischinger [13], who used trigonometric series to determine the stresses in continuous deep beams. The Portland Cement Association [8] have produced an expanded version of Dischinger's paper and added solutions for simply supported spans to give guidance for the design of deep beams. Photoelastic methods have also been used to investigate deep beam behaviour. It is pertinent to note that Saad and Hendry [22] have pointed out that, where there were holes in a deep beam, any theoretical elastic solution became very difficult or even impracticable.

The PCA [8] and other design methods [18, 21] which were based on the prediction of interal forces in deep beams from elastic theory were, in the past, consistent with the then accepted design criteria of service load requirements; but, because the elastic assumptions become increasingly invalid in reinforced concrete after the onset of cracking, these methods are no longer compatible with the current design criteria of ultimate limit states. For this reason, further review of research which related primarily to elastic analysis would not be appropriate.

1.2.2 DEEP BEAM TESTS

In 1964, in the Introduction to the 'Recommendations for

an International Code of Practice for Reinforced Concrete'[23], it was stated, "the Comité Européen du Béton considered that the Principles and Recommendations should be fundamentally and solely based on experimental knowledge of the actual behaviour of the combination of steel and concrete conceived as forming a single whole..... subjected to the action of external or internal forces and tested to failure".

In 1965 and 1966 respectively, the results of the practical deep beam tests conducted by de Paiva and Siess [24] in Illinois, and Leonhardt and Walther [25] at Stuttgart, were reported. These two test centres, together with the more recent work of Crist [26] at New Mexico, have expanded the knowledge of actual deep beam behaviour and have significantly influenced design practice. Over the last seven years, a comparatively large volume of research has been carried out on deep beams by the Nottingham - Cambridge team under the direction of Kong [1, 27-38].

In what follows, a brief description of details of the test studies carried out by de Paiva and Siess, Leonhardt and Walther, and Crist is presented, together with an outline of previous work by the Nottingham - Cambridge team.

1.2.2.1 de Paiva and Siess's tests [24].

Possibly the earliest comprehensive study of deep beam behaviour based on practical tests on reinforced concrete specimens was made by de Paiva [24, 39] and colleagues [40, 41], working at the University of Illinois. This work, a digest of which was reported in a paper by de Paiva and Siess [24] in

1965, has since been a guiding influence on the projects of other deep beam research workers [11, 12, 26].

The tests, that were reported in 1965, consisted of 19 simply supported reinforced concrete beams subjected to third point top loading (Fig.1.1). The object of the test programme was to investigate the behaviour of moderately deep beams; that is beams with span/depth ratios(L/D) of between 2 and 6. The major variables studied were the quantity of main tensile steel, the quantity of web (shear) reinforcement, and the span/depth ratio. The beams were tested over a constant span of 610 mm and their depths varied from 178 mm to 330 mm, to give L/D ratios of 1.8 to 3.4. The main longitudinal reinforcement consisted of one or two intermediate grade deformed bars in a single layer, anchored at the ends by welded steel plates. Web reinforcement, where provided, consisted of vertical or inclined stirrups of No.7 black annealed wire.

From the results of the tests, it was deduced that the inclined cracks, that originate in deep beams near the support and propagate upward and inward toward the midspan, had a greater influence on behaviour than the flexural type cracks at sections of maximum moment. Evidence from concrete and steel strain measurement showed that the propagation of the inclined cracks led to a redistribution of internal forces resulting in the formation of a 'tied arch'. (Fig.1.1). This arch behaviour causes high stresses in the tension reinforcement at the supports and hence provision must be made for positive end anchorage of the reinforcement.

Three failure modes were defined to describe the collapse of the beams: 'flexure' failure which occurred through rupture of the steel tie; 'shear proper' failure which resulted from crushing of the inclined 'strut' that formed between two inclined cracks; and 'flexure-shear' where the failure was not clearly either of the former modes.

The effect of the type and amount of web reinforcement provided was found to be not significant in changing the failure modes, but it was observed that increasing the quantity of main steel changed the failure mode from flexure to shear.

From an analysis of the test results, de Paiva and Siess [24] derived the following equation to compute the ultimate shear strength, P''_s:

$$P''_s = 0.8 \left(1 - 0.6\frac{x}{D}\right) P'_s \qquad (1.1)$$

where P'_s was determined using Laupa's [41] formula for shear stress (v_s), as derived from the results of tests on ordinary shallow beams (large L/D) with small shear span/depth ratios.

$$P'_s = 2\, v_s\, bD \qquad (1.2)$$

where $v_s = 200 + 0.188\, f'_c + 21{,}300\, p_t$

in which

$$p_t = A\, \frac{(1 + \sin\alpha_o)}{b\, D}$$

The quantity A $(1 + \sin\alpha_o)$ referred to the 'total' steel area crossing a vertical section between the load point and support; α_o was the angle of inclination of the reinforcement.

It is to be noted that two significant test observations are explicit in Eqn. (1.1): firstly, that the shear strength is related to the x/D ratio; and secondly that conventional vertical stirrups have little effect on ultimate strengths.

1.2.2.2 Leonhardt and Walther's tests [25]

Leonhardt and Walther [25] reported the results of their experimental study on deep beams in 1966, and the significant influence of their work at Stuttgart on the drafting of the CEB-FIP Recommendations (1970)[5] is clearly evident (cf.Chpt.2.2.1). The study included several tests (7 beams) which considered aspects of deep beam behaviour outside the scope of this thesis; namely, the behaviour of continuous, indirectly supported and bottom loaded deep beams, and hence the review here will refer only to the top-loaded simply supported deep beam tests.

A total of 5 comparatively large scale beams were tested under this condition; each 1600 x 1600 x 100 mm, with an overall span L of 1440 mm. The load was applied uniformly, spread over a length 0.8L by a system of distributing beams and rollers. Normal weight aggregate concrete was used for all beams and the main longitudinal tension reinforcement consisted of 8 mm diameter ribbed bars in quantities which ranged from 0.125% bD to 0.25% bD. In some beams the main steel was concentrated near the bottom;in others it was distributed over $\frac{1}{8}$ of the height;and in some cases a proportion of the main

steel was bent up over the supports. Anchorage of the reinforcement was achieved by the use of either vertical or horizontal hooks, and in all of the beams a nominal amount of web reinforcement was provided, consisting of an orthogonal mesh of 5 mm diameter bars.

Analysis of concrete and steel strain measurements confirmed that considerable redistribution of internal forces takes place in reinforced concrete deep beams compared with the elastic theory of vertical plates, and arch action behaviour of deep beams was apparent. The more common mode of failure was found to be flexural, caused by the collapse of the tension chord. Failure also occurred as a result of destruction of the concrete at the supports: it was thought that the failure there might have been caused by the unfavourable action of the vertical anchorage hooks.

In summary, from the basis of the test experience Leonardt and Walther [25] recommended the following design rules:

1. The quantity of main longitudinal steel should be determined from Eqns.(1.3), which follow

$$\text{for } L/D \geqslant 1 \quad T = M/0.6D$$
$$\text{for } L/D < 1 \quad T = M/0.6L \qquad (1.3)$$

where M is the maximum applied bending moment, and T is the resulting tension chord force.

2. The reinforcement determined from the above should extend from support to support and be positively anchored using

horizontal hooks or anchor plates.

3. To limit crack widths, the main reinforcement should be uniformly distributed over the bottom 0.15 to 0.2 times the beam depth. (Fig.1.2).

4. A light orthogonal mesh of vertical stirrups and horizontal bars, arranged more closely at the supports, should be provided for web reinforcement. (Fig.1.2).

Rule No.4 above, reflected the view that shear failure was not a problem in deep beams. It was contended that shear cracks would not occur if the main reinforcement was well anchored and extended from support to support without cut-offs. (In retrospect, it might be mentioned here that, with the benefit of later deep beam tests, it seems likely that shear failure was not observed in Leonhardt's tests because early collapse occurred as a result of either premature flexural failure - ~~and it is to be noted that the quantity of main reinforcement was relatively small~~ - or premature bearing failure at the supports.)

1.2.2.3 Crist's tests [26]

Together with the work of de Paiva and colleagues[24,39-41] at Illinois, Crist's [26] experimental work at the University of New Mexico formed the main basis of the deep beam design guidance, which is given in the current issue of the ACI Building Code [4].

Crist's experimental programme consisted of 9 static tests and 3 dynamic tests on uniformly top-loaded reinforced concrete beams. The object of the research was to develop behavioural equations for reinforced concrete deep beams;

especially as regards shear capacity.

All the test specimens were 203 mm thick and were simply supported over a span of 2438 mm. The depths of the beams were varied to give a range of L/D ratios of 1.6 to 3.8. Normal weight concrete with a nominal compressive strength of 25.9 N/mm^2 and intermediate grade ASTM A15 steel reinforcement were used. All of the beams contained longitudinal tensile reinforcing, and in five of the statically tested beams, an orthogonal array of web reinforcement coincident with the longitudinal axis of the beam was provided.

The statically loaded beams were all tested to collapse. There were no beams that failed prior to beam yield, and the failure modes were predominantly flexure in those beams with web reinforcement and shear in those without. None of the dynamically loaded beams was taken to complete failure, but each was found to behave similarly, as regards crack formation and development, to the companion statically tested beams.

Static behavioural equations for deep beams were derived on the lower boundary of data represented by nine tests mentioned above and seventy-three tests from other research. The total static shear capacity, it was argued, can be given conservatively at a critical section, $x_c = 0.2L$ (for $x_c \leqslant d$), by

$$V_u = V_{uc} + V_{us} \qquad (1.4)$$

in which the concrete capacity is

$$V_{uc} = \left[3.5 - \frac{4}{3}\left(\frac{M}{V}\right)_c \frac{1}{d}\right]\left[1.9\sqrt{f'_c} + 2500\left(\frac{V}{M}\right)_c pd\right] \qquad (1.5)$$

and the web reinforcement capacity is

$$V_{us} = 1.5\, f_y d \left[\frac{A_v}{s_v}\ \frac{1}{12}\ \left(1 + \frac{L}{d}\right) + \frac{A_h}{s_h}\ \frac{1}{12}\ \left(11 - \frac{L}{d}\right)\right] \qquad (1.6)$$

where $\left(\frac{M}{V}\right)_c$ = Ratio of applied moment to applied shear force at the critical section.

A_v, A_h = the area of vertical and horizontal web steel in spacing s_v and s_h respectively.

d = the effective depth measured to the centroid of the main longitudinal steel.

p = the ratio of main steel area to the area bxd of the concrete section.

Upper limits on nominal shear stress were established in the capacity calculations and these were found to control in a minor number of cases. The limits were as follows:

$$V_{uc}/bd < 6\sqrt{f'_c} \qquad (1.7)$$

$$V_u/bd < 8\sqrt{f'_c} \qquad (1.8)$$

Crist concluded that reinforced concrete deep beam inclined-cracking-load behaviour is little different from that observed in normal beams with large L/d ratios, but that in deep beams there is a reserve of strength beyond diagonal cracking, which is not usually available in normal beams. Hence, in Eqn.(1.5), the second bracketed term is conveniently the same term as that used in the ACI Building Code [4] for the inclined cracking load of normal beams: in such beams the diagonal cracking load is taken as a measure of the useful capacity of

the beam without shear reinforcement. The first bracketed term gives a measure of the reserve of strength of deep beams beyond diagonal cracking and was derived empirically from the test data.

The web reinforcement capacity, given by Eqn.(1.6), represents the capacity of an orthogonal array of reinforcement coincident with the longitudinal axis of a beam. The equation was based on a shear friction analogy originally developed by Mast [42]. The analogy assumes that normal forces, developed on an inclined crack plane by web bars crossing the plane, give rise to frictional forces which resist the applied shear force.

1.2.2.4 NOTTINGHAM - CAMBRIDGE tests

Research by the Nottingham-Cambridge team on the behaviour of reinforced concrete beams has been ongoing under the general guidance of Dr.F.K. Kong for the past nine years. At the beginning of the research programme, computer solutions based on the assumption of an uncracked section were sought[10,43] but as the research progressed, there was mounting experimental evidence that practical tests on concrete specimens would provide the most fruitful approach. Many of the details and results of the tests have been published in technical journals [27-32], and the new CIRIA design guide contains some design guidance which is based on the design proposals of the Nottingham - Cambridge team [33].

The culmination of the research up to 1972 on deep beams without openings was the publication of a proposed formula [33]

for the design of solid reinforced concrete deep beams, which it was argued, embodied many of the recorded test observations. The proposed method was based on a further evaluation of the research experiments previously carried out at Nottingham [30] and the proposed formula took the following form:-

$$Q_{ult} = C_1 \left(1 - 0.35\frac{x}{D}\right) f_t bD + C_2 \sum^{n} A \frac{y}{D} \sin^2\alpha \qquad (1.9)$$

$$= \frac{W}{2} \text{ for two-point top loading}$$

where, with reference to Fig.(1.3):

Q_{ult} is the ultimate shear strength of the beam, in Newtons.

W is the ultimate shear load, in Newtons, computed from the above formula; in the case of two-point top loading, $W = 2\ Q_{ult}$.

C_1 is an empirical coefficient equal to 1.4 for normal weight concrete and 1.0 for lightweight concrete.

C_2 is an empirical coefficient equal to 130 N/mm^2 for plain round bars and 300 N/mm^2 for deformed bars.

f_t is the cylinder splitting tensile strength, in N/mm^2, or 0.1 times the cube strength if f_t is not available.

b is the breadth or thickness of the beam, in mm.

D is the overall depth of the beam, in mm.

A is the area of the individual web bar, in mm^2, and for the purpose of this equation the main longitudinal bars are also considered as web bars.

y is the depth, in mm, measured from the top of the beam, at which an individual bar intersects the line joining the inside edge of the bearing block at the support to

the outside edge of that at the loading point.

α is the angle between the bar being considered and the line described in the definition of y above $(180 \geqslant \alpha \leqslant 0)$

n is the total number of web bars, including the main longitudinal bars, that cross the line described in the definition of y. Thus, the quantity $\sum A(y/D) \sin^2\alpha$ is to be summed for all n bars.

Using the test data from Nottingham and elsewhere, a plot of the measured ultimate loads (W_1) and the computed ultimate loads (W_2, as determined from Eqn.(1.9) above) was presented,and is reproduced here in Fig.(1.4). It may be seen that Eqn.(1.9) gives a reasonable estimate of the ultimate strengths of solid deep beams.

The experimental work [27-32] which formed the basis of the proposed formula included tests to destruction carried out on 135 simply supported rectangular deep beams. The test specimens were 76.2 mm thick and had spans of either 762 mm or 1524 mm. The depths of the beams and the geometry of the two point top loading system were varied to give a range of L/D and x/D ratios; namely, L/D varied from 1 to 3; x/d from 0.23 to 0.7. Both normal weight aggregate and lightweight aggregate concretes were used and five principal arrangements of web reinforcement were considered (Fig.1.5). The web reinforcement ratio, p_{web}, defined as the ratio of the volume of web steel to that of the concrete in the beam, varied from zero to about 0.025. Both plain round and deformed bars were used, and their yield strengths were approximately 300 N/mm^2 and 400 N/mm^2 respectively. The main longitudinal bars were

anchored at their ends to steel blocks to prevent possible anchorage failure.

The more important test observations reported [27-32], itemised here for brevity, are as follows:-

1. The ultimate shear strength of a deep beam is composed of two parts, the contribution of the concrete and that of the web reinforcement.

2. The concrete contribution increased linearly with a decrease in the x/D ratio, and is more closely related to the cylinder splitting strength f_t than to the cube strength f_{cu}.

3. The potential diagonal crack is approximately the line joining the inside face of the load-bearing block at the support to the outside face of that at the loading point, i.e., it is inclined at $\cot^{-1}$ (x/D) to the horizontal.

4. The more nearly a web bar is perpendicular to the diagonal crack, the more effective it is in resisting shear: its effectiveness also increases with the depth at which it intersects the diagonal crack.

5. Within practical limits, ultimate shear strength is independent of the yield stress of the reinforcement.

6. The main longitudinal reinforcement forms an important contribution to the shear strength of reinforced concrete deep beams.

It is to be noted that observation (2) above means that the clear-shear span ratio x/D is interpreted to be more important than the span/depth ratio L/D. Observation (2) also

implies that diagonal cracking in a deep beam is akin to the splitting of a cylinder in the Brazilian test, an analogy which was first described by Brock [44, 45], in connection with normal beams with small shear span/depth ratio (a_v/d), and subsequently applied to deep beams by Ramakrishnan and Ananthanarayana [46]. (Brock's 'split-cylinder' analogy is explained in Section (1.12) and Fig. (1.12) of the Shear Study Group's Report [47]).

As regards web reinforcement, there are two significant and interesting differences between the results of Crist's tests and those of the Nottingham-Cambridge team. Firstly, Crist assumes that the contribution of the reinforcement crossing the diagonal crack is uniformly distributed down the effective depth. The expression given above, Eqn.(1.9), reflects a triangular distribution with the maximum ordinate at the beam soffit. The second difference is that Crist assumes that the yield strain of the reinforcement develops before failure whereas observation (5) above, states that it may not.

C H A P T E R T W O

THE DESIGN OF R.C. DEEP BEAMS IN CURRENT PRACTICE

2.1 INTRODUCTION

2.2 OUTLINES OF CURRENT DESIGN METHODS

2.2.1 CEB-FIP Recommendations

2.2.2 ACI Building Code

2.2.3 Portland Cement Association

2.3 GENERAL COMMENTS

C H A P T E R T W O

THE DESIGN OF R.C. DEEP BEAMS IN CURRENT PRACTICE

2.1 INTRODUCTION

With the issue of the CIRIA design guide [9] in January 1977, some form of authorative, British guidance on the design of reinforced concrete deep beams became available for the first time. The guide joined ranks with (but provides more detailed guidance than) the CEB-FIP Recommendations [5], the ACI Building Code [4], and the PCA ST66[8]; each of which containing some provisions for deep beams is currently used in British design practice.

In this chapter the three major design methods mentioned above are described, and design examples are given to illustrate their usage. The CIRIA guide, which is likely to have a significant impact on future design practice and also contains some provisions for the design of deep beams with web openings, is reviewed in greater detail in Chapter 9.

2.2 OUTLINES OF CURRENT DESIGN METHODS

2.2.1 The CEB-FIP Recommendations [5].

According to the CEB-FIP Recommendations [5], simply supported beams of span/depth ratio L/D less than 2 or continuous beams of L/D ratio less than 2.5 are to be designed as deep beams. The area of the main longitudinal steel should be calculated from the largest bending moment in the span,

using the following values for lever arm z:-

$$z = 0.2\ (L + 2D) \quad \text{for } 1 < L/D < 2 \qquad (2.1)$$

$$z = 0.6\ L \quad \text{for } L/D < 1$$

It is thus seen that for $L/D < 1$, the lever arm z is independent of the depth D of the beam: for L/D from 1 to 2, z increases with D but at a lower rate.

The main longitudinal reinforcement, determined as explained above, should extend without curtailment from one support to another and be anchored securely at the ends. Also, the required area of the steel is not to be concentrated at one level, but should be uniformly distributed over a depth equal to (0.25D - 0.05L), as shown in Fig.(2.1). The CEB-FIP drew attention to the importance of detailing of the main steel in the form of a number of small diameter bars to limit the width and development of cracks and to facilitate anchorage at the supports.

The design shear force should not exceed

$$0.1bDf_c'/\gamma_m \quad \text{or} \quad 0.1bLf_c'/\gamma_m \quad \text{(whichever is less)}$$

where b is the beam width, D the depth, L the span, f_c' the characteristic cylinder strength of the concrete and γ_m the partial safety factor for materials.

As regards web reinforcement, the Recommendations state that it will generally be sufficient to provide an orthogonal mesh consisting of vertical stirrups and horizontal bars placed near each face and surrounding the extreme vertical bars. The

required area of one bar of the mesh is given by $A = 0.0025bs$ for a smooth round bar, and by $A = 0.0020bs$ for a high bond deformed bar, where s is the spacing between the bars of the mesh and b is the beam thickness. The total web steel ratio required, expressed as (volume of web steel)/(volume of concrete) is, therefore, 1.0% and 0.8% for plain and deformed bars respectively. Near the supports, additional web bars should be provided particularly in the horizontal direction, as shown in Fig.(2.1).

Design example for CEB-FIP Recommendations

A tentative scheme for part of a heavy industrial structure is shown in Fig.(2.2a). It is proposed to utilize Wall 'A' as a deep beam, to give required column free access below. If the total uniformly distributed load w (including selfweight) is 400 kN/m and the load in each column B and C is 3300 kN, design the main longitudinal and web reinforcement.

Idealising the problem, the loading, properties and geometry of the deep beam structural element are shown in Fig. (2.2b), where W/2 equals the column load plus half the total distributed load.

$$L/D = 6000/4800 = 1.25 < 2$$

$\therefore$ CEB-FIP Recommendations apply.

$$\text{Lever arm } z = 0.2\ (L + 2D) = 3120 \text{ mm}$$

$$\text{Design bending moment} = \gamma_f \times \frac{W}{2} \times 2000$$

(where $\gamma_f = 1.4$, say, is the overall partial safety factor for dead and live loading, and $W = 9{,}000$ kN)

$$\text{Moment of resistance} = \frac{f_y}{\gamma_m} \times A_s \times z$$

(where γ_m, the partial safety factor for material, is 1.15 for steel, $f_y = 410\ N/mm^2$ and $z = 3120$ mm as calculated)

$$1.4 \times \frac{9000 \times 10^3}{2} \times 2000 = \frac{410}{1.15} \times A_s \times 3120$$

Longitudinal steel area $A_s = 11327\ mm^2$

Use 24 No.25 mm diameter bars ($11782\ mm^2$)

These main bars are arranged in 8 rows of three bars, extended without curtailment from support to support, and distributed over a depth of (0.25D - 0.05L) = (0.25 x 4800-0.05 x 6000) = 900 mm measured from the bottom.

Next, the required beam width b is determined from the condition that:

$$\text{Design shear force } \gamma_f \times \frac{W}{2} \not> 0.1 \frac{bD f'_c}{\gamma_m}$$

Taking $\gamma_f = 1.4$ and $\gamma_m = 1.5$ for concrete

$$\frac{1.4 \times 9000 \times 10^3}{2} \not> 0.1 \times b \times \frac{4800 \times 22.5}{1.5}$$

$\therefore b = 875$ mm.

Web reinforcement: say, bar spacing s = 150 mm.

Area required for each bar = 0.2 per cent of b x s

i.e., $0.002 \times 150 \times 875 = 262\ mm^2$.

Provide an orthogonal mesh of 20 mm diameter deformed bars at 150 mm centres in each face ($A_v = A_h = 314.2\ mm^2$/bar) and at 75 mm spacing near supports.

The detailing is shown in Fig.(2.3).

2.2.2 ACI Building Code: ACI 318-71[4].

Special provisions are given in the 1971 ACI code [4] for deep beams; the emphasis is on the capacity to resist shear force. These shear provisions apply to both simple and continuous beams when the span/depth ratio L/D is less than 5. The calculations are carried out for the critical section, which is defined as follows. For a concentrated load, the critical section is located midway between the load and the face of the support; for a uniformly distributed load it is at 0.15 l from the support where l is the clear span distance face to face of supports.

First the nominal shear stress v_u is calculated from the given design shear force V_u:

$$v_u = \frac{V_u}{\phi\, bd} \qquad (2.2)$$

where ϕ is the capacity reduction factor (taken as 0.85)

b is the width of the beam

d is the effective depth measured to the centroid of the main longitudinal steel.

The designer should ensure that the dimensions b and d of the beams are large enough for v_u not to exceed the following limits:

$$v_u \not> 8\sqrt{f'_c} \quad \text{when} \quad l/d < 2$$

$$v_u \not> 2/3\ (10 + l/d)\sqrt{f'_c} \quad \text{when} \quad 2 \leqslant l/d \leqslant 5 \qquad (2.3)$$

where f'_c is the concrete cylinder compressive strength.

Next, the nominal shear stress v_c carried by the concrete is calculated:-

$$v_c = \left[3.5 - 2.5 \frac{M_u}{V_u d}\right] x \left[1.9 \sqrt{f'_c} + 2500p \frac{V_u d}{M_u}\right]$$

$$\not> 2.5 \left[1.9 \sqrt{f'_c} + 2500p \frac{V_u d}{M_u}\right] \quad (2.4)$$

$$\not> 6 \sqrt{f'_c} \quad (2.4_a)$$

where M_u is the design bending moment at the critical section

f'_c is the specified concrete cylinder compressive strength.

p is the ratio of the main steel A_s to the area b x d of the concrete section.

V_u, b and d are as defined in Eqn.(2.2)

Irrespective of the values of v_u and v_c so calculated, an orthogonal mesh of web reinforcement is mandatory; the area of the vertical web steel should not be less than 0.15 per cent of the horizontal concrete section bL, and that of the horizontal web steel not less than 0.25 per cent of the vertical concrete section bd. When v_u exceeds v_c the web reinforcement should also satisfy the requirements of Eqn.(2.5)below:-

$$\frac{A_v}{s_v}\left[\frac{1 + 1/d}{12}\right] + \frac{A_h}{s_h}\left[\frac{11 - 1/d}{12}\right] = \frac{(v_u - v_c)b}{f_y} \quad (2.5)$$

where A_v is the area of the vertical web steel within a spacing s_v.

A_h is the area of the horizontal web steel within a spacing s_h.

l is the clear span distance.

b is the beam width.

f_y is the specified yield strength of the steel.

Design example for ACI code.

Consideration is given again to the design of the beam shown in Fig.(2.2). (In using the ACI code it must be noted that all equations are intended for use with Imperial units. However, in practice, Imperial units need only be used in Eqn.(2.4) and in evaluating $\sqrt{f'_c}$).

The ACI code does not contain detailed requirements for designing deep beams for flexure. In the commentary [48] and notes [49] to the code, the designer is referred to other documents, such as the PCA bulletin [8]. The PCA method is explained later, and only the final result of the flexural calculations will be given here.

Main steel provided: 13 No. 40 mm diameter bars (16336 mm^2).

The critical section is located (Fig.2.2) at 0.5 x (2000 - 0.5 x 600) = 850 mm from the face of support, or 850 + 0.5 x 600 = 1150 mm from the centre of support.

Design bending moment $M_u = 1.4 \times \frac{9000}{2} \times 1150 = 7245$ kNM

(where 1.4 is the partial safety factor for loading).

Design shear force $V_u = 1.4 \times \frac{9000}{2} = 6300$ kN

A suitable beam width b may be chosen from Eqn.(2.3).

$$\frac{V_u}{\phi\, bd} = 8\sqrt{f'_c} \quad \text{(Assuming d = 4500 mm say)}$$

(f'_c = 22.5 N/mm^2 = 3260 lbf/in^2 $\therefore \sqrt{f'_c}$ = 57.2 lbf/in^2 = 0.394 N/mm^2)

$$\frac{6300 \times 10^3}{0.85\ b \times 4500} = 8 \times 0.394$$

$$b = 525 \text{ mm say}$$

Referring to Eqn. (2.4),

$$\left[3.5 - 2.5\ \frac{M_u}{V_u d}\right] = \left[3.5 - \frac{2.5 \times 7245 \times 10^3}{6300 \times 4500}\right]$$

$$= 2.86 > 2.5$$

Use 2.5 (See Eqn.(2.4)

$$v_c = 2.5\left[1.9\sqrt{f'_c} + 2500\ p\ \frac{V_u d}{M_u}\right]$$

$$= 2.5\left[1.9 \times 57.2 + 2500 \times \frac{16336}{525 \times 4500} \times \frac{6300 \times 4500}{7245000}\right] \text{ lbf/in}^2$$

$$= 441 \text{ lbf/in}^2 = 3.04 \text{ N/mm}^2$$

But $6\sqrt{f'_c} = 6 \times 0.394 = 2.36$ N/mm^2

From Eqn. (2.2)

$$v_u = \frac{6300 \times 10^3}{0.85 \times 525 \times 4500} = 3.14 \text{ N/mm}^2$$

Since v_u exceeds v_c, the web reinforcement must satisfy the requirement of equation (2.5). Only orthogonal web reinforcement is acceptable to the code. Assuming the same size bars (A_{web}) are used in a square pattern at, say,

150 mm spacings, equation (2.5) gives

$$\frac{A_{web}}{150}\left[\frac{1 + (6000 - 600)/4500}{12}\right] + \frac{A_{web}}{150}\left[\frac{11 - (6000 - 600)/4500}{12}\right]$$

$$= \frac{(3.14 - 2.36)}{410} \times 525$$

$$\therefore A_{web} = 150 mm^2$$

Check minimum requirements $A_h = 0.0025 \times 525 \times 150$

$$= 197 \text{ mm}^2$$

$$A_v = 0.0015 \times 525 \times 150$$

$$= 178 \text{ mm}^2$$

Provide 16 mm diameter bars at 150 mm spacing horizontal and vertical ($A_v = 201 \text{ mm}^2$, $A_h = 201 \text{ mm}^2$)

The detailing is shown in Fig. (2.4).

2.2.3 Portland Cement Association [8].

The PCA's Concrete Information ST66[8] is based on elastic analysis and not on the results of ultimate load tests. It applies to simply supported beams of span/depth ratio L/D not exceeding 1.25 and to continuous beams of L/D ratio not exceeding 2.5. The design is carried out with the help of a number of charts. Briefly, the procedure is as follows. First two characteristic ratios ε and β are calculated; these are nominally referred to as the support to span ratio and the depth to span ratio respectively. For a continuous span, ε is equal to the ratio of the length C of a support

(for example, the dimension of a column in the direction of the span) to the span L, and β is D/L. For a simple span, ε and β need careful interpretation. It would seem that for a simply supported beam under uniformly distributed load,

$$\varepsilon = \frac{1}{2} \quad \text{and} \quad \beta = \frac{D}{2L} \qquad (2.6$$

For a simply supported beam under a point load applied at midspan,

$$\varepsilon = \frac{C}{2L} \quad \text{and} \quad \beta = \frac{D}{2L} \qquad (2.7$$

From the values of ε and β, the tensile force T to be resisted by the main longitudinal steel A_s is obtained from a chart, reproduced here in Fig.(2.5).

Then

$$A_s = T/f_s \qquad (2.8$$

where f_s is the allowable stress in the steel; the value of f_s is left to the judgment of the designer.

As regards shear resistance, the PCA document [8] states that conventional vertical stirrups as used in ordinary beams are ineffective in deep beams. No specific recommendations are given for the design of the web reinforcement, but it is suggested that the shear force V applied to the beam should not exceed that given by Eqn.(2.9).

$$\frac{V}{\frac{7}{8}bD} \not> \frac{1}{3} \quad (1 + \frac{5D}{L}) \quad v \qquad (2.9$$

where v is the allowable shear stress for an ordinary beam

made of similar quality concrete; the value of v is again left to the discretion of the designer.

Design example for PCA method.

Once again, consideration is given to the design of the beam shown in Fig.(2.2). (Note: the PCA method is based on allowable stresses. Therefore, the partial safety factors of γ_f and γ_m do not appear).

The beam is under point loads W/2 applied at third points. To apply PCA's design chart (Fig.2.5) it is first necessary to approximate the beam to one with a span of 2L/3 having a point load at midspan; the maximum moments in the two beams are then the same. Next, the characteristic ratios ε and β are calculated from Eqn.(2.7) by writing 2L/3 for L:-

$$\varepsilon = \frac{C}{2(2L/3)} = \frac{600 \times 3}{4 \times 6000} = \frac{1}{13.3}$$

$$\beta = \frac{D}{2(2L/3)} = \frac{4800 \times 3}{4 \times 6000} = 0.6$$

Referring to Fig.(2.5) it will be conservative to use the solid curves to interpolate T for ε = 1/13.3 and β = 0.6.

By visual interpolation

$$T = 0.29W = 0.29 \times 9000 \text{ kN} = 2610 \text{ kN}$$

To determine A_s from Eqn.(2.8) it is necessary to adopt a value for the allowable steel stress f_s. A reasonable value (see Section 8.10.1 of ACI code [4]) would be f_s = 24000 lbf/in^2 = 165 N/mm^2. Then

$$A_s = \frac{T}{f_s} = \frac{2610 \times 10^3}{165} = 15818 \text{ mm}^2$$

Provide 13 No. 40 mm diameter bars (16336 mm^2) and note the PCA guide requires the main tensile steel to be placed close to the bottom of the beam.

Next, the required beam width is determined from Eqn.(2.9) using a reasonable value of $1.1\sqrt{f'_c}$ for the allowable shear stress v (see ACI code [4]: Sections 8.10.3 and 11.4.1).

$$v = 1.1\sqrt{f'_c} = 63 \text{ lbf/in}^2 = 0.44 \text{ N/mm}^2$$

Using Eqn.(2.9) with D/L replaced by D/(2L/3)

$$\frac{0.5 \times 9000 \times 10^3}{\frac{7}{8} \times b \times 4800} \not> \frac{1}{3}\left(1 + \frac{5 \times 4800}{2 \times 6000/3}\right) \times 0.44$$

$$b = 1050 \text{ mm (say)}$$

The PCA method does not call for web reinforcement. The detailing is shown in Fig.(2.6).

2.3 GENERAL COMMENTS

The most widely used of the four methods, namely, that of the PCA[8], was prepared some thirty years ago when little experimental data on reinforced concrete deep beams were available. Consequently, it was based on the theoretical work of Dischinger [13], who used the classical theory of elasticity and assumed the beam to be homogeneous. The method,

therefore, cannot be expected to reflect accurately actual behaviour. For example, the stress distribution in a concrete deep beam at ultimate load is not the same as that predicted. However, because of the built-in factors of safety, the PCA method is likely to be conservative in most cases, although its use would not be recommended.

The CEB-FIP Recommendations [5], published in 1970 were based mainly on the tests of Leonhardt and Walther [25], although they may have been influenced by the earlier tests carried out in Sweden by Nylander and Holst [50]. The Recommendations concentrate on flexural design and do not give specific guidance on how to calculate the web steel areas to resist specified shear forces. In contrast, the ACI's recommendations [4], which were based mainly on tests carried out in America by Crist [26], de Paiva and Siess [24], emphasize shear design and do not give specific guidance on how to calculate flexural steel areas to resist specified bending moments.

Since the publication of the ACI and CEB-FIP's recommendations, a comparatively large volume of research has been carried out on deep beams in the U.K. [27-32]. It is now known for example, that inclined web reinforcement (which is not covered by the ACI code and the CEB-FIP Recommendations) is the most efficient type of web reinforcement for deep beams, that the effectiveness of a web bar depends on where and how it intercepts the critical diagonal crack, and that the main longitudinal reinforcement is an integral part of the web reinforcement. Many of these aspects of deep beam behaviour are reflected in the design method proposed by the Nottingham -

Cambridge team [33,34] (Chapter 1.2.2.4: Eqn.(1.9)). This method gives reasonable estimates of the ultimate shear capacity of reinforced concrete deep beam without openings and now forms part of the provisions given in the new CIRIA design guide.

The design of deep beams with web openings is not covered by any of the design methods outlined in this chapter and, as will be shown, the CIRIA provisions for openings are rather restrictive (Chapter 9). As in the case of solid deep beams previously, data on the ultimate behaviour of deep beams with openings are required to facilitate the development of reasonable methods of predicting the ultimate shear capacity. As a step towards providing such data, the present experimental programme was carried out, a description and the results of which are presented in the succeeding four chapters.

C H A P T E R T H R E E

THE EXPERIMENTAL PROGRAMME

3.1 INTRODUCTION

3.2 MATERIALS

3.2.1 Cement

3.2.2 Lightweight aggregates

3.2.3 Normal weight aggregates

3.2.4 Reinforcement

3.3 CONCRETE MIXES

3.3.1 Lightweight concrete

3.3.2 Normal weight concrete

3.4 BEAM MANUFACTURE

3.4.1 Formwork

3.4.2 Reinforcement fabrication

3.4.3 Casting and curing

3.5 CONTROL SPECIMENS

3.6 TESTING

3.6.1 Test equipment

3.6.2 Test preparation

3.6.3 Test procedures

C H A P T E R T H R E E

THE EXPERIMENTAL PROGRAMME

3.1 INTRODUCTION

Previous work using practical laboratory tests on reinforced concrete specimens has proved fruitful in providing an appreciation of deep beam behaviour and has led to the development of practical design guidance. It is possible that, in the near future, advances in mathematical techniques such as refinements to the finite element method [51] could provide mathematical models capable of simulating post cracking behaviour on the computer; but at the present time, because of the complex nature of the behaviour of deep beams after cracking, laboratory testing would remain the primary investigatory tool available to the researcher. Such testing, as drafting committees for codes of practice have emphasized, should form the basis of practical design recommendations.

The primary object of the present experimental programme was to study the behaviour of reinforced concrete deep beams with web openings; a topic which, as mentioned earlier, has received little attention in the past, and one which may be expected to occur frequently in practice because of the wall like geometry and uses of deep beams. Due to the lack of previous test data, the present investigation was, of necessity, a developing one. It began with a pilot investigation in which 24 lightweight concrete specimens were tested to destruction. These exploratory tests, during which crack development, crack widths and beam deflection were recorded, covered a wide range

of opening size, shape and position and broadly investigated the effect of beam geometry. Further tests were then planned as a follow up and a series of 39 beams was designed to systematically test the more important observations recorded in the pilot study and provide information on the effects of web reinforcement.

In both of these two test series, lightweight aggregates were used in concrete making because test data of lighweight concrete beams were particularly scarce; for example, ACI Committee 408 has recommended that "experimental research should be conducted on lightweight concrete elements, which would evaluate the ability of lightweight concrete to develop bond in a variety of environments" [52]. Furthermore, some engineers [53,54] expect that, in the not too distant future, "lightweight concrete will achieve greatly enhanced use"[55].

In a final series of tests, which comprised 16 beams, normal weight aggregates were used in concrete making to provide information on any differences in behaviour between lightweight concrete deep beams and normal weight concrete deep beams. Nine of the second series of lightweight concrete test specimens were thus repeated and a further seven complementary normal weight deep beams with openings were designed to investigate the effectiveness of an inclined system of web reinforcement.

Some guidance for the early planning of the test programme was derived from a survey of the literature appertaining to the effects of openings on ordinary shallow beams (large span/depth ratios). The main conclusion drawn from the survey was that openings located in the predominantly flexural regions do

not reduce capacity, whereas openings located in regions of high shear may significantly do so. For this reason all the openings in the present tests were located within the shear spans. The test specimens were also designed to be complementary to the previous tests at Nottingham on solid deep beams, and a similar simple two point loading configuration was normally adopted.

In this chapter, the general experimental details of the test programme are described. The description and notation of each of the three series of the test specimens, together with the presentation and discussion of each set of test results, are given separately in the succeeding three chapters.

Two subsidiary deep beam topics were also investigated: the requirements for end anchorage of the main longitudinal tension reinforcement (9 tests), and the effects of repeated loading on deep beams (3 tests). These tests and theirresults are described in Appendices 1 and 2 respectively.

3.2 MATERIALS

3.2.1 Cement

Ordinary Portland Cement conforming to B.S.12 was used for both normal weight and lightweight concrete. Quantities of cement, sufficient to permit cement from the same batch to be used for the manufacture of all beams within each test series, were successively ordered and carefully stored in airtight containers. All cement was supplied by the Blue Circle Group.

3.2.2 Lightweight aggregates

Lightweight aggregates of sintered pulverized fuel ash (supplied in two grades under the name "Lytag") were used for the lightweight concrete test specimens:-

Fine aggregates: Lytag fine grade (5 mm down).

Coarse aggregates: Lytag medium grade (13 mm nominal size).

Both grades were well dried before use. Storage problems necessitated two batches being ordered, but, as shown by the results of sieve analysis presented in Table (3.1), the differences between the batches were not significant.

3.2.3 Normal weight aggregates

The following aggregates were used in normal weight concrete:-

Fine aggregates: dried Hoveringham River Sand (5 mm down)

Coarse aggregates: dried Hoveringham River Gravel (10 mm nominal)

The results from sieve analysis are given in Table (3.2).

3.2.4 Reinforcement

Deformed bars of high yield steel (Unisteel 410) were used throughout. The reinforcement was ordered as a single batch and, for quality control, samples of reinforcement picked at random from the fabrication workshop were simply tested for ultimate tensile strength. The coefficient of variation for the results of these tests was satisfactory, being approximately 3%. The typical tensile properties of the reinforcement (Table 3.3) were determined by tests on a smaller random sample, using the standard test procedures recommended in B.S.18:1962 and B.S.4449:1969. Typical load v. extension curves for the 20 mm

and 8 mm diameter bars are presented in Fig.(3.1). It is to be noted that the 8 mm bars and similarly the 6 mm and 10 mm bars possessed no definite yield point: for these bars the value of the 0.2 per cent proof stress was taken as representative of the 'yield strength'.

3.3 CONCRETE MIXES

3.3.1 Lightweight concrete

The proportion of dry weight of materials used was in accordance with recommendations [56] given by the manufacturers:

Mix proportions by weight	1:1.25:1.55
Total water/cement ratio	0.8
Cement per cu m.	383 kg/m^3

The average wet and hardened properties of the concrete produced were as follows:-

Slump, immediately after mixing	70 mm
Wet density	1810 kg/m^3
Air dry density	1780 kg/m^3
Cube strength (28 day)	37.90 N/mm^2 (5.4% coeff. of variation)
Cylinder crushing strength (28 day)	31.60 N/mm^2 (5.4% coeff. of variation)
Cylinder splitting strength (28 day)	2.5 N/mm^2 (9.4% coeff. of variation)

3.3.2 Normal weight concrete

The mix was designed for a target strength comparable to that of the lightweight concrete and after a series of trial

mixes, a mix of the following proportions was selected:-

Mix proportions by weight	1:1.75:3.25
Total water/cement ratio	0.47
Cement per cu.m	350 kg/m^3

Representative values for the properties of the mix are as follows:-

Slump	70 mm
Wet mix density	2450 kg/m^3
Cube strength (28 day)	53.25 N/mm^2 (6.0%coeff.of variation)
Cylinder crushing strength (28 day)	41.95 N/mm^2 (6.0% coeff.of variation)
Cylinder splitting strength (28 day)	3.75 N/mm^2 (5.7% coeff.of variation)

3.4 BEAM MANUFACTURE

3.4.1 Formwork

Four upright wooden moulds were used to cast the beams. Each mould was a bolted assembly of 20 mm thick Wisaform sides, with stop-ends and a base of 100 mm x 75 mm planed softwood. Prior to assembling, all the internal surfaces were coated with a thin release oil and all joint surfaces were liberally coated with thick heavy grease. This application of grease served successfully to seal the mould.

The openings in the test specimens were formed by blocks of expanded polystyrene. These blocks, which were easily and accurately shaped on a purpose built hot-wire cutter, were coated with grease during assembling to prevent the ingress of

of mortar. An array of 8 mm diameter holes drilled through the sides of each mould facilitated the fixing of the blocks in any of a wide range of locations. Each block was sandwiched between the sides of the mould and secured in compression by four lateral bolts 150 mm long. Those 8 mm diameter holes, which were not required for the opening location of a particular test specimen, were plugged effectively with plasticine.

Lateral bulging of the mould was prevented by three U-shaped metal frames positioned at the third points of each mould. The outer frames also functioned as mountings for two Bosch external vibrators, which were fixed across the top by bolts. The frames in turn were mounted on rubber pads, which served to reduce the clatter and give smoother vibration.

3.4.2 Reinforcement fabrication

The reinforcement for all the beams was fabricated in the workshop of the University's Applied Science Faculty. The main longitudinal reinforcement for all beams consisted of 1 No. 20 mm diameter deformed bar which, for the purpose of affixing external end anchorage blocks, had been cut longer than the beam and had screw threaded ends. All joints on the web reinforcement were made with light tack welds. After degreasing, the reinforcement was positioned in the mould and held in position by spacers at the top and by the main longitudinal bar passing through the ends of the formwork at the bottom. In order to simplify transportation of the beams, two 12 mm diameter lifting bolts to be cast in were fixed to the top bar of each reinforcement assembly.

3.4.3 Casting and curing

The beams for each test series were cast consecutively at weekly intervals in groups of 3 or 4. Each mixing session normally consumed approximately two tonnes of concrete and to spread the work load, the aggregates and cement were carefully weighed out into tins on a previous day.

Both normal weight and lightweight concretes were mixed for about 3 minutes in a 3 cu ft. (0.085 m^3) capacity Cumflow horizontal drum mixer. Prior to the first mix, the drum was 'buttered' to compensate for initial loss of mortar. Slump tests were carried out on each batch, with compaction factor tests being carried out at random. For most batches of concrete a slump of 70 mm was obtained; however, slumps 20 mm either side were accepted. If the slump was less than 50 mm additional water was added and following remixing, a new slump taken.

The concrete was placed in the forms with shovels and continuously compacted with the external Bosch vibrators. A set of control specimens, consisting of 3 standard cubes (100 mm) and 6 standard cylinders (150 mm diameter) for each deep beam, were cast in steel moulds and compacted on a vibrating table. Several hours after casting, the top surface of the beams in the region of the loading points was trowelled smooth and the control cylinders were capped with neat cement paste.

On the following day, the test beams were removed from their moulds and cured for a further 6 days under three layers of wet hessian. The beams were then stored in the laboratory (at approximately 23°C and 50% R.H) until tested.

3.5 CONTROL SPECIMENS

The properties of the concrete in each test beam were determined from tests on 3 cubes (100 mm) and 6 cylinders (150 mm diameter x 300 mm). The control specimens were manufactured and cured in accordance with B.S.1881-1970, with the exception of the cylinders of lightweight concrete. B.S.1881-1970 does not differentiate between normal weight and lightweight concretes and the special procedure recommended by ASTM Standard C330 for lightweight cylinders was adopted; namely, moist cured for 7 days followed by storage at 50 per cent relative humidity until the time of test. It is to be noted that the main effect of the curing conditions is on the tensile splitting strength, and in a separate study consisting of tests on 30 cylinders it was found that the ASTM method curing resulted in a reduction in the splitting strength (f_t); the average ratio f_t (ASTM)/f_t (B.S.1881) being 0.74. Similar results have been reported by Teychenne [57] and Hanson [58]. For this reason, it was important that the test beams and control cylinders of lightweight aggregates were cured under comparable conditions.

Each set of control specimens was tested on a 120 tonne capacity Denison grade 'A' machine, immediately following the testing of the corresponding deep beam. The three cubes and three capped cylinders were used to determine the crushing strength. The cylinder splitting strength was determined from tests on the further three cylinders, the load being applied through 3 mm thick plywood strips along diametrically opposite lines.

3.6 TESTING

3.6.1 Test equipment

The beams were tested under static top-loading applied hydraulically by means of a 500 tonne capacity M.A.N. testing machine and frame. The applied load was measured by a precision pendulum manometer operating a load indicator hand over a large 360^0 scale.

The test set-up and its mode of operation are illustrated in Fig.(3.2).

The beam to be tested was mounted on the travelling base beam which was then winched along rails into position under the upper load distribution beam. The height of the upper beam on the screwed columns could be adjusted by an A.C. motor. Early in the test programme particular attention was given to making the process of mounting a beam up for test a safe and speedy one-man operation. To this end special steel jigs were designed which were clamped to each end of the base beam (Fig.3.2). The jigs ensured that the test beam automatically assumed a correct alignment as it was lowered by crane onto the support reactions and provided temporary lateral support whilst the travelling base beam was being winched into position.

All the test specimens were simply supported and the support reactions were applied through 52·7 mm ($2\frac{3}{4}$ in.) diameter rollers attached to the top surface of the base beam. The rollers were free to rotate in planes both parallel and perpendicular to the axis of the trolley and each permitted a limited horizontal translation of approximately 2 mm. The

loading to the top surface of the test beam was applied through 25 mm diameter rollers sandwiched between the steel bearing plates: the upper distribution beam itself had rotational freedom about a spherical seating joint.

The deflections of a test beam were measured by three Mercer dial gauges (1 div = 0.01 mm). The gauges were attached to a rigid frame, which was clamped to the travelling base beam of the M.A.N. test frame, and operated on three right-angled brackets fixed just above the soffit of the test beam with Devcon plastic steel (Fig.3.3). The two outer gauges above the supports registered the support settlements, the average of which was used to correct the central gauge reading.

Crack widths were measured to 0.025 mm using an illuminated hand microscope of 25 magnifications.

3.6.2 Test preparation

The casting and testing programme was organised into cycles of 4 weeks of one day per week casting followed by 4 weeks of testing. Each set of beams cast together was therefore tested during week five after casting, with the result that all the beams had the similar test age of 28 days plus or minus a maximum of 2 days.

A week prior to testing, the face of each beam was painted with a thin coat of white emulsion paint to assist crack detection and measurement, and a 100 mm square reference

grid was marked on in pencil. Steel anchor blocks (100 x 75 x 25 mm), each having a central hole through which the main reinforcement bar could pass, were bedded to each end of the beam on a thin (3 mm) layer of high-alumina cement mortar. After hardening of the mortar, nuts threaded on each end of the main bar were tighten ed up with a torque spanner.

On the day prior to testing, the prepared test beam was installed into the loading frame. By using a small screw jack to raise each end of the beam in turn, steel bearing blocks (100 x 100 x 30 mm) were positively bedded to the beam at the support points on a thin layer of quick-setting gypsum plaster. Similar blocks were bedded to the concrete at the loading points by using the A.C. motor operating the upper distribution beam to apply a fractional top-loading. Finally, the right-angled brackets for deflection measurement were affixed and, following a check on the beam's position and verticality, the beam was ready for test: the lateral temporary support offered by the alignment jigs was then released.

3.6.3 Test procedures

The single cycle of loading, which was adopted, had the advantage of producing identical, simple loading histories for all the test beams. The load was applied incrementally in units of 20 kN up to collapse of the test specimen . (Note: some tests were carried out to investigate the effect of re-peated loading on deep beam behaviour; these tests are reported in Appendix 2).

After each increment of load, the deflection gauge readings were observed and recorded and, with the aid of a hand lamp and lens, the surface of the beam was inspected to detect the development of cracks. The width of each significant crack was measured on formation and its position and extent was marked on the beam surface with a thin pencil line, together with the value of the load which was written at the two extremities of the crack. Subsequent growth was similarly monitored at later load increments.

After collapse, the final crack pattern was recorded in a sketch and by photography. The beam was then removed from the test rig for storage for a minimum of five weeks, during which time the test data was processed.

C H A P T E R F O U R

LIGHTWEIGHT CONCRETE DEEP BEAMS WITH OPENINGS: PILOT STUDY

4.1 TEST PROGRAMME

4.2 TEST RESULTS

4.2.1 Crack patterns and modes of failure

4.2.2 Crack widths and deflection

4.2.3 Ultimate loads

4.3 GENERAL COMMENTS

CHAPTER FOUR

LIGHTWEIGHT CONCRETE DEEP BEAMS WITH OPENINGS: PILOT STUDY

4.1 TEST PROGRAMME

The test specimens consisted of 24 simply supported deep beams (Fig.4.1 and Table 4.1) of span L 1500 mm, overall depth D 750 mm and width (thickness) b 100 mm. Two clear shear spans x were used, giving x/D ratios of 0.4 and 0.25 respectively. The span/depth ratio L/D was kept constant at 2, because it is believed [31] that the x/D ratio is a more important parameter than the L/D ratio.

The test beams were divided into two groups: Group O beams had no web reinforcement, whilst Group M beams had a rectangular-mesh web reinforcement of 6 mm diameter deformed bars of 425 N/mm^2 yield stress, giving a total web steel ratio of 0.0048 (0.0020 vertical and 0.0028 horizontal). The longitudinal tension reinforcement consisted of one 20 mm diameter deformed bar of 430 N/mm^2 yield stress, anchored to steel blocks at the ends. Reinforcement cages were used at the support and loading points (Fig.4.1) to avoid local crushings which had been observed at these places in a previous investigation of beams without openings [31]. Lytag sintered fly-ash lightweight aggregates were used in concrete making; details of concrete strengths are given in Table (4.1).

All the web openings were rectangular and, in the Group M beams, each opening was trimmed with one loop of 6 mm

diameter deformed bar (Fig.4.1: Note 2 (ii)). The positions and sizes of the openings are indicated by reference numbers, which range from 0 to 13 and which are explained in Fig.(4.2).

The beams were tested under static two-point loading as shown in Fig.(4.1).

The general experimental details have been given in Chapter 3.

4.2 TEST RESULTS

4.2.1 Crack patterns and modes of failure.

The crack patterns at failure of all the beams are shown in Fig.(4.3), where the beam notation is as explained in the footnote to Table (4.1). The circled numbers indicate the sequence in which the oracks were observed. and the other figures, giving the load in 10 kN units, mark the extent of cracking at a particular load interval. (Note: the vertical steel supports seen at each end of a beam (Fig.4.3) served only to support the beam laterally during test preparations - see Chapter 3.6).

A study of the crack patterns revealed that the crack patterns and modes of failure depended mainly on the extent to which the opening intercepted a notational 'load-path' joining the loadbearing blocks at the support and loading point (Fig.4.4), and that the size, shape and position of an opening were significant only in so far as these affected the extent and location of such an interception. Where an opening was reasonably clear of the above-mentioned 'load-path' the crack pattern and mode of failure were

essentially those of a comparable beam without openings. For example, Beams M-O. 4/5, M-O. 4/11, O-O. 4/5, O-O. 25/5, which had openings, all collapsed following the formation and propagation of diagonal cracks, which ultimately caused the beams to be split into two approximately along a line joining the inside and outside edges of the loadbearing blocks at the support and loading point respectively. The failure mode, designated Mode 1, is shown diagrammatically in Fig.(4.5a). Previous work [27, 28] has demonstrated that this failure mode is typical of solid top-load deep beams containing little or ineffective arrangements of web reinforcement.

Where an opening intercepted the load path as shown in Fig.(4.4), the general sequence of behaviour was as follows:-

(a) The first cracks to form were those at the beam soffit and at the corners A and C of the opening (Fig. 4.4: cracks 1 and 2), which were being opened by the applied load. Corners B and D which were being closed by the applied load remained intact at this stage.

(b) As the load was increased the corner cracks 1 and 2 became wider and propagated rapidly towards the load bearing blocks. Other cracks might form in the flexural region, for example crack 7. More important was the possible formation of crack 5, which initiated from the vertical edge of the beam, and crack 6, which initiated from the top surface of the beam, as these cracks could influence later behaviour.

(c) Upon further increase in loading the diagonal cracks 8 and (or) 9 would appear. These were the dangerous cracks because they either caused the immediate collapse of the beam or led to its eventual failure; for this reason cracks 8 and 9 were referred to respectively as the 'critical lower diagonal crack' and the 'critical upper diagonal crack'. These critical diagonal cracks possessed two distinctive properties: (1) They usually formed with a definite noise and (2) they initiated not from the opening nor from the load-bearing blocks regions, but from the region between the opening and the bearing blocks where subsequently the width of the crack was at a maximum. These two properties had previously been observed to be characteristic of the critical diagonal cracking in deep beams without openings [27,28,32], and this provided evidence that the formation of the critical lower and upper diagonal cracks in the present beams was due to the same cause as that of the diagonal cracks in the previous beams without openings.

(d) The final increment in loading caused collapse in either of two distinct modes. In the first, which is designated Mode 2 (Fig.4.5b), the propagation of the critical upper diagonal crack or the sudden appearance of a new upper diagonal crack completely split the chord above the opening, along a line joining the outside edge of the bearing-block at the loading point to the outside top corner of the opening. Similar simultaneous failure of the lower chord or the widening of an existing crack resulted in the beam being split into two over its full height. In the second failure mode, designated Mode 3 (Fig.4.5c), diagonal cracking in the chord above

the opening did not occur and collapse occurred as a result of the lower critical diagonal crack splitting the lower chord into two, whilst that portion of the beam outside the opening deformed plastically with hinges at the head of cracks 1 and 5 (or possibly 6) (Fig.4.4).

Typical examples of those beams which failed in Mode 2 were Beams M-0.4/3, M-0.4/8 and M-0.4/12, and in Mode 3, Beams M-0.4/9, M-0.4/13, O 0.4/4 and O-0.25/4 (Fig.4.3).

4.2.2 Crack widths and deflection

The maximum crack widths of the beams are shown in Fig.(4.6), where the beam notation is as explained in the footnote to Table (4.1). The maximum crack width in each beam was generally recorded across a corner crack close by the opening. An illustrative example of the behaviour of crack widths under increasing load is given in Fig.(4.7), which depicts the behaviour observed in Beam M-0.4/4. The flexural cracks in the central region of the beam were rarely found to exceed 0.2 mm, whilst the corner cracks frequently grew to exceed 1.0 mm before the instant of collapse. At collapse, the critical diagonal cracks became the widest and the corner cracks frequently closed up.

It was found that each group of beams could be divided into sub-groups according to the maximum crack widths. For example, the Group M beams in Fig.(4.6a) could be divided into:

Sub-group M1: comprising beams M-0.4/0, M-0.4/1, M-0.4/5 and M-0.4/11,

Sub-group M2: comprising Beams M-0.4/12, M-0.4/8, M-0.4/4, M-0.4/3 and M-0.4/2,

and

Sub-group M3: comprising Beams M-0.4/13, M-0.4/10, M-0.4/9 and M-0.4/6.

Maximum crack widths were smallest in sub-group M1, in which the beams either had no web openings or had openings which were reasonably clear of the 'load path'; they were widest in sub-group M3, in which the openings seriously interrupted the 'load path'. An examination of Fig.(4.6a) in conjunction with Table (4.2) shows further that openings which resulted in low ultimate loads also resulted in large maximum crack widths.

A study of Fig.(4.6b) shows that the above observations on the effects of the openings applied equally to the beams in Group O, which had no web reinforcement. A comparison of the crack widths in Fig.(4.6a) with those in the top part of Fig.(4.6b) shows that, in beams having the same type of openings, the web reinforcement was highly effective in controlling maximum crack widths. This may be demonstrated further by a comparison of Figs.(4.7) and (4.8), which depict the behaviour under increasing load of Beams M-0.4/4 and O-0.4/4 respectively. It is evident that, whilst the web reinforcement predictably had little effect on the load at which the corner cracks appeared, significant control was subsequently exercised over the width of the corner cracks and also as a consequence over the width of the horizontal edge cracks.

In Fig.(4.9), the average crack widths of the beams are presented. For the purpose of Fig.(4.9), the average crack widths were taken to be the average of the four widest cracks, which, in general, were the four corner cracks in each beam. It is, therefore, perhaps not surprising that it was found that the above observations concerning maximum crack widths were equally applicable to such average crack widths. However, this result serves to demonstrate the symmetrical behaviour of the beams.

The effect of the openings on deflection was found to be similar to their effect on crack widths, though less pronounced. The deflections of the beams, as shown in Fig. (4.10), were generally small, being only of the order of 1 or 2 mm (1/1500 to 1/750 of the span) at 60 per cent ultimate load. Examination of Fig.(4.10), in conjunction with Fig.(4.6) and (4.9), revealed that the deflection plot for each beam roughly parallelled the corresponding maximum and average crack widths plots, and indicated that shear deflection, resulting from the formation of corner cracks and at later load stages, diagonal cracks, was more significant than flexural deflection. It was also evident that prior to cracking (Fig.4.10: load 60 to 100 kN), the openings had relatively little effect on the stiffness of the beams.

4.2.3 Ultimate loads

The measured ultimate loads of all the beams, W_1, are presented in Table (4.2). In the right hand column of Table (4.2), the ratio (W_1/W_0) gives the ratio of the ultimate

load of a beam with openings to that of the similar beam without openings. It may be seen that, in Beams M-0.4/1, M-0.4/11, M-0.4/12 and in those beams with opening Type 5, the reductions in ultimate load were quite small, the ratio (W_1/W_0) being greater than 0.8. However, serious reductions occurred in the remaining beamsand in particular those beams with opening Type 6, where the ratio W_1/W_0 was less than 0.5.

Thetest results have indicated that the effect of an opening on the ultimate strength depended on the extent to which it interrupted the 'load path' joining the bearing blocks at the loading and reaction points. For those beams in which the openings were reasonably clear of the 'load path' the ultimate loads were high and comparable to that achieved by a beam without openings. Indeed, as noted earlier, the failure modes of these beams were essentially similar and were in fact as described previously for beams without openings [27, 28]. Where the opening completely interrupted the 'load path', the lowest ultimate strengths occurred, and with reference to Fig.(4.3), it may be seen that these beams collapsed in failure Mode 3 (Fig.4.5c).

It would seem that, in the beams tested here, most of the applied load was transmitted directly from the loading point along the 'load path'. If this path was intercepted by an opening, the reduction in ultimate strength would depend on whether this load path could be successfully rerouted, along the paths ABC and AEC in Fig (4.11) When the forces in BC and AE reached sufficiently high values the lower and upper critical diagonal cracks would occur.

For a given applied load the forces in AE and BC depended on the angles which were made with the horizontal, i.e., the angles $\emptyset'$ and $\emptyset$ in Fig.(4.11), which, in turn, depended on the size and location of the opening. It is, therefore, reasonable to expect the ultimate load carrying capacity of the beam to depend on the locations of corners B and E of the opening. Table (4.2) shows that, where the locations were such that the angles $\emptyset$ and $\emptyset'$ were little different from the inclination of the critical diagonal crack of a beam without openings, the ultimate load was high; for example, Beam M-0.4/12 (520 kN). The lower ultimate loads in Table (4.2) were recorded for those beams in which an upper diagonal crack did not occur. With reference to Fig.(4.11), it may be seen that the upper path AEC would be comparatively ineffective, because a substantial tensile force EE' would be required except when the angle $\emptyset'$ between AE and EE was large. In these beams the capacity was mainly dependent on the effectiveness of the lower path ABC, and when the 'strut' BC failed as a result of the propagation of the lower critical diagonal crack collapse occurred by Mode 3 (Fig.4.5).

The amount of web reinforcement provided in Group M beams was found to have an effect on the ultimate strength of only certain beams. Comparison of the ultimate loads of the Group M beams with similar beams in Group O (Table 4.2) shows that where the beams were without openings or where the openings were reasonably clear of the 'load-path' (as in Beams M-0.4/5 and O-0.4/5 for example) the web reinforcement had little effect on ultimate strengths. However, where the

openings intercepted the 'load path' (as in Beam M-0.4/6 and 0-0.4/6) the effect of the web reinforcement was to significantly increase the ultimate strength. In beams such as M-0.4/6 the lower path was clearly not highly effective (Fig.4.3): the effect of the web reinforcement was therefore to provide a horizontal tensile capacity along EE', and increase the capacity of the upper path and hence the ultimate capacity of the beam. Again, comparison of the ultimate loads of Beam M-0.4/4 (Table 4.2: 450 kN) and Beam 0-0.4/4 (Table 4.2: 340 kN) shows a similar result, and with reference to Fig.(4.3) it may also be seen that the web reinforcement caused a change in the failure mode. Hence, it seemed likely that the effects of web reinforcement could be more important in deep beams with openings than in deep beams without. However, the type and amount of reinforcement provided had little effect on the growth of the critical diagonal cracks, which were the prime cause of collapse in all three failure modes (Fig.4.5). Therefore, on the basis of the pilot test results it was concluded that, in general, the web reinforcement provided had little effect on ultimate strengths.

4.3 GENERAL COMMENTS

It is noted that discussions of the experimental results of the pilot tests have also been presented elsewhere [35], and that certain of the deductions then reported [35] have since been developed in the light of further testing. Further analysis of the results of pilot tests is therefore deferred, here, until after the presentation of the results of the follow-up tests in both lightweight concrete (Chapter 5)

and normal weight concrete (Chapter 6), where in Chapter 7 a structural idealization of deep beams with openings is argued from a basis of all the test data.

However, it would be useful and interesting to illustrate the developing nature of the investigation and, in what follows, a brief description of the previously proposed method of analysis [35] and a list of the previously reported conclusions [35] is given.

It was suggested that the following equations offered a simple means of calculating the ultimate shear strength of reinforced concrete deep beams with web openings:-

$$Q_{ult} = C_1 \left(1 - 0.35 \frac{x}{D}\right) f_t \, bD + C_2 \sum A \frac{y}{D} \sin^2\alpha \qquad (4.1)$$

$$Q_{ult} = C_1 \left(1 - 0.35 \frac{k_1 x}{k_2 D}\right) f_t \, b \, k_2 \, D + C_2 \sum A \frac{y}{D} \sin^2\alpha \qquad (4.2)$$

in which the notation is as explained in Fig.(4.12).

Eqn.(4.1) is the equation derived from the results of earlier tests at Nottingham of deep beams without openings (cf.Chapter 1.2.2.4). On the basis of the pilot test results, it was argued that this equation could be used for estimating the ultimate strength of deep beams, which had openings that were clear of the 'load path' joining the loading point and support. Where an opening intercepted the load path, an approximate estimate of the ultimate strength might then be made using Eqn.(4.2), which was based on the proposition that the lower load path ABC was the primary path and that the web reinforcement in deep beams both with and without openings

had similar functions. Hence, the first term of Eqn.(4.1) which estimates the concrete contribution was modified by the factors $k_1 x$ and $k_2 D$ to give the capacity of the lower chord, whilst the second term, the reinforcement contribution, was left unchanged.

The main conclusions from the test results were then as follows:-

(i) The effect of an opening on the ultimate shear strength depends primarily on the extent to which it intercepts the 'load path' joining the load bearing blocks at the loading point and the support reaction point and on the location at which this interception occurs.

(ii) Where an opening is reasonably clear of the 'load path', the ultimate shear strength may be computed as for a beam without openings using Eqn.(4.1) above.

(iii) Where the opening intercepts the 'load path' the ultimate shear strength may be calculated using Eqn.(4.2).

(iv) Web reinforcement of the type and amount provided can be effective in controlling crack widths but its contribution to the ultimate strength is not as important.

(v) Trimming the openings with reinforcement loops has no beneficial effect on ultimate shear strengths.

C H A P T E R F I V E

LIGHTWEIGHT CONCRETE DEEP BEAMS WITH OPENINGS: FURTHER TESTS.

5.1 INTRODUCTION

5.2 TEST PROGRAMME

5.3 TEST RESULTS

5.3.1 Crack Patterns and modes of failure

5.3.2 Crackwidths and deflection.

5.3.3 Ultimate loads.

C H A P T E R F I V E

LIGHTWEIGHT CONCRETE DEEP BEAMS WITH OPENINGS: FURTHER TESTS

5.1 INTRODUCTION

Since it was thought that the results and conclusions of the pilot study had potential applications in deep beam design where openings had to be provided for access or for services, and since the design of such beams was not yet covered by the major codes of practice, a further study including tests on 39 beams was carried out. The purpose of the tests was to provide further data to establish the behaviour and failure modes of deep beams with web openings, and in particular the tests had four specific aims. The first aim was to check the validity of Conclusion No.1 of the pilot study (Chpt.4.2.4), using a series of beams in which the position and size of the openings were systematically varied. Secondly, the pilot tests had shown that in a deep beam with web openings, there could be two critical diagonal cracks (lower and upper) as against only one in a deep beam without openings; therefore the mere inclusion of the parameters k_1 and k_2 to modify Eqn.(4.1) into Eqn.(4.2) needed further examination, particularly as there was an ambiguity regarding the value of α (Eqn.4.2) which depended on the direction assumed for the critical diagonal crack. Thirdly, the type and amount of web steel used in the pilot study failed to provide information on the function of such steel and hence failed to provide guidelines for the proper design of the web steel. Fourthly, Conclusion No.5 was unexpected and merited confirmation.

5.2. TEST PROGRAMME

The test specimens were designed to complement those in the pilot study, and consisted of 39 simply supported lightweight concrete deep beams (Fig.5.1 and Table 5.1). Thirty-six of the beams, of which four were duplicate specimens to test repeatability (see Beam notation; Table 5.1), were of overall depth D 750 mm, width b 100 mm, with span lengths L of 1125 mm and 750 mm, giving L/D ratios of 1.5 and 1 respectively. Similarly, two clear-shear span distances x were used, giving x/D ratios of 0.3 and 0.2 respectively. The other three beams (prefix WM; see Beam notation, Table 5.1). were manufactured from Imperial sized moulds, giving b 76 mm (3"), D 762 mm (30"), L 1524 mm (60"), and L/D and x/D ratios of 2 and 0.4 respectively.

The test beams were divided into two groups: the Group O beams had no web reinforcement while the Group W beams incorporated seven special types of web reinforcement (Fig.5.1; Type W1 to W7) and a uniform orthogonal mesh type of reinforcement (Fig.5.1; Type WM). The seven special types of reinforcement each consisted of 10 mm diameter deformed bars of 460 N/mm^2 yield strength and the web steel ratio * was as near as possible constant at 1.2 per cent (Table 5.1) so that the weight of the web steel in each of these beams was very nearly the same.

The Type WM reinforcement consisted of a mesh of 6 mm diameter deformed bars in each face, giving a web steel ratio of 1.13 per cent (0.38% vertical and 0.75% horizontal); in addition, beam prefixed WM' contained a single loop in each face of 6 mm

---

* The web steel ratio p_{web} was calculated as the ratio (volume of steel)/(volume of concrete)

diameter deformed bar around each opening. The main longitudinal steel in each beam consisted of one 20 mm diameter deformed bar of 430 N/mm^2 yield strength, anchored to external steel blocks at the ends (Fig.5.1). Lytag sintered fly-ash lightweight aggregates were again used in concrete making; details of the concrete strengths are given in Table (5.1).

The positions and sizes of the web openings complemented those in the pilot study, and are indicated by reference numbers ranging from 0 to 18 as explained in Fig.(5.2). Briefly, in openings referenced 0 to 16, the size of an opening is given by a_1 x by a_2D, where the height factor a_2 was kept constant at 0.2 but the breadth factor a_1 varied by increments from 0.3 to 1.5. As illustrated clearly in Fig.(5.4), where the notation is as explained in the footnote to Table (5.1), the centroids of opening 1 to 10 were at mid-depth of the beam; those of openings 11. 12 and 13 were at 175 mm from the beam top, while those of 14, 15 and 16 at 175 mm from the beam soffit. Opening reference number 17 was used in the next series of tests using normal weight concrete specimens. Opening reference number 18 was located at the centre of the shear span at mid-depth. with both a_1 and a_2 equal to 0.25.

In the pilot study, all of the beams were tested under two-point loading; in the present investigation 35 of the beams were also tested this way. However, in practice the distributed load condition is a common one for deep beams; and, as a crude but convenient approximation for this condition, four-point top loading (Fig.5.3) was used for four of the beams, to give some indication of whether the conclusions drawn from

tests using two-point loading could be broadly applicable to the uniformly distributed load condition.

5.3 TEST RESULTS

5.3.1 Crack patterns and modes of failure.

The crack patterns at failure of the Group 0 beams without web reinforcement are shown in Fig.(5.4a) and (5.4b).

The present tests broadly confirmed the observations recorded in the pilot study and in particular provided further evidence to substantiate the observation that, the effect of an opening on the behaviour of a deep beam was mainly dependent of the extent to which the opening intercepted the 'load path' between the load bearing blocks at the support and loading point.

As in the pilot tests, the present tests have shown that, where the opening was clear of the load path the failure mode remained essentially that of a comparable solid deep beam: a comparison of the crack patterns of beams 0-0.3/0, 0-0.3/12 and 0-0.3/14 clearly shows that in each beam the failure plane was defined by the positions of the load bearing blocks at the support and loading point and was unaffected by the presence of an opening (cf.Chapter 4: Fig.4,5a; failure Mode 1). Where an opening intercepted the load path the typical sequence of crack formation was again basically that described in the pilot tests, but from a study of the crack patterns at failure of the beams in the present tests, clear trends in ultimate be-

haviour now became obvious. Examination of the crack patterns of Beams 0-0.3/1, 0-0.3/2, 0-0.3/3 and 0-0.3/4 (Fig.5.4a), shows that as the horizontal dimension of the opening was increased, effecting an increased interception to the load path, the diagonal failure planes which occurred in the chords above and below the opening were consistently defined by the corners of the opening, until in Beam 0-0.3/4 the upper failure plane ceased to occur. It is therefore evident that failure Mode 2, which was described in Chapter 4 and of which Beam 0-0.3/2 (Fig.5.4) is a typical example, would occur only in those beams - without web reinforcement - in which the opening intercepted the load path from the interior of the beam: that is, for large values of angle $\emptyset'$ (Fig.4.11). In the majority of the beams the failure mode was found to be Mode 3 (Chapter 4:Fig.4.5) and it occurred not only in those beams in which the opening completely intercepted the load path, for example, beams with openings Types 4, 13, 16 (Fig.5.2), but also for any beam in which the opening encroached into the load path from the support side of the beam, as for example, in Beam 0-0.3/7 (Fig.5.4). Hence, the crack patterns of Beams 0-0.3/7, 0-0.3/8, 0-0.3/9, 0-0.3/4 and 0-0.3/10 were sensibly similar and were unaffected by changes in the size of the opening.

In Fig.(5.4d) the crack patterns at failure of Beams 0-0.3/2R, 0-0.3/3R, 0-0.3/4R and 0-0.3/5R are presented: these beams were duplicates of Beams 0-0.3/2, 0-0.3/3 etc. A comparison of the crack patterns recorded for the two sets of beams would not immediately suggest any great differences in behaviour. However, it was found that the ultimate loads of the beams in a similar pair coulddiffer by an amount which

seemed greater than that which might typically be the result of the effects of normal experimental scatter and the small measured differences in concrete strengths (Table 5.1): for example, the difference in ultimate load between Beam 0-0.3/4 (Table (5.2); 260 kN) and Beam 0-0.3/4R (215 kN) would have been more reasonably expected. In the other pairs of beams the difference in ultimate load could be as large as 50% (Table 5.2). In beams without web reinforcement it would seem that the regions above and below the openings are very susceptible to diagonal cracking, and that if a diagonal crack occurred at an early load, the ultimate load would be reduced. The results would indicate that the formation of the early corner cracks had an influence on the diagonal cracking load: in beams where the lower corner crack (Fig.4.4 crack 2) propagated sufficiently rapidly, the critical lower diagonal crack (Fig.4.4: crack 8) would form at a very late stage, or might not form until the collapse load was reached. This happened for example in Beam 0-0.3/2 as compared with beam 0-0.3/2R. Also, the early formation of an extensive flexural-shear crack near to the support reaction point (Fig.4.4: crack 4) was likely to inhibit the formation of the critical lower diagonal crack and hence increase the ultimate strength of the beam. This happened, for example, in Beam 0-0.3/5R as compared with 0-0.3/5.

As pointed out earlier, the pilot tests did not show how the web reinforcement should be most effectively arranged. The present tests have yielded useful information on this point. Fig.(5.4c) shows the crack patterns at failure of the Group W beams which incorporated the seven types of web reinforcement as described in Fig.(5.1). The sequence of early

behaviour in these beams was in general similar, and was comparable to Beam O-O.3/4, which had no web reinforcement; that is, the formation of cracks at the corners (Fig.4.4 cracks 1 and 2) was followed by cracks 3, 4 and 7 (Fig.4.4).

The effect of the different types of web reinforcement on later behaviour and on the failure modes will be more fully discussed in the section on 'Ultimate Loads'. Suffice to say, here, that where the web reinforcement was wholly below the opening (as in Beam W1-O.3/4) or wholly above the opening (as in Beam W2-O.3/4) the consequent failure modes resulted in only moderate increases in ultimate load. The trimming of an opening by surrounding it with several loops of reinforcement (Beam W5-O.3/4) only served to locally control the propagation of the corner cracks without being able to control that of the critical diagonal cracks - in fact such trimming resulted in a rather low ultimate strength and the failure mode was little different from that of a beam with no web reinforcement. However, the inclined web reinforcement in Beam W4-O.3/4, and particularly that in Beam W6-O.3/4, most effectively restrained the width of the critical diagonal cracks so that they remained narrow up to the instant of collapse. The crack pattern for Beam W6-O.3/4 clearly shows that the collapse was due to failure of that portion of the beam outside the support reaction point; also, there were fairly wide flexural cracks near the midspan. This is evidence that the inclined web reinforcement effectively protected the diagonal cracking region above and below the web opening so that the final failure of the beam had to occur by a different mode, and the result was an outstandingly high ultimate load.

The crack patterns at failure of the beams with the commonly used orthogonal mesh type reinforcement are shown diagrammatically in Fig.(5.4e). (Note: the photographic record of these beams was unfortunately destroyed in processing). The failure mode of the beam without openings was typical of similar beams which have been reported elsewhere [28]. The crack patterns of the two beams with openings were nearly identical and again it is clear that the loops of reinforcement trimming the openings in Beam WM' - 0.4/4 had little effect on ultimate behaviour. More important, it is apparent from the failure mode that the reinforcement had only moderate effect on the control of the upper and lower critical diagonal cracks.

5.3.2 Crack widths and deflection

The maximum crackwidths for the Group 0 beams are presented in Fig.(5.5) and the results confirm the conclusion drawn from the pilot tests, namely, that the maximum crack-widths increased with the extent to which the web opening intercepted the 'load path'. For example, Fig.(5.5a) illustrates clearly how the progressive increases in the extent of such interception led to progressive increases in maximum crack width.

Some new observations are presented in Fig.(5.5c), which shows the crack widths of the four beams with L/D= 1 and x/D = 0.2: Beams 0-0.2/0, 0-0.2/4, 0-0.2/13 and 0-0.2/16. It can be seen that opening No.16 led to the widest crack width, No.4 the second widest, followed by No.13 and No.0. This agreed with the results from Beams 0-0.3/16, 0-0.3/4, 0-0.3/13

and 0-0.3/0, in which L/D = 1.5 and x/D = 0.3. In the pilot study only a single L/D ratio of 2 was used and it was not then possible to say whether the conclusion referred to above would not be affected by a change in the L/D ratio. The present tests have shown that it is unlikely to be so affected. The pilot tests and the present tests together covered L/D ratios of 1, 1.5 and 2; in deep beams the L/D ratio usually lies within the range 1 to 3.

Fig.(5.5d) shows the effects of different types of web reinforcement on maximum crack widths. The crack width curves are drawn against a grid mesh of 0.3 mm unit width. This represents a limit state for maximum crack-width commonly accepted in design, and it can be seen that this limiting width was quickly exceeded in Beams W1-0.3/4, W2-0.3/4 and, particularly, in Beam W5-0.3/4 where the web steel was used to surround the opening. The inclined web reinforcement in Beam W6-0.3/4, however, not only substantially increased the ultimate strength but also effectively restrained the crack width so that the 0.3 mm limit was not exceeded until the applied load reached 580 kN, and, as was noted earlier, the widest cracks were not diagonal cracks but flexural cracks at mid-span. The combined vertical horizontal system in W7-0.3/4 was also effective; the vertical bars restrained the lower and upper diagonal cracks (Fig.4.4: crack 8 and 9), while the horizontal bars restrained the corner cracks (Fig.4.4: crack 1 and 2). Similarly, the combined inclined-horizontal system in Beam 4-0.3/4 was also effective.

Fig.(5.5e) also shows the four beams with suffix A

which were tested under four-point loading to simulate a uniformly distributed load condition; apart from the difference in loading, Beam W1/(A) was identical to Beam W1-0.3/4, Beam W3(A) to Beam W3-0.3/4, and so on. The figure shows that the behaviour of Beam W7(A) and that of Beam W7-0.3/4, were remarkably similar; this was true of Beams W4(A) and W4-0.3/4, and also of W3(A) and W3-0.3/4. Beams W1(A) and W1-0.3/4 formed the exceptional pair and hence it would seem from the other results, that the effect of loading condition becomes less important for beams with effective arrangements of reinforcement. Judging from the results of the latter mentioned beams, it may be deduced that, in fact, as far as crack widths were concerned the four-point loading system was a less severe form of loading, possibly as a result of the better distribution of the load obtained around the opening.

The maximum crack widths of the three beams containing the uniform mesh reinforcement (Fig.5.1 Type WM) are shown in Fig.(5.5f). In the pilot study it was found that the amount of mesh reinforcement used in the pilot test beams (Table 4.1; .48%) was insufficient to control the width of diagonal cracks. The present tests have shown that at least 1.0% web reinforcement is required to make any significant effect. For example, in Beam M-0.4/0 the 0.3 mm limit on crack width was exceeded at 50% ultimate load (Fig.4.6a) whereas in Beam WM-0.4/0 the limit was not exceeded until 85% ultimate load. The mesh reinforcement, however, was not so effective in controlling the crack widths in the beams with openings (Fig.5.5f: Beams WM' - 0.4/18 and WM-0.4/18): the limit of 0.3 mm was exceeded at 60% ultimate load.

The behaviour of the beams as measured by central deflection is illustrated in Fig.(5.6). As in the pilot study the effect of openings on deflection was found to be similar to their effect on crack widths, and a comparison of Fig.(5.5) with Fig.(5.6) shows again that the deflections were a result primarily of the effects of cracking within the shear spans. Examination of Fig.(5.6d) showed the effect of the different types of reinforcement on deflection and it was noticeable that the deflection plot for Beam W6-0.3/4, which had inclined web reinforcement, was particularly linear up to 650 kN: this provided a further indication of the ability of this type of reinforcement to control crack widths within the shear span. After approximately 650 kN, the flexural crack widths and the deflection resulting from flexural beam behaviour, increased more rapidly until collapse of the beam.

5.2.3 Ultimate Loads

The measured ultimate loads of all of the beams are presented in Table (5.2). The results of the Group O beams broadly confirmed the deduction made from the pilot test results; namely, that the effect of a web opening on the ultimate strength of a deep beam depends primarily on where and by how much it intercepts the 'load path' joining the load bearing blocks at the loading point and the support reaction point.

Where the opening was clear of the load path, for example, in Beams O-0.3/12 and O-0.3/14 (Fig.5.4b), the ultimate loads (Table 5.2; 560 kN each) were comparable to that

of the beam without openings, Beam O-0.3/O (595 kN). A close examination of the crack patterns at failure of these three beams shows that the openings were located either in regions which remained uncracked in the solid beam (as in the case of opening No.12), or in regions where inclined flexure-shear cracks originated from the beam soffit (as in the case of opening No.14). The only significant effect opening No.14 had on the crack pattern, was to reduce the load at which the inclined flexure-shear cracking developed; that is the corner cracks numbered 1 and 3 of Beam O-0.3/14 (Fig.5.4) had a similar secondary effect on the ultimate load and behaviour as the inclined flexure-shear crack numbered 6 of the solid beam, O-0.3/O. The results of numerous previous tests [11, 12] of solid deep beams have indicated that this type of cracking has indeed little effect on ultimate strength, unless, the proportion of main steel is so small that as a result, a flexure-shear type failure mode occurs similar to that reported by de Paiva [24].

Where the opening intercepted the load path, the crack pattern typical of a solid deep beam was no longer obtained and as a result significant reductions in ultimate load were then recorded. A study of the drack patterns at failure (Fig.5.4) in conjunction with the ultimate loads (Table 5.2) showed that the amount of interception required to cause some reduction was quite small. Fig.(5.7a), in which the ultimate loads are shown against the opening breadth factor a_1 (Fig.5.2), gives an idea of the way in which the ultimate load reduced as the opening size increased, from

opening type 1 through opening types 2,3,4,5 to 6 (Fig.5.4), to effect a greater interception of the load path. Similarly, opening type 7 through types 8,9, 4 to type 10, which were increasing in breadth from the support side of the beam (Fig. 5.4), caused progressive reductions in the ultimate loads as illustrated in Fig.(5.7b). It is worth mentioning that these figures serve only to indicate the trends: indeed, the post-cracking behaviour of the beams was so complex that it would be difficult to isolate uniquely the particular effect of particular geometrical parameters on the ultimate load. However, a simple structural idealization was found which did offer a useful understanding and visualization of the load transfer mechanism in deep beams with openings and gave reasonable predictions of their ultimate strengths. The idealization will be explained in Chapter 7 after the results of all the tests have been presented; as mentioned in Chapter 4, the idealization was a development of the method of anal ysis tentatively proposed on the basis of the results of the pilot tests.

The tests on the Group O beams provided useful information on the behaviour of deep beams with web openings in circumstances that were not complicated by the effects of web reinforcement. The Group W beams, which contained web reinforcement. yielded further complementary information and demonstrated that the effects of web reinforcement on ultimate strength could be substantial. For example, the inclined type web reinforcement increased the ultimate strength of Beam W6-0.3/4 to 825 kN (Table 5.2), as compared with the ultimate strength of 260 kN for Beam O-0.3/4 which had no web reinforcement.

As has been mentioned earlier, the tests on beams without web reinforcement have shown that there are two vulnerable regions to be protected by web reinforcement: one above and one below the opening. The measured ultimate loads in Table (5.2), studied in conjunction with the web steel details in Fig.(5.1), and the crack patterns in Fig. (5.4c), show that:

(a) Where the web reinforcement protected only the lower region (Fig.5.1: Type W1) or only the upper region (Type W2) or where it was used to trim the opening (Type W5), the ultimate loads were low - Table (5.2): Beam W1-0.3/4 (400 kN), Beam W2-0.3/4 (490 kN); Beam W5-0.3/4 (370 kN).

(b) Where the reinforcement protected both the upper and lower regions, as in Beams W4-0.3/4 (660 kN), W6-0.3/4 (825 kN) and W7-0.3/4 (630 kN), the ultimate loads were much higher - higher in fact than that of the solid beam 0-0.3/0 (595 kN).

(c) Web steel was most efficiently used in the form of Type W6 inclined web reinforcement. The Group W beams each had the same amount of web steel, but the ultimate load of Beam W6-0.3/4 was much higher than those of the others.

(d) The failure of Beams W6-0.3/4 and W4-0.3/4 was the result of tensile failure of the concrete outside the shear span and hence the shear capacity of the web reinforcement was not in fact achieved. (Fig.(5.3) shows the result of maintaining the applied load after the onset of serious breakdown in the region above the support and it can be seen that the failure was a result of splitting along the line of anchorage hooks

of the reinforcement. In contrast, Fig.(5.9) shows the effect of maintaining the applied load on Beam W7-0.3/4 and it is clear that the failure was within the shear span and was a consequence of loss of anchorage to the vertical bars of the reinforcement system. Fig.(5.10) of Beam W5-0.3/4 shows that the web reinforcement Type W5 was totally ineffective because of its inability to distribute the load into adjacent region of the beam, and the distortion of the opening due to shear is clearly visible.

(e) The web reinforcement Type W3 effected a useful increase in ultimate load mainly as a result of controlling the corner cracks and hence changing the failure mode from Mode 3 to Mode 2 (Fig.4.5).

(f) The effects of the loading condition, that is whether two point or four point, were insignificant compared with the effects of the relative positions of the openings and the effects of web reinforcement. It would seem from the present test results, that for a uniformly distributed load the assumption of a statically equivalent two point loading system would be a safe one.

(g) It was noted earlier that as a result of the susceptability to diagonal cracking, the duplicate sets of beams without reinforcement had significant differences in the measured ultimate load. Following on from (f) above, if it is tentatively assumed that the difference in loading condition had very little effect, then it would be seen by comparing the results of say, Beam W4(A) with Beam W4-0.3/4, and so on (Table 5.2),

that the web reinforcement acted to produce much more reliable and consistent results. This point is amplified further by a comparison of the ultimate load of Beam WM-0.4/4 and Beam WM'- 0.4/4; as mentioned previously their ultimate loads were identical.

(h) One final point concerning the effect of web reinforcement on deep beams without openings. In the pilot study, as mentioned previously, the amount of web reinforcement then provided was found to have little effect on ultimate loads. Beam WM-0.4/0 in the present tests and Beam M-0.4/0 of the pilot study differed primarily in as much that the beam thickness of the former beam was 25% less but contained approximately 0.5% additional web reinforcement (Table 4.1 and 5.1). The ultimate load recorded for both beams being the same would indicate that significant savings in concrete costs and self weight might be gained by the provision of a relatively small, additional quantity of web reinforcement. As will be seen in the next Chapter, the use of an inclined arrangement of web reinforcement could result in much greater benefits still.

C H A P T E R S I X

NORMAL WEIGHT CONCRETE DEEP BEAMS WITH WEB OPENINGS

6.1 INTRODUCTION

6.2 TEST PROGRAMME

6.3 TEST RESULTS

6.3.1 Crack patterns and modes of failure

6.3.2 Crack widths and deflection

6.3.3 Ultimate loads

C H A P T E R S I X

NORMAL WEIGHT CONCRETE DEEP BEAMS WITH WEB OPENINGS

INTRODUCTION

A third test programme was carried out to investigate the behaviour of normal weight reinforced concrete deep beams with web openings and to determine the general effectiveness of the inclined system of web reinforcement.

In studies of previous test results, significant differences have been reported [27, 28] between the behaviour of lightweight concrete and normal weight concrete deep beams. However, in these previous studies the data available consisted of normal weight beams reinforced with plain round bars and lightweight beams reinforced with deformed bars. Hence, it is not clear whether the reported differences in behaviour were actually due to concrete type or to reinforcement type.

The effectiveness of an inclined arrangement of web reinforcement in deep beams with web opening was demonstrated in the lightweight deep beam tests reported earlier in this thesis. Only a single type of opening was then considered, and it was therefore desirable to test the behaviour of deep beams with inclined reinforcement, for a number of different opening locations.

In this chapter the results of the tests on normal weight concrete deep beams are presented, and whenever

possible their performance is discussed in relation to the lightweight test specimens.

6.2 TEST PROGRAMME

The test specimens were designed to complement those used in the lightweight concrete test programmes, and comprised 16 simply supported normal weight concrete deep beams (Fig.6.1 and Table 6.1) of overall depth D 750 mm and width b 100 mm. A single span length L of 1125 mm and a single clear shear span length x of 225 mm were used, giving L/D and x/D ratios of 1.5 and 0.3 respectively.

Nine of the tests specimens were repeats of nine of the lightweight concrete beams. These beams are designated as their lightweight twins but have been given an additional prefix N to discriminate between the two types of concrete. Hence, for example, Beam NO-0.3/4 in normal weight concrete - like Beam O-0.3/4 in lightweight concrete - contained no web reinforcement and opening reference No.4 (Fig.5.2). All of the lightweight beams with the special types of web reinforcement (Fig.5.1) were repeated together with the solid beam and the beam mentioned above, both of which contained no web reinforcement.

The other seven beams all contained the same inclined pattern of web reinforcement; one beam was a control beam and had no openings, the others each contained openings as shown in Fig.(6.2b) and explained in Fig.(5.2). The web reinforcement in each of these beams consisted of 6 mm diameter deformed bars of 425 N/mm^2 yield stress, arranged

in each face at 30° to the horizontal and at a uniform horizontal spacing of 125 mm (Fig.6.1: web reinforcement type 6A). Reinforcement bars that were in line with the openings were ommitted, so that the total web steel ratio for each beam varied slightly and was in a range 0.0049 to 0.0065 (Table 6.1).

Details of the concrete mix and other general experimental details are given in Chapter 3. Details of the concrete strengths for each beam are given in Table (6.1).

6.2 TEST RESULTS

6.2.1 Crack patterns and modes of failure.

The crack patterns at failure of all the normal weight beams are presented in Fig.(6.2).

A comparison of the similar beams in normal weight and lightweight concrete (Fig.6.2a and 5.4a & c) showed that the crack pattern and mode of failure were little affected by concrete type - in fact the crack patterns of each pair of similar beams were near identical. In general it was found that the cracking in the normal weight beams occurred at only slightly higher applied loads.

The crack patterns at failure of the series of beams containing the type W6A inclined web reinforcement (Fig.6.2b) showed that the reinforcement provided was effective in controlling the propagation of the corner cracks (Fig. 4.4 crack types 1 and 2), so that the failure mode of each beam was similar and was typically Mode 2 as described in

Chapter 4 (Fig.4.5). More important the web reinforcement protected the vulnerable regions above and below the opening and acted to control the width and propagation of the critical diagonal cracks with the result that high ultimate loads were achieved in all of the beams. It is clear from a comparison of the crack patterns at failure of Beams NW6-0.3/4 and NW6A-0.3/4 that the amount of Type W6A reinforcement could be increased to effectively prevent the diagonal failure mode. In Beam NW6-0.3/4 the web steel ratio (Table 6.1) was 1.25% compared to 0.47% in the latter mentioned beam and, as in the case of the lightweight concrete specimens, collapse in beams containing this greater quantity of inclined web reinforcement followed as a result of failure outside the shear span.

A comparison of the crack patterns at failure of the two solid beams NO-0.3/0 and NW6A-0.3/0 revealed some interesting information on the behaviour of deep beams without openings. It has been argued recently that web reinforcement has only limited effect on the behaviour of deep beams (CIRIA guide [9] 1977). However, the evidence of these two tests, which will be discussed more fully in the Section on 'Ultimate Loads', would support results of previous investigations [27, 28, 29], which have reported the benefits of inclined web reinforcement.

6.2.2 Crack widths and deflections

It was found that the effect of web reinforcement on the crack widths in normal weight concrete deep beams with web openings was similar to that in the lightweight concrete

specimens. It may be seen (Fig.6.3a) that, of the special types of reinforcement the inclined web reinforcement, Type W6 again produced the most effective control over crack widths: the 0.3 mm maximum crack width limit was not exceeded until approximately 650 kN and as in the similar lightweight beam of the previous tests the maximum crack width was again in fact on a flexural crack. Examination of Fig.(5.5d) in conjunction with Fig.(6.3a) showed that the difference in cracking behaviour, between similar beams of lightweight and normal weight concrete, was not significant: in general the lightweight beams reached the 0.3 mm crack width slightly earlier than the normal weight beams. This similarity between the behaviour of the two types of concrete is evidence that the effects of the reinforcement predominate.

The effectiveness of the Type W6A web reinforcement is demonstrated clearly in Fig.(6.3b). It is to be noted that the 0.3 mm limit for each beam containing the smaller openings was not exceeded for applied loads up to approximately 500 kN and in several of the beams the applied load at this serviceability limit state of cracking was considerably greater than the collapse load of the solid Beam NO-0.3/0. As mentioned earlier, it is also clear that the amount of web reinforcement provided is a major factor in controlling beam behaviour: the performance of Beam NW6-0.3/4 with 1.25% inclined steel was far superior to Beam NW6A-0.3/4 with 0.47% inclined web steel (Fig.6.3b).

The effect of the inclined web reinforcement on the behaviour of the solid beam NW6A-0.3/0 was found to be

substantial. Whereas in the similar beam without web reinforcement, Beam NO-0.3/0, the crack width limit of 0.3 mm was reached at 350 kN, in Beam W6A-0.3/0 containing 0.65% web steel the load at this serviceability limit state of cracking was 1000 kN - an increase in load of over 200%.

In Fig.(6.4), the deflections recorded for the beams are presented. Generally, these results again confirmed the observations made in the lightweight concrete tests and as before the deflection behaviour was found to reflect the ability of each type of web reinforcement to control crack widths in the shear spans.

6.2.3 Ultimate Loads

The present normal weight concrete tests have broadly shown that the effects of web openings on the ultimate behaviour of deep beams is little affected by the type of structural concrete used. A study of the measured ultimate loads of the normal weight beams containing opening ref.No.4 (Table 6.2), made in conjunction with the web steel details in Fig.(6.1) and the crack patterns in Fig.(6.2), resulted in observations similar to those drawn previously from the results of the tests on the comparable beams of lightweight concrete (Chapter 5.3.3). Hence, it seems reasonable to deduce that all the observations made from the results of both the pilot tests and further tests (Chapters 4 and 5) would be broadly applicable to normal weight reinforced concrete deep beams.

In general, from a comparison of the ultimate loads of each pair of similar beams (Tables 5.2 and 6.2) it was found that the higher ultimate loads recorded for the normal weight beams were not inconsistent with the higher strength - as measured by the control cube and cylinders tests - of the normal weight concrete. An interesting result was obtained by dividing the ultimate loads of each beam in each particular set of beams by the corresponding solid beam without reinforcement: thus the ultimate load of Beam NW1-0.3/4 was divided by that of Beam NO-0.3/0, and Beam W1-0.3/4 by O-0.3/O and so on. In Table (6.3) it may be seen that the result of this exercise is to produce two sets of figures which are clearly comparable. This result provided further evidence to suggest that the performance of the reinforcement - as regards bond in particular - was similar in both normal weight and lightweight reinforced concrete deep beams.

The results of the series of beams containing the same type of inclined web reinforcement provided some new information on the behaviour of deep beams with web openings. It was found that, by the provision of approximately 0.5% (Table 6.1) of web reinforcement in an inclined pattern, the ultimate loads of deep beams containing openings in any of a number of locations could achieve high ultimate loads. For example, in Beam NW6A-0.3/15 the location of the opening was such that the 'load path' joining the load bearing blocks at the supports was intercepted ataposition close to the beam soffit. The results of the tests on lightweight beams

have shown that such openings could drastically reduce the strength of deep beams without effective systems of web reinforcement. In contrast, Table (6.2) shows that due to the web reinforcement the measured ultimate load of Beam NW6A-0.3/15 was high; indeed, it was greater than that of the solid beam NO-0.3/0. Similarly all of the other beams, with similarly sized openings and Type W6A web reinforcement, recorded ultimate loads which were greater than the measured capacity of the solid beam; and even Beam NW6A-0.3/4, which contained openings that completely intercepted the 'load path', obtained a load comparable to that of the unreinforced solid deep beam (Table 6.3).

As mentioned earlier some reservations have been expressed [9] over the ability of web reinforcement to increase the strength of beams without openings. In the case of inclined web reinforcement, the present tests have shown by the performance of Beam NW6A-0.3/0, which contained 0.65% inclined web steel, that the increase in ultimate load could be in fact substantial: Table (6.2) shows that the ultimate load of Beam NW6A-0.3/0 was 1215 kN compared with 695 kN for the similar beam without web reinforcement, Beam NO-0.3/0. In the tests on solid beams with little or no web reinforcement reported herein (Chapter 4, Beams N-0.4/0, O-0.4/0, O-0.25/0; Chapter 5, Beams O-0.3/0, O-0.2/0; and Chapter 6, Beam NO-0.3/0), shear failure occurred as a result of the formation and progagation of a single critical diagonal crack, which at collapse split the beam into two. However, in Beam NW6A-0.3/0 examination of the crack pattern

at failure (Fig.6.2) shows that the web reinforcement acted to control the propagation of the diagonal cracks such that failure occurred as a result of a pure shearing action on the 'strut'- like portion of the beam between two diagonal cracks. This result would also suggest that, the apparent crushing failure of this strut-like portion observed in previous tests [24, 27], should not be construed as an axial compression failure of the web: indeed, the present tests of beams with web openings and larger quantities of effective web reinforcement have shown that such a compression failure mode is unlikely to occur. In summary, therefore, the results of the present tests have shown and confirmed that shear failure in reinforced concrete deep beams both with and without openings is essentially a diagonal splitting type failure, which may be controlled - and even realistically prevented - by the proper arrangement of the web steel.

CHAPTER SEVEN

A STRUCTURAL IDEALIZATION FOR DEEP BEAMS WITH WEB OPENINGS

7.1 THE STRUCTURAL IDEALIZATION

7.2 GENERAL DISCUSSION

CHAPTER SEVEN

A STRUCTURAL IDEALIZATION FOR DEEP BEAMS WITH WEB OPENINGS

7.1 THE STRUCTURAL IDEALIZATION

The arguments that follow are based on the sum total of the evidence from all of the tests reported in Chapters 4,5 and 6. In summary, the tests, a total of 79 beams, together covered: (a) span/depth ratios L/D of 1, 1.5 and 2; (b) clear-shear span/depth ratios x/D of 0.2, 0.25,0.3 and 0.4; (c) 13 combinations of the opening-size factors a_1 and a_2 (Fig.4.2 and Fig.5.2); (d) 22 combinations of the opening-location factors k_1 and k_2; (e) 8 arrangements of web reinforcement (Fig.4.1, Fig.5.1 and Fig.6.1), (f) both normal weight and lightweight concrete.

The ultimate shear strength of a deep beam may be calculated using the structural idealization of Fig. (7.1), which shows that the applied load is transmitted to the support mainly by a 'lower path' ABC and partly by an'upper path' AEC. The structural idealization suggests that the effectiveness of the lower path should increase with the angle $\emptyset$, whilst that of the upper path with $\emptyset'$. Let us consider, for the time being, that the opening occurs at a fixed level, i.e.,the dimensions to k_2D and $k_2'D$ are fixed. Then, if $\emptyset$ is kept constant by keeping the dimension $k_1'x$ constant, and $\emptyset$ is progressively reduced by increasing the dimension k_1x, it would be reasonable to expect a progressive reduction in ultimate strength.Beams O-0.3/7 to O-0.3/10(Fig.5.4a) were designed to test this argument, and the W_1 values in Table (5.2)shows that ultimate loads were indeed progressively reduced: from 420 kN for Beam O-0.3/7

through 380 kN, 280 kN, 260 kN, to 210 kN for Beam 0-0.3/10. On the other hand in Beams 0-0.3/1 to 0-0.3/6 (Fig.5.4a), the angle Ø was kept constant while Ø' was progressively reduced; again, the W_1 valuesin Table (5.2) confirm that the general trend was a reduction in the ultimate load.

In the absence of the opening, the upper and lower paths in Fig.(7.1) become one, which is the 'natural load path' joining the loading and reaction points; for such a solid beam, it has been shown [33] that the ultimate shear strength Q_{ult} could be predicted by Eqn.(7.1) below

$$Q_{ult} = C_1 \left(1 - 0.35 \frac{x}{D} \right) f_t \; bD + C_2 \sum A \frac{y}{D} \sin^2\alpha \quad (7.1)$$

where the notation is explained in Fig.(7.2a).

The structural idealization suggests that if the opening is small or is so located as not to interfere significantly with the natural load path, a reasonable estimate of the ultimate strength should be obtainable from Eqn.(7.1). This was indeed supported by the test results; in Table (7.1) the W_2 values marked with a symbol (‡) have been calculated using Eqn.(7.1) and the W_1/W_2 ratios for these beams are reasonably close to unity.

If the opening interrupts the natural load path, the ultimate strength equation takes the modified form:

$$Q_{ult} = C_1 \left(1 - 0.35 \frac{k_1 x}{k_2 D} \right) f_t \; b \; k_2 \; D + \sum \lambda C_2 \; A \frac{y_1}{D} \sin^2\alpha_1 \quad (7.2)$$

$$= W_2/2$$

where the notation is explained in Fig.(7.2b).

It should be noted that y_1 is now the depth at which a typical reinforcement bar intersects the 'strut' EA of the upper path or the 'strut' CB of the lower path as the case may be, and α_1 is the angle between the typical bar and the strut EA or EB.

The anomoly in the previously proposed equation, which was based on the pilot study test data (Chapter 4; Eqn. 4.2), has thus been corrected: in the pilot study the proposed equation took the form:

$$Q_{ult} = C_1 \left(1 - 0.35 \frac{k_1 x}{k_2 D}\right) f_t \; b \; k_2 D + C_2 \sum_A \frac{y}{D} \sin^2\alpha \qquad (7.3)$$

where α and y were measured with reference to the natural load path, which often bears little relation to the critical diagonal cracks in a beam with openings.

In the first term on the right-hand side of Eqn.(7.2), the quantity $C_1 f_t b k_2 D$ ($= C_2 f_t b \overline{CB} \sin \phi$) is a measure of the load-carrying capacity of the 'strut' CB of the lower path in Fig.(7.1), and the factor $(1-0.35 k_1 x/k_2 D)$ allows for the experimental observation of the way in which the load capacity varied with cot ϕ, where ϕ is the inclination of the 'strut' CB to the horizontal. The first term is therefore a semi-empirical expression for the capacity of the lower path; when this capacity is reached, the 'strut' CB fails in a splitting mode (hence the splitting strength f_t is used) resulting in the formation of a so-called critical diagonal crack along CB.

The second term on the right-hand side of Eqn.(7.2) represents the contribution of the reinforcement to the shear

strength of the beam; experimental observation has shown that the reinforcement has two functions. Firstly, it controls the widening and propagation of corner cracks (Fig.4.4; crack types 1 and 2) which would otherwise cause failure in Mode 3 (Fig.4.5). Hence, the reinforcement enables a proportion of the load to be carried along the 'upper path' AEC. However, the capacity of 'strut' EA itself has not explicitly been included in Eqn.(7.2) because, in the absence of web reinforcement, the upper path was found to be ineffective except for very large values of $\emptyset'$ (say 75°), when the behaviour of the beam is then better described by Eqn. (7.1). Hence, the concrete contribution in Eqn.(7.2) has been restricted, conservatively, to that given by the lower path, while the contribution of the upper path is implicitly allowed for in the reinforcement contribution term, as explained later. The second important function of the web reinforcement is to restrain the propagation and widening of any critical diagonal cracks along EA and CB. Unless arrested, such propagation and widening leads to failure Mode 2 (Fig.4.5), in which the beam is split into two by the diagonal cracks along EA and CB. The ability of the reinforcement to restrain the diagonal cracks was shown by the test results to depend on the quantity of reinforcement provided and on the angle with which the typical reinforcement bar crosses a critical diagonal crack. It would also seem that the propagation and widening of the diagonal cracks could result in the end portion of the beam moving outwards in a predominantly rotational motion about the loading point. The structural idealization (Fig.7.1) explains why the ability of a reinforcement bar to restrain such rotation increases with the distance y_1 and similarly y in Eqns.

(7.2) and (7.1) respectively.

It is appropriate to point out one significant difference between the function of the web reinforcement in a beam without openings and that of a beam with openings. In a deep beam without openings [27, 33], the vulnerable region is between the soffit and about D/3 from it. As mentioned above the term $C_2 \sum A_y \sin^2\alpha/D$ in Eqn.(7.1) increases with the distance y; this suggests that one way to detail the web steel is to arrange it in a closely spaced band near the beam soffit; and previous experience [25, 27, 32], has shown that this is indeed acceptable, especially for the deeper beams (L/D greater than 1.5). However, in a deep beam with openings the upper and lower paths are less efficient in carrying loads than the natural path of a solid beam, and are more sensitive to imperfections - such as diagonal cracks. The effect of web reinforcement is hence more pronounced in deep beams with openings and also, as noted earlier, the effectiveness of the upper path is in any case largely dependent on the provision of web reinforcement to provide a tensile capacity along EE' (Fig.7.1).

It was therefore required to introduce a further empirical factor into Eqn. (4.1) (repeated above as Eqn.7.3) in order to implicitly allow for the contribution of the upper load path and to allow for the increase in strength which was experimentally observed for the types of web reinforcements that protected both the vulnerable regions above and below the opening. By a systematic process of inspection and trial it was found that the empirical factor λ could reasonably allow for the experimental observations: the factor λ distin-

guishes between the main longitudinal reinforcement and the web steel proper; for the main steel $\lambda = 1$; for the web steel proper, that is reinforcement detailed above and below the opening, $\lambda = 1.5$. (See General Discussion below: Item 1).

The use of Eqn.(7.2) is perhaps best illustrated by a simple worked example, and for this purpose the ultimate shear capacity of Beam W3-0.3/4 will be calculated.

EXAMPLE:

The properties of the Beam W3-0.3/4 have been extracted from Fig.(5.1) and Table (5.1) and are shown in Fig.(7.3).

With reference to Fig.(7.2) and Fig.(7.3)

$f_t = 2.87\ N/mm^2$ $\qquad$ $D = 750$ mm

$k_1 x = 225$ mm $\qquad$ $b = 100$ mm

$k_2 D = 300$ mm $\qquad$ $C_1 = 1.35$

then the shear strength contribution of the concrete is given by the first term on the right hand side of Eqn.(7.2)as follows

$$1.35\ (1 - 0.35\ \frac{k_1 x}{k_2 D})\ f_t\ b\ k_2\ D$$

$$= 1.35\ (1 - 0.35\ \frac{225}{300})\ x\ 2.87\ x\ 100\ x\ 300\ x\ 10^{-3}\ kN$$

$$= 85.7\ kN.$$

The shear strength contribution of the steel is calculated using the second term on the right hand side of Eqn.(7.2). Referring to Fig.(7.2)and Fig.(7.3),the steel contribution is given by

$$\sum \lambda \times 300 \times A \times y_1/D \times \sin^2\alpha_1$$

$$= 1 \times 300 \left(314.2 \times \frac{710}{750} \times 0.64\right) \times 10^{-3}$$

main steel term; $\lambda = 1$

$$+ 1.5 \times 300 \times \frac{157}{750} (190 + 230 + 270 + 480 + 520 + 560) \times 0.64 \times 10^{-3}$$

web steel term; $\lambda = 1.5$

$$= (57.1 + 135.6) \text{ kN}$$

This gives a computed ultimate shear load of

$$Q_{ult} = 85.7 + 57.1 + 135.6 \text{ kN}$$

$$= 278.4 \text{ kN}$$

$Q_{ult} = W_2/2$ where W_2 is the total applied load

$W_2 = 557$ kN

With reference to Table (5.2) the measured ultimate load W_1 of Beam W3-0.3/4 was 560 kN.

As a final illustration let us consider the ultimate strength predicted for a replica beam without web reinforcement. From Table (5.1) $f_t = 2.69$ N/mm^2 for Beam 0-0.4/0, and since the geometry of the beam and the main longitudinal reinforcement are identical to Beam W3-0.4/0 described in Fig.(7.3), the ultimate shear strength is as follows,

$$Q_{ult} = 85.7 \times \frac{2.69}{2.89} + 57.1$$

$W_2 = 275$ kN.

With reference to Table (5.2) the measured ultimate load W_1 of Beam 0-0.3/4 was 260 kN.

In Table (7.1) the computed ultimate loads for all the beams, using Eqn.(7.2) or Eqn.(7.1) as appropriate, are compared with the measured values and it can be seen that apart from a few exceptions the agreement is generally good. This agreement is exhibited further in Fig.(7.4) where it can be seen that the line $W_1 = W_2$ represents a reasonable mean profile.

7.2 GENERAL DISCUSSION

1.) In Table (7.1), W_2 values are not shown against Beams W1-0.3/4, W2-0.3/4, W5-0.3/4, W1(A) and the similar beams of normal weight concrete. If, for example, Eqn.(7.2) is applied to Beam NW1-0.3/4, the computed W_2 will be over 800 kN; this artificially high computed load arises from the fact that the web reinforcement detailing (Fig.6.1: Type W1) was such as to leave the upper region weak and hence the potential capacity of the lower path could not be realized before the collapse of the beam occurred.

2.) In Eqn.(7.2) the concrete contribution, as represented by the first term on the right-hand side, is based on the capacity of the lower path, which without proper detailing of the web reinforcement is normally the primary path. Under special circumstances, however, the lower path might be much weaker than the upper path. This happened, for example, in beams 0-0.3/16 and 0-0.2/16 which were designed to test the structural idealization. It is clear from Fig.(5.4) that the lower paths in these beams were weak relative to the upper paths; Table (7.1) shows that for such beam Eqn.(7.2) is grossly

conservative. In any event, however, the shear strength of a beam is likely to be low if the values of k_2 and the angle ϕ ($= \cot^{-1}(k_1 x/k_2 D)$; see Fig.(7.1) are low, unless special attention is given to the detailing of the web reinforcement; and hence, the conservative estimate from Eqn.(7.2) is justified. If proper web reinforcement is provided, then, as shown by Beam NW6A-0.3/15 (Fig.6.1), the predicted ultimate load becomes reasonably less conservative for such an opening location: in Table (7.1) the ratio W_1/W_2 for Beam NW6A-0.3/15 is 2.0.

3.) Beams W1(A), W3(A), W4(A) and W7(A) were tested under four-point loading to simulate the distributed-load condition, as shown in Fig.(5.3). The results in Table (7.2) show that Eqn.(7.2) may also be used for this loading condition. In Eqn.(7.2), the dimensions $k_1 x$ and $k_2 D$ are independent of the loading condition. To define all the y_1 and α_1 values, it is only necessary to choose a reasonable line to represent the strut EA in Fig.(7.2).

4.) With reference to Eqn.(7.2), it is reasonable to expect, that, for a given beam, there is an upper limit to the shear strength, irrespective of how much web steel is used. In the tests, that limit was not reached at a web steel ratio of 1.2%, which already represented a rather heavy web reinforcement for a deep beam.

In beams with normal span/depth proportions, recent tests have shown that shear behaviour could be influenced by the scale of the test specimens. The size of the test specimens used in the present test programme was chosen to be as large

as practicable in consideration of the wide range of parameters to be tested. At the University of Cambridge a test programme using large deep beams has commenced; the test specimens both in normal weight and lightweight concretes are of depth 1800 mm, thickness 250 mm and span length 3,500 mm and contain openings across the shear span at mid-depth similar to opening type 4 (Fig.5.2) of the present tests. The webs of the beam are reinforced either by an orthogonal mesh or by inclined arrangements of reinforcement. Only a single result has, at present, been reported [62] but the indications are that the prediction of ultimate strength given by Eqn.(7.2) is not likely to be significantly affected by a scale effect. The measured ultimate load of a beam, containing openings as described above and approximately 1.34% of web reinforcement in an orthogonal mesh, was 3000 kN; using Eqn.(7.2) a predicted ultimate load of 2530 kN was obtained. Hence as seen by the ratio of measured to calculated ultimate load, 1.18, the agreement was reasonably good and comparable to the results of the present tests.

CHAPTER EIGHT

A PROPOSED METHOD FOR THE DESIGN OF DEEP BEAMS WITH WEB OPENINGS

8.1 INTRODUCTION

8.2 PROPOSED DESIGN EQUATIONS FOR SHEAR

8.3 DESIGN HINTS

8.4 DESIGN EXAMPLE

C H A P T E R E I G H T

A PROPOSED METHOD FOR THE DESIGN OF DEEP BEAMS WITH WEB OPENINGS

8.1 INTRODUCTION.

The design of reinforced concrete deep beams with web openings is not yet covered by the major codes of practice [3-5]. In Great Britain, the Construction Industry Research and Information Association, has just issued a design guide [9] for practising engineers, but the provisions for web openings are necessarily very restrictive because extensive surveys [6,7,9], have shown that little information is available in the literature, on the effects of web openings on the ultimate load behaviour of concrete deep beams.

The exact analysis of reinforced concrete deep beams with openings presents formidable problems [22, 36], but the results of the experimental research presented in this thesis indicates that the restrictions on web openings need not be so severe. The structural idealization presented in Chapter 7 should prove a powerful tool to the designer, both for the visualization of the load transfer mechanism in deep beams with web openings and for the prediction of their ultimate strengths. In this chapter, a simple method for the design of deep beams with openings is suggested, and design hints are given together with a design example to illustrate the method's ease of use.

8.2 PROPOSED DESIGN EQUATIONS FOR SHEAR

It should be noted that Eqns.(7.1)and (7.2) are

intended to predict actual collapse loads. Hence, there is no built-in factor of safety and also there is likely to be a certain amount of scatter in comparing predicted and actual strengths. Therefore, in order to modify the equations to be appropriate for design, it is necessary to multiply the empirical coefficients C_1 and C_2 by a factor to obtain a safe lower bound. Examination of Fig.(7.4), showed that a reasonable lower bound to the experimental results is given by a factor of 0.75. In addition, it is necessary to relate the lower bound strengths to the ultimate limit state design loads by the application of the partial safety factor for material, γ_m.

It is also noted that the characteristic cube strength is usually the concrete strength parameter adopted in design practice, and hence it is appropriate to substitute an estimated value based on the cube strength, for the cylinder splitting strength which is used in Eqn.(7.1) and (7.2) and which may not normally be available. In the CIRIA design guide [9], the relationship between the cube and cylinder splitting strength is taken as $f_t = 0.52 \sqrt{f_{cu}}$. For normal weight aggregate concrete this relationship is within the experimental range of the present tests and will be adopted here. For lightweight aggregate concrete, however, this relationship over estimates the splitting strength: from the results of the testing of the control specimens a relationship $f_t = 0.44 \sqrt{f_{cu}}$ was obtained, and this is the value adopted for lightweight concrete. (It is pertinent to point out again, that the splitting strength of lightweight concrete

is dependent on curing conditions: in the present tests f_t for lightweight concrete was obtained in accordance with ASTM 330 - see Chapter 3.5). Taking into account the partial factor of safety for material, which is given in CP110[3] as 1.5 for concrete, the concrete strength parameters for design purposes are derived as follows:

$$\frac{f_t}{\gamma_m} = 0.52\sqrt{\frac{f_{cu}}{1.5}} = 0.42\sqrt{f_{cu}} \text{ for normal weight concrete}$$

$$\frac{f_t}{\gamma_m} = 0.44\sqrt{\frac{f_{cu}}{1.5}} = 0.36\sqrt{f_{cu}} \text{ for lightweight concrete}$$

The design equations for ultimate shear strength then become:

$$Q_{ult} = C_1^{\bullet}(1-0.35\,x/D)\sqrt{f_{cu}}\,bD + \sum C_2^{\bullet} A \frac{y}{D} \sin^2\alpha \qquad (8.1)$$

$$Q_{ult} = C_1^{\bullet}(1-0.35\,k_1x/k_2D)\sqrt{f_{cu}}\,bk_2D + \sum \lambda C_2^{\bullet} A \frac{y_1}{D} \sin^2\alpha_1 \qquad (8.2)$$

where the geometrical notation is as explained again in Fig.8.1

and $C_1^{\bullet}$ = 0.44 for normal weight aggregate concrete

$C_1^{\bullet}$ = 0.36 for lightweight aggregate concrete

$C_2^{\bullet}$ = 1 95 N/mm^2 for deformed bars (f_y = 410 N/mm^2)

$C_2^{\bullet}$ = 85 N/mm^2 for plain round bars (f_y = 250 N/mm^2)

λ = 1.0 for main longitudinal bars (A_s)near beam soffit

λ = 1.5 for web reinforcement proper (A_w)

f_{cu} = characteristic cube strength of concrete

A = area of main steel bar or web bar as the case may be

8.3 DESIGN HINTS

The following design hints based on the experimental observations, are given to qualify and to aid the use of Eqns.(8.1) and (8.2).

(1) Equations (8.1) and (8.2) are intended to apply to beams with span/depth ratios and clear shear-span/depth ratios comparable to those of the test specimens: namely, $1 \leqslant L/D \leqslant 2$ and $0.2 \leqslant x/D \leqslant 0.4$. The equations should be applied only to deep beams under top loading conditions; static loads only are covered.

(2) Whenever possible, web openings should be kept clear of the natural 'load path' joining the loading and reaction points. If the opening is reasonably clear of the natural load path, the ultimate shear strength may be calculated from Eqn.(8.1).

(3) In using Eqn.(8.1), it is recommended that the steel contribution, as given by the second term of the equation, should not be less than 20% of the design shear force (Q_{ult}).

(4) If the opening intercepts the natural load path, the designer should ensure that the factor k_2 is not less than approximately 0.2 and the angle $\cot^{-1}(k_1 x/k_2 D)$ not less than about 30° (Fig.8.1). The ultimate shear strength may then be calculated from Eqn. (8.2).

(5) In using Eqn.(8.2), it is possible that the contribution from the concrete term together with that of the main steel (A_s) might be found to be sufficient to meet the design shear

loads, However, the test experience has shown that to ensure the mobilisation of the potential capacity of the unreinforced web, it is advisable to provide web reinforcement to protect the regions above and below the opening. For this purpose it is recommended that where the total steel contribution exceeds 20% of Q_{ult}, then at least 25% of the steel contribution should be made by the web steel proper (A_w), and the web steel A_w must be detailed properly.

(6) It is worth noting that in meeting the recommendation given in (5) above, the total quantity of web reinforcement so provided is unlikely to be significantly greater than the mandatory quantity of reinforcement required for temperature and shrinkage effects by CP110[3] (Clause 5.5) and may be less than the so-called nominal web reinforcement required for solid deep beams by the CEB-FIP Recommendations [5] (see Chapter 2.2.1).

(7) The ultimate shear strength may be substantially increased by providing designed quantities of web reinforcement. In detailing the web reinforcement the designer should again ensure that both the regions above and below the opening are protected. Web reinforcement not meeting this requirement should be disregarded when using Eqn.(8.2).

(8) Inclined web reinforcement (Fig.6.1: Type W6 and W6A) is particularly effective for increasing the ultimate shear strength (and for crack control - see Chpts.5.2.2 and 6.2.2). This type of web reinforcement is likely to be more expensive to bend and fix than others. However, where there are restrictions on the overall dimensions of the beam, and an

adequate ultimate strength is the main concern, then Type W6 may be the best choice.

(9) Trimming web openings locally with loops of reinforcement has little beneficial effect on ultimate shear strengths and any reinforcement that is provided locally for crack control should be disregarded in using Eqn.(8.2).

(10) In the design of shallow beams and of the majority of solid deep beams [31, 32], it is usually necessary to consider shear for the ultimate limit state only. In the design of deep beams with openings, however, shear may also be an important consideration for the serviceability limit state of cracking (see Chpts.5.2.2 and 6.2.2).

(11) It is suggested that the equations should be applied only where positive end anchorage is provided for the main longitudinal steel. Little experimental data on the end anchorage requirements in deep beams are available, and both the ACI Building code [4] and the CEB-FIP Recommendations [5] are very cautious on this point. In all of the present tests, the main longitudinal bars were anchored at their ends to steel blocks as a precautionary measured against load failure (see also Appendix 1).

8.4 DESIGN EXAMPLE FOR A DEEP BEAM WITH OPENINGS

The geometry and properties of the beam used for this example are similar to those used previously in the illustration of the design of solid deep beams as given in Chapter 2. It is required to include an opening in the beam located as shown in Fig.(8.2); design the main steel and web

steel.

Examination of Fig.(8.2) shows that the opening intercepts the notional loadpath joining the load and support reaction and is therefore likely to seriously disrupt the normal distribution of internal forces and stresses within the beam. It is therefore necessary to compute the ultimate shear strength using Eqn.(8.2).

First, though, an estimate should be made of the necessary main bending steel required.

Because the proportion of main steel required is normally relatively small and the amount provided also contributes to the ultimate shear strength, a simple approximate estimate is only necessary (cf.Chpt. 9.2).

In this example it is suggested that the main longitudinal reinforcement be conservatively calculated as follows:-

$$\text{Design bending moment } M = 0.75\, k_2 D\, A_s\, \frac{f_y}{\gamma_m} \qquad (8.3)$$

With reference to Fig.(8.2) and using a partial safety factor of 1.4 for loading, the design shear force and moment are then as follows:-

Design shear force $V = 1.4 \times 4500 = 6300$ kN

Design bending moment $M = 1.4 \times 4500 \times 2.0 = 12600$ kNm

Using Eqn.(8.3) with $\gamma_m = 1.15$ for steel

$$12600 = 0.75 \times 2600 \times A_s \times \frac{410}{1.15} \times 10^{-6}$$

$$A_s = 18124 \text{ mm}^2 \quad (A_s/bD = 0.58\%)$$

Use 6 No.40 mm bars + 14 No.32 mm bars (18792 mm^2)

Next, we consider shear. From Fig.(8.2) $k_1x/k_2D = 0.462$

The concrete resistance to shear is given by the first term in Equation (8.2) as -

$$0.44\ (1-0.35 \times 0.462)\sqrt{30} \times 2600 \times b = 5.25\ b\ kN$$

Dimension b may be chosen so that the concrete resists say 55 per cent of the design shear force, then

$$5.25b = 6300 \times 0.55$$

$$b = 650 \text{ mm say}$$

From Eqn.(8.2) the shear resistance of the beam with main bars (A_s) only is

$$\left[5.25 \times 650\right] + \left[1 \times 195 \times 18792 \times \frac{4400}{4800} \text{ (say)} \times \sin^2\alpha_1 \times 10^{-3}\right]$$

(where $\alpha_1 = \cot^{-1} k_1x/k_2D = 65^\circ$; $\sin^2\alpha_1 = 0.82$)

$$= (3412 + 2754) = 6166 \text{ kN}$$

The contribution required by the web reinforcement = 6300 - 6166 = 134 kN, but it is noted that the required total steel contribution (6300 - 3412 = 2888 kN) is greater than 20% Q_{ult} and therefore a minimum amount of web reinforcement is required: web steel proper should contribute 25% x 2888 = 722 kN.

From Eqn. (8.2)

$$722 \times 10^3 = \sum 1.5 \times 195 \times A_w \times \frac{y_1}{4800} \sin^2\alpha_1$$

Assuming horizontal stirrups at uniform spacing are used to protect the regions above and below the opening: $\sin^2\alpha_1 = 0.82$ as before and $\sin^2\alpha_1' = \sin^2 (\cot^{-1} 750/1200) = 0.72$. For design purposes it is sufficient to take an average value of $\sin^2\alpha_1$ and $\sin^2\alpha_1'$ and an average value of y_1 (say $y_1 = 1800$).

From above,

$$A_w = 8548 \text{ mm}^2 \quad (A_w/bD = 0.27\%)$$

Use 18 No.25 mm diameter bars (8836 mm^2).

These bars must be arranged to protect both regions above and below the opening. The detailing is shown in Fig.(8.3). (Note: secondary nominal reinforcement, which might be provided elsewhere in the beam for temperature and shrinkage effects, and additional reinforcement at the supports and loading points to provide adequate bearing capacity has been omitted for clarity).

CHAPTER NINE

A CRITICAL REVIEW OF THE CIRIA DESIGN GUIDE FOR DEEP BEAMS

9.1 INTRODUCTION

9.2 CIRIA DESIGN METHOD: SOLID TOP-LOADED DEEP BEAMS

9.3 COMPARISON OF DESIGN LOADS WITH TEST RESULTS

9.4 CIRIA GUIDE: PROVISIONS FOR DEEP BEAMS WITH HOLES

C H A P T E R N I N E

A CRITICAL REVIEW OF THE CIRIA DESIGN GUIDE FOR DEEP BEAMS

9.1 INTRODUCTION

The recently issued CIRIA Guide 'The design of deep beams in reinforced concrete' [9] is the most comprehensive design Guide published to date (1977). Because of its likely impact on future design practice and on future revisions of codes of practice, the Guide is reviewed and discussed here in some detail.

The Guide [9] is based on an exhaustive study of published literature and of research reports on deep beams, and it is stated, "owes much to the work of Leonhardt [25], Kong [27-35] and to the CEB-FIP International Recommendations [5]". It contains 'simple rules' for designing the simpler forms of reinforced concrete deep beams and 'supplementary rules' to cover the more complex cases, in which the load capacity may be affected by elastic instability, or where the applied loads are concentrated or indirect, or where the supports are indirect. The Guide is also unique in including for the first time some provisions for the design of deep beams with web openings.

In the review here it will be appropriate to examine only those sections of the Guide which are relevant to the experimental research of this thesis; namely, simply supported top loaded deep beams and deep beams with web openings. In what follows, the recommendations for the design of solid deep beams are explained and illustrated with a simple design example

in section (9.2); in section (9.3) comparison is drawn between the measured ultimate loads of the test beams (solid) reported herein and the design loads which would obtain both according to the CIRIA Guide and according to the three currently used design methods (cf. Chapter 2); and finally in section (9.4) the CIRIA provisions for the design of beams with openings are examined.

9.2 CIRIA DESIGN METHOD: SOLID TOP-LOADED DEEP BEAMS

According to the Guide [9] the 'simple rules' may be applied to a beam which satisfies the conditions of being a flat plate, with no significant openings, subjected to essentially uniformly distributed loading. Then, using the simple rules for bonding the main tension steel required is calculated from Equation (9.1) as follows:

$$A_s > \frac{M}{0.87\ f_y z} \qquad (9.1)$$

where M is the design moment at ultimate limit state

z is the lever arm and for single spans $z = 0.21 + 0.3\ h_a$

l is the effective span (Fig.9.1)

h_a is the effective height (Fig.9.1)

If $l/h_a > 1.5$ it is required to confirm the strength of the concrete in compression due to bending and the condition $M < 0.12\ f_{cu}\ b\ h_a^{\ 2}$ must be satisfied.

The reinforcement calculated by Eqn.(9.1) above is not to be curtailed in the span and may be distributed over a depth

of 0.2 h_a. The bars must be anchored to develop 80% of the maximum ultimate force beyond the face of the support, and 20% of the maximum ultimate force at or beyond a point 0.2 l_o from the face of the support or at or beyond the far face of the support, whichever is less (Fig.9.1).

It is worth noting that the provisions for flexural design are similar to those contained in the CEB-FIP Recommendations (cf. Chapter 2.2.1) and are therefore related to the work of Leonhardt (cf. Chapter 1.2.2.2). The lever arm factors for bending are in fact based upon the elastic stress distribution which obtains prior to cracking and hence, as might be expected, there is a substantial in-built factor of safety on collapse for simply supported beams. (Note: Appendix (1) of this thesis includes a description of some test beams that collapsed in the flexural failure mode). Compared to, say, the flexural design of normal beams (large span/depth ratios) Equation (9.1) would therefore seem irrational in the context of the philosophy of limit state of collapse: however, it is the philosophy of the Nottingham/Cambridge team that the following good reasons may be found as to why the equation is acceptable from a practical design point of view [33, 34, 51].

Firstly, because of the relatively large size of the internal lever arm flexural failure due to flexural crushing of the concrete prior to yield of the main steel will rarely occur: flexural collapse of deep beams is therefore a lesser problem than in normal beams. Secondly, the proportion of main steel required is relatively small compared to that required in normal beams and hence, whether the lever arm is nominally

taken as 0.6D or say, 0.8D, would not make significant differences to the cost. Thirdly, and more important, any reinforcement bar that intersects the critical diagonal crack (Fig.9.2) will form an integral part of the shear reinforcement [27 - 34]. Therefore, all the main bars provided in accordance with Eqn.(9.1) also act as web bars; that is, to quote Kong, Robins and Sharp [34] "the laws of equilibrium are unaware of the designer's discrimination between bars labelled as 'flexural reinforcement' and bars labelled as 'shear reinforcement' ".

The requirements for anchorage of the main steel stem from the understanding of the manner in which the stress in the steel becomes uniform within the span as the beam approximates to a'tied-arch'(cf. Chapter 1.2.2.1 and 1.2.2.2). However, it does seem that the anchorage capacity of the tension reinforcement might be significantly increased in the presence of the high compressive stresses in the support regions, although Kong, Singh and Sharp [37] have commented that the experimental evidence is insufficient as yet to recommend a relaxation in the current prudent recommendations. (Note: Appendix 1 describes the details of a series of exploratory tests [37] carried out to investigate the requirements for end anchorage of the main steel).

As regards shear, the 'simple rules' specify two conditions for the shear capacity of beams with unreinforced webs; these are to be satisfied as follows:-

$$V < 2\, bh_a^{\,2}\, v_c\, k_s/x_e \qquad (9.2)$$

$$V < bh_a\, v_u \qquad (9.3)$$

where V is the applied shear force

x_e is taken to be the least of

(a) L/4 for uniformly distributed load.

(b) the clear shear span for a load which contributes more than 50% to the total shear force at the support.

(c) the weighted average of clear shear spans where more than one load acts and none contributes more than 50% to the shear force at the support.

v_c is the ultimate concrete shear stress taken from CP110 Tables 5 and 25 for normal weight aggregate and lightweight aggregate concretes, respectively.

v_u is the maximum value for shear stress taken from CP110 Tables 6 and 26, respectively, for the two types of concrete.

k_s = 1.0 for $h_a/b < 4$

= 0.6 for $h_a/b > 4$

Equation (9.2) may be recognised as being an extension of the design equation for shear in normal beams (cf.CP110[3]: Clause 3.3.6.2) with modifications being made in an attempt to produce a single continuous provision for all types of beams. The factor $2\ h_a/x_e$ corresponds to the factor $2\ d/a_v$, which was included in CP110's provisions for normal beams to allow for the increased shear capacity exhibited by normal beams with small shear span/depth (a_v/d) ratios [47, 59]. For such beams it

has been reported [47] that the failure mode in shear in certain respects resembles a deep beam failure mode; namely, that failure in both types of beam may be initiated by the formation of diagonal (splitting) cracks between the loading and support points

There is a further factor k_s included in Equation (9.1), the value of which depends on the aspect ratio h_a/b. As deep beams usually have aspect ratios greater than the minumum of 4, the effect of the factor k_s is to reduce the CP110 values by 40%. The explanation regarding k_s, as given in the Guide, is that Kani [60] and later Taylor [61] have drawn attention to the probability that beams unreinforced for shear with aspect ratios exceeding 4 will exhibit reduced shear capacity against that predicted on the basis of normal shallow beam theory. It is not clear how these results can be directly extended to deep beams, as the shear failure mode in both Kani's and Taylor's tests was typical of that of shallow beams with large (a_v/d) ratios and hence bore little resemblance to a deep beam failure mode. However, the reduction of 40% may be seen to be certainly necessary by comparing the nominal shear stresses obtained for the present tests with that givenby Equation (9.2) without the k_s factor. For example, Beam NO-0.3/0 (Chapter 6: Table 6.2) achieved a measured ultimate nominal shear stress of 4.5 N/mm^2 which compares with an allowable ultimate shear stress from Eqn.(9.2) of 3.66 x k_s N/mm^2. These figures would imply a factor of safety of $4.5/3.66\ k_s = 1.23/k_s$ which, taking k_s at its value of 0.6 then becomes 2.05.

The upper limit for shear stress is fixed by the condition given in Eqn.(9.3). It is worth mentioning that the use

of this limit in the simple rules is strictly not appropriate, as the limit has been derived as an upper limit for the shear strength of normal beams with designed quantities of shear reinforcement. However, in practice, under the simple rules either Eqn.(9.2) or more usually the rather conservative limit on support bearing pressures will govern [9]. The Guide recommends that the bearing pressures at the support should not exceed $0.4\ f_{cu}$.

The simple rules do not give specific recommendations for the design of web steel but stipulate the provision of nominal quantities of web reinforcement. The minimum amount should not be less than the reinforcement for shrinkage and temperature effects required for a wall under Clauses 3.11 and 5.5 of CP110: namely, 0.25% (for high yield steel) or 0.3% (for mild steel) times the volume of the concrete is to be provided both horizontally and vertically. In the support regions the proportion of steel, related to the local area of concrete in which it is embedded, should not be less than $0.52\sqrt{f_{cu}}/0.87\ f_y$; that is sufficient steel to provide a tensile resistance of not less than that of the uncracked concrete: for example, taking $f_{cu} = 30\ N/mm^2$ and $f_y = 410\ N/mm^2$ the percentage required in each direction would equal 0.8%.

Where a beam is subjected to concentrated loads or where the unreinforced web shear capacity given by Eqn.(9.2) is exceeded, then the nominal web reinforcement may be augmented under the 'supplementary rules' to improve the top load capacity.

Under the supplementary rules [9] the ultimate shear capacity is given by, with reference to Fig.(9.2):

$$V = \lambda_1\left(1-0.35\ \frac{x_e}{h_a}\right)\sqrt{f_{cu}} + \lambda_2\sum\frac{100\ A_r\ y_r\ \sin^2\theta_r}{b\ h_a^{\,2}} \qquad (9.4)$$

where λ_1 = 0.44 for normal weight aggregate concrete

= 0.32 for lightweight aggregate concrete

λ_2 = 1.95 N/mm^2 for deformed bars

= 0.85 N/mm^2 for plain round bars

Equation (9.4) is based on the analysis [33,34] of the results of the Nottingham - Cambridge tests [27-32]: it is, in fact, Eqn.(1.9) as given in Chapter 1. The equation is intended to apply to beams under top loads with clear shear span/depth ratios (x_e/h_a) in the range 0.23 to 0.7; this being the range considered in the tests [27-32]. The coefficients λ_1, and λ_2 are based on the empirical coefficients C_1 and C_2 of Equation (1.9), having been modified [34] by a factor of 0.75 to give a lower bound to experimental results, and by the partial factor of safety for materials.

The ultimate shear capacity is subject to the condition expressed as follows:

$$V/bh_a < 1.3\ \lambda_1\sqrt{f_{cu}} \qquad (9.5)$$

This limit, judging from the Nottingham-Cambridge tests [27-32], may or may not be very conservative depending, for example, on how well the beam is reinforced against bearing failure. In the tests [27-32] the measured nominal shear stress acting over the cross-sectional area (width x depth) varied from about 4 N/mm^2 to 7 N/mm^2 depending on geometry (mainly the clear-shear-span/depth ratio) and on the effectiveness of the web reinforcement. The limit given by Eqn.(9.5),

for example, equals 3.12 N/mm^2 for a normal weight aggregate concrete of 30 N/mm^2 cube strength. For beams with effective inclined web reinforcement, the present tests reported herein would indicate that the limit restricts the possible ultimate shear stress potential by a factor of at least 2 (cf.Chapter 6: Table (6.2) , the ultimate load of beam NW6A - 0.3/0 is 1215 kN which represents a nominal shear stress of 8.1 N/mm^2 and nominal support bearing pressures of 60.8 N/mm^2).

As regards bearing capacity, the Guide permits the maximum bearing stress at the support to be increased from the limit of 0.4 f_{cu} in the simple rules to 0.6 f_{cu}, provided that suitable binding reinforcement is added to the support zones to provide lateral confinement to the concrete. It will be generally found, in fact, that the bearing capacity stipulation for simply supported beams is the limiting factor governing the design capacity of the beam. Whilst it is at present reasonable to expect conservative limits to be placed on bearing pressures - for the reason that the bearing pressures achieved under laboratory conditions may not be achieved, it is thought [9] , in practice - it also seems likely that too great an importance has been attached to the bearing failures reported by Leonhardt[25], (cf. Chapter 1.2.2.2). At Nottingham [32], tests have indicated by the use of cine-film that bearing failure might be a secondary effect of the propagation of diagonal cracks into the support zones: by proper arrangement of web reinforcement to control diagonal cracking,bearing failures might therefore be avoidable. It is notable also that in the present tests simple confining cages of reinforcement at the load and support points helped to

prevent the occurrence of a single bearing type failure.

Two worked design examples are given in the Guide to illustrate the application of the rules over the wide range of loading and support conditions covered. These examples are rather comprehensive and are not so suitable for the specific illustration of the design of a simply supported top-loaded deep beam. Hence, a simple worked example of the design of such a beam will be given here. It is to be noted that as an aid to the designer Eqns.(9.3) and (9.4) are re-arranged algebraically in the Guide, so that the design may be carried out with the help of a number of Tables. These re-arranged equations and Tables are presented and used in the example.

Design example for the CIRIA Guide.

The design problem used is again that which was given in Chapter 2. With reference to Fig.(2.2) it is required to design the main steel and web steel using the CIRIA Recommendations [9].

The design procedures conform with the limit state principles of CP110[3], therefore, the design ultimate bending moment M and the design ultimate shear force V are determined as follows (Fig.2.2):-

$$M = 1.4 \times \frac{W}{2} \times 2 = 12600 \text{ kNm}$$

$$V = 1.4 \times \frac{W}{2} = 6300 \text{ kN}$$

where 1.4 is the partial factor of safety on the loading.

$$l/h_a = 4800/6000 = 1.25 < 1.5$$

hence there is no need to check the compression stresses (from bending) in the concrete.

The area of main steel (A_s) required is given by Eqn. (9.1)

$$A_s > \frac{M}{0.87\ f_y z} \qquad (9.1)$$

$$z = 0.2 \times 6000 + 0.4 \times 4800 = 3120 \text{ mm}.$$

$$\therefore A_s = \frac{12600 \times 10^6}{0.87 \times 410 \times 3120} = 11322 \text{ mm}^2.$$

Provide 24 No.25 mm diameter bars (11782 mm^2; $p = \frac{A_s}{b\ h_a} = 0.49\%$)

This reinforcement will be distributed in a band over a height 0.2 x 4800 = 1000 mm (say) and extend and be fully anchored across the complete span.

Next, consideration is given to the shear capacity of the beam.

The 'simple rules' of the Guide [9] are not applicable for concentrated loads, therefore, the supplementary rules [9] might be used.

Equations (9.2) and (9.3) have been algebraically re-arranged in the Guide as follows:-

$$\frac{V_c}{b\ h_a} = \lambda_1 v_x + (\beta_1\ v_{ms} + \beta_2\ v_{wh} + \beta_3\ v_{wv}) \qquad (9.6)$$

$$\frac{V_c}{b\ h_a} \not> \lambda_1 v_{max} \qquad (9.7)$$

where V_c is the shear capacity of the beam.

λ_1 = 0.44 or 0.32 as in Eqn.(9.2).

$\beta_1 = \beta_2 = \beta_3 = 1$ for deformed bars and 0.4 for plain.

The values v_x, v_{ms} etc., are given in a series of Tables (CIRIA Tables 4, 5, 6, 7. 8) reproduced here in (Fig.(9.3). Eqn.(9.6) is applicable to beams with orthogonal reinforcement arrangements only. In Eqn.(9.6), the first term on the right hand side represents the concrete contribution to shear and the terms in brackets give the contribution from the main steel, the horizontal web bars, and the vertical web bars respectively.

Using the limit on maximum shear stress as given by Eqn.(9.7), first a reasonable value for the beam width b may be determined. (Note: guidance on choosing a practical minimum beam width considering the concrete cover to steel, etc., is given in the Guide and the minimum thickness will normally be not less than 300 mm).

From Fig.(9.3) Guide Table 5; $v_{max} = 7.12$ N/mm^2: say, b = 500 mm then by substitution in Eqn.(9.7).

$$\frac{6300 \times 10^3}{500 \times 4800} \not< 0.44 \times 7.12$$

$$2.63 < 3.13 \quad \text{i.e., condition satisfied.}$$

Choose b = 500 mm.

The contribution of the concrete and main bars only is given by the terms $\lambda_1 v_x$ and $\beta_1 v_{ms}$ of Eqn.(9.6),namely:

$$(0.44 \times v_x + 1 \times v_{ms}) \times 500 \times 4800 \text{ N}$$

Where Fig.(9.3); Guide Table 4 for $f_{cu} = 30$ N/mm^2 and

$x/h = 1400/4800 = 0.29$, $v_x = 4.9$ N/mm^2

; Guide Table 6 for $p_{ms} = 0.49\%$ and $x/h = 0.29$,

$v_{ms} = 0.86$ N/mm^2

then $(2.156 + 0.86) \times 500 \times 4800 \times 10^{-3} = 7238$ kN.

Hence, the capacity of the concrete and main bars only is sufficient. It may be noted that the main steel bars contribute a significant proportion of shear strength: if, for example, the main steel for bending had been determined from a more rigorous equation (than Eqn.9.1) then it would have been necessary to provide extra horizontal web bars above the main steel to compensate for the loss to the shear capacity.

The CIRIA Guide requires in all cases the provision of a nominal quantity of web reinforcement; 0.25% both horizontally and vertically.

With reference to Eqn.(9.6) and Guide Tables 7 and 8 (Fig.9.3) the contribution given by the nominal mesh is

$$(0.22 + 0) \quad 500 \times 4800 \times 10^{-3} = 528 \text{ kN}.$$

$$\text{Total } V_c = 7238 + 528 = 7766 \text{ kN}$$

i.e., $V_c/V = 1.2$

The detailing of the reinforcement is shown in Fig.(9.4).

(Note that the CIRIA Guide requires an increased minimum percentage of reinforcement in the support zones; as mentioned previously for f_y = 410 N/mm^2 and f_{cu} = 30 N/mm^2 the area required equals (0.8% x b x s) both vertically and horizontally, where b is the beam thickness and s bar spacings. Note also that it is preferable to continue the horizontal bars so provided across the full span).

9.3 COMPARISON OF DESIGN LOADS WITH TEST RESULTS

The design ultimate shear loads of those beams tested herein without web openings have been calculated using the three commonly used design Guides (which were described in Chapter 2; namely, the CEB-FIP Recommendations [5], and ACI Building code [4] and the PCA document ST66[8]) and the new (1977) CIRIA design Guide.

By comparing the design shear load with the corresponding measured ultimate load (W_1) it is possible to estimate the effective in-built factor of safety against shear collapse. In Table (9.1) the ratios (W_1/W_4 to W_1/W_7) represent the factors of safety for each of the above design methods respectively. With reference to Table (9.1), it may be seen that the PCA method is very conservative; the average value for the factor of safety on the working load is over 6.

The CEB-FIP Recommendations are also rather conservative for those beams with web reinforcement, which would imply, since a relatively heavy percentage of nominal reinforcement is mandatory, that the minimum factor of safety on the design ultimate load may be significantly greater than 2.

The ACI and the CIRIA Guides are reasonably less conservative and are more consistent; and of the two, the CIRIA Guide as may be seen would result in the more satisfactory design.

As stated in Chapter 2, the earlier workers concentrated on the elastic analysis of deep beams, and the PCA method, published in 1946, is based on the results of Dischinger's theoretical work. The CEB-FIP Recommendations, which are based mainly on the tests carried out by Leonhardt and Walther, centre on flexural design and do not give specific guidance on how to calculate the web steel area to resist specified shear forces. The ACI's recommendations and CIRIA's recommendations are based on the test studies of Crist, de Paiva and Siess, and the Nottingham - Cambridge team respectively, both of which centred on the shear behaviour of reinforced concrete deep beams.

9.4 CIRIA GUIDE: PROVISIONS FOR DEEP BEAMS WITH HOLES

The exhaustive literature study conducted by CIRIA during the compilation of the Guide [9], failed to find sufficient test data on the effects of web openings on deep beams. Indeed, the only reference quoted in the CIRIA Guide is a paper co-authored by the Author [35]. As a result the recommendations are necessarily restrictive.

Any opening, which is likely to significantly disturb the stress pattern that would obtain in a solid deep beam, is deemed 'inadmissible' under the rules. Typical stress patterns derived by elastic analysis are given in a series of diagrams which detail the conditions to be satisfied for an opening to be considered 'admissible'. As an example, the diagram which gives the conditions for a top-loaded beam is reproduced here

in Fig.(9.5). The Guide does not include a diagram for the two point loading condition of the present tests, but from an examination of Fig.(9.5) it may be deduced that the spirit of the Guide's recommendations would result in restrictions similar to that shown in Fig.(9.6). It may be seen (Fig.9.6) that, except for opening type 11 (Fig.5.2), all of the other openings in the present tests (cf.Fig.4.2 and 5.2) are deemed 'inadmissible'.

Openings, that are admissible under the rules, are assumed by the Guide to be unlikely to disturb the overall behaviour of the beam. The Guide, therefore, requires that reinforcement around the opening, need only be provided to prevent local excessive cracking. For this purpose, the opening is considered to be located in a sensibly uniform, possibly biaxial, field of stress, and the amount of reinforcement required is to be determined as follows. Each side of the opening is considered to act as a simply supported deep beam, subjected to the resolved forces set up within the primary deep beam. This system of notional deep beams is shown in Fig.(9.7). The load system assumed to act on each notional beam is derived either directly from a consideration of the primary loading or by the use of a number of principal stress diagrams. One such diagram is reproduced here in Fig.(9.8). The load acting on each pair of notional deep beams is determined by calculating, from the given stresses at the centre of the opening, the total force in each direction that would have crossed that region in the solid beam occupied by the opening. Having established the loading system each notional beam is then reinforced according to the 'simple rules' as described earlier. Where the principal stresses are

not orthogonal to the opening, the reinforcement is determined from consideration of an equivalent hole as shown in Fig.(9.9), which also shows the recommended local reinforcement pattern.

The origins of the theoretical elastic basis of the CIRIA provisions for openings would appear to be founded in a method described by Uhlmann [13] in 1952. Ulhmann's method was similarly based on a calculation of notional forces acting on an opening and similarly made use of the elastic stress patterns obtained for solid deep beams. To determine the design tensile forces, from which the required amounts of reinforcement would be calculated, Uhlmann modified the notional forces by stress concentration factors; these having been derived from a photo-elastic study of the effects of holes on uniform stress fields.

To sum up this section, it may be broadly concluded that the results of the tests on deep beams with openings, which are reported herein, would indicate that the CIRIA provisions for openings should produce serviceable designs. It has been stated [35] that 'the effect of an opening on the ultimate strength of a deep beam depends primarily on the extent to which it intercepts the load path joining the load bearing blocks at the loading point and at the support reaction point': hence, by definition, the type of small opening considered 'admissible' by the Guide has little effect on the overall behaviour of a beam and hence on the ultimate limit state. As regards the provisions for the design of the reinforcement around the 'admissible' opening; it does seem that these are rather over elaborate when it is considered that their purpose is to attempt to satisfy serviceability limit state conditions.

Indeed, the elastic assumptions on which the reinforcement provisions are based, are only applicable at best, to the service load condition.

In the absence of any specific test evidence on the behaviour of small 'admissible' openings, it may reasonably be inferred from the broad experience gained from the present range of tests, that the serviceability problem of possible local cracking at such openings could be solved simply by a provision which specified a minimum qnntity of nominal reinforcement. The amount of reinforcement required might be conservatively based on the 'lost' tensile capacity of the opening; that is (a) x (b) x (f_t) where (a) is the dimension of the opening for the direction being considered; (b) is the beam thickness; and (f_t) is the tensile strength of the concrete (or assume say (f_t) = 0.52 $\sqrt{f_{cu}}$ for normal weight concrete). For example, taking f_y = 410 N/mm^2 and f_{cu} = 30 N/mm^2 the percentage of reinforcement along each side of the opening (size say (a) x (a)) would be $\frac{1}{2}$ (0.52 $\sqrt{f_{cu}}$/0.87 x 410) x (a) x (b) x 100 = 0.4% x (a) x (b). It is recommended here, that bars detailed to trim the opening should be fully anchored and preferably extend at least a length 2 x (a) each side of the opening, to ensure an effective distribution of the tensile forces into the surrounding concrete. (Note: the tests reported herein demonstrated that too local a system of reinforcement (for example Fig.(5.1) and Fig.(6.1): web reinforcement Type 5) - and this could include the one recommended by CIRIA (Fig.9.9) - might not be satisfactory).

Where the location or size of a particular opening is

unavoidable and it is such that it fails to satisfy the admissibility criteria given in the Guide, then consideration has to be given to the opening's possible effect on the ultimate limit state capacity. The tests reported herein have demonstrated that the best thing then is to consider the actual failure mode, but this is not easy because engineers do not yet have sufficient experience with deep beams. However, it is suggested that the proposed structural idealization given in Chapter 7 of this thesis and the simple design method presented in Chapter 8 are useful in this respect. The proposed structural idealization should prove a powerful tool to the designer, both for the visualization of the load transfer mechanism in deep beams with openings and for the prediction of their ultimate strengths.

CHAPTER TEN

CONCLUSIONS AND SUGGESTIONS FOR FURTHER RESEARCH

10.1 CONCLUSIONS

10.2 SUGGESTIONS FOR FURTHER RESEARCH

CHAPTER TEN

CONCLUSIONS AND SUGGESTIONS FOR FURTHER RESEARCH

10.1 CONCLUSIONS

The design of reinforced concrete deep beams with web openings is not yet covered by the major codes of practice, such as CP110:1972, ACI318-71, and the CEB-FIP Recommendations (1970). Little information is available in the literature on the effects of web openings, and as a result the provisions for the design of deep beams with web openings as given in the (new) CIRIA guide are necessarily restrictive.

It is hoped that the conclusions of the research work presented here will be of direct use to engineers engaged in this branch of reinforced concrete design and that it will assist in the advancement of this aspect of engineering science.

It is to be noted that discussions of some of the experimental results have already been presented elsewhere [35, 63]. The following list of conclusions is based on the sum total of the work reported herein, which included tests to destruction carried out on 79 reinforced concrete deep beams:

(i) The effect of a web opening on the ultimate shear strength, on crack widths, and on deflection depends primarily on the extent to which the opening intercepts the natural 'load path' joining the loadbearing blocks at the

loading point and the support reaction point, and on the location at which this interception occurs.

(ii) Where the opening is clear or reasonably clear of the 'load path' mentioned in paragraph (i), the ultimate shear may be estimated from Eqn.(7.1). Where the opening intercepts the 'load path' the ultimate shear strength may be estimated from Eqn.(7.2).

(iii) Web reinforcement substantially increases the ultimate load capacity of deep beams with web openings, but proper detailing of the reinforcement is critically important. Inclined web reinforcement is the most effective type as regards both ultimate shear strength and crack width control. Local reinforcement in the form of bars trimming the openings has little effect on ultimate shear strength.

(iv) The general behaviour of normal weight concrete and lightweight concrete deep beams is very similar, and any differences in cracking loads and in ultimate shear strengths may be accounted for by the difference between the potential tensile capacity of structural normal weight concrete and that of structural lightweight concrete.

(v) The simple design method suggested in this thesis is reasonably satisfactory and is applicable to a wide range of opening locations. The proposed structural idealization should prove a powerful tool to the designer, both for the visualization of the load transfer mechanism in deep beams and for the prediction of their ultimate strengths.

10.2 SUGGESTIONS FOR FURTHER RESEARCH

(i) The size of the test specimens used in the present

investigation was as large as was compatible with the range of variables investigated. Further selective tests using large scale specimens are required to confirm that the present results are not affected by scale.

(ii) Inclined web reinforcement is more expensive to bend and fix than conventional orthogonal mesh reinforcement but the performance of inclined reinforcement is significantly better than all other types used in current practice. Further tests to investigate the optimum percentage of inclined reinforcement would be valuable.

(iii) Taylor [61] of the Cement and Concrete Association has conducted some special tests on ordinary shallow beams in shear, and made some useful deductions about the relative significance of the various shear parameters, such as aggregate interlock, dowel action, and the compression zone. Parallel tests of deep beams may lead to some interesting observations.

(iv) The results of the exploratory tests on end anchorage of the main steel (Appendix 1) have indicated that further tests are desirable to establish design criteria for anchorage requirements in deep beams.

(v) The deep beam data collected by the Nottingham - Cambridge team would seem to be the most comprehensive to date and would justify further detailed examination and re-evaluation, which might well lead to yet a better understanding of deep beam behaviour and a yet more efficient design procedure.

A P P E N D I X O N E

ANCHORAGE OF TENSION REINFORCEMENT IN LIGHTWEIGHT CONCRETE DEEP BEAMS

A1.1 INTRODUCTION AND BACKGROUND

A1.2 TEST PROGRAMME

A1.3 TEST RESULTS

A1.3.1 Deflection control

A1.3.2 Crack control

A1.3.3 Crack patterns and modes of failure

A1.4 GENERAL COMMENTS

A P P E N D I X O N E

ANCHORAGE OF TENSION REINFORCEMENT IN LIGHTWEIGHT CONCRETE DEEP BEAMS.

A1.1 INTRODUCTION AND BACKGROUND

It would seem that, for some time yet, the design assumptions regarding the end anchorage requirements of the longitudinal tension reinforcement must remain rather conservative, because extensive surveys [6,7,9-12] have confirmed that very few systematic investigations have been carried out to provide information on the effects of various amounts of end anchorage on the strength and crack control of deep beams. For example, many of the conclusions previously reported were based on tests in which end-anchorage failure had been precluded by anchoring the longitudinal tension bars to steel blocks [11,12,24] or by using other devices [26,64].

In deep reinforced concrete beams, the full tensile force must be developed in anchorage at the supports, because of the arch action behaviour which is thought to occur at ultimate loads [24,25]. Untrauer and Henry [66] have reported that pressures normal to the tension reinforcement may have significant influence on bond strength: in tests made on 37 pull-out specimens, which were subjected to a range of normal pressures, the bond strength was found to increase in proportion to the square root of the applied normal pressure [66].

At the University of Nottingham, tests recently carried out by Singh [12] have indicated that the usual design

assumptions, regarding end anchorage of the main steel in deep beams, might be unnecessarily conservative. In a test programme consisting of 24 lightweight concrete deep beams, the amount of end anchorage provided for the main longitudinal tension steel was varied systematically from zero to an embedment length of twenty-five times bar diameter. In all of the beams web reinforcement was provided; either inclined web reinforcement or an orthogonal mesh satisfying Section 11.9.6 of ACI318-71 [4]. (Fig. A1.1).

Singh's tests provided some valuable information on deep beam behaviour but it was not clear what effects the provision of web reinforcement had had on the requirements for end anchorage, particularly as analysis of the flexural strengths showed that the quantity of web reinforcement provided could have contributed as much as 50% of the ultimate flexural strength. It was therefore desirable to supplement Singh's test programme with further tests on comparable deep beams but without web reinforcement. In this Appendix, the details and results of nine follow-up tests are given, and general observations are drawn from the evidence of all thirty-three tests.

A1.2 TEST PROGRAMME

The test specimens were designed to be complementary to Singh's [12] tests and as previously [12], in planning the test programme where reference to a code of practice was desirable, ACI318-71 [4] was used as the main guide (the current British Code CP110: 1972 [3] does not yet cover deep beams).

The test specimens consisted of 9 simply supported sintered-fly-ash lightweight concrete deep beams (Fig.A1.2 and Table A1.1), of width b 102 mm and overall depth D 762 mm (Note: the beams were cast in Imperial sized moulds). Two different span lengths L were used: 1524 mm span in three beams with a clear-shear-span/depth ratio x/D of 0.55 and 952 mm in six beams with an x/D ratio of 0.30.

The concrete materials and proportions, reinforcement properties and other general experimental details were the same as those given in Chapter 3. Details of concrete strengths are given in Table (A1.1).

The main longitudinal reinforcement in each beam consisted of two 8 mm dia. deformed bars; no web reinforcement was provided. These bars were anchored by different embedment lengths beyond the centre line of the support reaction (Table A1.1, Column 4). In those beams with an x/D ratio of 0.3, the anchorage was either an ACI standard hook (ACI318-71: Section 7.1.1.1)[4] or one of the following embedment lengths: 25 times bar diameter d_b, 20 d_b, 15 d_b, 10 d_b, or nil, plus one of (25 d_b + standard hook). In those beams with an x/D ratio of 0.55, the anchorage was either a standard hook or 10 d_b embedment length or nil. The equivalent embedment length of a standard hook, computed from Section 12.8.2 of ACI318-71, is 17.25 d_b. Hence all the embedment lengths used in the tests (except for the one beam with 25 d_b+ hook) were substantially less than the development length l_d specified by Section 12.5 of ACI318-71, which is 305 mm (12 in), i.e., 38.1 d_b for 8 mm diameter bars.

Details of the test procedures and equipment have

been given in Chapter 3. Briefly, the loads and reactions (Fig.A1.2) were applied through circular rollers and 102 x 89 x 29 mm steel bearing blocks bedded to the concrete with quick setting plaster. One of the support reaction assemblies was specially mounted on steel rollers to give freedom for a larger range of axial translation (Fig.A1.5, see Beam 0-0.3(0) for example, left hand support). Central deflections were measured with 0.01 mm dial gauges, compensation being made for support settlements as measured; crack widths were measured with a hand microscope of 25 magnifications.

A1.3 TEST RESULTS

A1.3.1 Deflection control

Fig.(A1.3) shows that within the individual series of each group of beams with the same x/D ratio, progressive reduction of the embedment length of the tension reinforcement did not increase deflections by significantly large amounts. All of the beams exhibited a marked increase in deflections at the load producing the first flexural crack, indicating that the tension bars yielded at the first-cracking load. Beams 0-0.55(0) and 0-0.30(0) failed prematurely as a result of complete loss of end anchorage. Apart from these two beams, the effect of the amount of end anchorage was not clearly observable.

A1.3.2 Crack control

The flexural cracks were usually widest at the beam soffit at formation, but after a few more load increments the

widest part of a flexural crack was always about 150 mm to 300 mm up the soffit, irrespective of the embedment length. Fig.(A1.4), shows that the crack widths were usually as wide as ½ mm at formation, and the cracks opened up to about 10 mm before ultimate collapse occurred. As in the case of deflection control, Fig.(A1.4) shows that the anchorage of the tension reinforcement did not have a clearly observable effect except for Beams 0-0.55(0) and 0-0.30(0) which had zero embedment lengths and failed prematurely.

A1.3.3 Crack patterns and modes of failure.

The tests showed the crack pattern and failure mode (Fig.(A1.4)) were not influenced by the amount of end anchorage, except that the two beams 0-0.55(0) and 0-0.30(0) failed by the pulling-out of the tension reinforcement. The failure mode in all of the other beams was in flexure: collapse was preceded by yielding of the reinforcement and a single central flexural crack, to which all other flexural and inclined flexure-shear cracks were like tributaries, penetrated the compression zone to within 25 mm of the beam top to cause crushing of the concrete adjacent to the loading point. Similar flexural failures for beams with small amounts of tension reinforcement (0.125% in the present tests) have been reported by others, for example, Leonhardt and Walther (see Chpt.1.2.2.2). It is noted that the diagonal splitting type cracks which caused failure in those solid beams without web reinforcement reported in Chpts.4,5 and 6 did not occur. In those beams the amount of tension reinforcement provided was 0.42%.

A1.3.4 Ultimate loads

Table (A1.2) shows the measured ultimate loads and, again, except for Beams 0-0.55(0) and 0-0.3(0), no observable effects of the amount of end anchorage were evident.

Analysis of the ultimate loads showed that at collapse the stress in the reinforcement approached the ultimate tensile stress of the steel. In the flexural design of deep beams, the usual procedure in current practice is to calculate the main steel requirements on the basis of an assumed value for the internal lever arm of approximately 0.6D, where D is the overall depth. For example, in the new CIRIA design guide [9] the lever arm z is taken as $z = 0.2\ L + 0.3D$ and the required amount of tension reinforcement A_s is given by

$$A_s = \frac{M}{0.87 f_y z} \qquad \text{(see Chapter 9:Eqn.9.1)}$$

In Column 2 of Table (A1.2) the ratios of measured ultimate load to the design load according to the equation given above are presented, and it may be seen that there is an in-built factor of safety on collapse of approximately 3 for beam with x/D of 0.3, and 2.5 for beams of x/D equal to 0.55.

A1.4 GENERAL COMMENTS

The tests here reported together with those of Singh [12] were necessarily exploratory in nature; hence it is desirable to summarise the main observations rather than draw firm conclusions. It was observed that: [37]

1. The progressive reduction of the end anchorage of the tension

reinforcement down to an embedment length of ten bar diameters did not produce clearly observable detrimental effects on ultimate loads, maximum crack widths, or deflections

2. Within each series of test beams, an embedment length of ten bar diameters was not less efficient than an ACI standard hook.

3. The present tests showed that web reinforcement as provided in Singh's beams could contribute significantly to the flexural strength. The provision of an orthogonal mesh satisfying Section 11.9.6 of ACI 318-71 or of an equivalent amount of inclined web reinforcement could almost double the ultimate load.

Observation 3 above follows from the laws of equilibrium, which are unaware of the designer's distinction between "flexural reinforcement" and "shear reinforcement". Observation 2 was unexpected, and Observation 1 indicates that the current assumptions regarding the end-anchorage requirements of the tension reinforcement are possibly too conservative, particularly for deep beams with web reinforcement (and, in practice, the provision of a proper system of web reinforcement is virtually mandatory). However, it is not prudent to recommend a relaxation of the current end-anchorage requirements on the evidence from one test programme. The ACI Committee 408 has called for further experimental research on bond and development in lightweight concrete structural elements [52] and the ACI Committee 439 has also pointed out that "there has been little experimental research on the bond strength of reinforcing

bars with a minimum yield strength greater than 414 N/mm^2 (60 ksi)" [65]. It is hoped that, together with Singh's tests at Nottingham, the test results presented herein, besides providing information on deep beam behaviour, will stimulate others to further investigations. It does seem that the anchorage capacity of the tension reinforcement might be significantly increased in the presence of the high compressive stresses in the support regions of deep beams.

APPENDIX TWO

SHEAR STRENGTH OF LIGHTWEIGHT DEEP BEAMS SUBJECTED TO REPEATED LOADS

A2.1 INTRODUCTION

A2.2 TEST PROGRAMME

A2.2.1 Test specimens

A2.2.2 Testing

A2.3 TEST RESULTS

A2.3.1 Deflection and crack widths

A2.3.2 Crack patterns and modes of failure

A2.3.3 Ultimate loads

A2.4 SUMMARY

A P P E N D I X 2

SHEAR STRENGTH OF LIGHTWEIGHT DEEP BEAMS SUBJECTED TO REPEATED LOADS.

A2.1 INTRODUCTION AND BACKGROUND

Recent literature surveys [9,11] have shown that little test data are available on lightweight concrete deep beams subjected to repeated loadings. Indeed, the effect of repeated loading on all types of structural reinforced concrete members has received scant consideration from codes of practice: codes merely mention that vibrations should be considered, but without stating how. Contrary to general opinion, Crockett [67] has recently claimed that reinforced concrete structures designed to current codes may collapse under fatigue loading conditions and that the number of load applications should be as important a design factor as load magnitude if progressive cracking and failure is to be avoided.

At the University of Nottingham an exploratory programme of repeated load tests was carried out by Singh [12,32] on 18 lightweight concrete deep beams. The aims of the programme were to investigate whether the various static shear strength formulas proposed for deep beams could be applied to lightweight beams which had a repeated-load history, and to compare the relative effectiveness of three types of web reinforcement under the repeated loading condition. From the results of the tests, it was observed that the loadcyclings had no appreciable over-all effects on the ultimate shear strengths.

However, it was suggested that it would seem desirable to investigate the effect of substantially increasing the number of cycles.

In this Appendix, the details and results of three further tests carried out to supplement Singh's test programme are presented. In these tests the repeated-loading history given to each beam consisted of 520,000 cycles; in Singh's tests each beam was subjected to 45,000 load cycles. Whenever possible the results of the present tests are discussed in relation to the previous tests carried out by Singh.

A2.2 TEST PROGRAMME

A2.2.1 Test specimens

The test specimens (Table A2.1) consisted of 3 sintered fly-ash lightweight concrete deep beams of constant thickness b equal to 76 mm; the other dimensions are as shown in Fig.(A2.1). Each beam was designed to be identical to one of Singh's [32] test specimens. The longitudinal tension reinforcement in each beam consisted of one 20 mm diameter deformed bar of yield stress 440 N/mm^2. 6 mm deformed bars of yield stress 445 N/mm^2 were used for all web reinforcement. The three types of web reinforcement were used as shown in Fig.(A2.1) (A) An orthogonal system satisfying the steel ratio requirements of Section 11.9.6 of ACI318-71 (as given here in Chpt.2.2.2); (B) An orthogonal system in which the horizontal stirrups were more closely spaced near the beam soffit, and (C) An inclined system, which had previously been found to be highly effective

for static loading condition [28, 29, 31]. The web steel ratio P_{web} for all the beams was kept constant at 0.012, being 3 times the minimum value specified by Section 11.9.6 of ACI318-71.

The general experimental details of beam manufacture were the same as those given in Chapter 3. Details of concrete strengths are given in Table (A2.1).

A2.2.2 Testing

Two-point top loading (Fig.A2.1 and Fig.A2.5) was applied through hydraulic pulsatable jacks; steel load-bearing blocks of size 89 x 76 x 29 mm were used. Each beam was first loaded, statically, to the ACI design load, 2 V_u, where V_u is the design shear force computed from ACI318-71 (see Chapter 2.2.2). The load was then cycled in stages at a frequency of about 10 cycles per minute. Stage 1 consisted of 120,000 cycles between the ACI load and 0.5 ACI load. The load was next increased statically to 1.25 times the ACI load and Stage 2 cycling was applied; this consisted of 300,000 cycles between 1.25 ACI load and 0.5 ACI. For the first of the three beams tested, Beam C-2/0.4, the load was then increased statically until collapsed occurred. For Beams A-2/0.4 and B-2/0.4 a third cycling stage was introduced prior to loading to collapse; Stage 3 consisted of 100,000 cycles between 1.5 ACI load and 0.5 ACI load.

A2.3 TEST RESULTS

A2.3.1 Deflection and crack widths

In Fig.(A2.2) and (A2.3), the mid-span deflections and maximum diagonal cracks widths are, respectively, plotted against the applied loads. Figure (A2.2) shows that deflections increased during each stage of load cycling. During Stage 1 the initial central deflection was increased by about 25% for Beam A-2/0.4 and B-2/0.4, but substantially less for Beam C-2/0.4, 13%. In Stage 2 the increase in deflection was comparable for all three beams, being about 20%. Stage 3 produced much smaller increases in deflection, about 6%. These increases in deflection were significantly greater than the increases observed in the previous tests: however, in Fig.(A2.4) the overall deflection behaviour of both the present and corresponding previous tests are compared, and it would seem that the increased repeated-loading history had very little overall effect (excluding the inexplicably poor performance of Singh's beam C-2/0.4*). It is also to be noted that no appreciable difference in the effectiveness between each type of web reinforcement was observable, and that the deflection just prior to collapse was in any case small, being only about 3 mm in each beam (1/500 times the span).

A2.3.2 Crack patterns and modes of failure

The crack patterns at failure are shown in Fig.(A2.5). In Beams A-2/0.4 and B-2/04, which contained, respectively, a mesh system and a modified mesh system of web reinforcement (Fig.A2.1), diagonal cracks formed before the Stage 1 cycling at the ACI load. In Beam C-0.2/4 the diagonal cracks occurred generally during the load cycling and the effectiveness of the web reinforcement in controlling the growth and

propagation of diagonal cracks is evident from the appearance of the crack pattern, which shows a large number of relatively small discontinuous cracks. The widths of these diagonal cracks remained small up to collapse, whereas the web reinforcements in Beam A-2/0.4 and B-2/0.4 were not so efficient; and the maximum diagonal crack widths for these beams exceeded 0.4 mm just prior to collapse (Fig.A2.3).

The failure modes of the beams were similar to those previously observed by Singh [32]. In all of the beams substantial crushing of the concrete occurred at collapse. In Beam C-2/0.4 (Fig.A2.5) flexural cracks penetrated into the compression zone below the loading point to cause an extensive crushing failure there. In Beam B-2/0.4 the failure mode would seem to be a pure bearing type failure at the supports, although cine-film records of Singh's tests have showed that such crushings were preceded by the penetration of diagonal cracks into the concrete zones near the bearing blocks [32]. In Beam A-2/0.4, diagonal cracking,accompanied by crushings at the loading and support points, caused the beam to be split into two. It is worth mentioning that at collapse the bearing pressures at the supports and loading points in all of the beams were greater than the cube strength of the concrete; the average bearing pressures were 52 N/mm^2 compared with cube strengths of 43 N/mm^2 (Table A2.1).

A2.3.3 Ultimate loads

The measured ultimate loads together with the computed ACI design loads and the measured diagonal cracking

loads are shown in Table (A2.2). The results, being not significantly different to the measured ultimate loads in Singh's tests (Table A2.2: Column 5), would indicate that the increased repeated load history had little effect on ultimate strengths. In connection with the ACI load computations, it should be pointed out that Sections 11.9.5 and 11.9.6 of ACI318-71 do not cover the web reinforcement types B., and C. However, in the computation of the ACI load here, the contribution of types B and C web reinforcement was assumed to be the same as that of type A web reinforcement. This approach was thought to be more reasonable than neglecting any web reinforcement not covered by ACI318-71.

A2.4 SUMMARY

The three tests reported herein were specifically designed to supplement similar previous tests carried out at Nottingham. The results of the tests would indicate that the observations previously recorded were not affected by the substantial increase in the number of loading cycles. However, it should be mentioned that fatigue failure in reinforced concrete normally follows gradual increase of cracking and deflection as progressive bond failure occurs between steel and concrete. In both the previous and the present tests, the main steel reinforcement was anchored to steel bearing blocks and deformed reinforcement bars were used. These two factors, which have a substantial influence on bond, may have contributed to the observed overall lack of sensitivity to repeated loading. Further testing of reinforced concrete deep beams with plain mild steel reinforcement would be valuable.

R E F E R E N C E S

1. KONG, F.K., and SHARP, G.R. Reinforced concrete deep beams with web openings. Paper presented at Cambridge University Mechanics Colloquium, 8 November 1973.

2. STEVENS, A., et al. (Draft) Design guidance for deep beams. Prepared under CIRIA's supervision, Ove Arup and Partners, 1975 (see also reference 9).

3. BRITISH STANDARDS INSTITUTION. CP 110: Part 1: 1972. The structural use of concrete. London. pp.154.

4. ACI COMMITTEE 318. Building code requirements for reinforced concrete: ACI 318-71. Section 11.9 - Special provision for deep beams. Detroit, American Concrete Institute, 1971, pp.78.

5. COMITE EUROPEEN DU BETON AND FEDERATION INTERNATIONALE DE LA PRECONTRAINT. CEB-FIP International recommendations for the design and construction of concrete structures. pp.80. Appendix 3: International recommendations for the design and construction of deep beams. London, Cement and Concrete Association, 1970. pp.17-24.

6. ANON. Bibliography on deep beams. London, Cement and Concrete Association, 1969. pp.8. Library Bibliography No. Ch. 71.

7. ALBRITTON, G.E. Review of literature pertaining to the analysis of deep beams. Vicksburg, U.S. Army Engineer Waterways Experiment Station, November 1965. pp.80 Technical Report No.1-701.

8. PORTLAND CEMENT ASSOCIATION. Concrete Information ST66: design of deep girders. Chicago 1946.

9. OVE ARUP and PARTNERS. The design of deep beams in reinforced concrete. London, Construction Industry Research and Information Association, January 1977, pp 131. CIRIA Guide 2.

10. COLE, D.F. Behaviour of deep reinforced concrete beams. M.Sc. thesis, University of Nottingham, 1968. 325 pp.

11. ROBINS, P.J. Reinforced concrete deep beams studied experimentally and by the finite element method. PhD. thesis, University of Nottingham, 1971. 258 pp.

12. SINGH, A. Static and repeated loads on lightweight concrete deep beams. MPhil. thesis, University of Nottingham, 1972. 111 pp.

13. DISCHINGER, F. Beitragzur Theorie der Halbscheibe und des wandartigen balken. Int. Assn. for Bridge and Structural Engineers Publications, Zurich, Vol.1, 1932. pp. 69-93.

14. COULL, A. Stress analysis of deep beams and walls. The Engineer. Vol. 22, No.5744. February 1966. pp.310-312.

15. SCIAMMERELLA, C.A. Effect of holes in deep beams with reinforced vertical edges. Engineering Progress at the University of Florida. Vol.17. No.12. December 1963.

16. SAAD, S., and HENDRY, A.W. Gravitational stresses in deep beams. The Structural Engineer. Vol.39. No.6. June 1961. pp.185-194.

17. ARCHER, F.E., and KITCHEN, E.M. Stress distribution in deep beams. Civil Engineering and Public Works Review. Vol.55, No.643. February 1960. pp.230-234.

18. CHOW, L.E., CONWAY, H.D., and WINTER, G. Stresses in deep beams. Transactions - American Society of Civil Engineers. Vol.118, Paper 2557. 1953. pp.686 - 708.

19. SAVIN, G.N. Stress concentrations around holes. Pergamon Press. 1961.

20. RAVILLE, M.E., and McCORMICK, F.J. Stresses in deep beams subjected to central and thirdpoint loading. Proc. A.S.T.M., Vol.59. 1959.pp.1230-1236.

21. UHLMANN, H.L.B. The theory of girder walls with special references to reinforced concrete design. The Structural Engineer. Vol.30. August 1952. pp.172-181.

22. SAAD, S., and HENDRY, A.W. Stresses in a deep beam with a central concentrated load. Exp. Mech., Vol.1. No.6. June 1961. pp.192-198.

23. COMITE EUROPEEN DU BETON. Recommendations for an International Code of Practice for Reinforced Concrete (English ed.). London, American Concrete Institute and Cement and Concrete Association, 1964.

24. DE PAIVA, H.A.R., and SIESS, C.P. Strength and behaviour of deep beams in shear. Proceedings A.S.C.E., Vol. 91, No. ST5. October 1965.pp.19-41.

25. LEONHARDT, F., and WALTHER, R. Wandartige Träger (Deep Beams). Deutscher Ausschuss für Stahlebeton. Bulletin 178, 1966, Wilholm Ernst und Sohn (Berlin). CIRIA Translation, January 1970.

26. CRIST. R.A. Static and dynamic shear behaviour of uniform ly reinforced concrete deep beams. Ph.D. thesis, University of New Mexico, 1971.

27. KONG, F.K., ROBINS, P.J., and COLE, D.F. Web reinforcement effects on deep beams. Journal of the American Concrete Institute. Proceedings Vol.67, No.12. December 1970. pp. 1010-1017.

28. KONG, F.K., and ROBINS, P.J. Web reinforcement effects on lightweight concrete deep beams. Journal of the American Concrete Institute. Proceedings Vol. 68, No.7. July 1971. pp.514-520.

29. KONG, F.K., ROBINS, P.J., KIRBY, D.F., and SHORT, D.R. Deep beams with inclined web reinforcement. Journal of the American Concrete Institute. Proceedings Vol. 69, No.3 March 1972. pp. 172-176.

30. KONG, F.K., and ROBINS, P.J. Shear strength of reinforced concrete deep beams. Concrete. Vol.6, No.3. March 1972. pp. 34-36.

31. KONG, F.K., and SINGH, A. Diagonal cracking and ultimate loads of lightweight concrete deep beams. Journal of the American Concrete Institute. Proceedings Vol. 69, No.8. August 1972. pp.513-527.

32. KONG, F.K., and SINGH, A. Shear strength of light-weight concrete deep beams subjected to repeated loads. Shear in reinforced concrete. Detroit, American Concrete Institute, 1974. ACI-ASCE Special Publication SP-42. Vol.2.pp. 461-476.

33. KONG, F.K., ROBINS, P.J., SINGH, A., and SHARP,G.R. Shear analysis and design of reinforced concrete deep beams. The Structural Engineer. Vol.50, No.10. October 1972. pp.405-409.

34. KONG, F.K., ROBINS, P.J., and SHARP, G.R. The design of reinforced concrete deep beams in current practice. The Structural Engineer. Vol.53, No.4. April 1975. pp.173-180.

35. KONG, F.K., and SHARP, G.R. Shear strength of lightweight reinforced concrete deep beams with web openings. The Structural Engineer. Vol.5, No.8. August 1973. pp. 267-275.

36. KONG, F.K., and KUBIK, L.A. Discussion of: Collapse load of deep reinforced concrete beams by P. KUMAR. Magazine of Concrete Research. Vol.29, No.98. March 1977. pp. 42-43.

37. KONG, F.K., SINGH, A., and SHARP, G.R. Anchorage of tension reinforcement in lightweight concrete

deep beams. Cambridge University Engineering Dept., Technical Report (in preparation).

38. STEVENS, A., and KONG, F.K. Reinforced concrete deep beams and CIRIA's draft design guide. Paper presented at Cambridge University Mechanics Colloquium, 8 May 1975.

39. DE PAIVA, H.A.R. Strength and behaviour in shear of reinforced concrete deep beams under static and dynamic loading. Ph.D. thesis, University of Illinois, 1961.

40. UNTRAUER, R.E. Strength and behaviour in flexure of deep reinforced concrete beams under static and dynamic loading. Ph.D.thesis, University of Illinois, 1961.

41. LAUPA, A., SIESS, C.P., and NEWMARK, N.M. Strengh in shear of reinforced concrete deep beams. Bulletin No.428. Eng. Expt. Station, University of Illinois. 1955. p. 59.

42. MAST. D.R. Design of auxiliary reinforcement in precast concrete connections. A.S.C.E. Structural Engineering Conference, Miami Beach, Florida, January 1966.

43. MOFFET, D.R. Stresses and strain in deep beams studied experimentally and by the finite-difference method. B.Sc. (Hons.) thesis, University of Nottingham, 1969.

44. BROCK, G. Effect of shear on the ultimate strength of beams with tensile reinforcement. ACI Journal. Proceedings Vol.56. January 1960. pp. 619-637.

45. BROCK, G. Discussion of: The riddle of shear failure and its solution by N.J. KANI. ACI Journal. Proceedings Vol.61, No.12. December 1964. pp. 1587-1590.

46. RAMAKRISHNAN, V., and ANANATHANARAYANA, Y. Ultimate shear strength of deep beqms in shear. ACI Journal. Proceedings Vol.65. No.2. February 1968. pp. 87-98.

47. SHEAR STUDY GROUP. The shear strength of reinforced concrete beams. Institution of Structural Engineers, London. January 1969. 170 pp.

48. ACI COMMITTEE 318. Commentary on building code requirements for reinforced concrete (ACI318-71). Detroit, American Concrete Institute, 1971.

49. PCA ENGINEERING SERVICES DEPT. Notes on ACI318-71. Chicago, Portland Cement Association, 1972.

50. NYLANDER. H., and HOLST, H. Reinforced concrete deep beams and slabs. Royal Technical University, Stockholm, 1946. (In Swedish; English translation by courtesy of Ove Arup and Partners, London).

51. ROBINS, P.J., and KONG, F.K. Modified finite element method applied to reinforced concrete deep beams. Civil Engineering and Public Works Review, Vol.68 November 1973. pp.963.

52. ACI COMMITTEE 408. Opportunities in bond research. ACI Journal. Proceedings Vol.67, No.11. November 1970. pp.857-867.

53. ANON. Lightweight concrete. News article. NCE, Magazine of the Institution of Civil Engineers. Thomas Telford Ltd., June 1974.

54. ANON. Lightweight concrete. Construction News Supplement. Northwood Publications Ltd., 6th.May 1976.

55. ACI BOARD COMMITTEE. Concrete - Year 2000. ACI Journal. Proceedings Vol.68, No.8. August 1971. pp. 581-589.

56. ANON. The all-round lightweight aggregate. Lytag general information brochure. September 1967. 8 pp.

57. TEYCHENNE. D.C. Structural concrete made with lightweight aggregates. Concrete. Vol.1, No.4 April 1967. pp. 111-122.

58. HANSON, J.A. Tensile strength and diagonal tensile resistance of structural lightweight concrete. ACI Journal. Proceedings Vol.58. July 1961.pp.1-37.

59. KONG, F.K., and EVANS, R.H. Reinforced and pre-stressed concrete. Nelson, London, 1975. 229 pp.

60. KANI, G.N.J. How safe are our large concrete beams? ACI J ournal. Proceedings Vol.65. March,1967.pp.124-141.

61. TAYLOR, H.P.J. Strength of large beams. Proceedings A.S.C.E., Vol.98, ST11. November 1972. pp.2473-2490.

62. BEAUMONT, C.J. An investigation of the behaviour of reinforced concrete deep beams. M.A. thesis, University of Cambridge, 1975.

63. KONG, F.K., and SHARP, G.R. Structural idealization for deep beams with web openings. Magazine of Concrete Research. Vol.29, No.99. June 1977.pp.81-91.

64. SMITH, K.N. and FEREIG, S.M. Effect of loading and supporting conditions on the shear strength of deep beams. ACI Publication SP42: Shear in reinforced concrete. American Concrete Institute, 1974,pp.441-460.

65. ACI COMMITTEE 439. Uses and limitations of high strength steel reinforcement. ACI Journal. Proceedings Vol.72, No.2. February 1973. pp.70-104.

66. UNTRAUER, R.E. and HENRY R.L. Influence of normal pressure on bond strength. ACI Journal. Proceedings Vol.62, No.5. May 1965. pp. 577-586.

67. ANON. Concrete fatigue - evidence of failure revealed. News article. NCE, Magazine of the Institution of Civil Engineers. Thomas Telford Ltd., 25 August 1977. (a paper for ICE is in preparation).

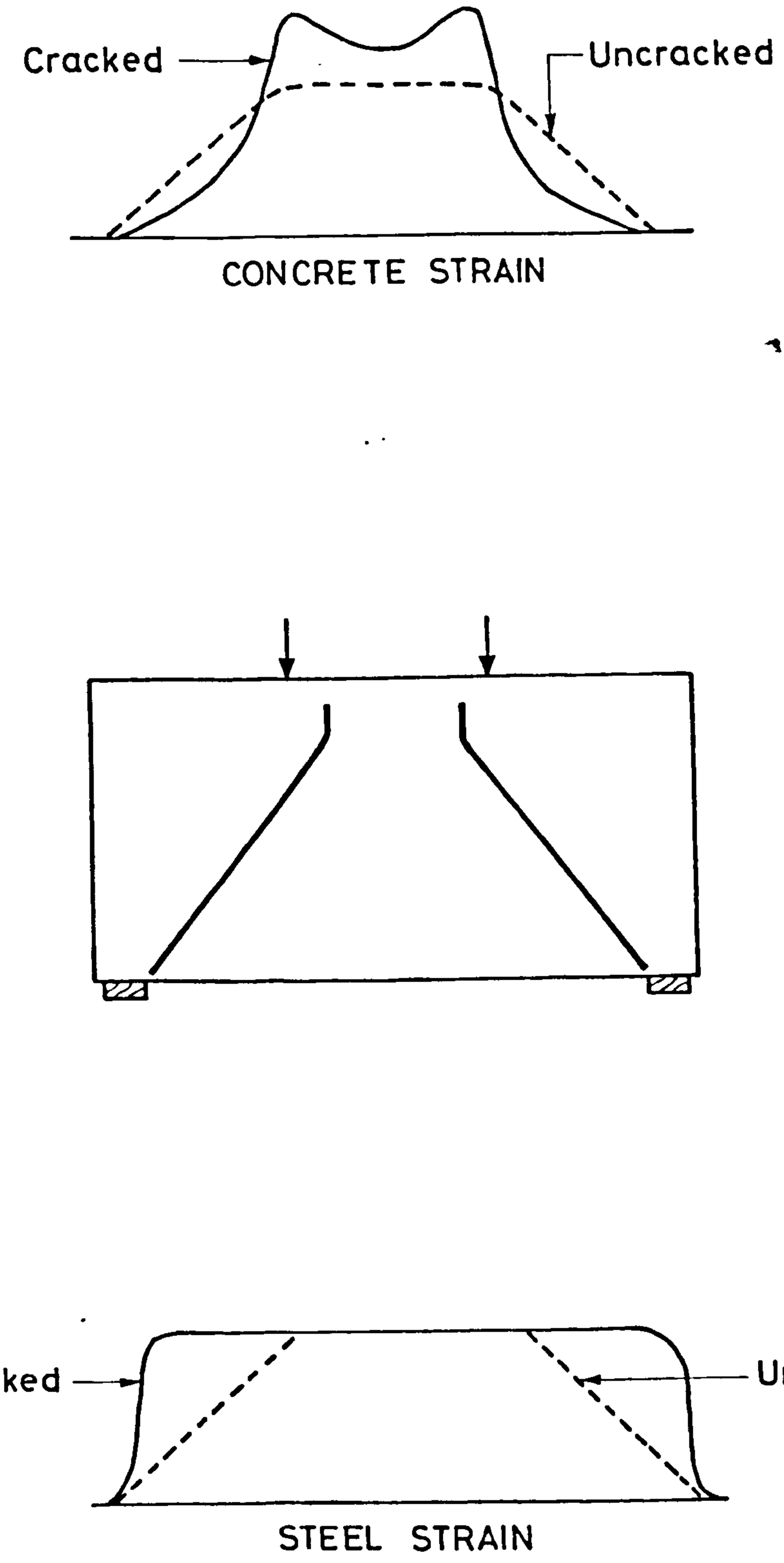

FIG.1.1 EFFECT OF INCLINED CRACKING ON STEEL AND CONCRETE STRAINS

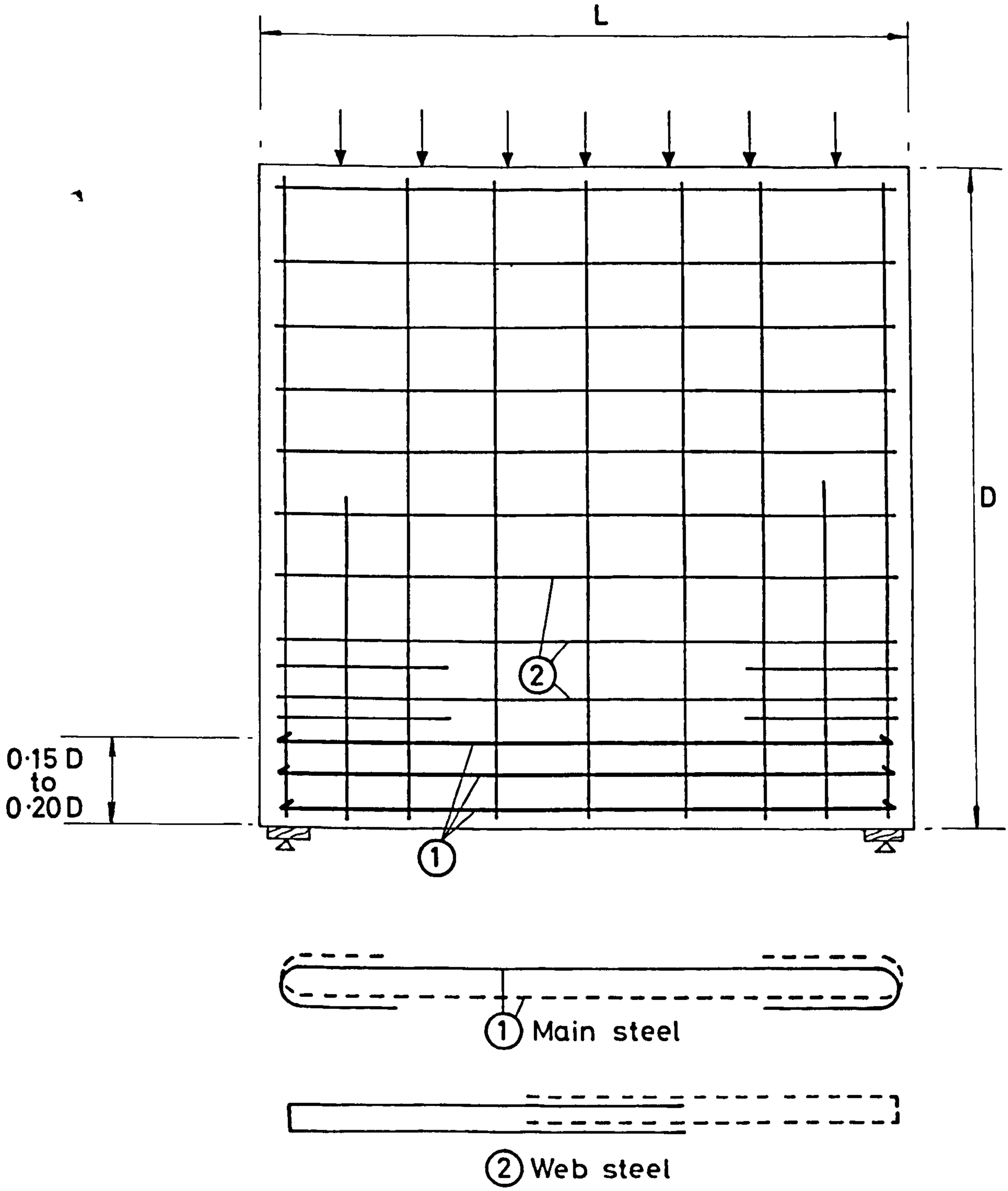

FIG.1.2 LEONHARDT AND WALTHER: REINFORCEMENT ARRANGEMENT

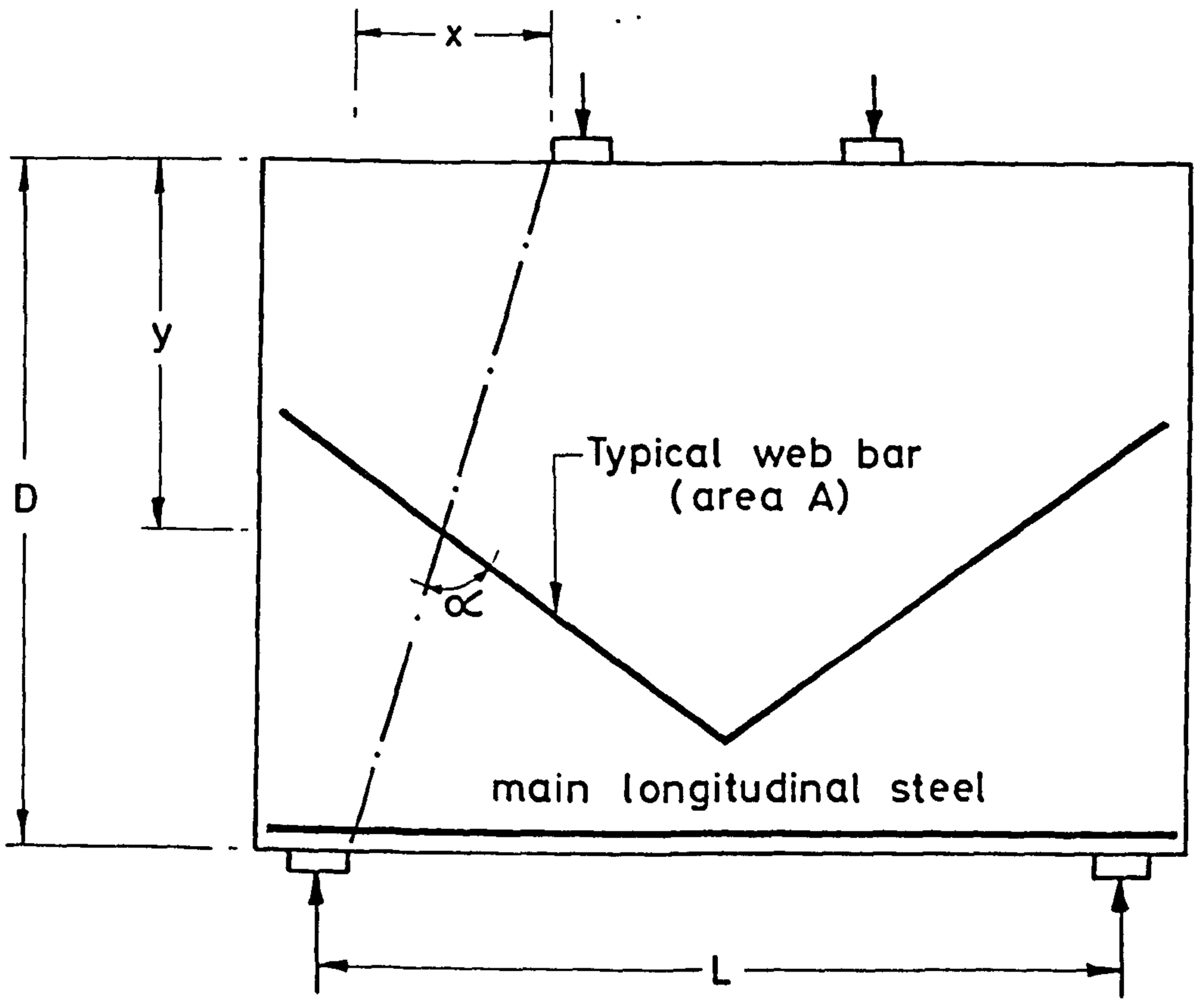

FIG.1.3 MEANINGS OF SYMBOLS

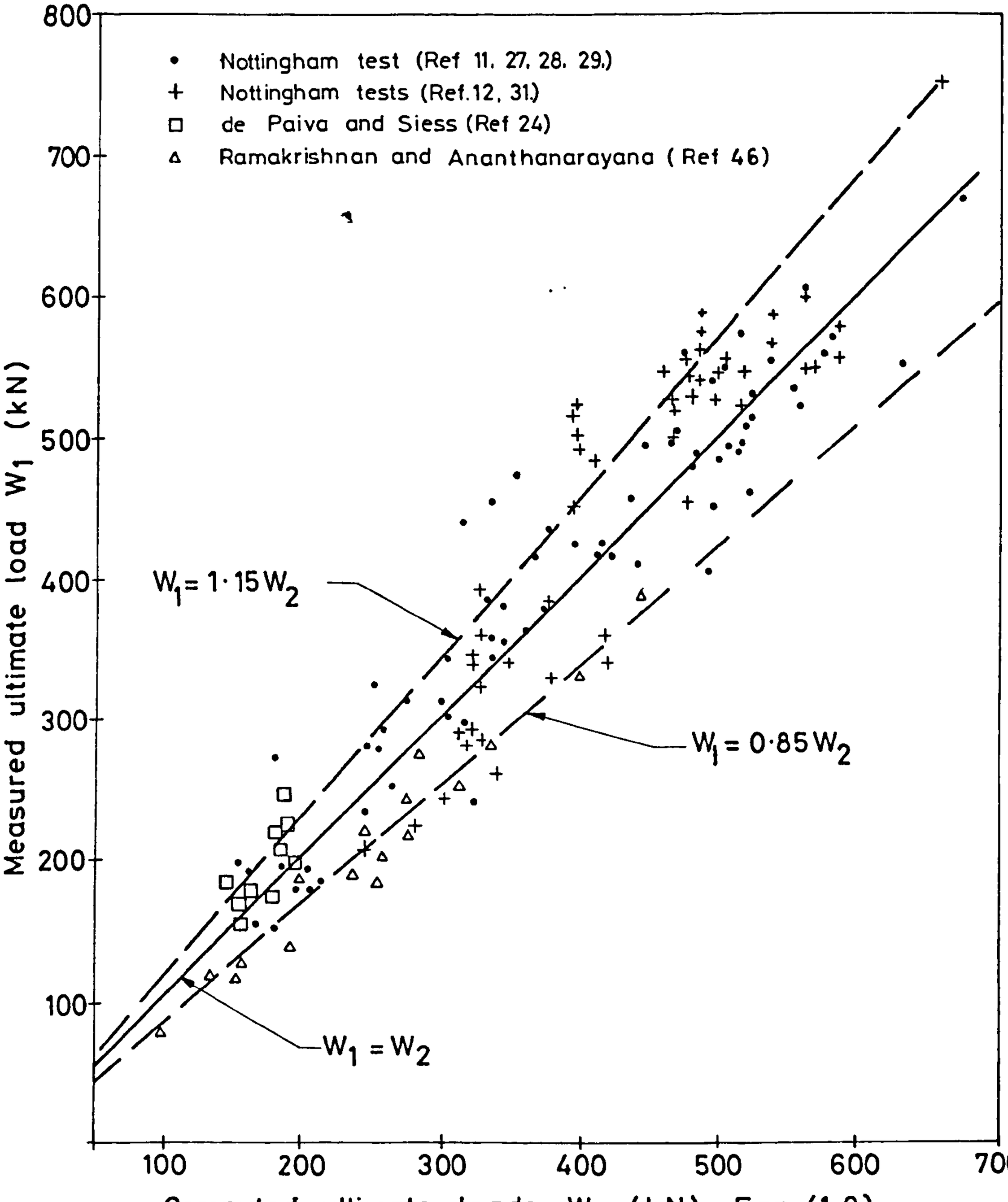

FIG.1.4 COMPARISON OF COMPUTED AND MEASURED ULTIMATE LOADS

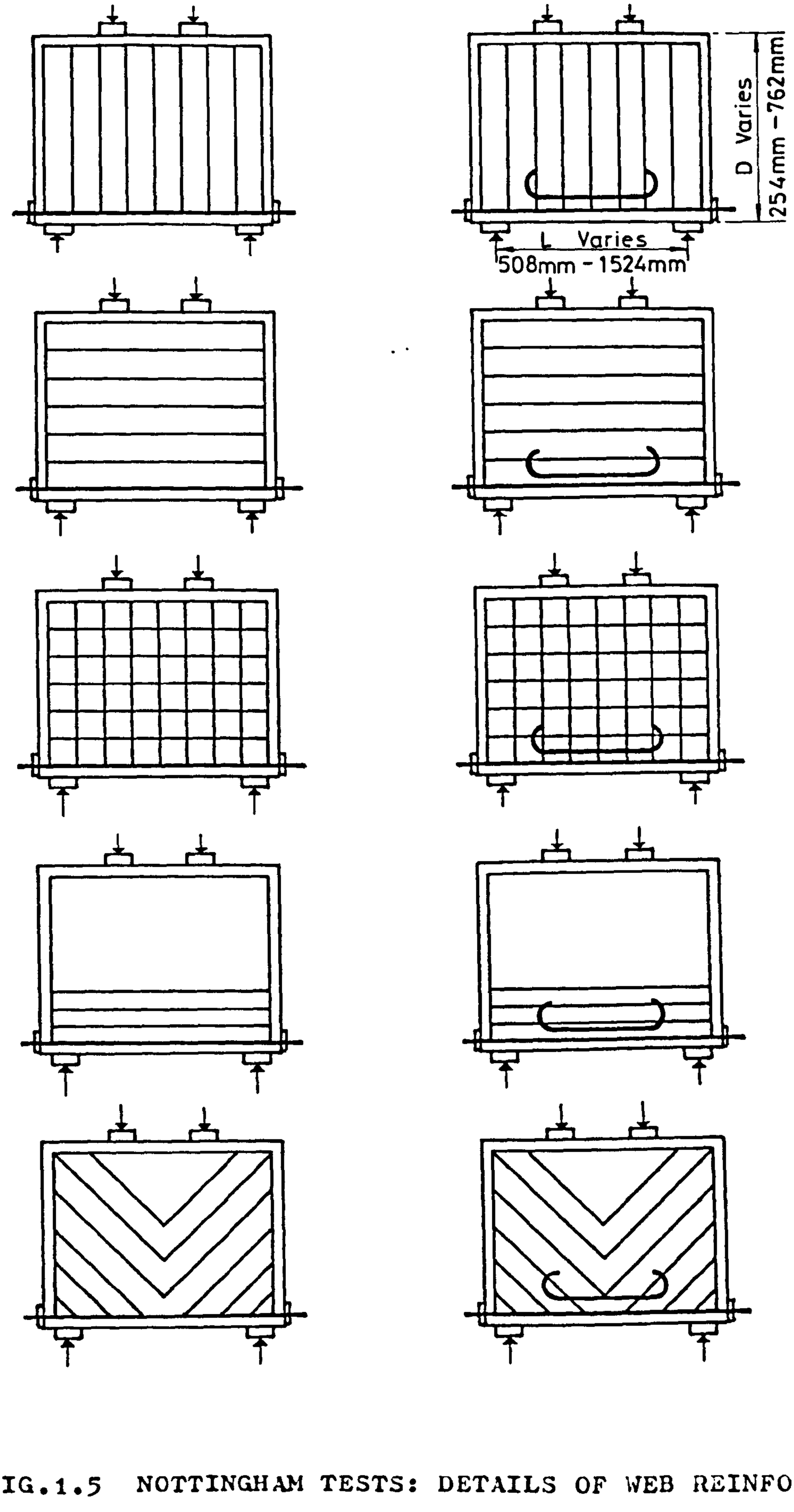

FIG.1.5 NOTTINGHAM TESTS: DETAILS OF WEB REINFORCEMENT

(Further details are given in references 27 to 31)

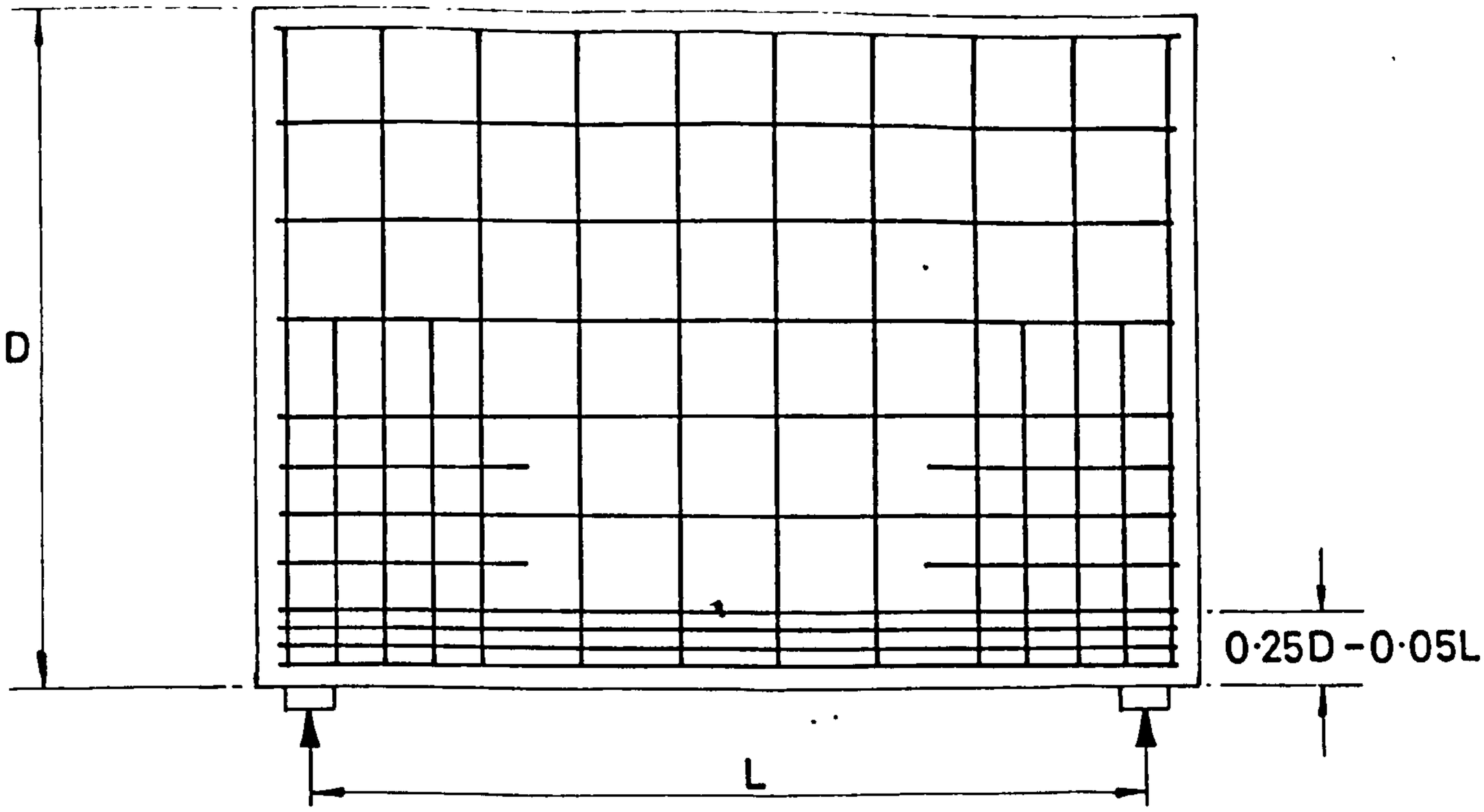

2.1(a) General layout

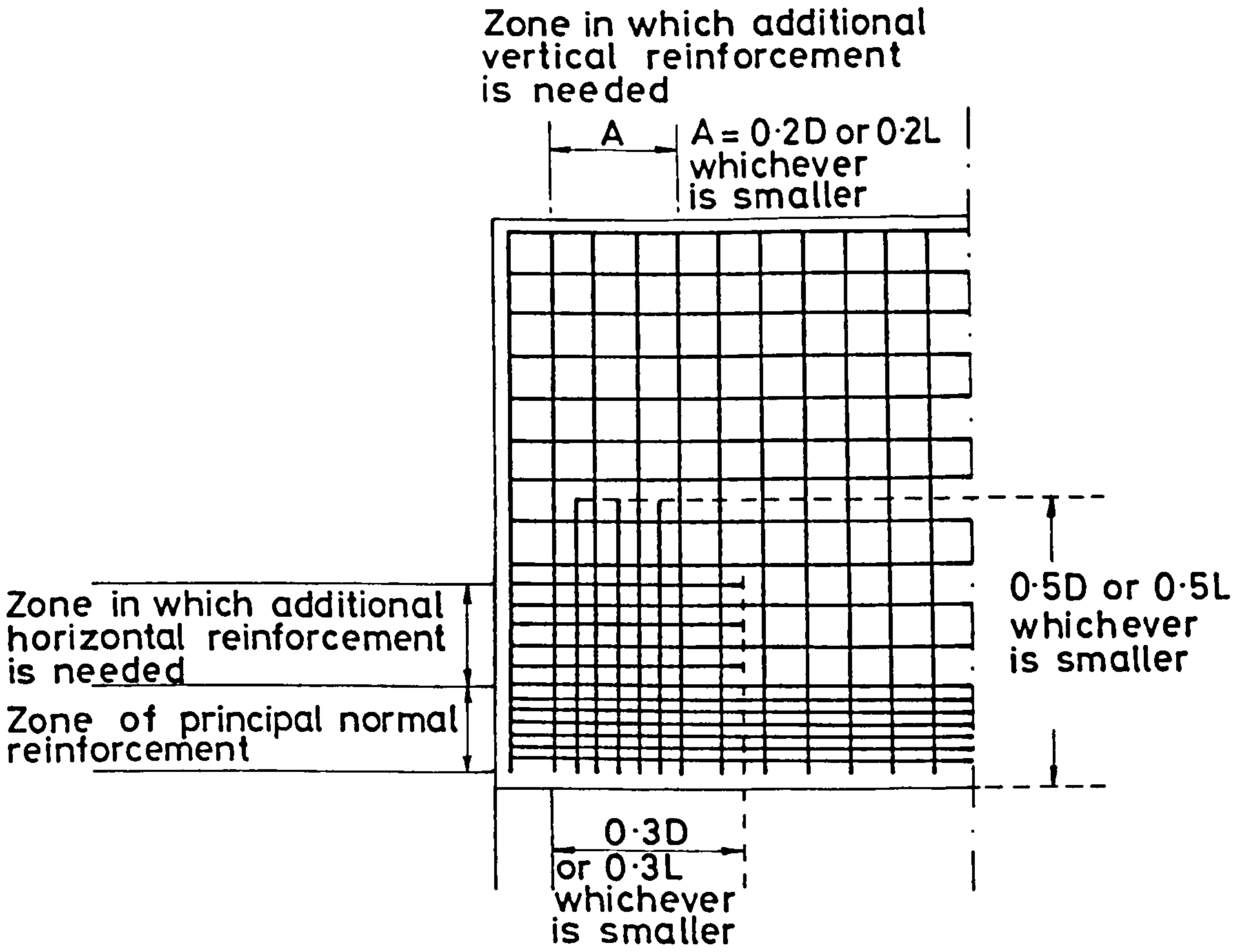

2.1(b) Detail at support

FIG.2.1 REINFORCEMENT PATTERN: CEB-FIP RECOMMENDATIONS

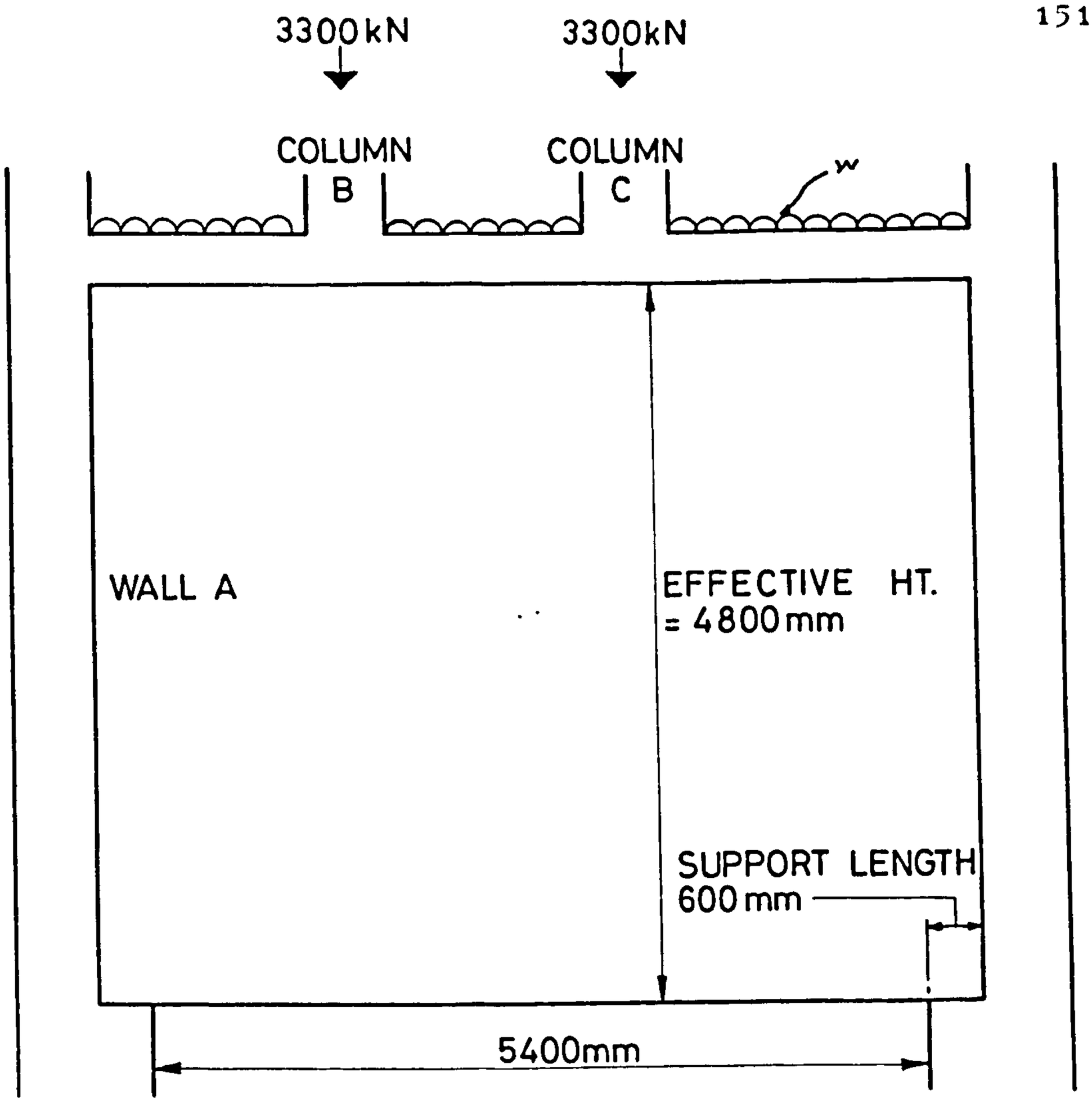

2.2(a) General arrangement

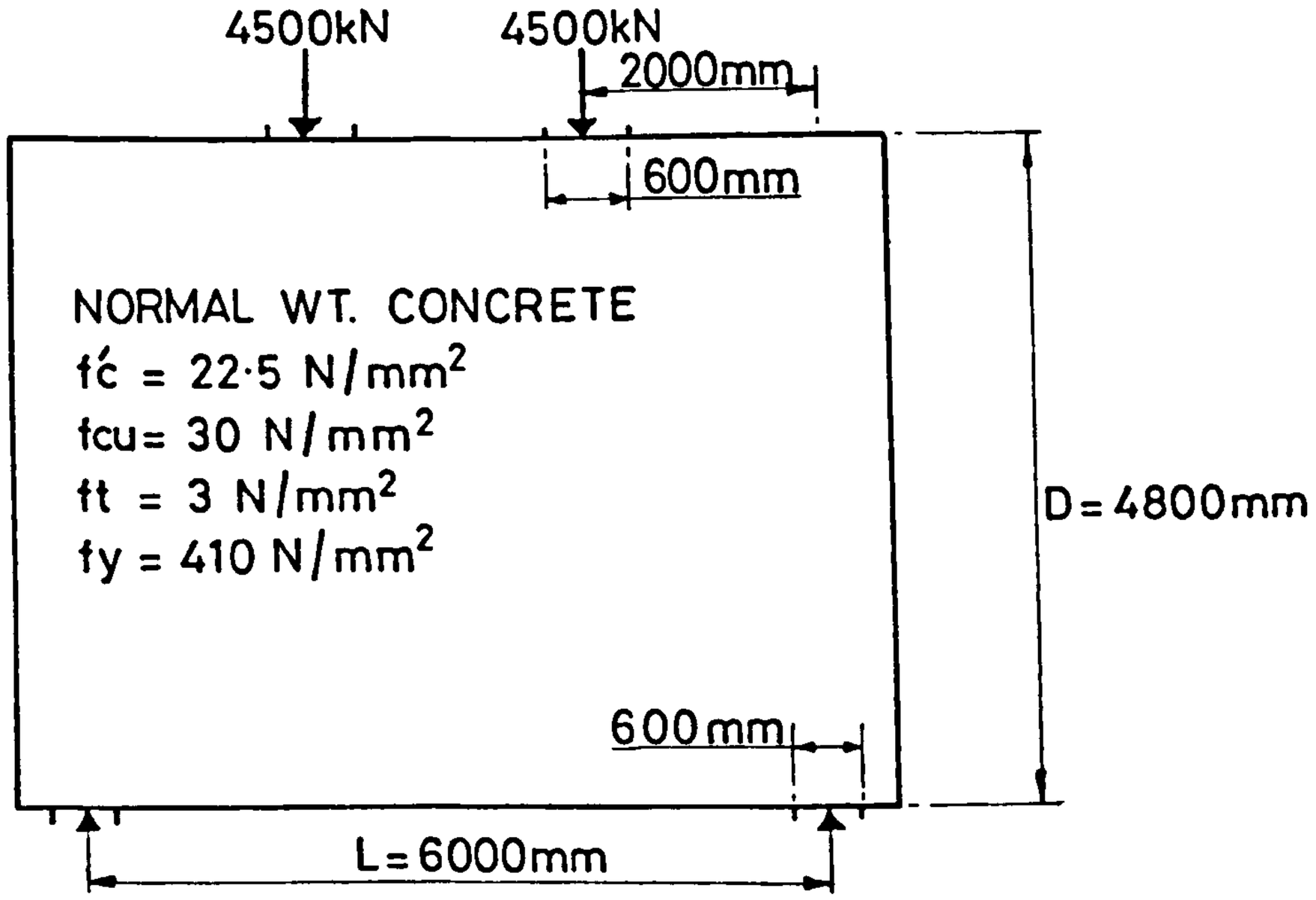

2.2(b) Structural deep beam element

FIG.2.2 DEEP BEAM IN DESIGN EXAMPLES

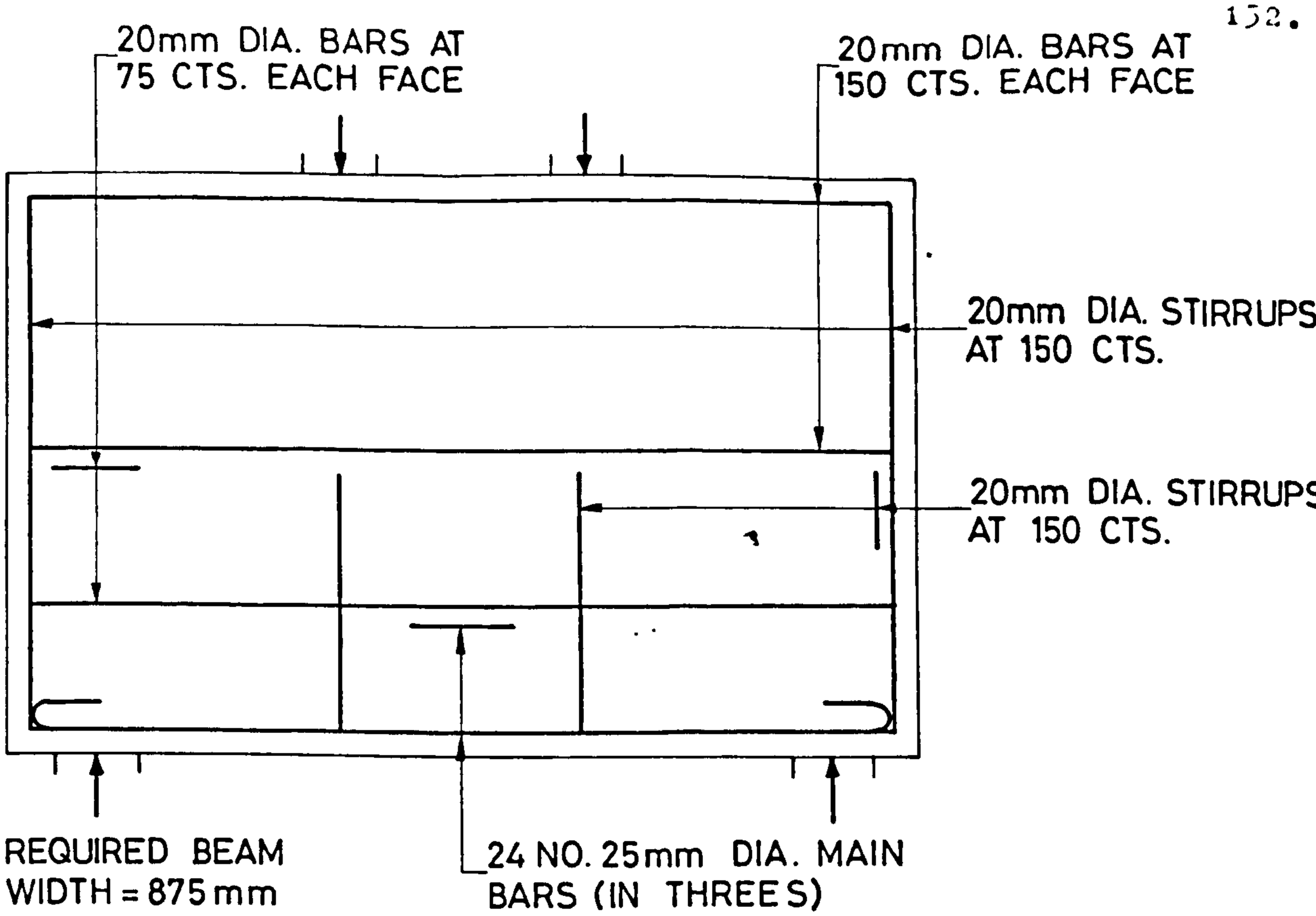

FIG.2.3 BEAM DESIGNED TO CEB-FIP RECOMMENDATIONS

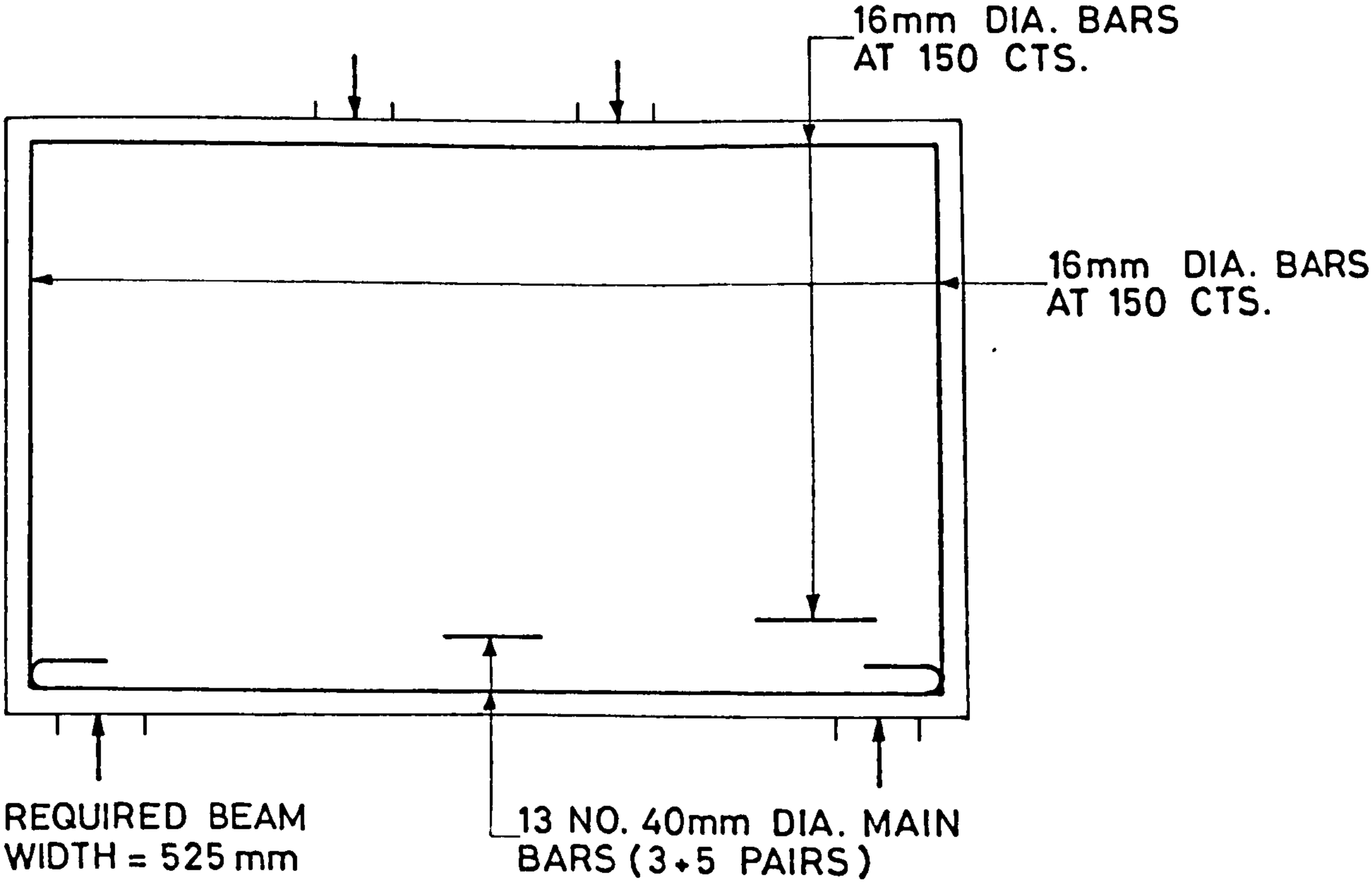

FIG.2.4 BEAM DESIGNED TO ACI BUILDING CODE

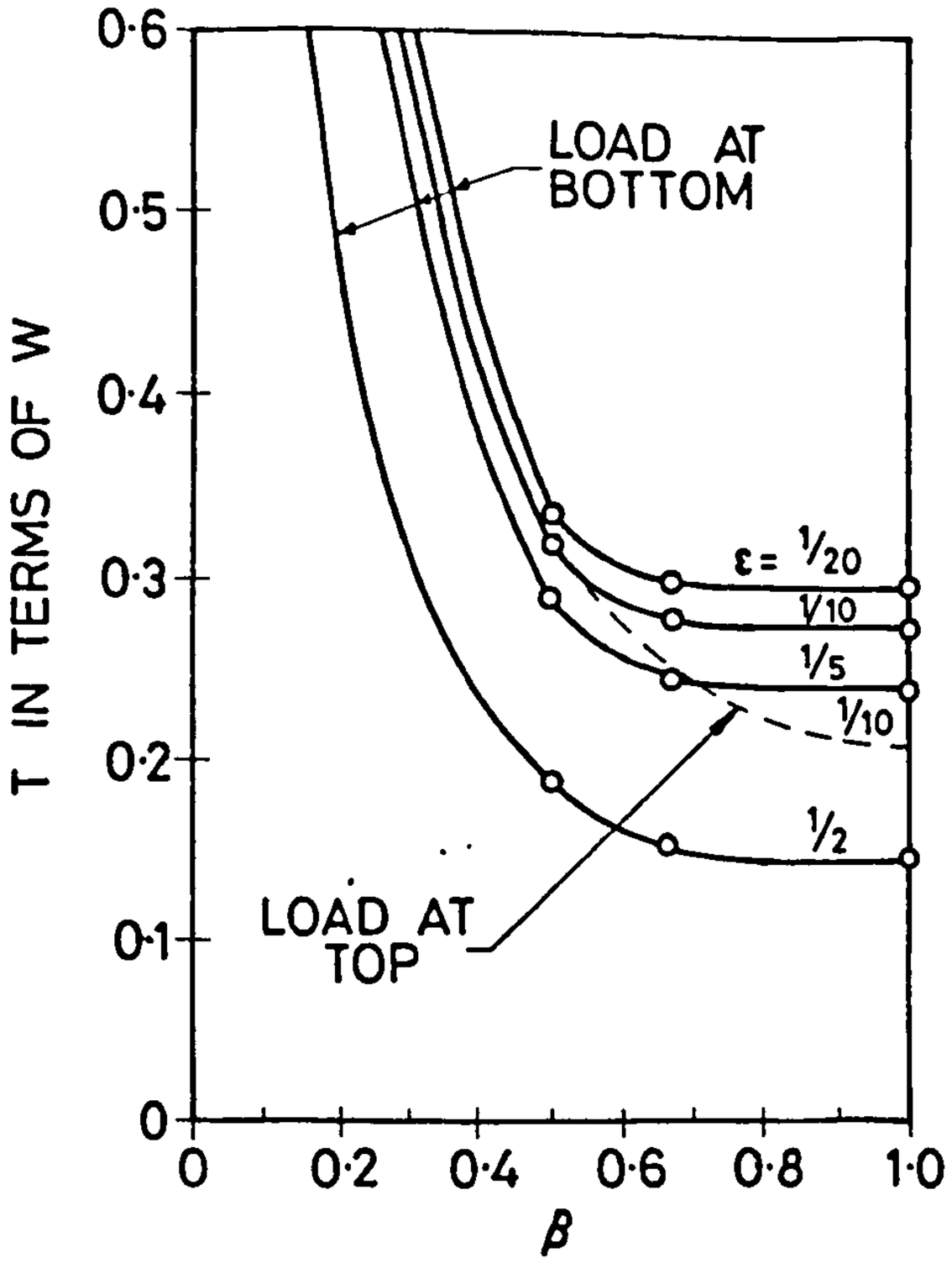

FIG.2.5 PCA's DESIGN CHART

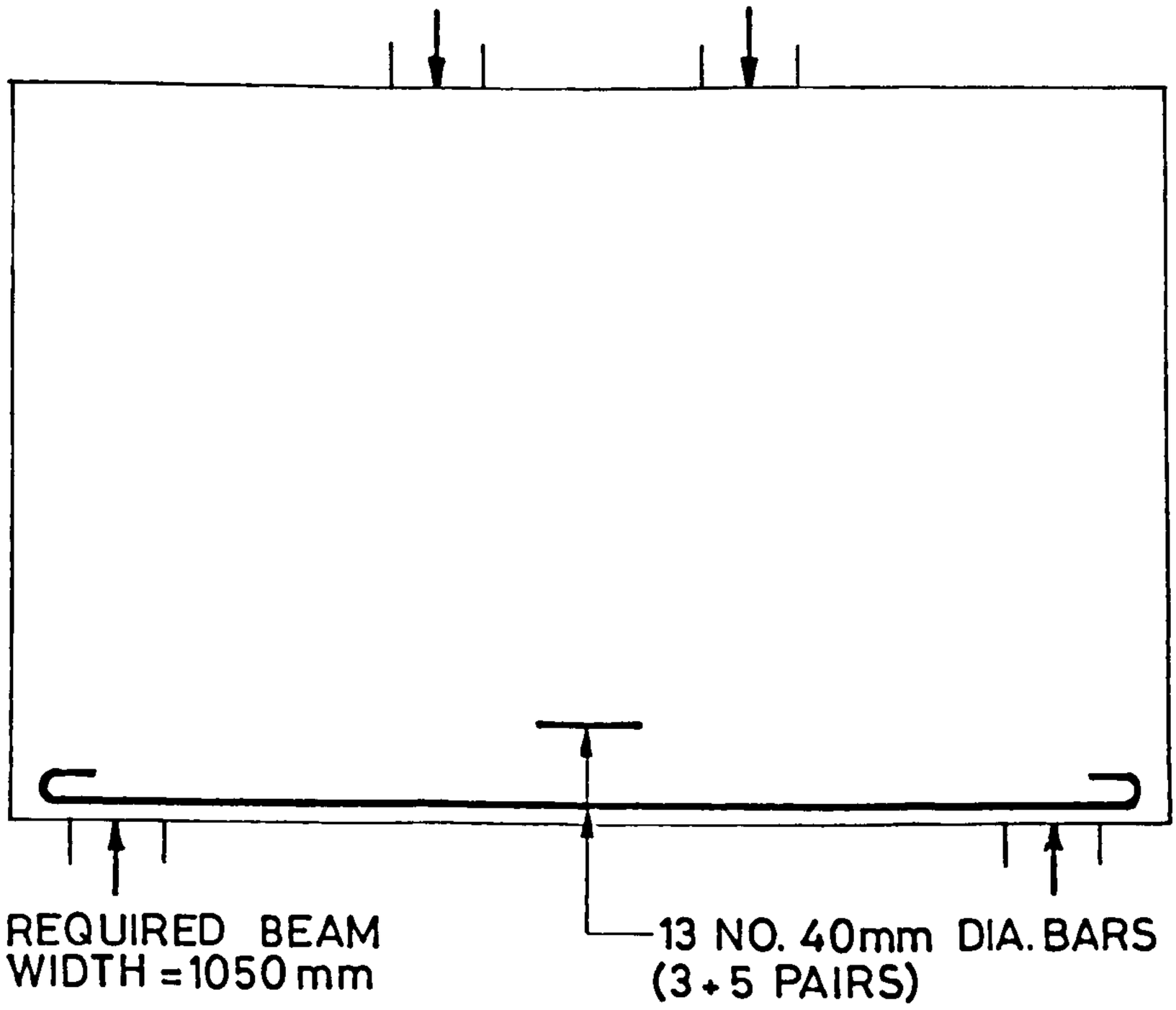

FIG.2.6 BEAM DESIGNED TO PCA DESIGN GUIDE

(A) LYTAG BATCH No.1

MEDIUM GRADE

B.S.Sieve Size	Cumulative % retained
¾	0
⅜	11.8
3/16	97.4
7	98.3
Pan	100.0

Fineness modulus = 6.075

FINE GRADE

B.S.Sieve Size	Cumulative % retained
3/16	0
7	15.4
14	34.7
25	48.4
52	55.8
100	63.2
Pan	100.0

Fineness modulus = 2.175

(B) LYTAG BATCH No.2

MEDIUM GRADE

B.S.Sieve Size	Cumulative % retained
¾	0
⅜	10.0
3/16	96.0
7	98.0
Pan	100.0

Fineness modulus = 6.030

FINE GRADE

B.S.Sieve Size	Cumulative % retained
3/16	0
7	27.8
14	47.4
25	51.3
52	55.2
100	59.9
Pan	100.0

Fineness modulus = 2.696

TABLE 3.1 SIEVE ANALYSIS OF LYTAG AGGREGATES.

COARSE GRADE

B.S.Sieve Size	Cumulative % retained
$\frac{3}{4}$	0
$\frac{3}{8}$	48.0
3/16	97.6
7	99.6
Pan	100.0

Fineness modulus = 6.452

FINE GRADE

B.S.Sieve Size	Cumulative % retained
3/16	4.1
7	19.3
14	32.1
25	49.3
52	89.2
100	99.6
Pan	100.0

Fineness modulus = 2.936

TABLE 3.2 SIEVE ANALYSIS OF HOVERINGHAM GRAVEL AGGREGATES.

BAR DIAMETER	YIELD STRESS	ULTIMATE TENSILE STRESS
mm	N/mm^2	N/mm^2
6	425	614
8	441	643
10	452	634
20	432	602

TABLE 3.3 TENSILE PROPERTIES OF REINFORCEMENTS.

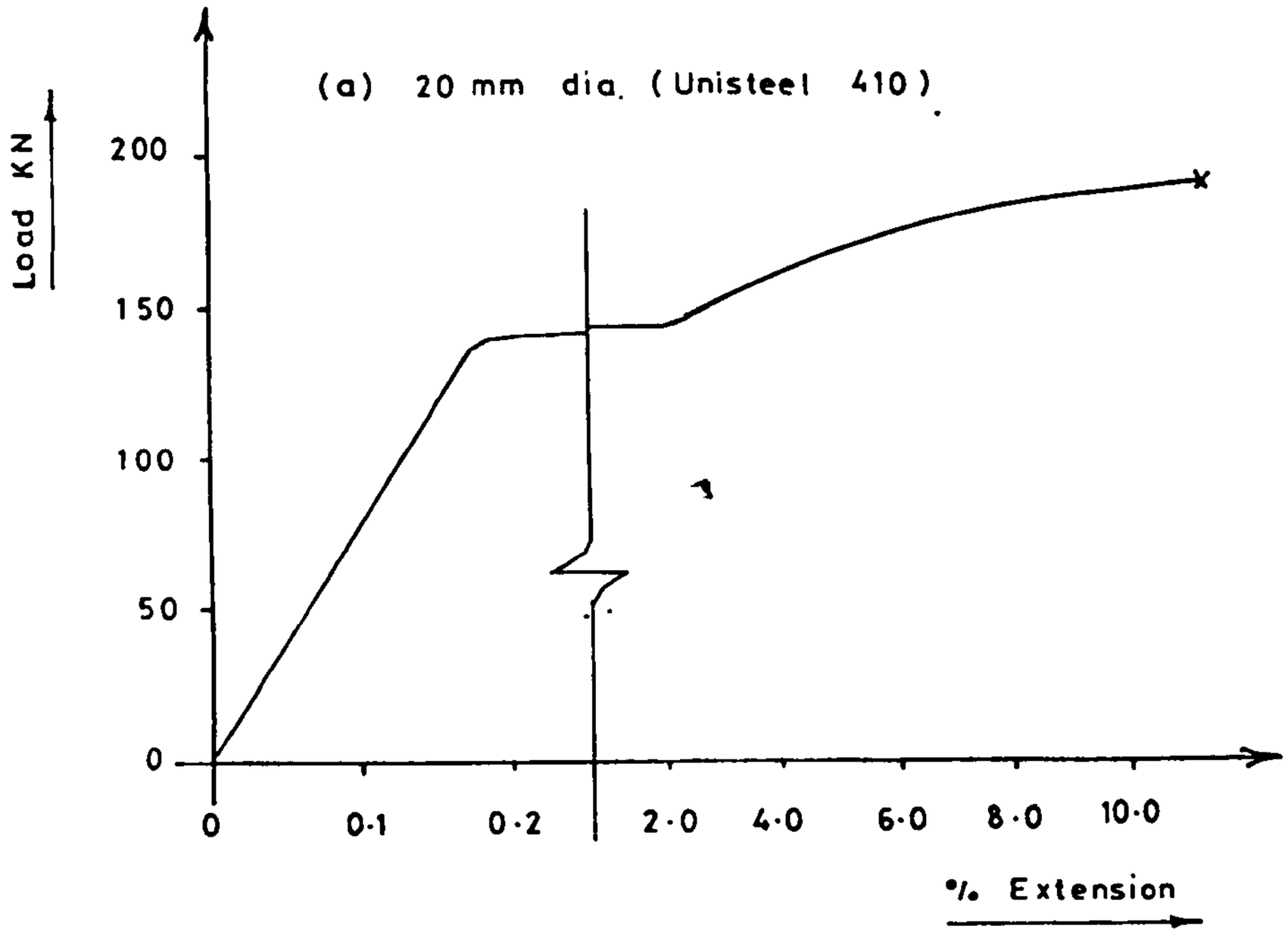

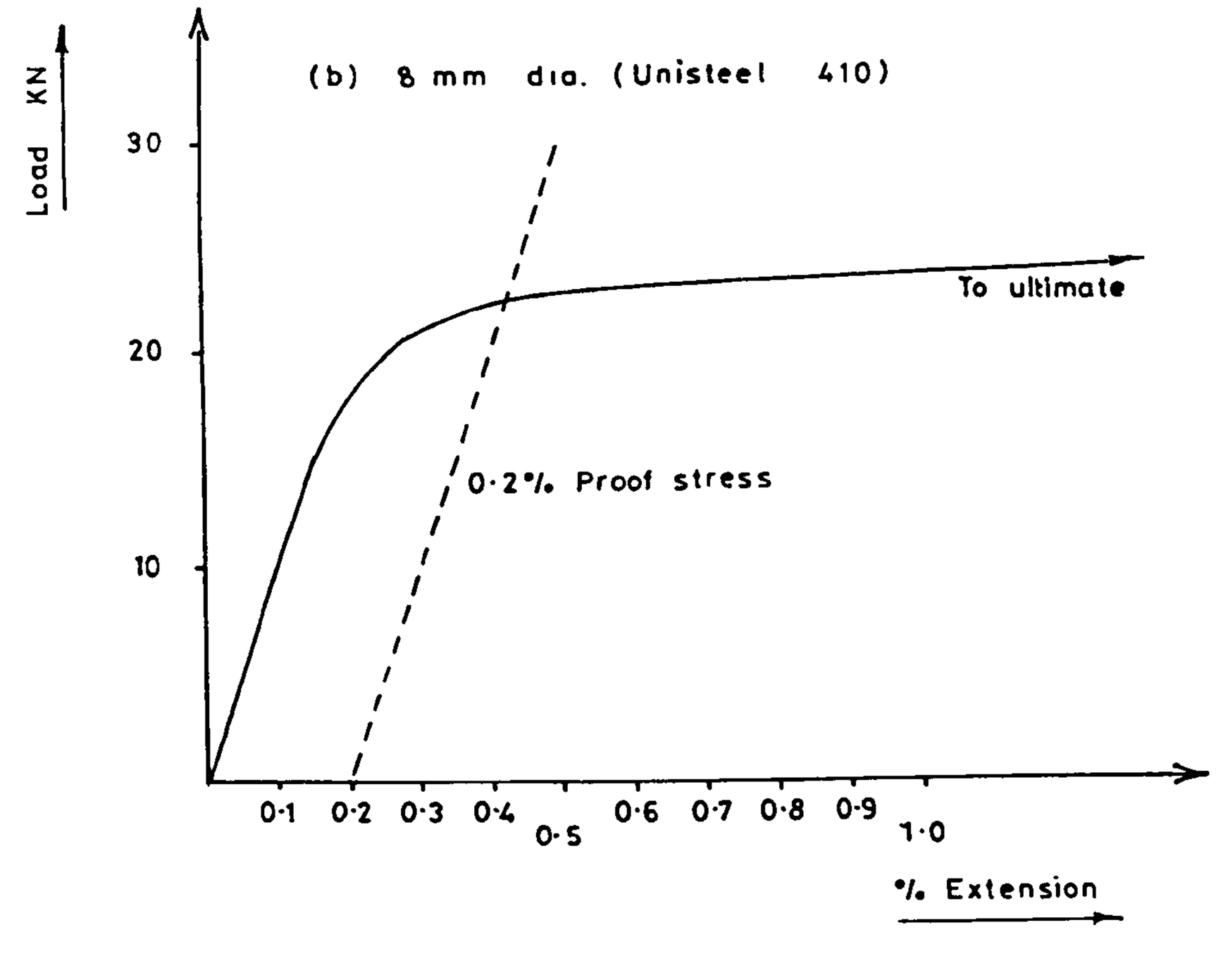

FIG.3.1 LOAD v. EXTENSION DIAGRAMS FOR REINFORCEMENT

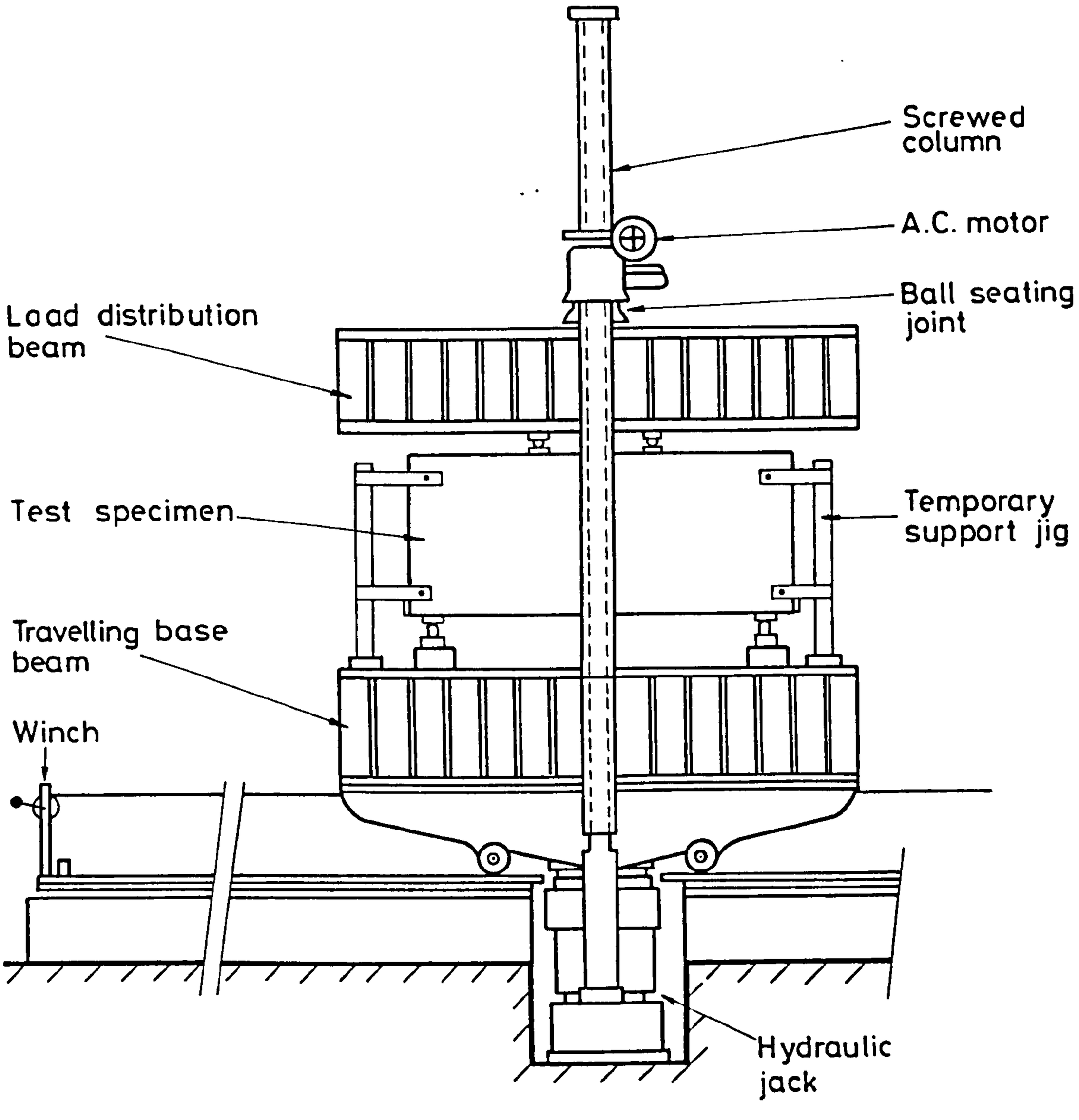

FIG.3.2 THE LOADING APPARATUS: GENERAL ARRANGEMENT

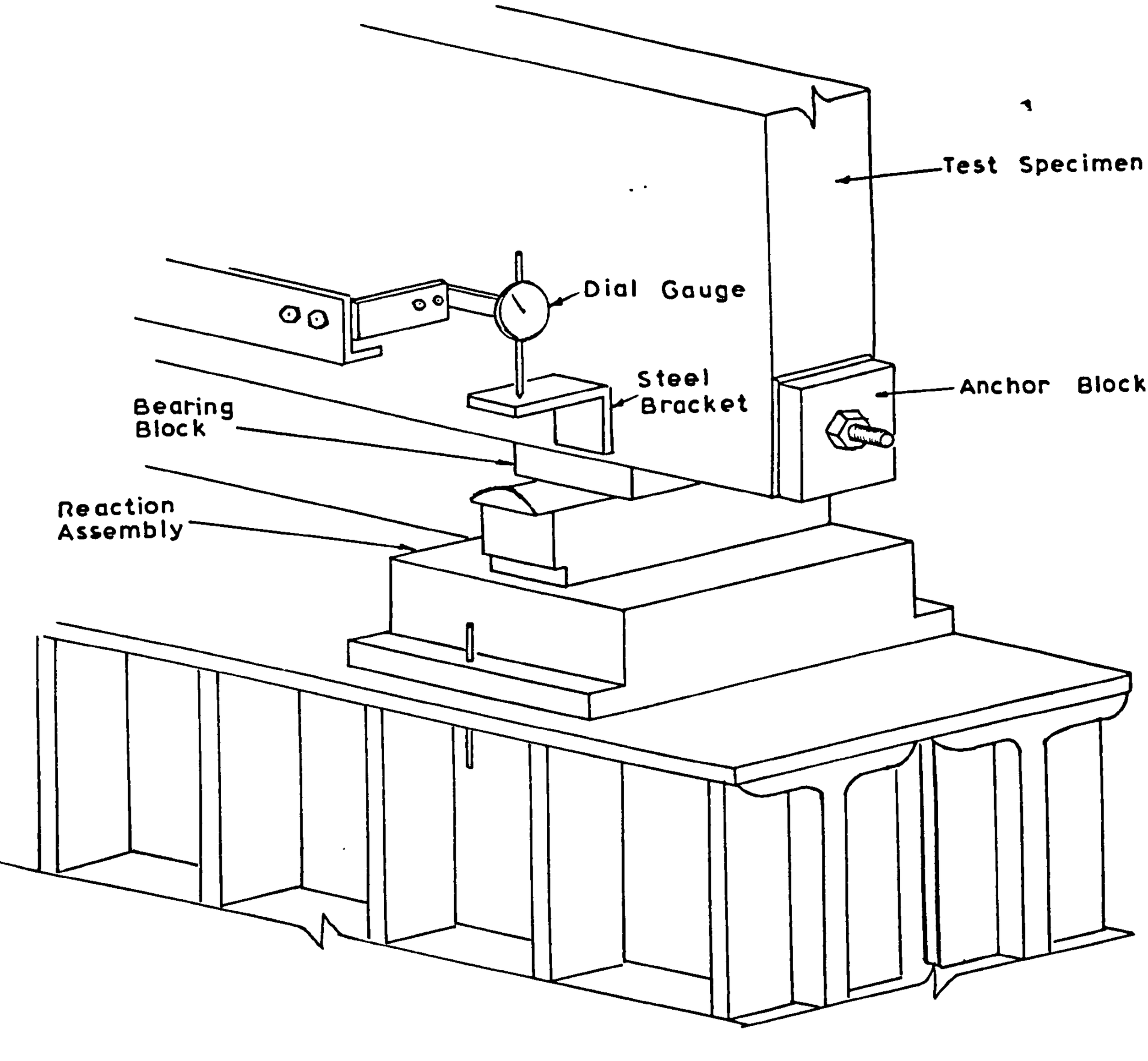

FIG.3.3 THE LOADING APPARATUS: DETAIL AT THE SUPPORTS

Beam * Ref.No.	$\frac{L}{D}$	$\frac{x}{D}$	Web opening ‡‡ Ref.No.	Web Steel %	f_{cu} ≠ N/mm^2	f_c' xx xx N/mm^2	f_t ** N/mm^2
M-0.4/0	2	0.4	0	0.48	39.6	31.6	2.84
M-0.4/1	2	0.4	1	0.48	39.5	26.5	2.90
M-0.4/2	2	0.4	2	0.48	38.9	30.1	2.50
M-0.4/3	2	0.4	3	0.48	41.5	32.5	2.18
M-0.4/4	2	0.4	4	0.48	36.4	29.3	2.16
M-0.4/5	2	0.4	5	0.48	40.9	31.3	2.30
M-0.4/6	2	0.4	6	0.48	33.2	32.4	2.84
M-0.4/8	2	0.4	8	0.48	35.3	30.4	2.74
M-0.4/9	2	0.4	9	0.48	35.8	29.2	2.60
M-0.4/10	2	0.4	10	0.48	35.8	34.0	2.78
M-0.4/11	2	0.4	11	0.48	38.7	33.8	2.62
M-0.4/12	2	0.4	12	0.48	38.1	32.0	2.60
M-0.4/13	2	0.4	13	0.48	38.7	33.8	2.62
0-0.4/0	2	0.4	0	0	37.1	32.6	2.50
0-0.4/2	2	0.4	2	0	38.1	32.4	2.45
0-0.4/4	2	0.4	4	0	39.8	32.2	2.72
0-0.4/5	2	0.4	5	0	39.3	32.7	2.28
0-0.4/6	2	0.4	6	0	39.9	34.7	2.63
0-0.4/7	2	0.4	7	0	38.0	31.0	2.46
0-0.25/0	2	0.25	0	0	38.4	34.0	2.68
0-0.25/2	2	0.25	2	0	42.6	36.4	2.80
0-0.25/4	2	0.25	4	0	37.5	34.1	2.80
0-0.25/5	2	0.25	5	0	41.4	35.8	2.83
0-0.25/6	2	0.25	6	0	41.8	37.2	2.58

* Beam notation: A letter M before the hyphen indicates a rectangular mesh web reinforcement, whilst a letter O indicates no web reinforcement; the x/D ratio is given after the hyphen, followed by the web-opening reference number. Thus O-0.4/2 refers to a beam with no web reinforcement, having an x/D ratio of 0.4 and a web opening type 2.

‡‡ Details of web openings are given in Figs.4.2 and 4.3

≠ f_{cu} = cube strength (100 mm).

xx xx f_c' = cylinder compressive strength (300 mm x 150 mm).

** f_t = cylinder splitting tensile strength (300 mm x 150 mm) in accordance with ASTM Standard C330.

TABLE 4.1 PROPERTIES OF TEST BEAMS
(Pilot tests; lightweight concrete).

Beam * Ref.No.	Measured W_1 kN	$\frac{W_1}{W_0}$ **
M-0.4/0	660	1.0
M-0.4/1	580	0.88
M-0.4/2	360	0.55
M-0.4/3	445	0.67
M-0.4/4	450	0.68
M-0.4/5	600	0.91
M-0.4/6	270	0.41
M-0.4/8	340	0.52
M-0.4/9	240	0.36
M-0.4/10	300	0.45
M-0.4/11	600	0.91
M-0.4/12	520	0.79
M-0.4/13	130	0.20
O-0.4/0	660	1.0
O-0.4/2	370	0.56
O-0.4/4	340	0.52
O-0.4/5	540	0.82
O-0.4/6	190	0.29
O-0.4/7	420	0.64
O-0.25/0	660	1.0
O-0.25/2	360	0.55
O-0.25/4	460	0.70
O-0.25/5	560	0.85
O-0.25/6	280	0.42

*Beam notation as in Table 4.1

**W_1/W_0 is the ratio of the measured ultimate load of a beam with openings to that of the corresponding solid deep beam.

TABLE 4.2 MEASURED ULTIMATE LOADS
(Pilot tests; lightweight concrete)

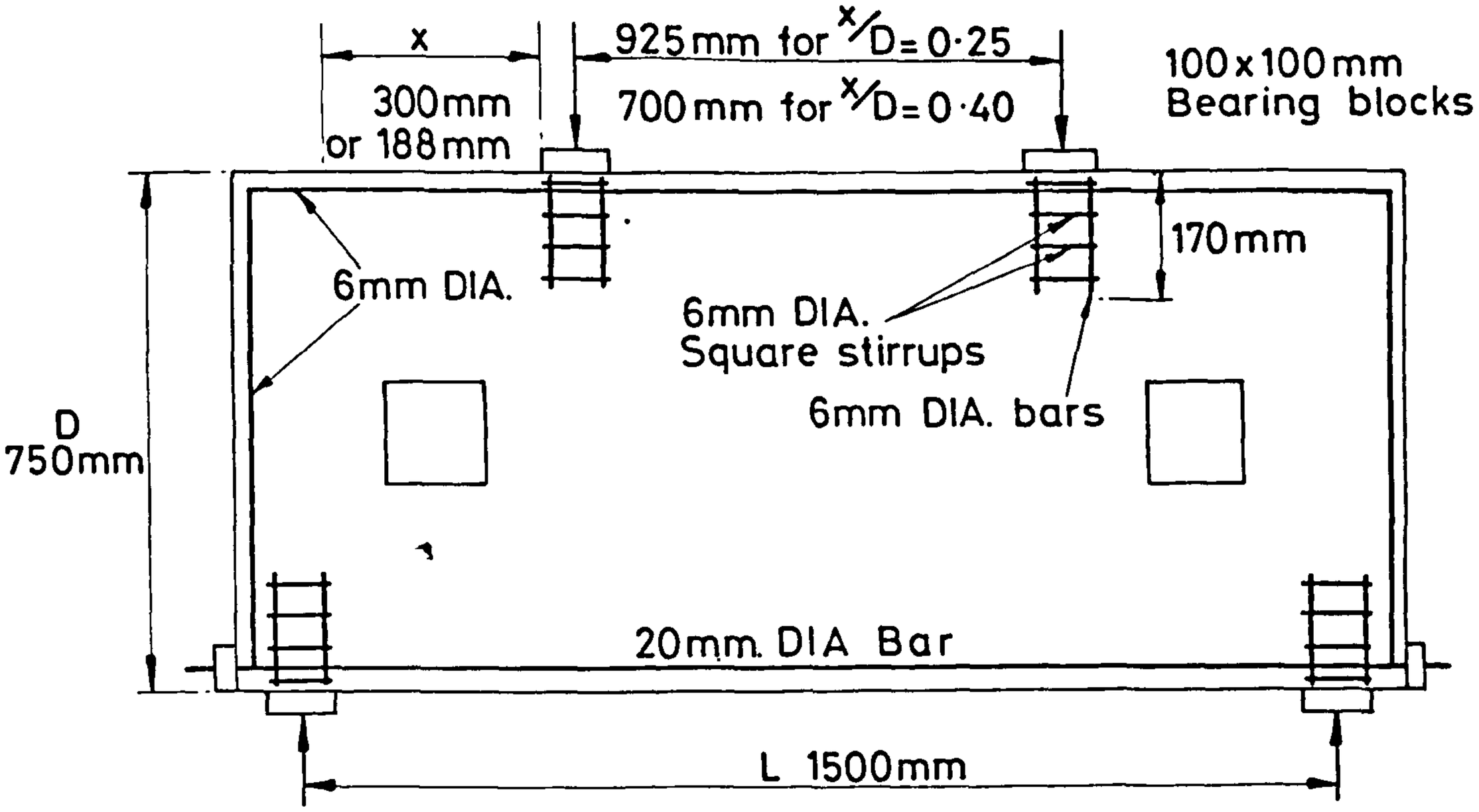

NOTES:-

1. Reinforcement details of group O beams were as shown above.
2. Reinforcement details of group M beams include in addition and as shown below:
   (i) A rectangular mesh of 6mm dia. bars at 100mm vertical spacings and 140mm horizontal spacings and
   (ii) A 6mm dia. rectangular loop to trim each opening.

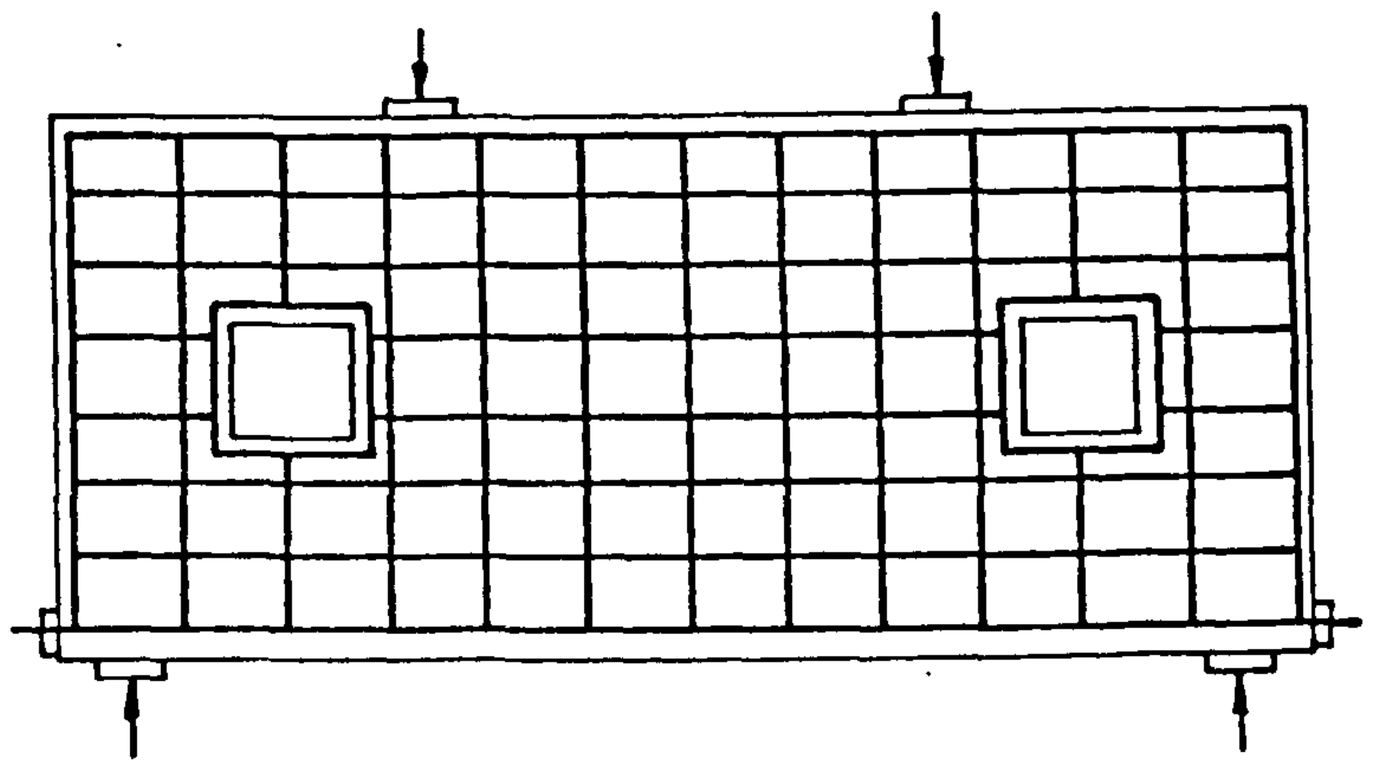

FIG.4.1 DIMENSIONS AND REINFORCEMENT DETAILS
(Pilot tests; lightweight concrete)

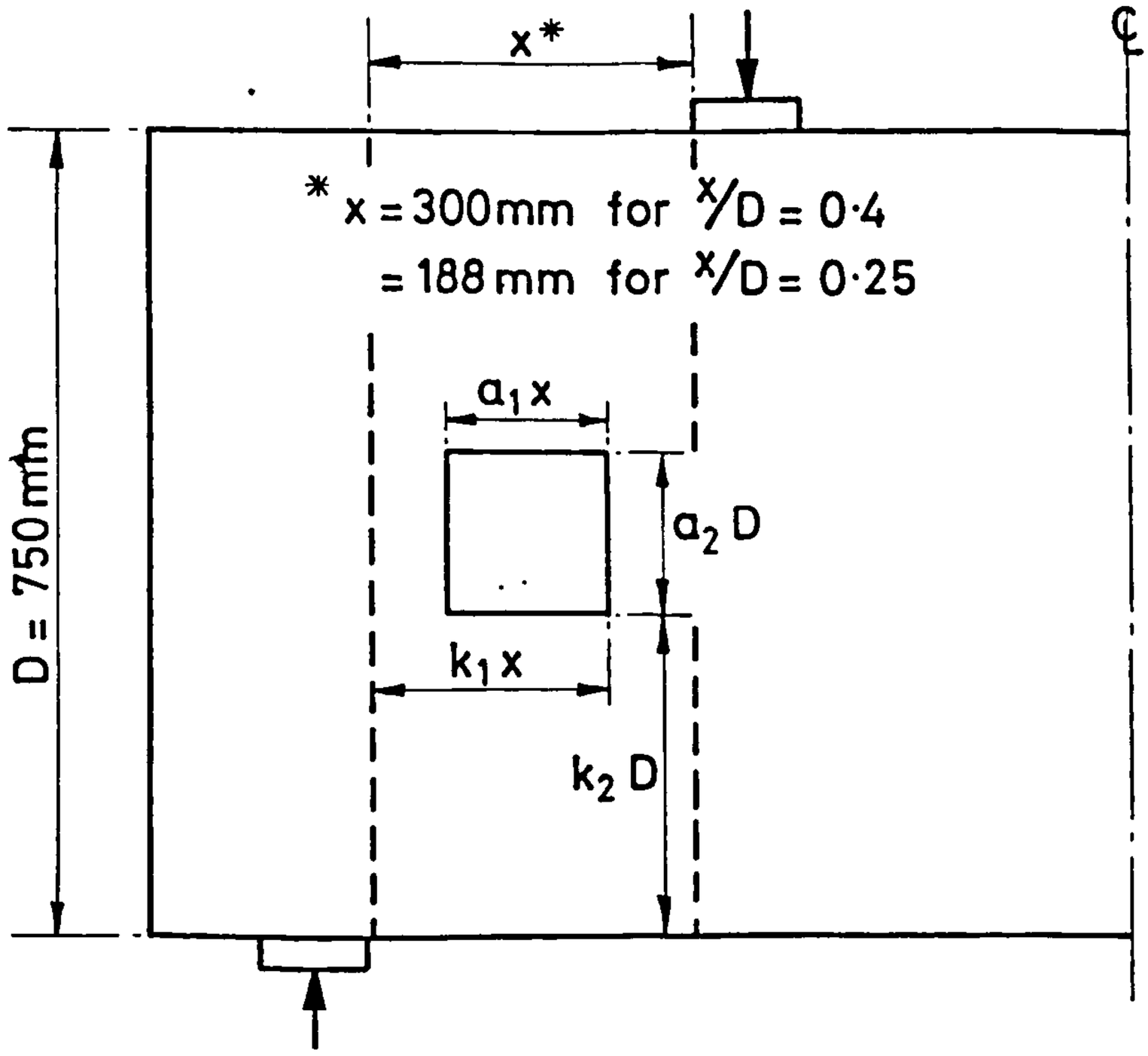

REF NO.	SIZE		POSITION	
	a_1	a_2	k_1	k_2
0	NO WEB OPENING			
1	0·5	0·2	1·0	0·8
2	0·5	0·2	1·0	0·6
3	0·5	0·2	1·0	0·4
4	0·5	0·2	0·75	0·4
5	0·5	0·2	1·0	0·12
6	0·5	0·2	0·5	0·12
7	0·5	0·2	0·5	0·6
8	0·25	0·4	1·0	0·3
9	1·0	0·1	1·0	0·45
10	0·25	0·4	0·63	0·3
11	0·25	0·1	1·0	0·45
12	0·25	0·1	0·63	0·45
13	1·0	0·4	1·0	0·3

FIG.4.2 OPENING REFERENCE NUMBERS: APPLICABLE TO BEAMS IN TABLE 4.1

FIG.4.3a TYPICAL CRACK PATTERNS AT FAILURE
- GROUP M BEAMS

(The circled numbers show the sequence in which the cracks were observed; the other numerical figures show the load, in 10 kN units, at which the extent of the cracks were as marked. Beam notation as in Table 4.1)

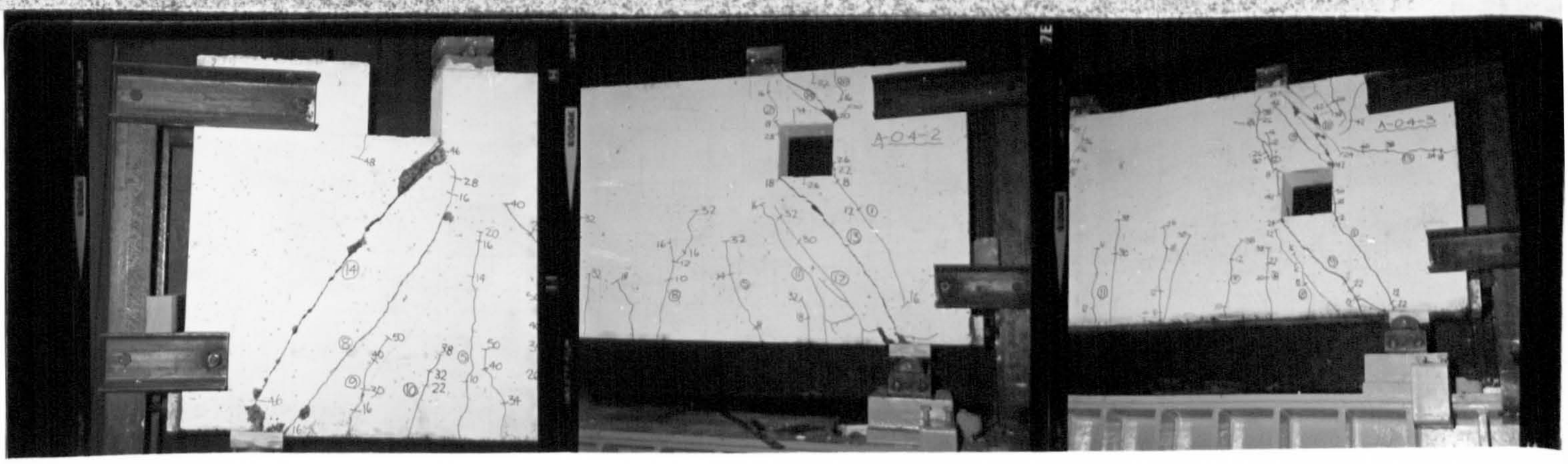

M-0·4/1 M-0·4/2 M-0·4/3

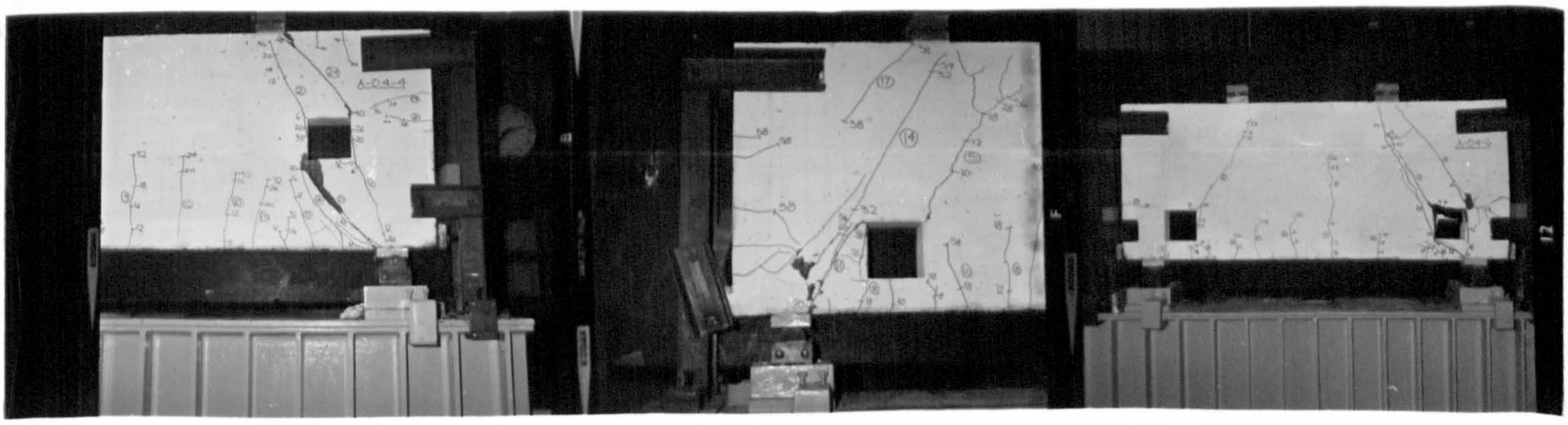

M-0·4/4 M-0·4/5 M-0·4/6

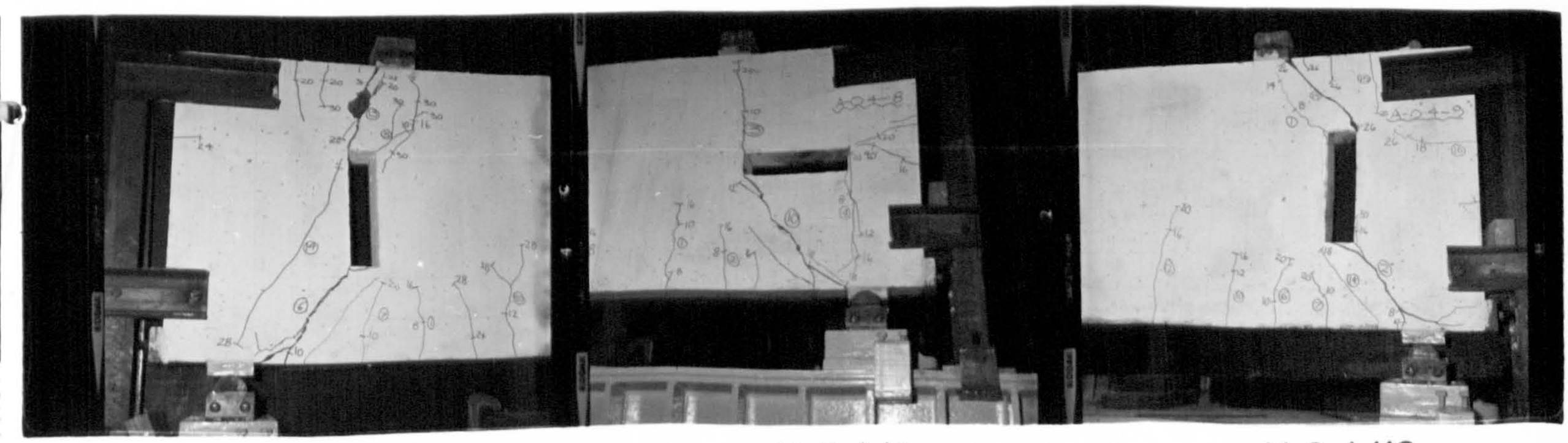

M-0·4/8 M-0·4/9 M-0·4/10

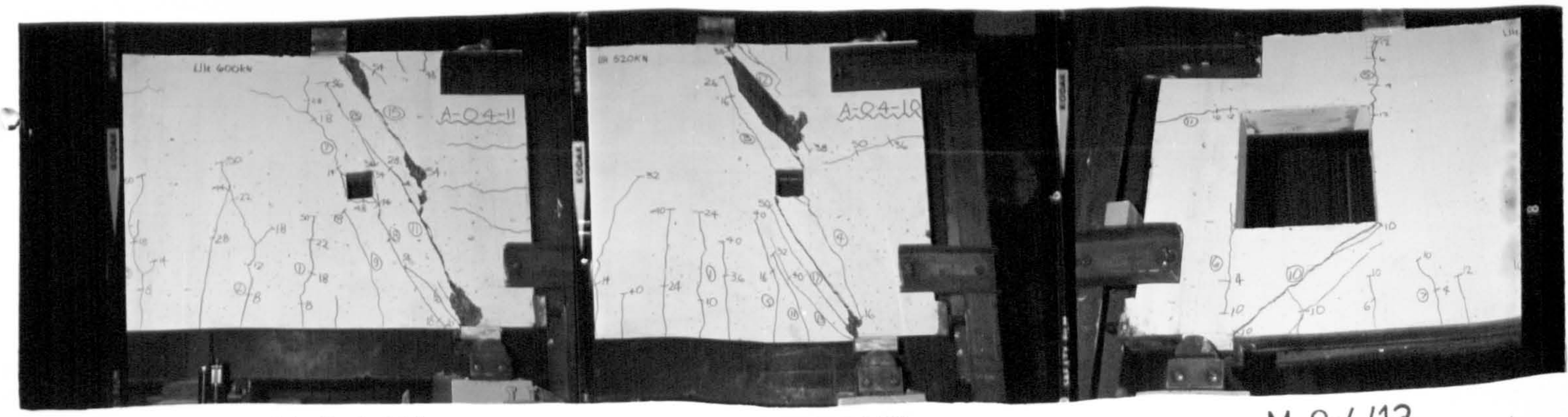

M-0·4/11 M-0·4/12 M-0·4/13

FIG.4.3b TYPICAL CRACK PATTERNS AT FAILURE
- GROUP O BEAMS

(The circled numbers show the sequence in which the cracks were observed; the other numerical figures show the load, in 10 kN units, at which the extent of the cracks were as marked. Beam notation as in Table 4.1)

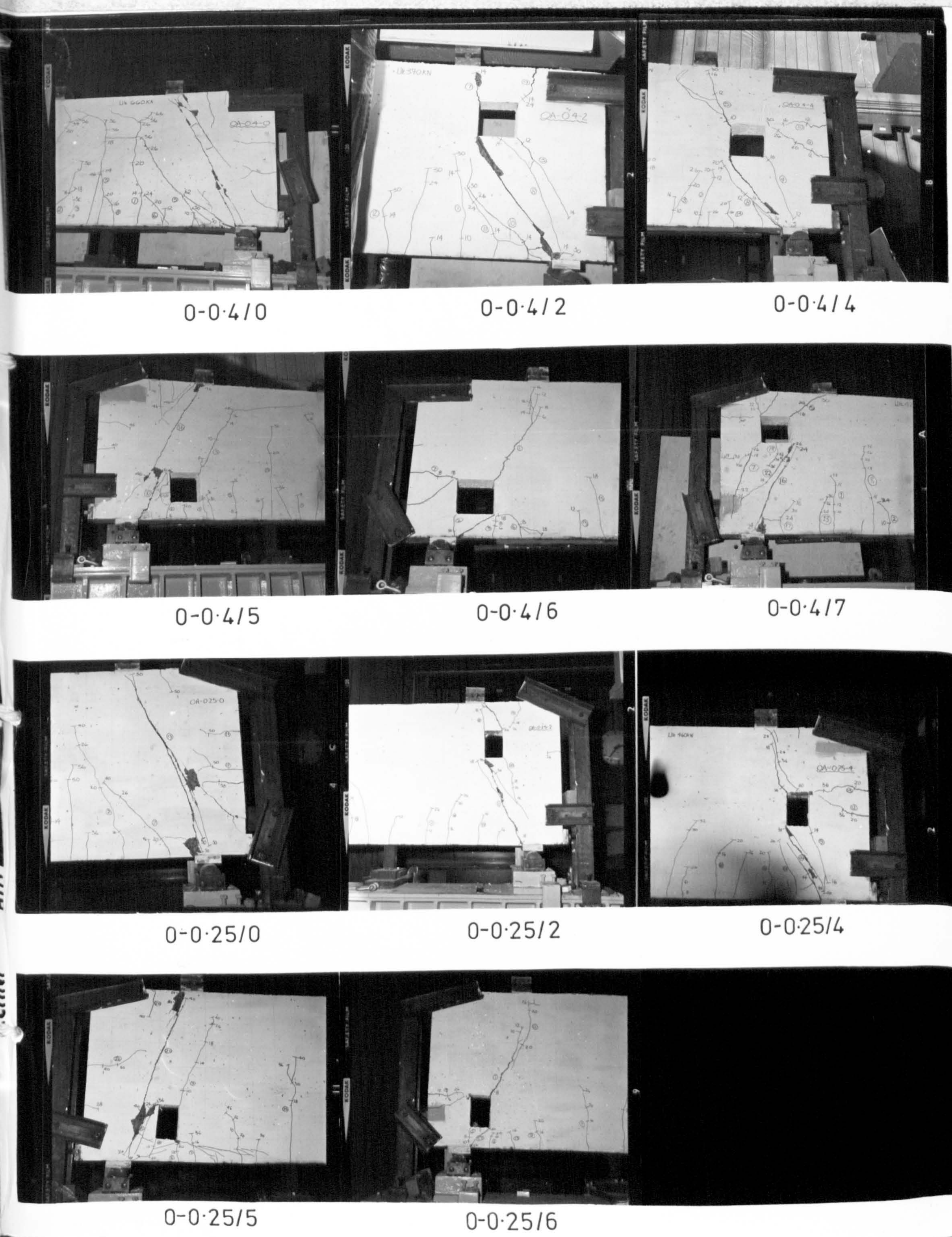

0-0·4/0 0-0·4/2 0-0·4/4

0-0·4/5 0-0·4/6 0-0·4/7

0-0·25/0 0-0·25/2 0-0·25/4

0-0·25/5 0-0·25/6

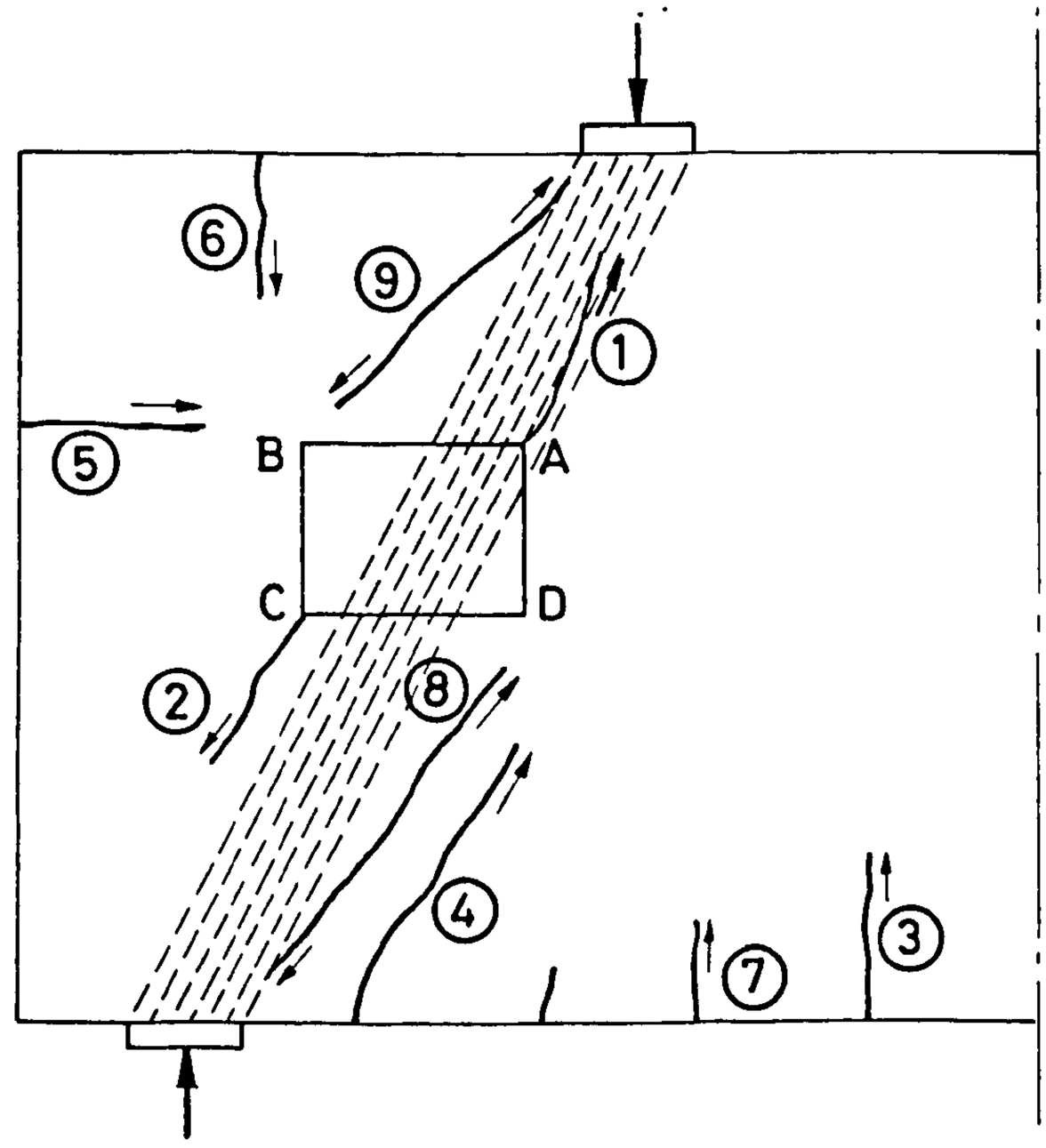

FIG.4.4 TYPICAL SEQUENCE IN WHICH THE CRACKS APPEARED

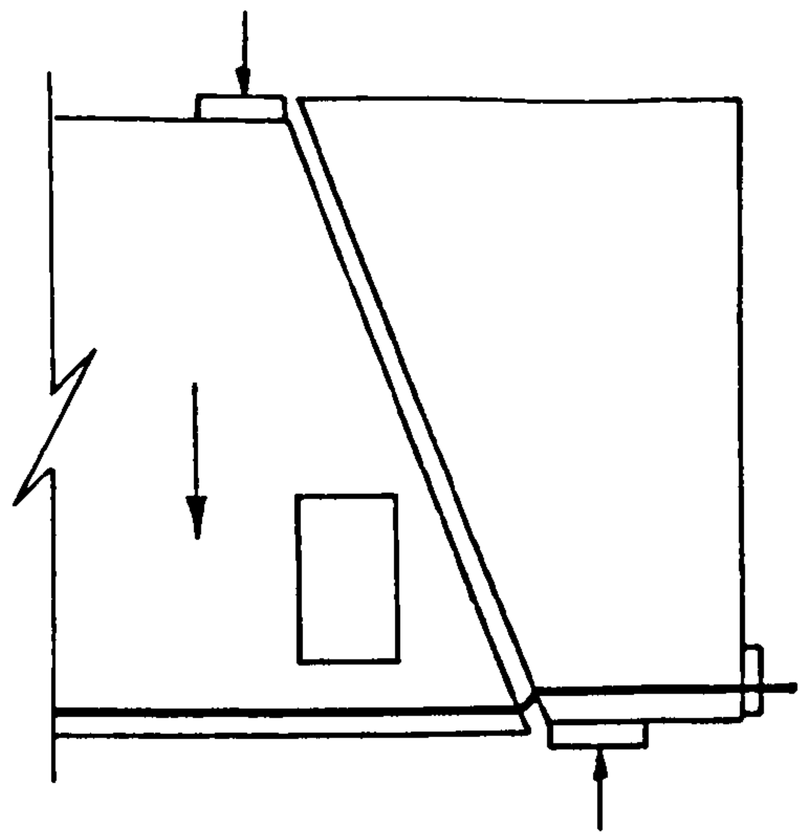

(a) FAILURE MODE 1

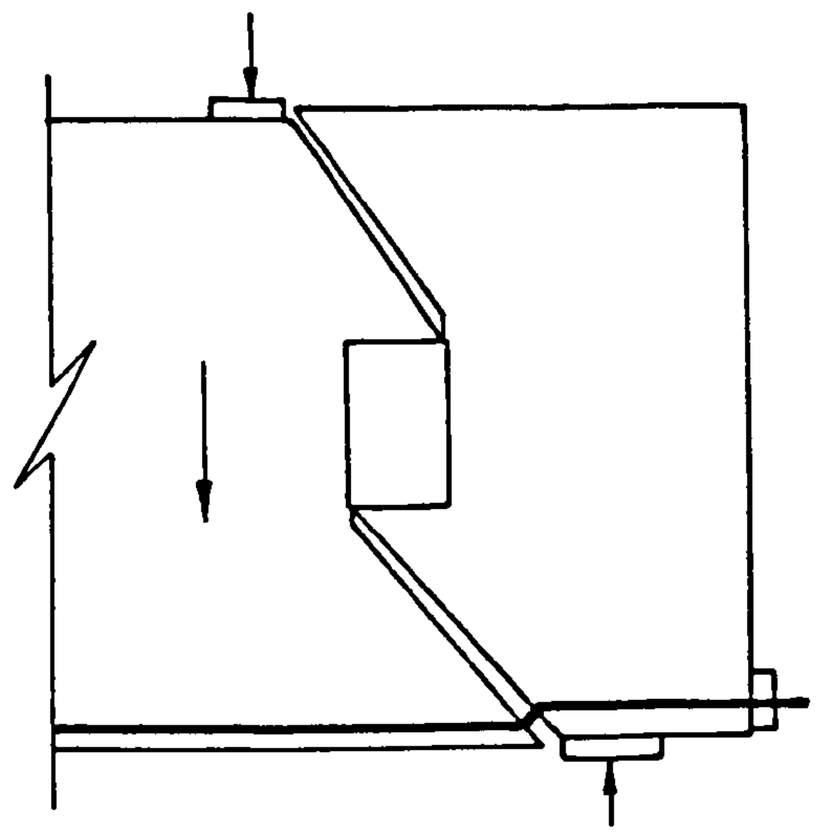

(b) FAILURE MODE 2

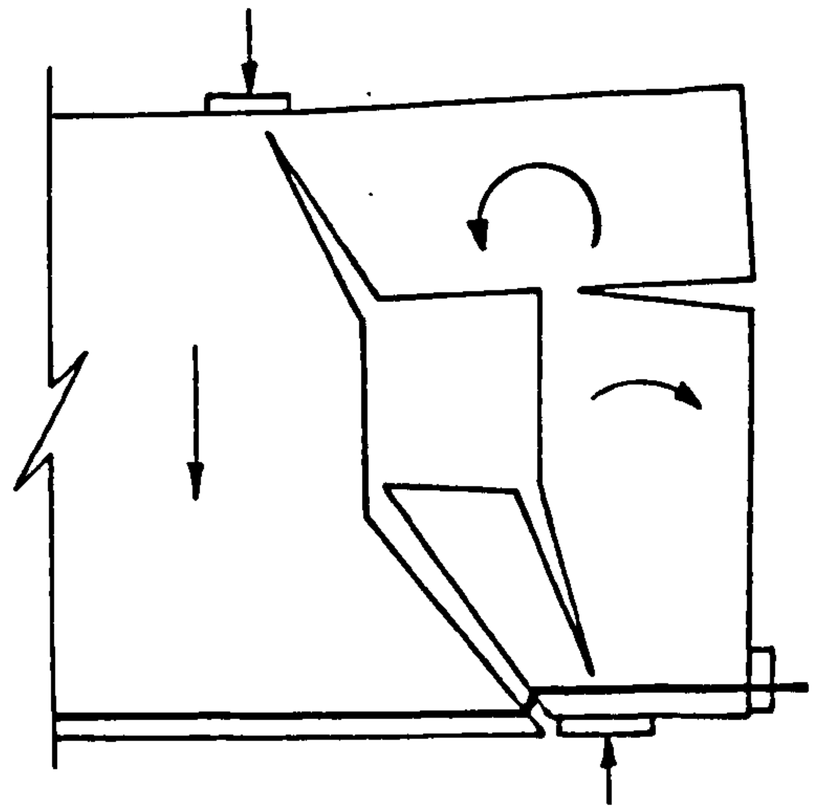

(c) FAILURE MODE 3

FIG.4.5 TYPICAL FAILURE MODES OF DEEP BEAMS WITH WEB OPENINGS

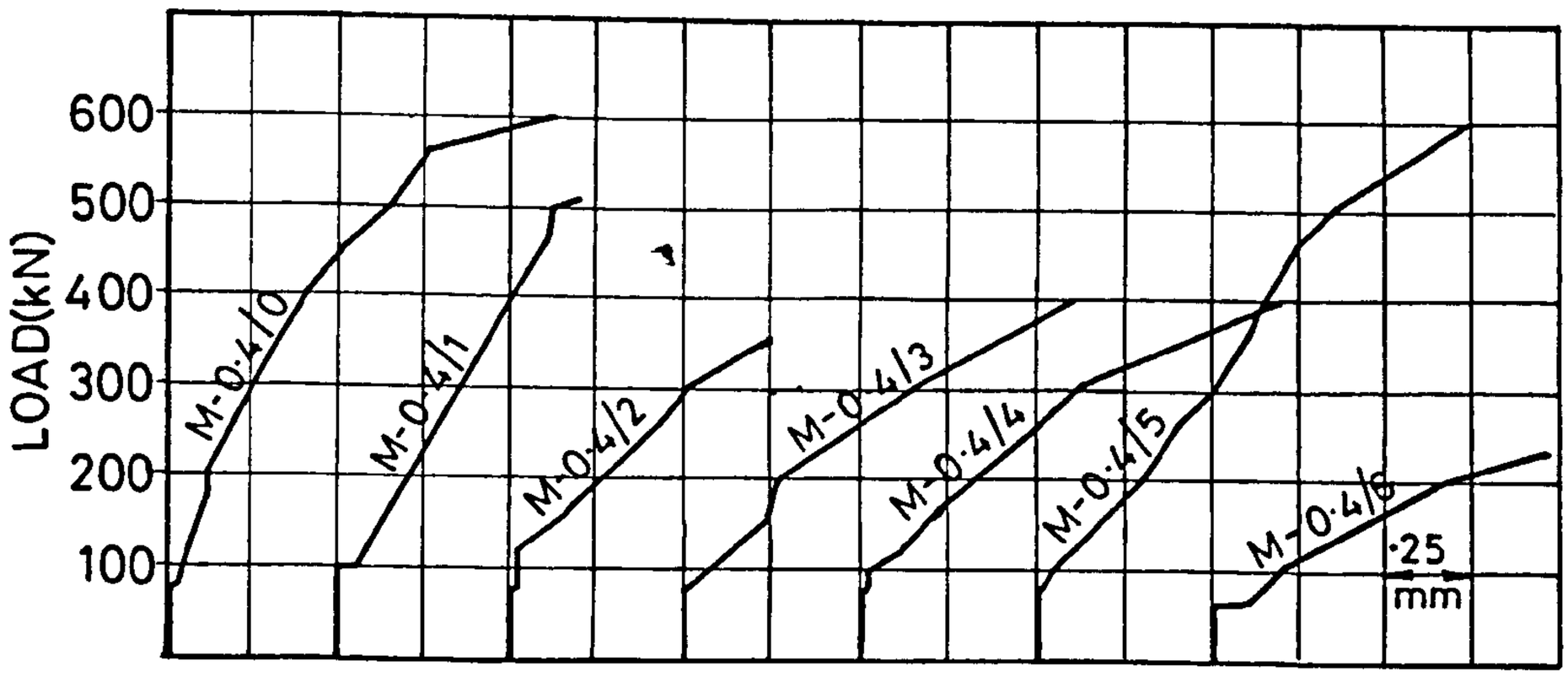

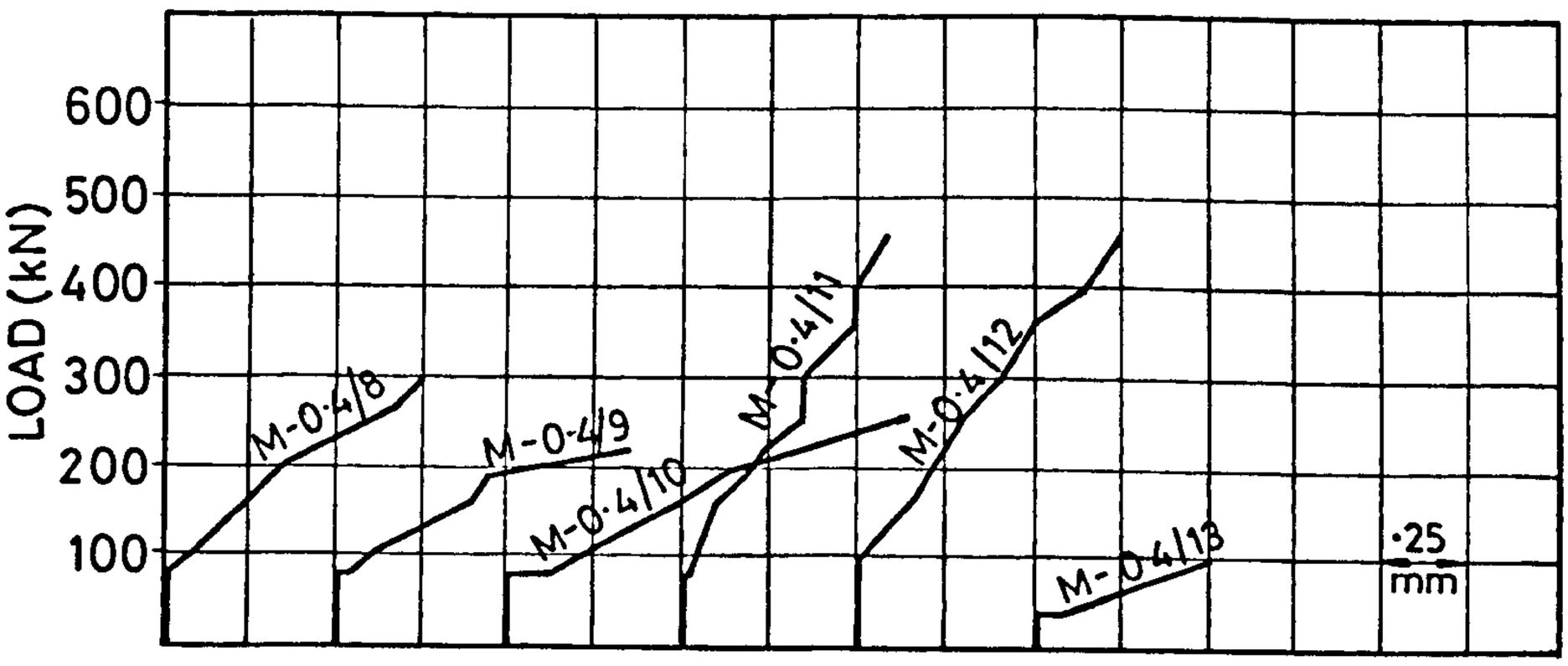

Beam notation as in Table (4.1)

FIG.4.6(a) MAXIMUM CRACK WIDTHS - GROUP M BEAMS

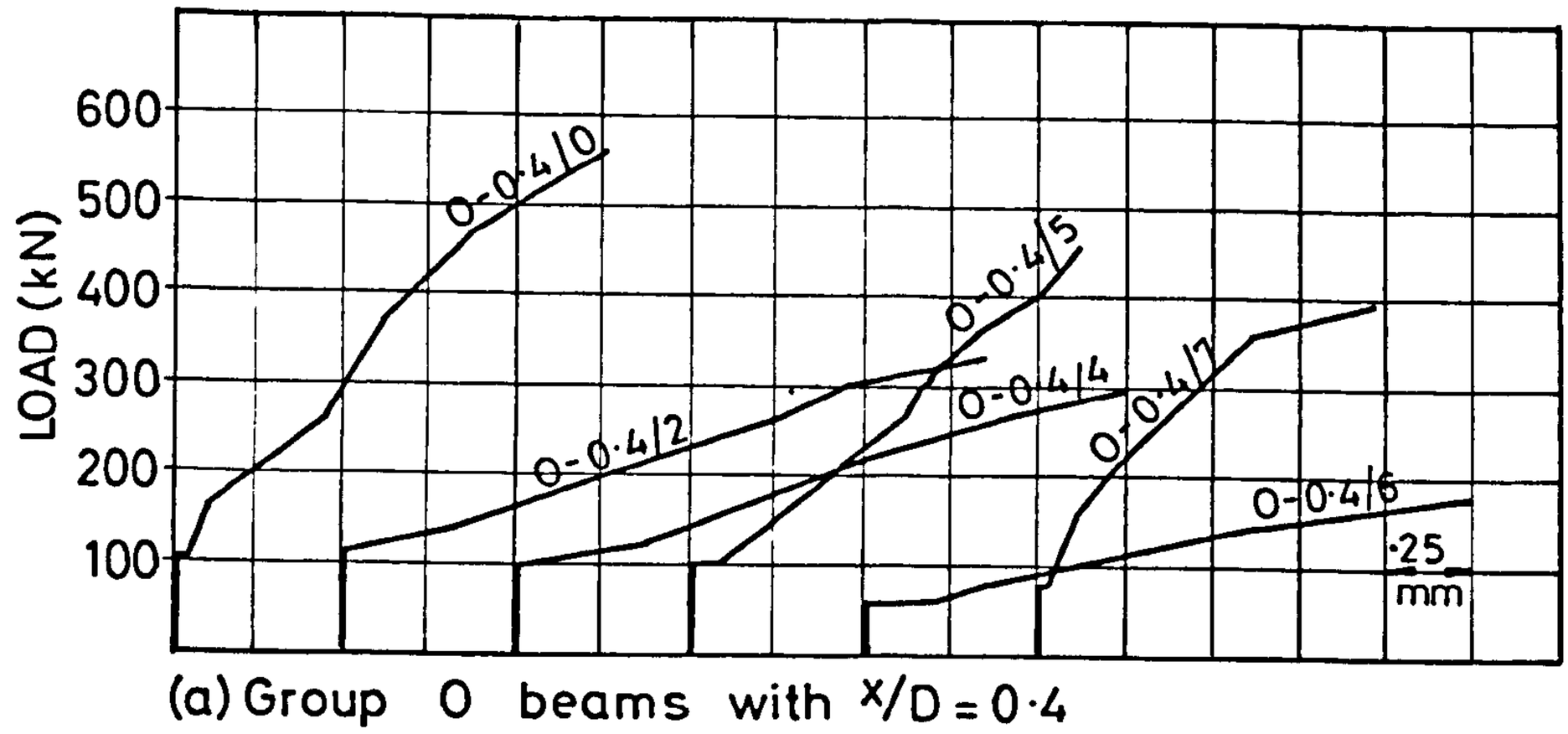

(a) Group O beams with $x/D = 0{\cdot}4$

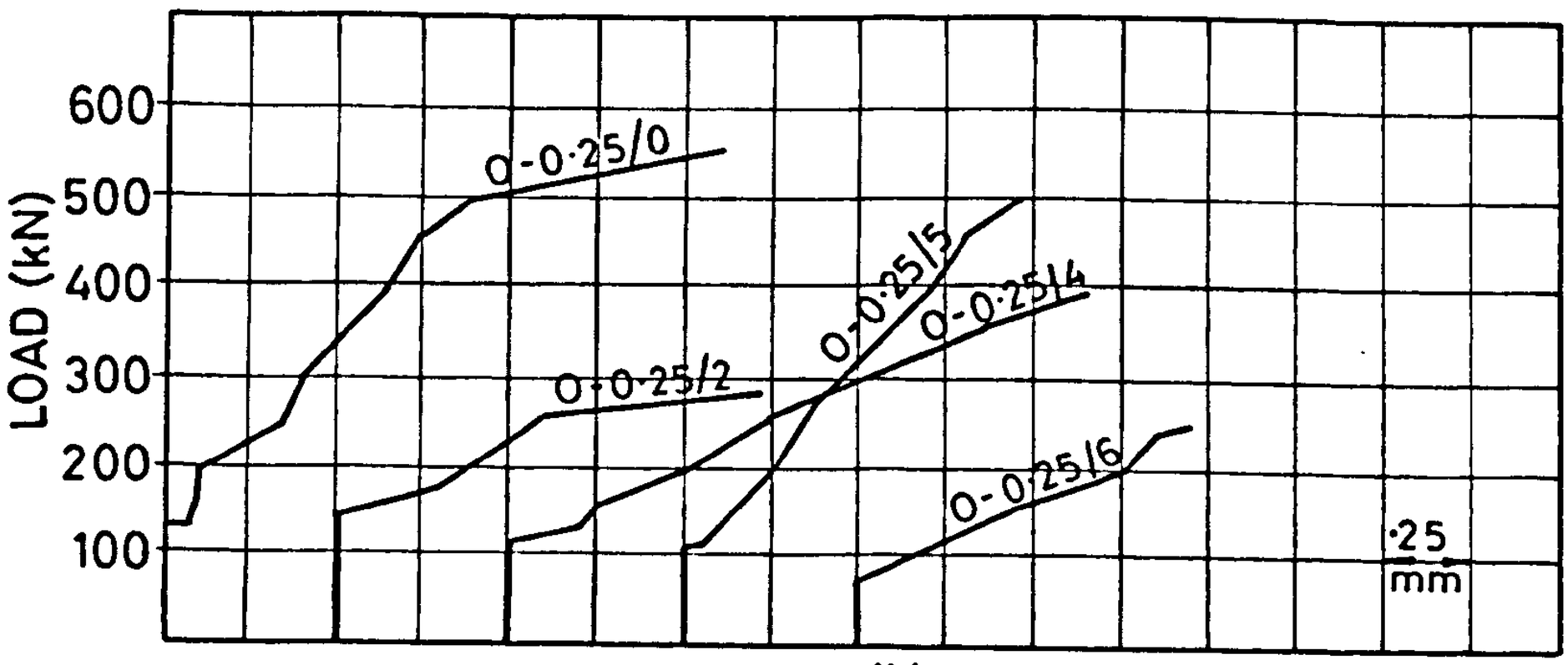

(b) Group O beams with $x/D = 0{\cdot}25$

Beam notation as in Table(4.1)

FIG.4.6(b) MAXIMUM CRACK WIDTHS - GROUP O BEAMS

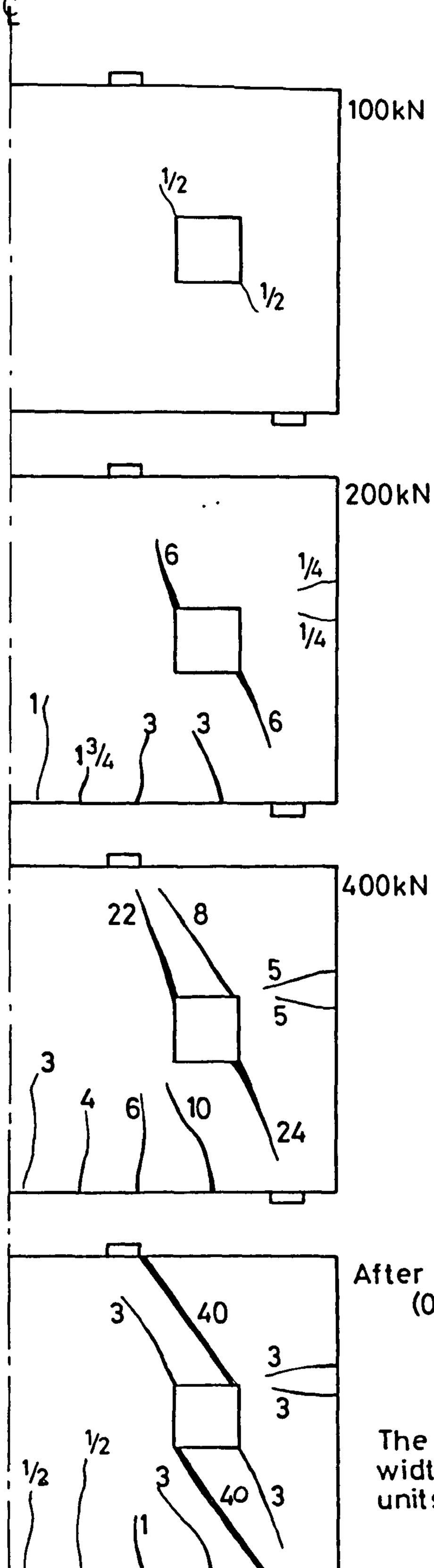

The numbers give the width of each crack in units of 0·05mm.

FIG.4.7 DEVELOPMENT OF CRACKING IN BEAM M-0.4/4

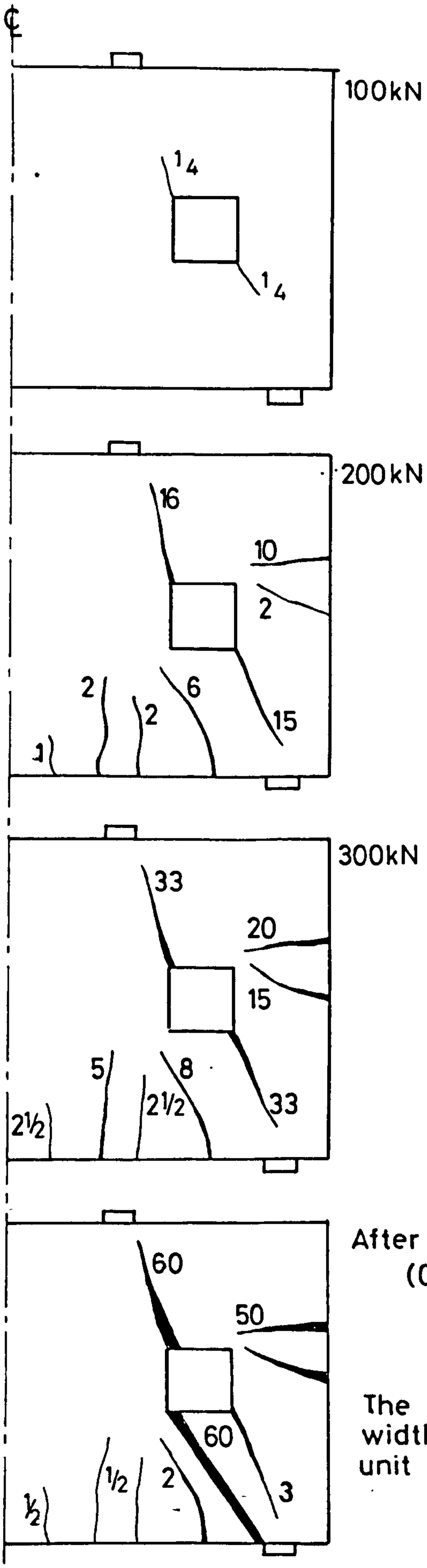

The numbers give the width of each crack in unit of 0·05mm

FIG.4.8 DEVELOPMENT OF CRACKING IN BEAM O-O.4/4

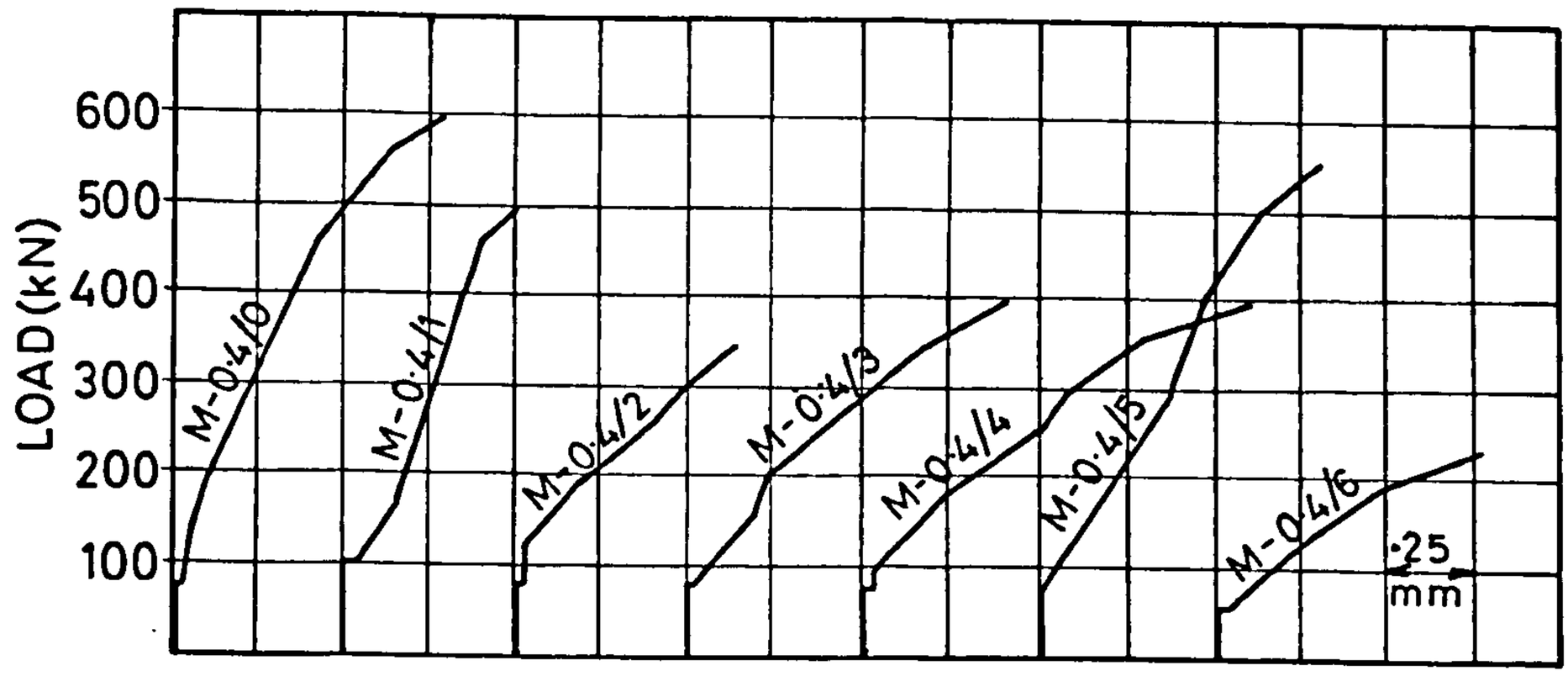

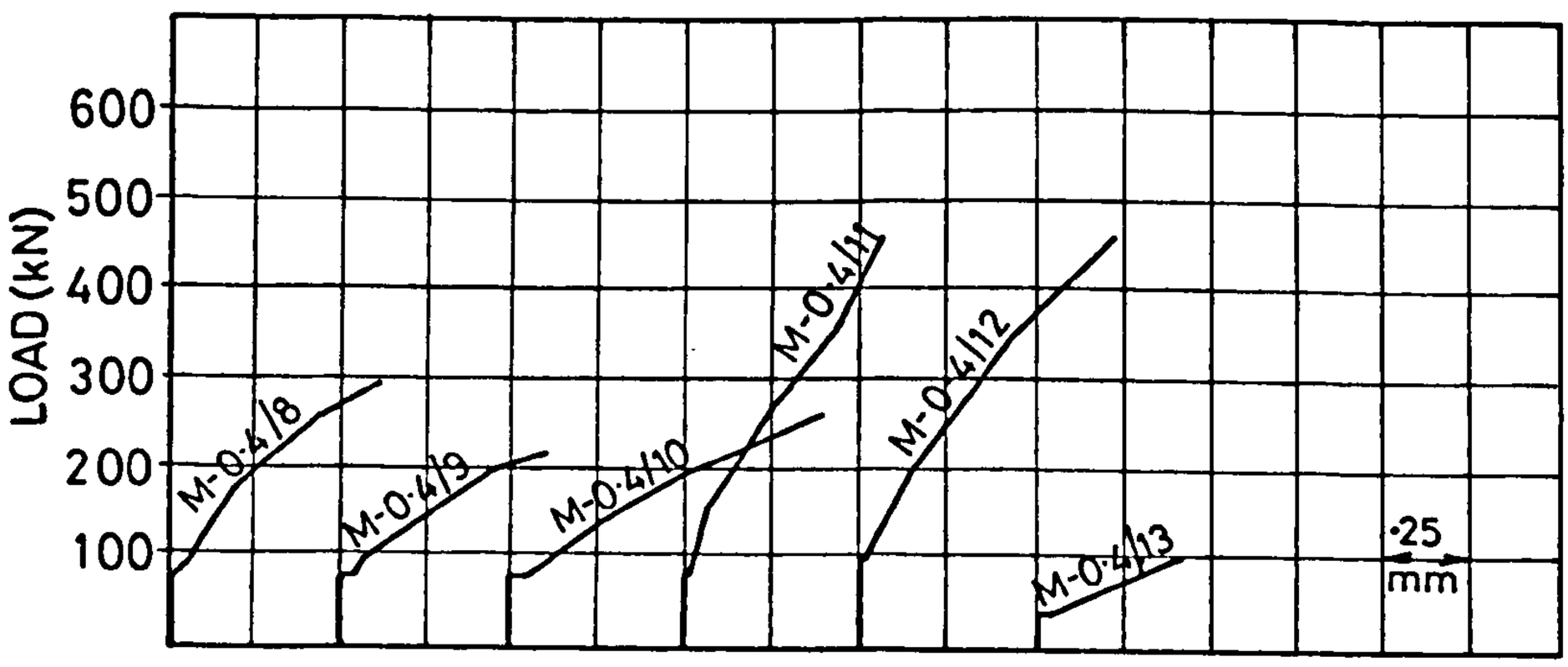

Beam notation as in Table (4.1)

FIG.4.9(a) AVERAGE CRACK WIDTHS - GROUP M BEAMS

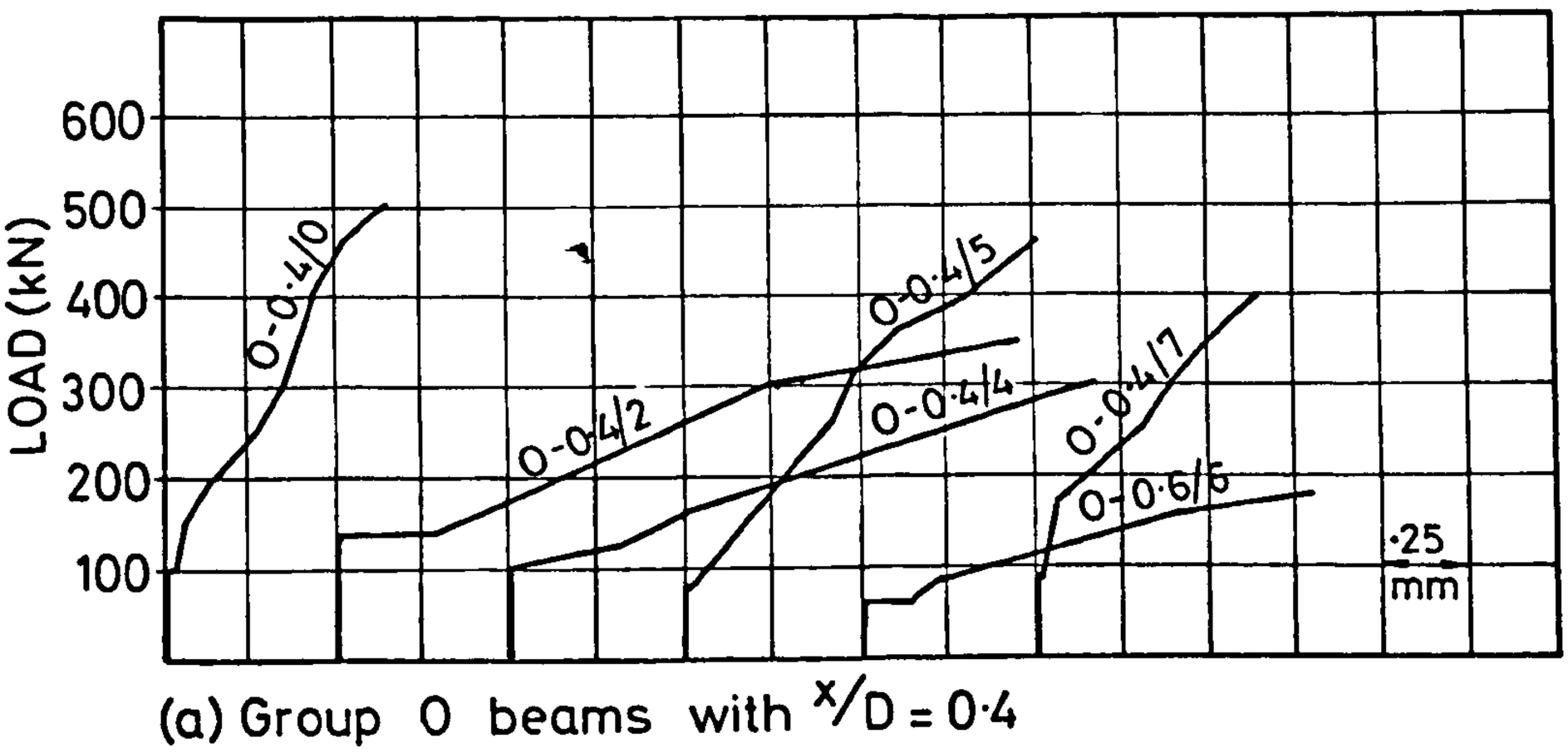

(a) Group O beams with $x/D = 0{\cdot}4$

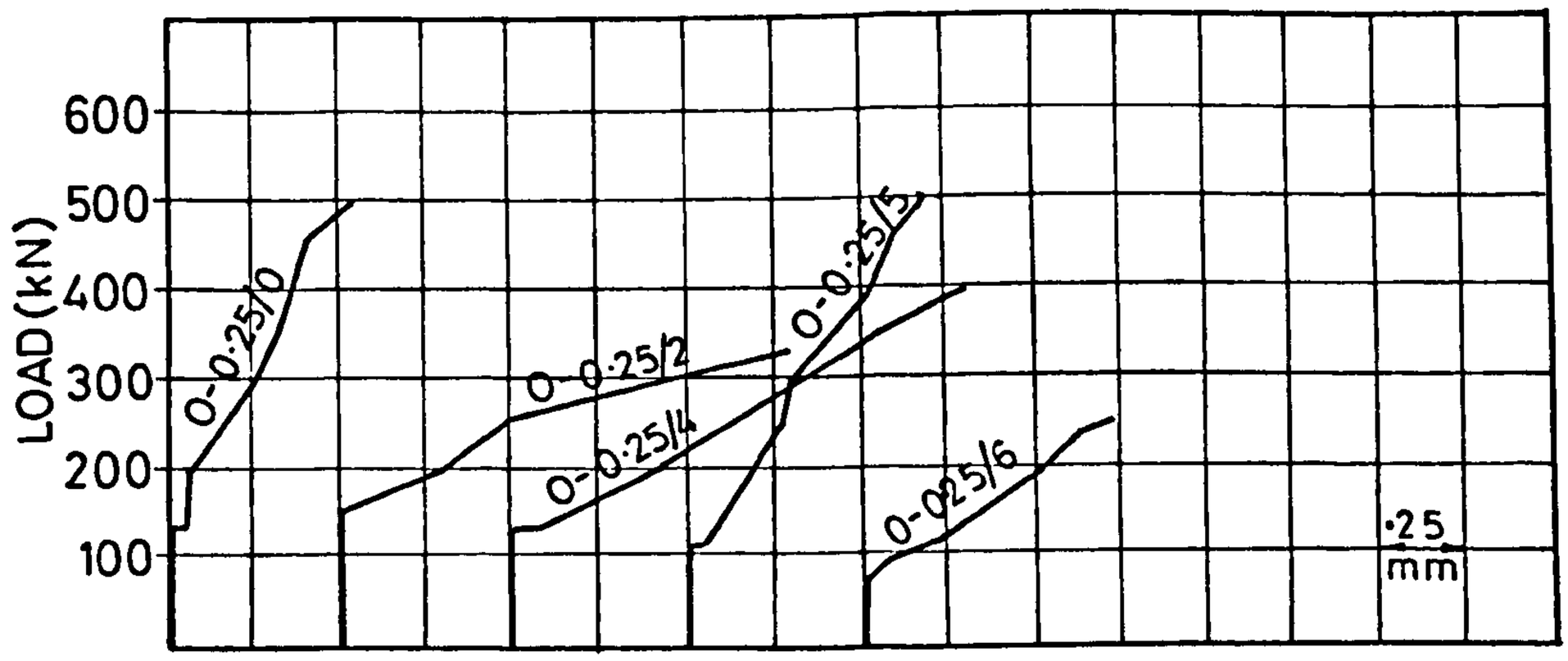

(b) Group O beams with $x/D = 0{\cdot}25$

Beam notation as in Table (4.1)

FIG.4.9(b) AVERAGE CRACK WIDTHS - GROUP O BEAMS

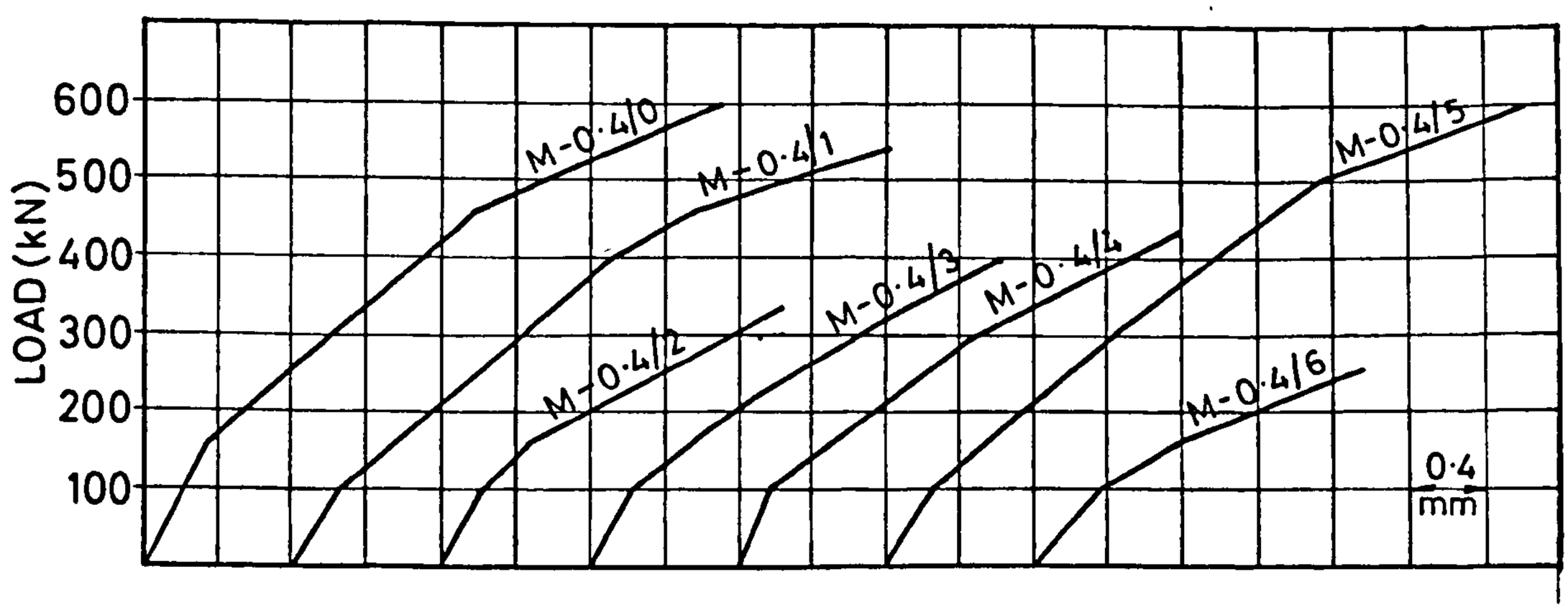

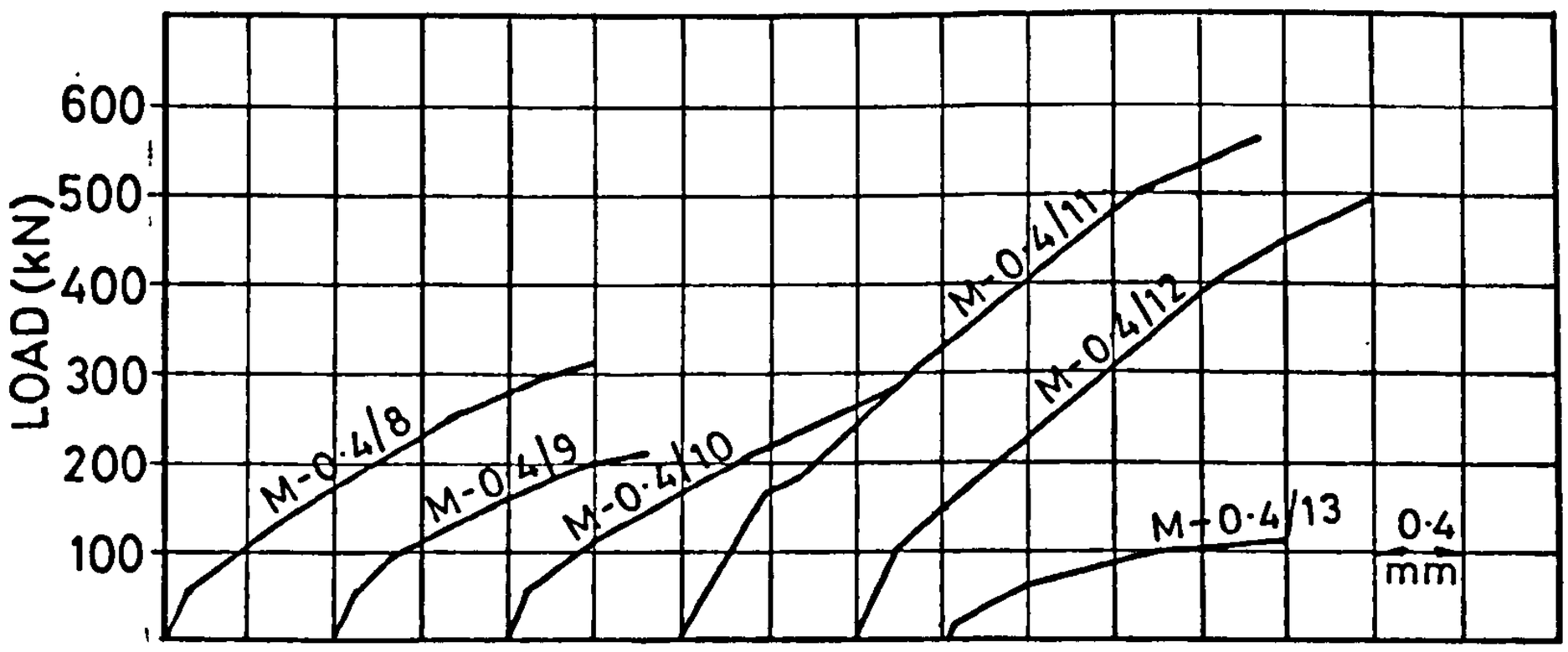

Beam notation as in Table (4.1)

FIG.4.10(a) CENTRAL DEFELECTIONS - GROUP M BEAMS

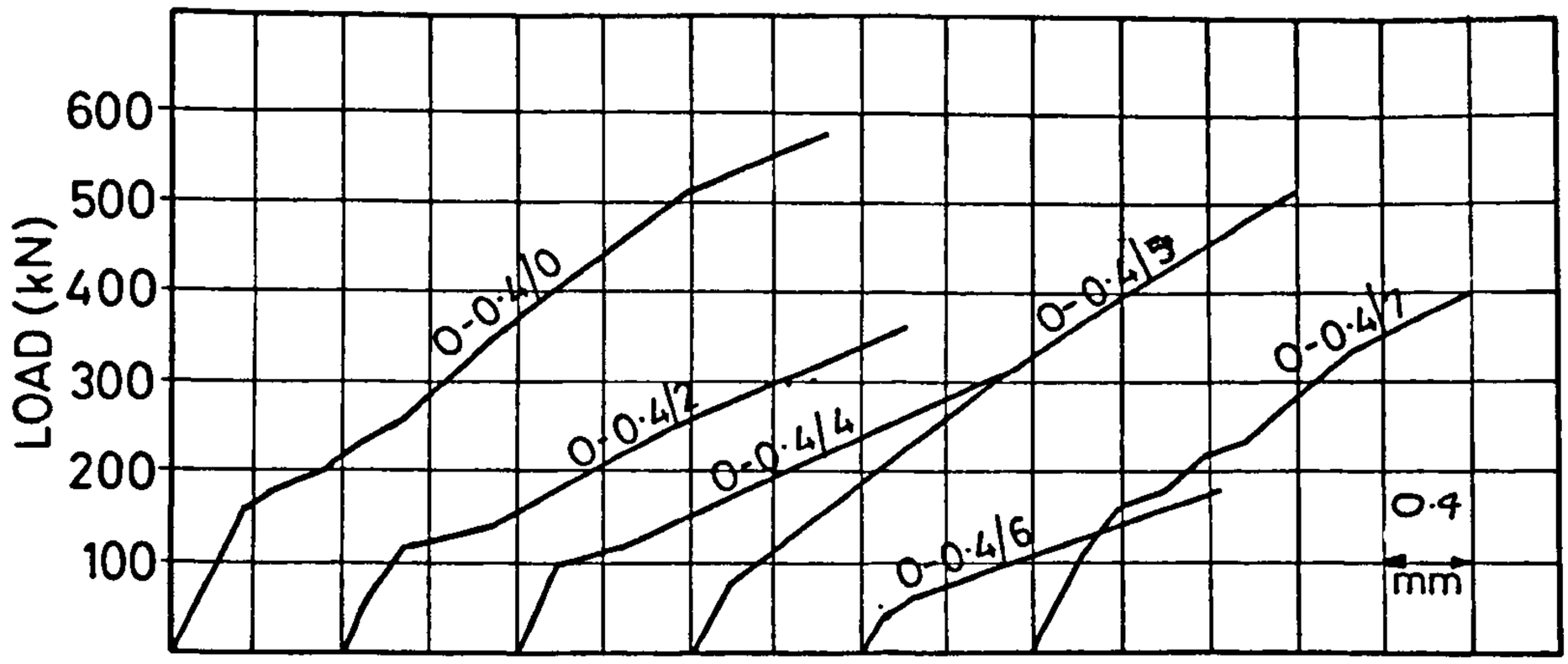

(a) Group 0 beams with $x/D = 0{\cdot}4$

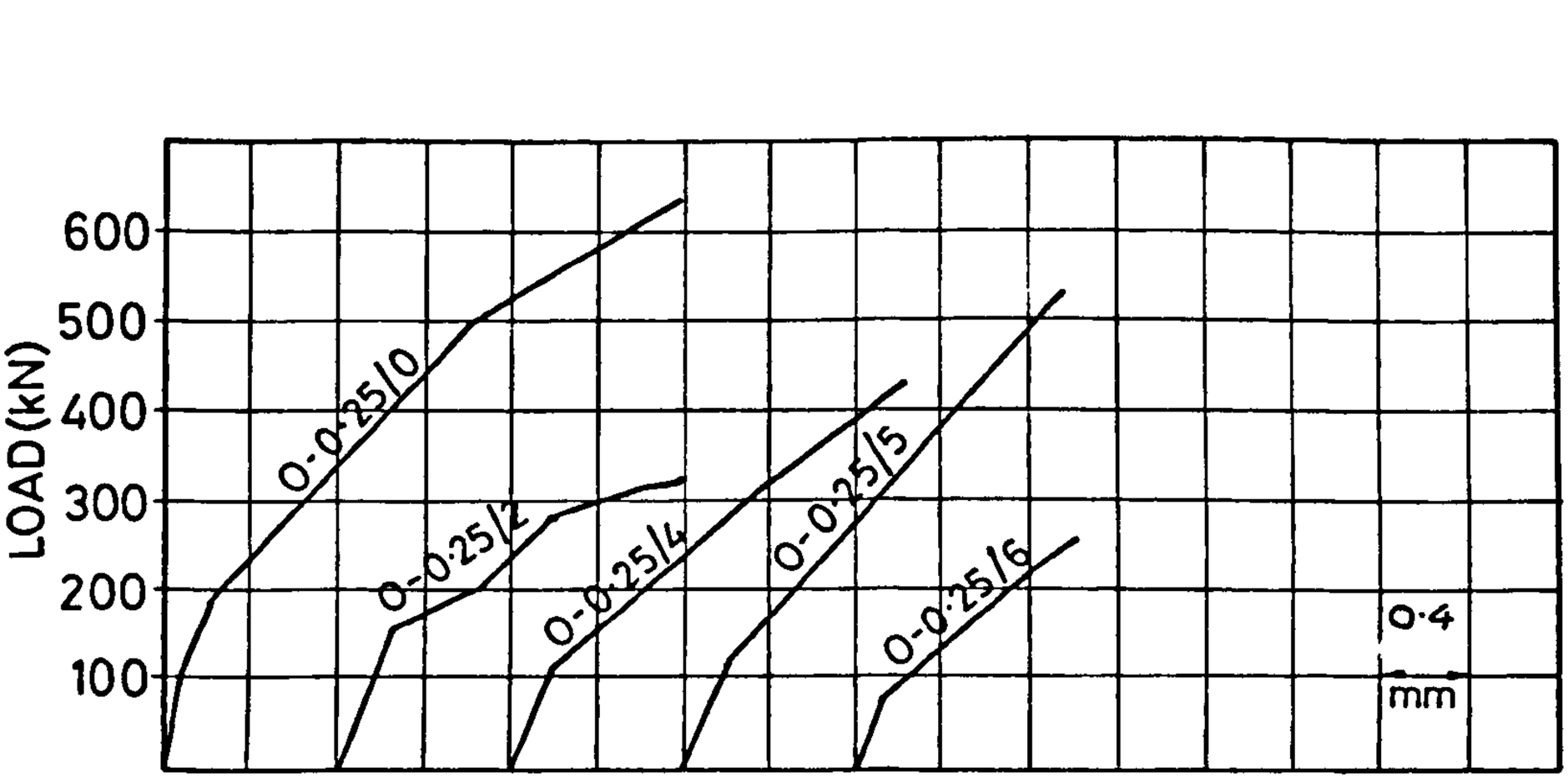

(b) Group 0 beams with $x/D = 0{\cdot}25$

Beam notation as in Table (4.1)

FIG.4.10(b) CENTRAL DEFLECTIONS - GROUP 0 BEAMS

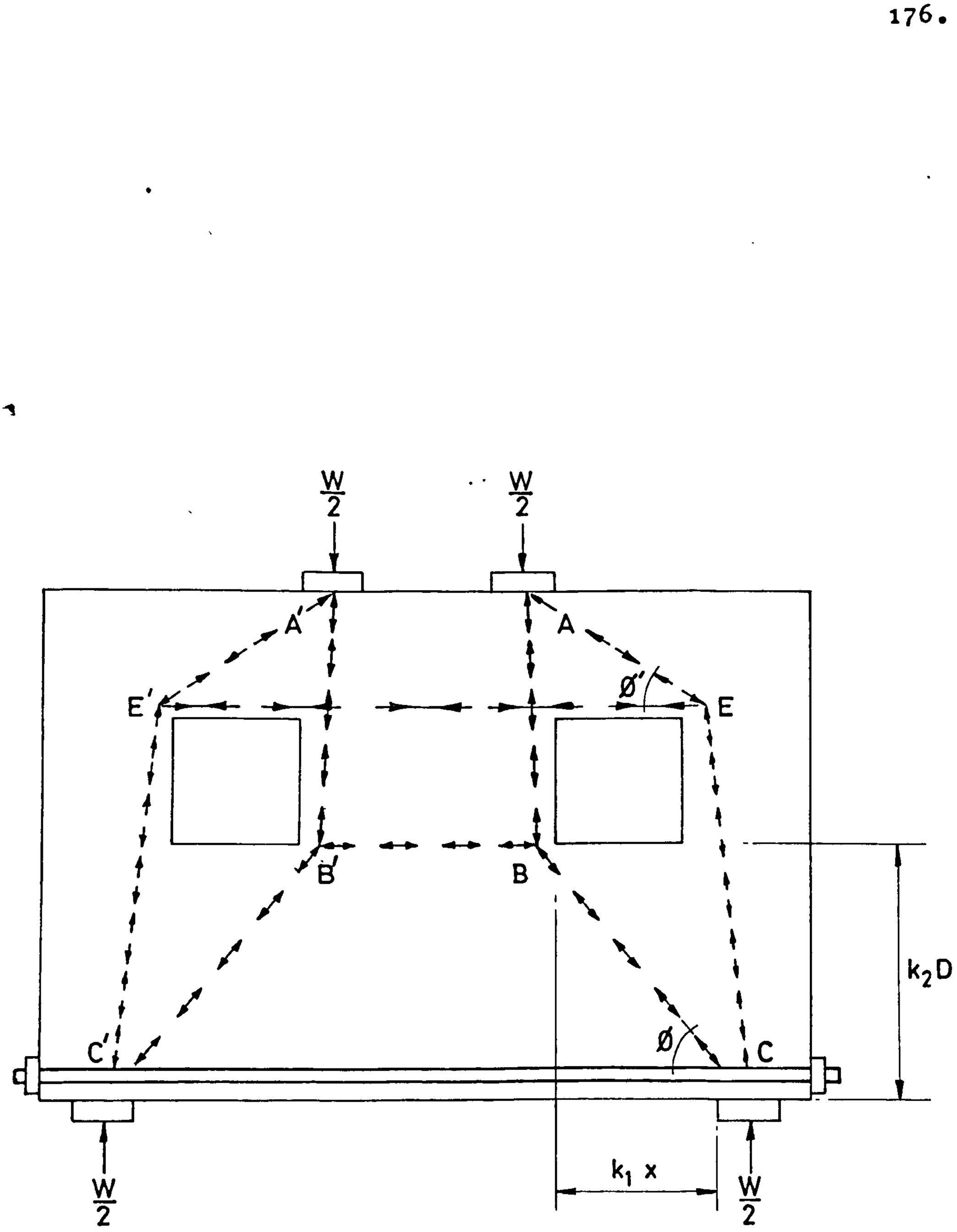

– FIG.4.11 LOAD-TRANSMISSION PATHS

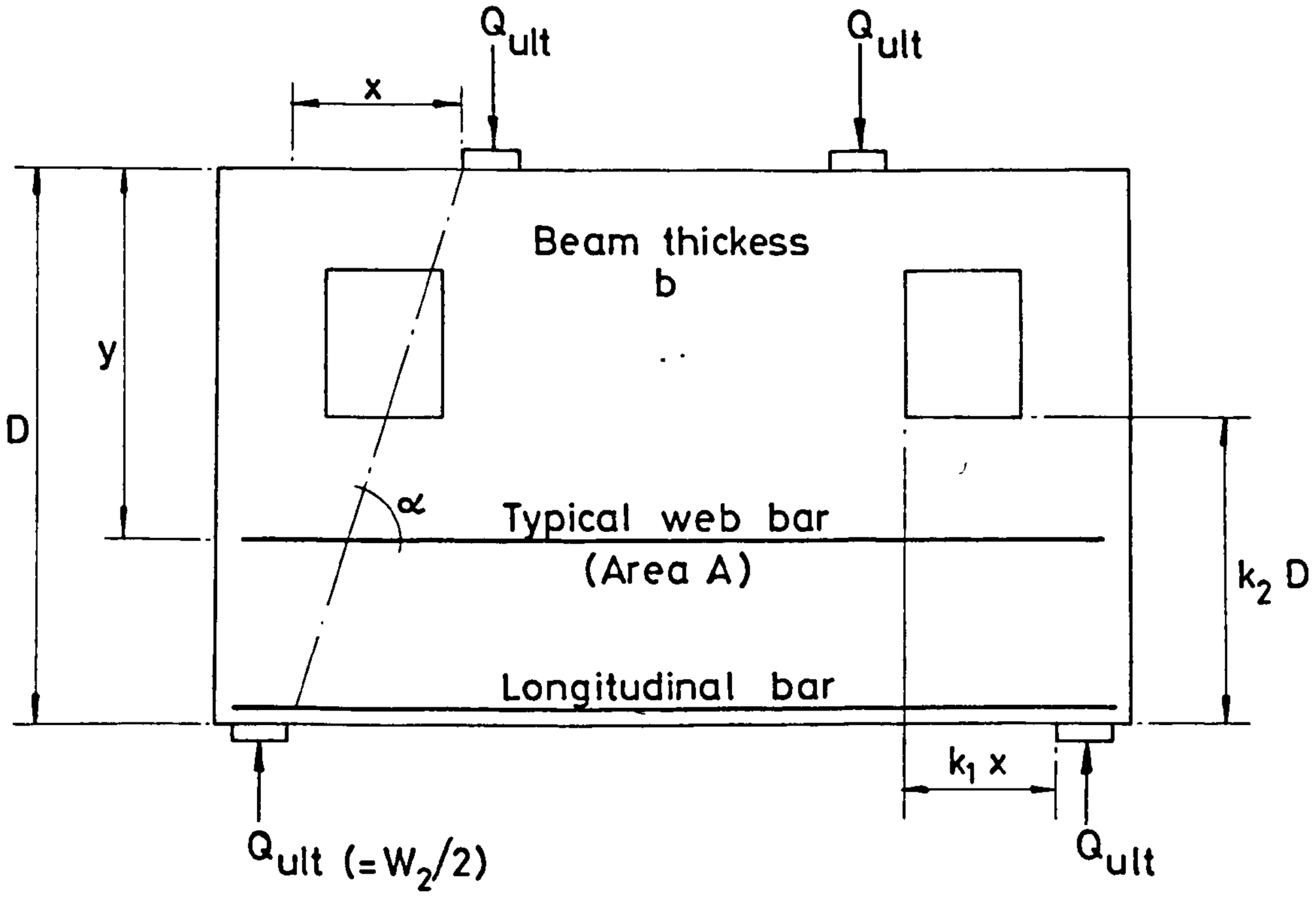

Notatation for equations (4.1) and (4.2)

1. Geometrical notation as shown above; all dimensions in millimetres.
2. C_1 and C_2 are empirical coefficients, being equal, respectively, to 1·35 and 300 N/mm^2.
3. ft is the cylinder splitting tensile strength - in accordance with A.S.T.M. standard C 330.

FIG.4.12 EXPLANATION OF SYMBOLS

Beam Ref.No. *	$\frac{L}{D}$	$\frac{x}{D}$	Web opening Ref.No. ‡‡	Web steel		f_{cu} N/mm^2 ≠	f_c' N/mm^2 xx xx	f_t N/mm^2 **
				Type	per cent			
0-0.3/0	1.5	0.3	0	These Group 0 beams had no web steel		39.0	37.0	2.69
0-0.3/1	1.5	0.3	1			40.4	35.6	2.61
0-0.3/2	1.5	0.3	2			41.3	36.9	3.06
0-0.3/3	1.5	0.3	3			41.7	35.5	2.69
0-0.3/4	1.5	0.3	4			40.8	34.7	2.69
0-0.3/5	1.5	0.3	5			39.2	35.0	2.74
0-0.3/6	1.5	0.3	6			33.4	33.3	2.89
0-0.3/7	1.5	0.3	7			43.7	39.2	3.04
0-0.3/8	1.5	0.3	8			33.0	31.8	2.61
0-0.3/9	1.5	0.3	9			45.0	38.1	2.80
0-0.3/10	1.5	0.3	10			36.0	33.6	2.85
0-0.3/11	1.5	0.3	11			30.8	33.3	2.78
0-0.3/12	1.5	0.3	12			36.7	33.1	3.11
0-0.3/13	1.5	0.3	13			41.3	37.8	2.92
0-0.3/14	1.5	0.3	14			33.2	30.2	2.76
0-0.3/15	1.5	0.3	15			35.2	33.6	2.92
0-0.3/16	1.5	0.3	16			43.4	37.6	3.07
0-0.2/0	1.0	0.2	0	These Group 0 beams had no web steel		39.6	37.4	2.93
0-0.2/4	1.0	0.2	4			42.0	39.6	3.19
0-0.2/13	1.0	0.2	13			38.5	39.5	2.85
0-0.2/16	1.0	0.2	16			40.4	38.9	2.76

(continued on next page)

* Beam notation: A letter O before the hyphen indicates no web reinforcement, whilst a letter W indicates the presence of web reinforcement; the x/D ratio is given after the hyphen, followed by web-opening reference number. Thus W1-0.3/4 refers to a beam with web reinforcement Type W1 (see Fig.5.1), having an x/D ratio of 0.3 and a web opening type 4.

‡ The four beams with a suffix A were tested under 4-point loading (see Fig.5.3); otherwise Beam W1(A) was identical to Beam W1-0.3/4. Beam W3(A) identical to Beam W3-0.3/4 and so on.

xx The four beams with a suffix R were repeat tests; viz., Beam O-0.3/2R was identical to Beam O-0.3/2, Beam O-0.3/3R identical to Beam O-0.3/3 and so on.

‡‡ , ≠ , xx xx , ** , see continuation next page.

TABLE 5.1 PROPERTIES OF TEST BEAMS
(Further tests; lightweight concrete)

Beam * Ref.No.	$\frac{L}{D}$	$\frac{x}{D}$	Web opening Ref.No. ++	Web steel Type	Web steel per cent	f_{cu} ≠ N/mm^2	f_c' xx N/mm^2	f_t ** N/mm^2
0-0.3/2R xx	1.5	0.3	2			34.2	32.1	2.84
0-0.3/3R	1.5	0.3	3			40.7	35.9	2.54
0-0.3/4R	1.5	0.3	4			45.0	35.3	3.03
0-0.3/5R	1.5	0.3	5			37.3	31.7	3.03
W1-0.3/4	1.5	0.3	4	W1	1.19	39.5	34.2	2.93
W2-0.3/4	1.5	0.3	4	W2	1.19	40.5	34.6	2.96
W3-0.3/4	1.5	0.3	4	W3	1.19	40.9	33.7	2.87
W4-0.3/4	1.5	0.3	4	W4	1.24	39.1	33.3	2.89
W5-0.3/4	1.5	0.3	4	W5	1.11	36.8	35.3	2.93
W6-0.3/4	1.5	0.3	4	W6	1.25	37.8	31.9	2.91
W7-0.3/4	1.5	0.3	4	W7	1.13	37.4	33.0	3.03
W1 (A) ‡	1.5	0.3	4	W1	1.19	34.5	31.8	2.82
W3 (A)	1.5	0.3	4	W3	1.19	34.3	33.6	3.04
W4 (A(	1.5	0.3	4	W4	1.24	35.2	32.5	2.89
W7 (A)	1.5	0.3	4	W7	1.13	37.7	31.9	3.04
WM-0.4/0	2	0.4	0	WM	1.13	30.6	26.4	3.03
WM-0.4/18	2	0.4	18	WM	1.13	35.1	26.1	3.16
WM-0.4/18	2	0.4	18	WM	1.13	31.6	26.1	3.16

*, ‡, xx, see previous page.

++ Details of web openings are given in Figs.5.2 and 5.4

≠ f_{cu} = cube strength (100 mm)

xx f_c' = cylinder compressive strength (300 mm x 150 mm)

** f_t = cylinder splitting tensile strength (300 mm x 150 mm) - in accordance with ASTM C330.

TABLE 5.1 PROPERTIES OF TEST BEAMS (Continued).

Beam Ref. No.*	Measured W_1 kN
0-0.3/0	595
0-0.3/1	460
0-0.3/2	390
0-0.3/3	280
0-0.3/4	260
0-0.3/5	200
0-0.3/6	250
0-0.3/7	420
0-0.3/8	380
0-0.3/9	280
0-0.3/10	210
0-0.3/11	360
0-0.3/12	560
0-0.3/13	300
0-0.3/14	560
0-0.3/15	260
0-0.3/16	195
0-0.2/0	655
0-0.2/4	360
0-0.2/13	500
0-0.2/16	340

Beam Ref. No.*	Measured W_1 kN
0-0.3/2R	260
0-0.3/3R	400
0-0.3/4R	215
0-0.3/5R	330
W1-0.3/4	400
W2-0.3/4	490
W3-0.3/4	560
W4-0.3/4	660
W5-0.3/4	370
W6-0.3/4	825
W7-0.3/4	630
W1(A)	475
W3(A)	500
W4(A)	650
W7(A)	670
WM-0.4/0	660
WM-0.4/18	500
WM'-0.4/18	500

*Beam notation as in Table 5.1

TABLE 5.2 MEASURED ULTIMATE LOADS
(Further tests; lightweight concrete).

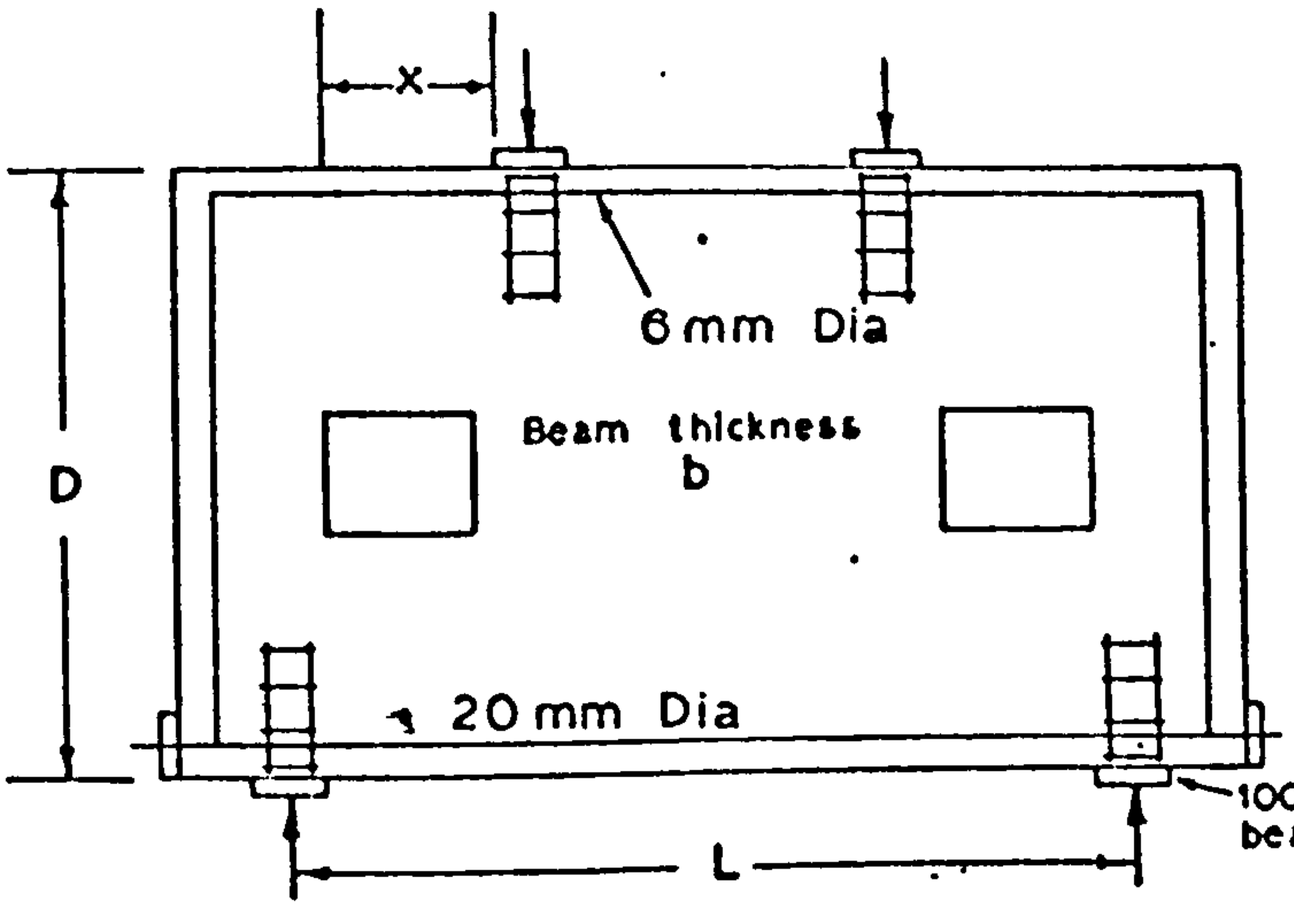

Beam Geometry (mm)				
	L	D	x	b
For $\frac{x}{D}$ = 0·2	750	750	150	100
$\frac{x}{D}$ = 0·3	1125	750	225	100
$\frac{x}{D}$ = 0·4	1524	762	304	76

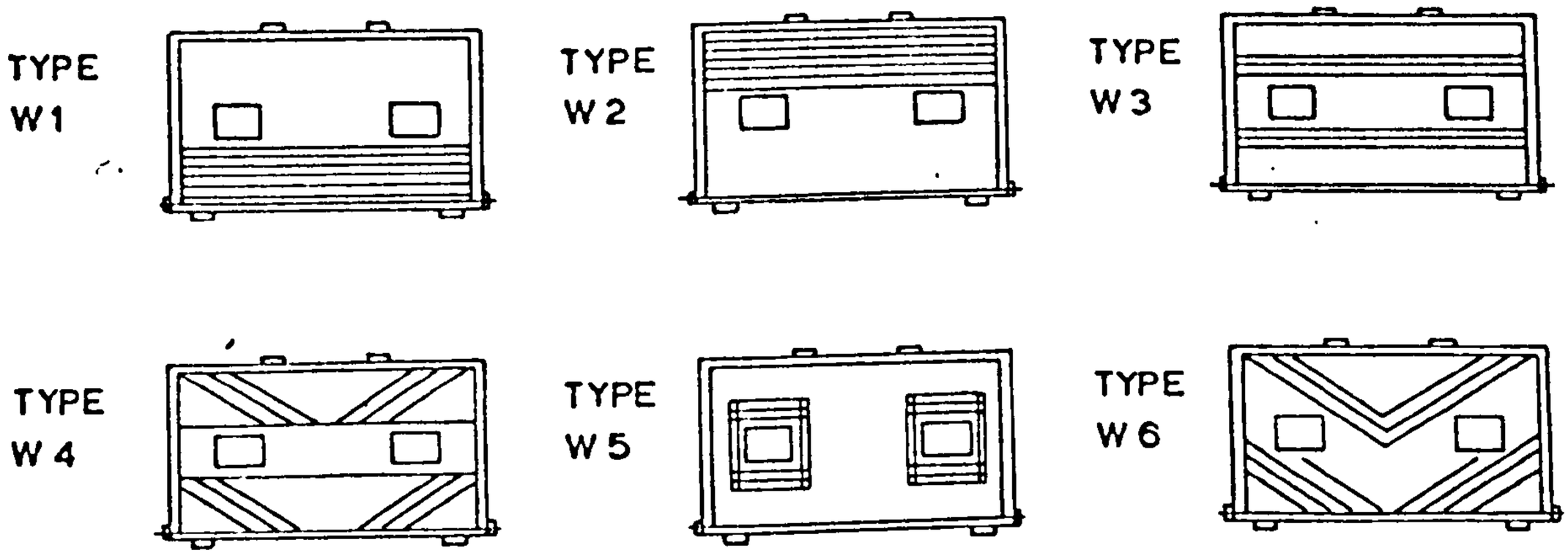

NOTES:

(1) Reinforcement details of Group 0 beams (no web reinforcement) as shown in top diagram above.

(2) Web reinforcement. Type W1 to W7 consisted of 10 mm diameter stirrups (web steel ratio = 1.2%)

(3) Web reinforcement Types WM and WM' consisted of 6 mm diameter stirrups (web steel ratio = 1.13%)

FIG.5.1 DIMENSIONS AND REINFORCEMENT DETAILS
(Further tests in lightweight concrete)

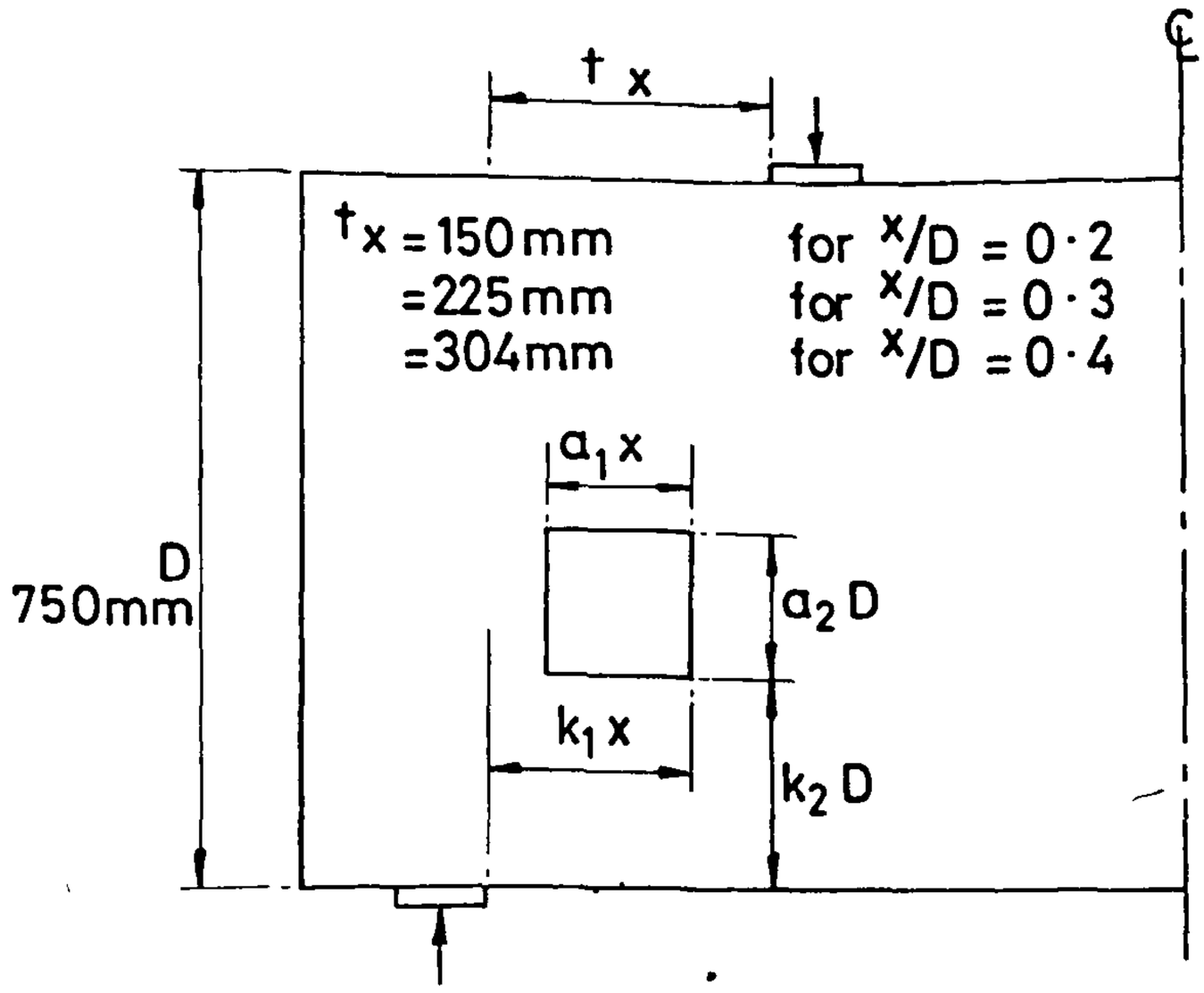

REF No.	SIZE a_1	a_2	POSITION k_1	k_2
0	NO OPENING			
1	0·30	0·20	1·00	0·40
2	0·50	0·20	1·00	0·40
3	0·70	0·20	1·00	0·40
4	1·00	0·20	1·00	0·40
5	1·20	0·20	1·00	0·40
6	1·50	0·20	1·00	0·40
7	0·30	0·20	0·30	0·40
8	0·50	0·20	0·50	0·40
9	0·70	0·20	0·70	0·40
10	1·30	0·20	1·30	0·40
11	0·30	0·20	1·00	0·666
12	0·30	0·20	0·30	0·666
13	1·00	0·20	1·00	0·666
14	0·30	0·20	1·00	0·134
15	0·30	0·20	0·30	0·134
16	1·00	0·20	1·00	0·134
17	0·30	0·20	0·65	0·40
18	0·25	0·25	0·622	0·375

FIG.5.2 OPENING REFERENCE NUMBERS: APPLICABLE TO LIGHTWEIGHT BEAMS IN TABLE 5.1 AND NORMAL WEIGHT BEAMS IN TABLE 6.1

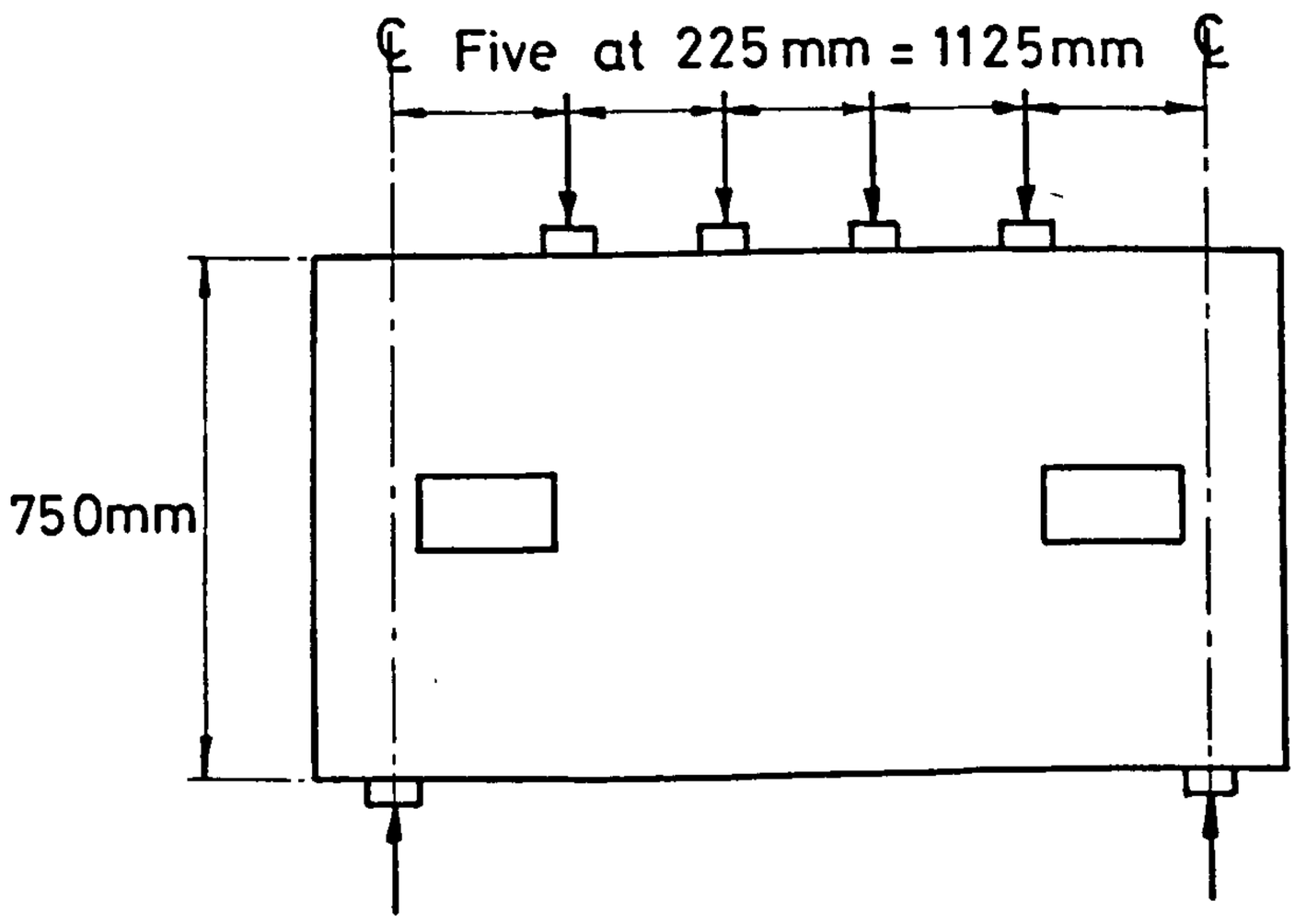

FIG.5.3 FOUR POINT LOADING - FOR BEAMS W1(A), W3(A), W4(A) and W7(A)

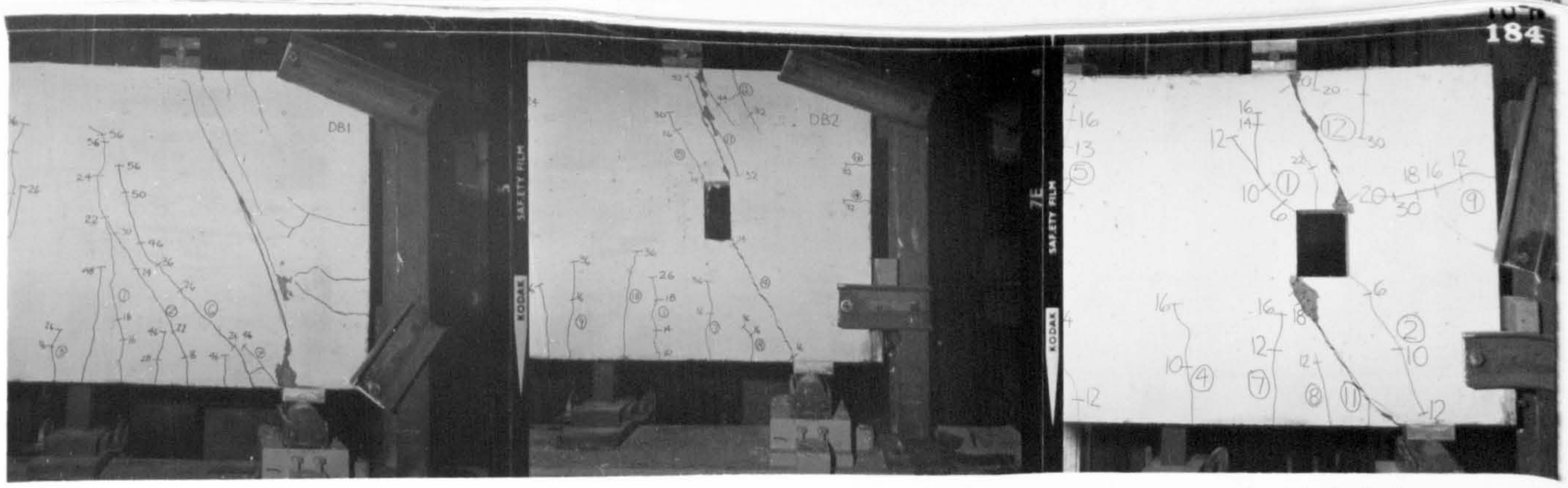

0-0·3/0 0-0·3/1 0-0·3/2

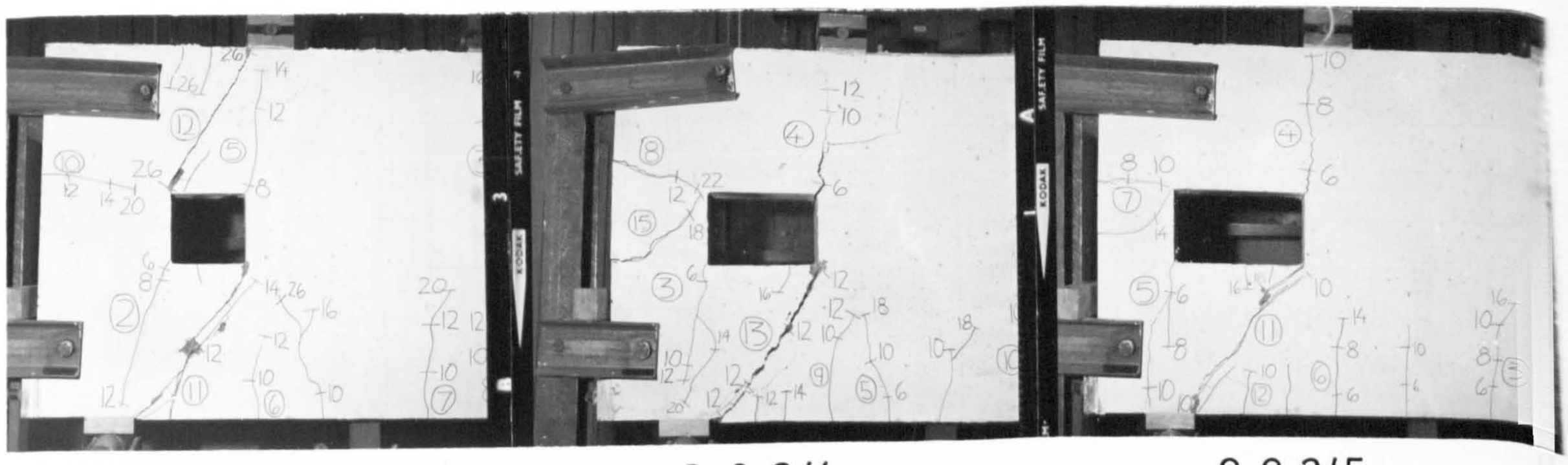

0-0·3/3 0-0·3/4 0-0·3/5

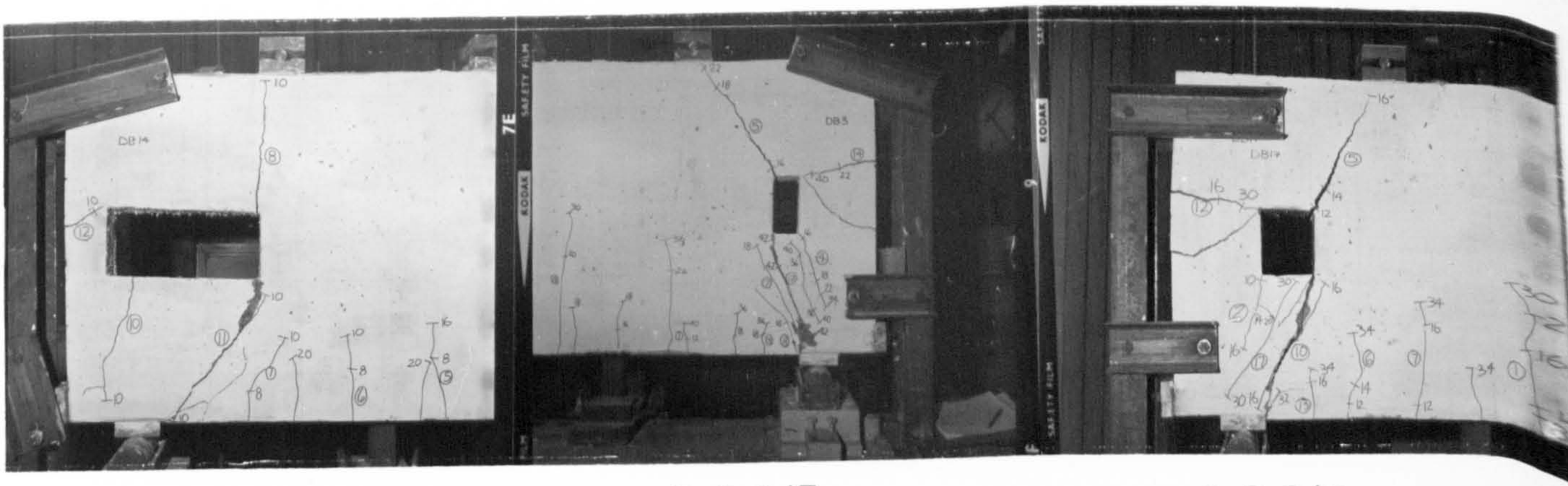

0-0·3/6 0-0·3/7 0-0·3/8

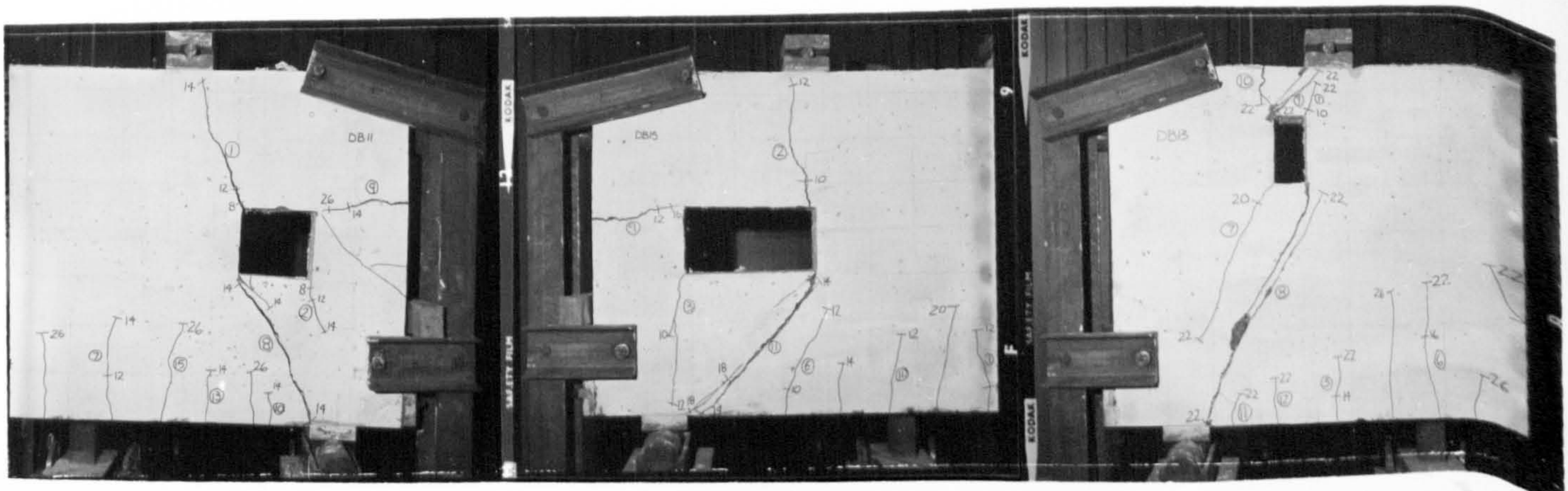

0-0·3/9 0-0·3/10 0-0·3/11

FIG.5.4a TYPICAL CRACK PATTERNS AT FAILURE
- GROUP 0 BEAMS (First twelve)

(The circled numbers show the sequence in which the cracks were observed; the other numerical figures show the load in 10 kN units, at which the extent of the cracks were as marked. Beam notation as in Table 5.1)

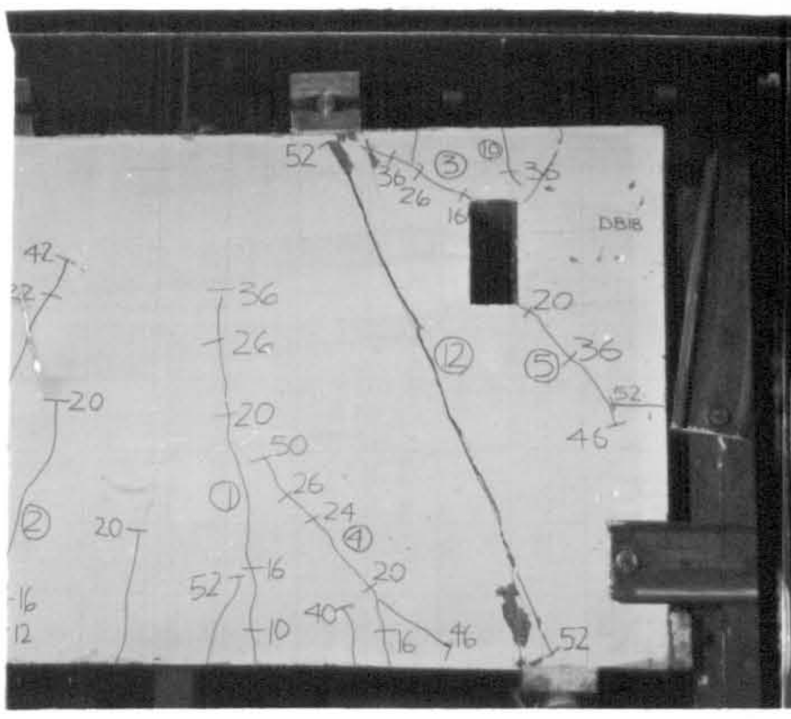

0-0·3/12

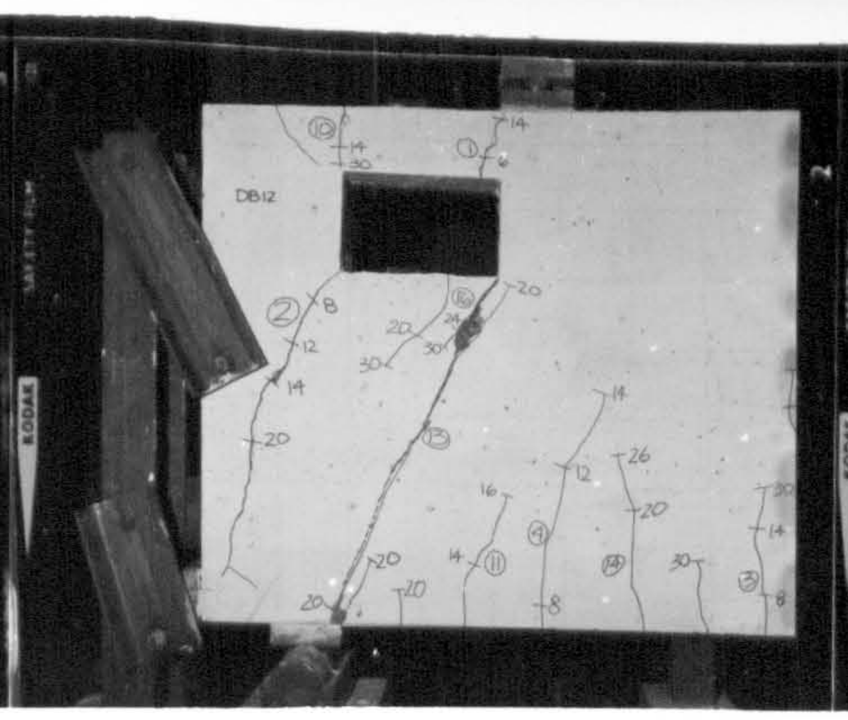

0-0·3/13

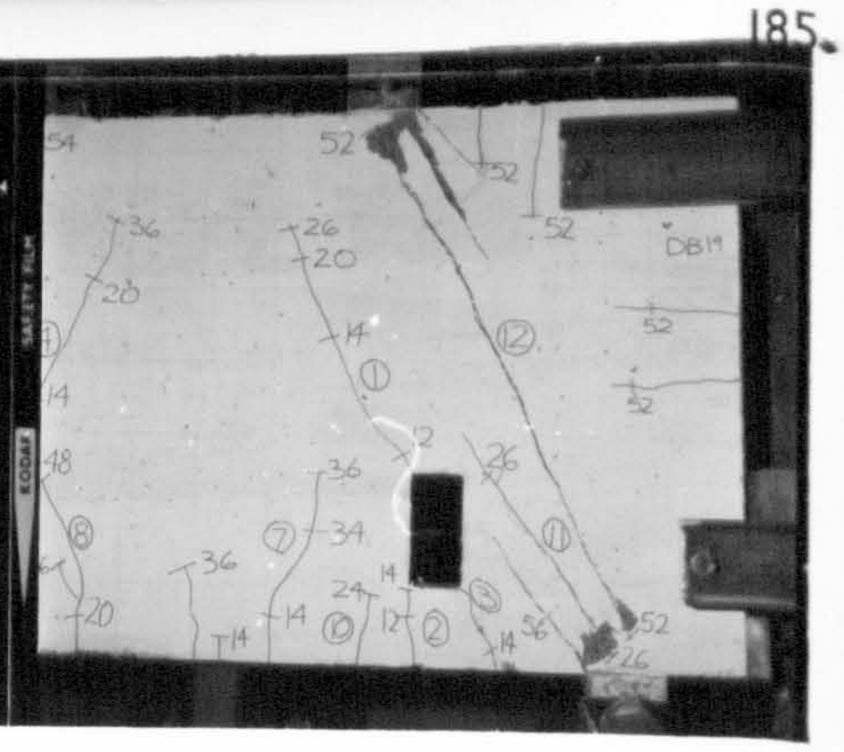

0-0·3/14

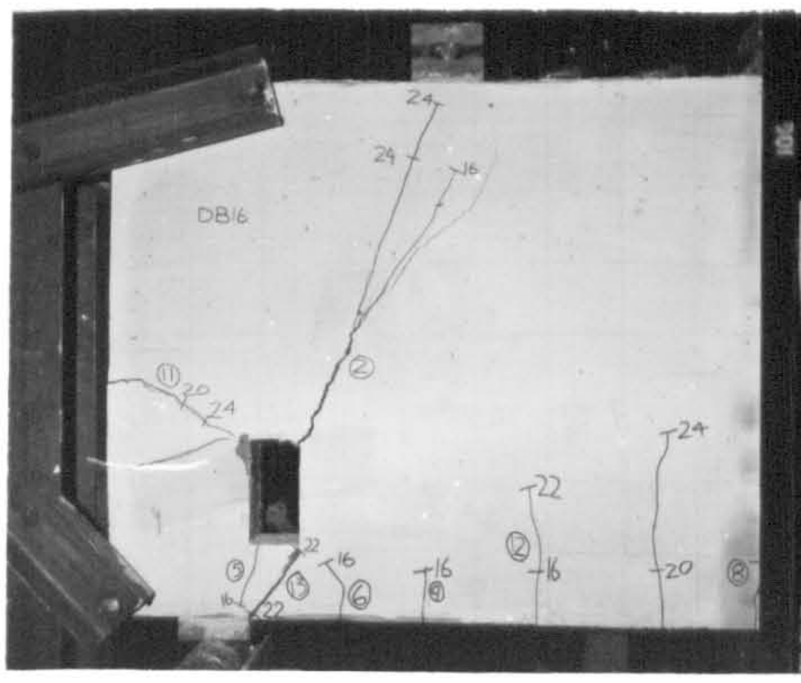

0-0·3/15

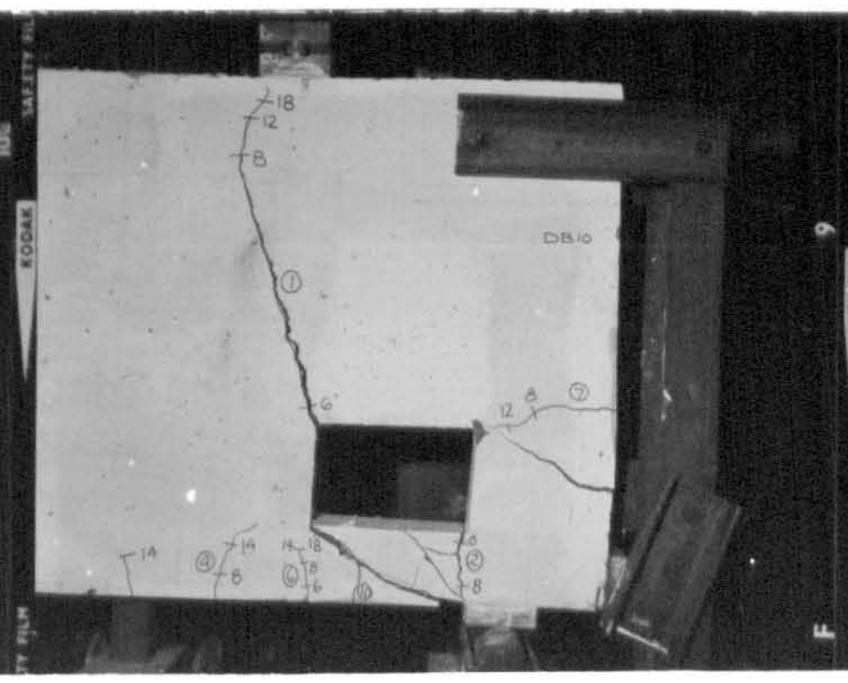

0-0·3/16

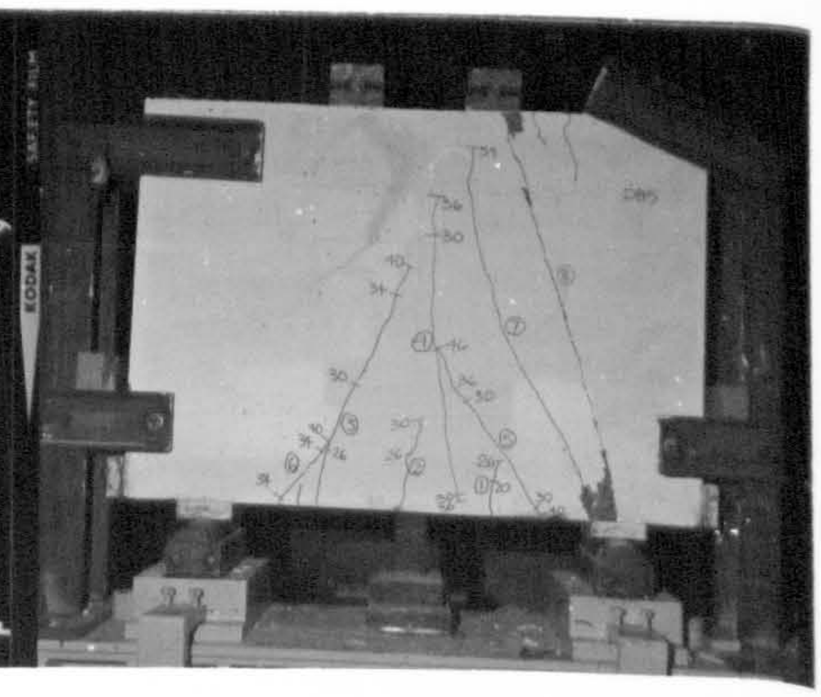

0-0·2/0

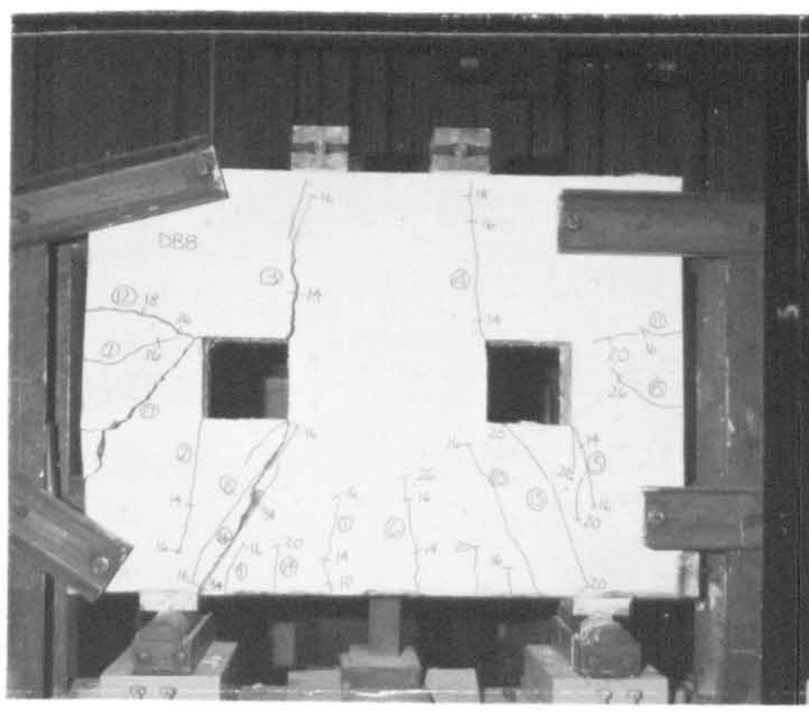

0-0·2/4

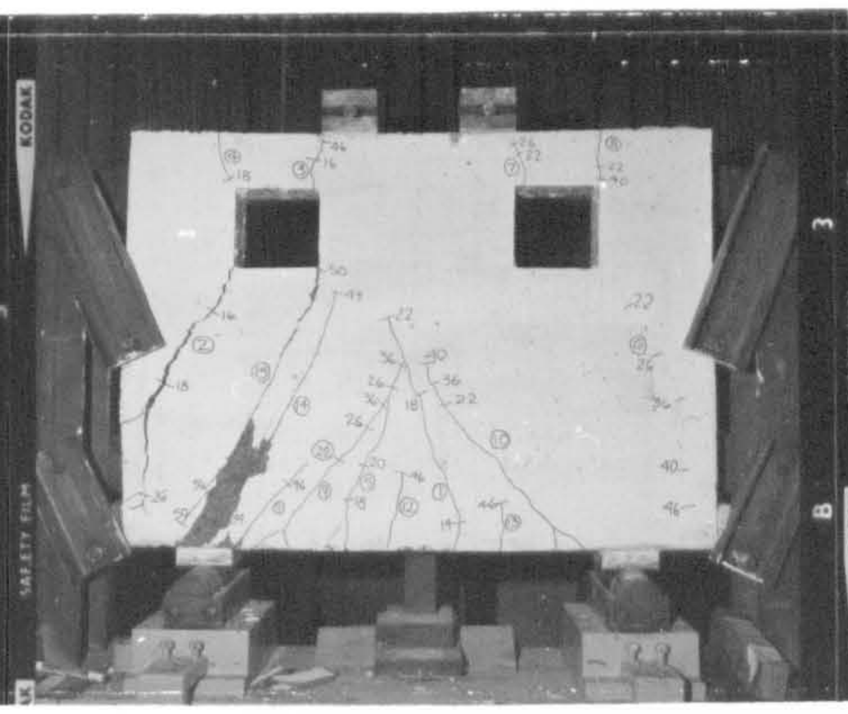

0-0·2/13

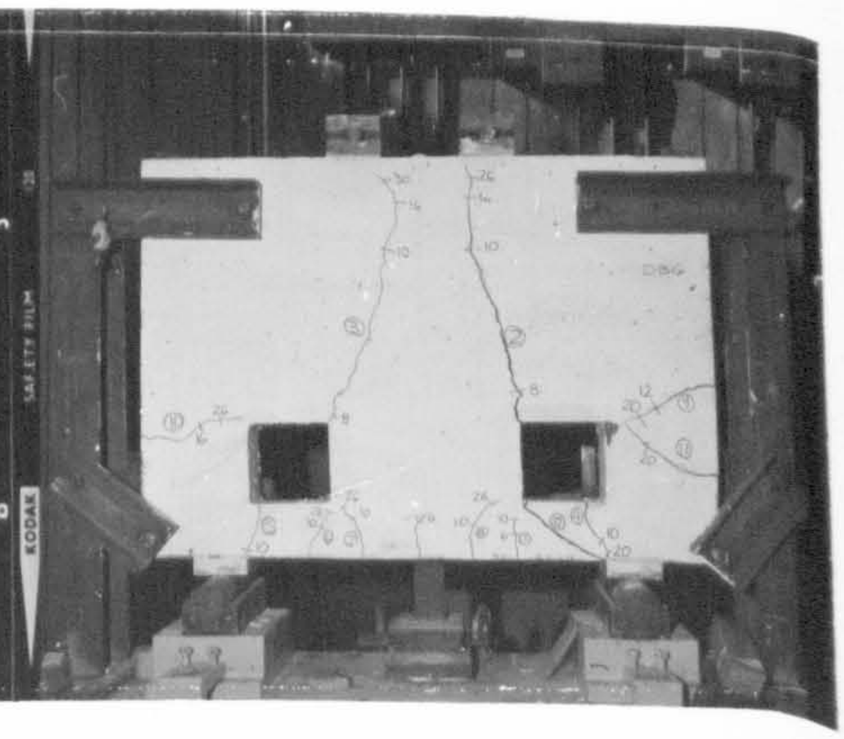

0-0·2/16

FIG.5.4b TYPICAL CRACK PATTERNS AT FAILURE
(The remaining Group 0 beams)

(The circled numbers show the sequence in which the cracks were observed; the other numerical figures show the load in 10 kN units, at which the extent of the cracks were as marked.
Beam notation as in Table 5.1)

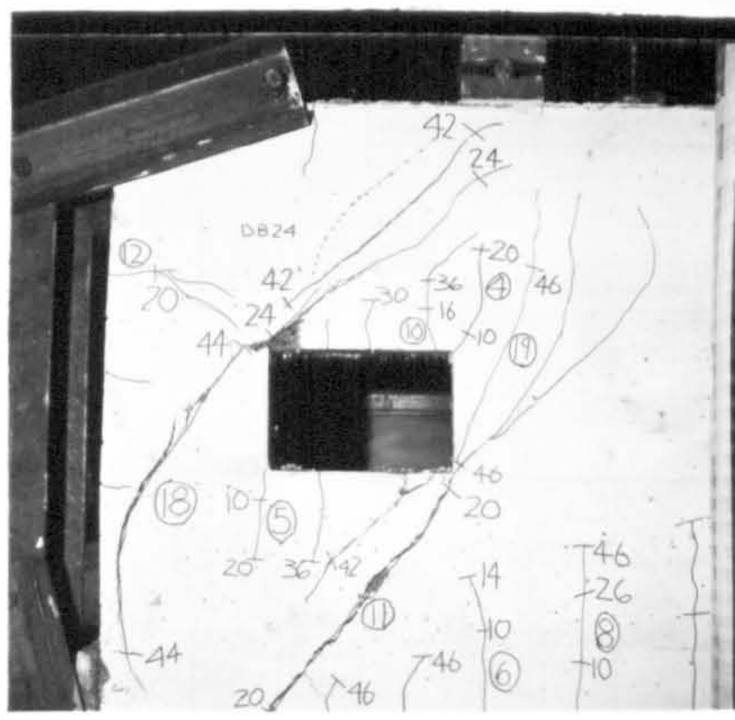

W1-0·3/4

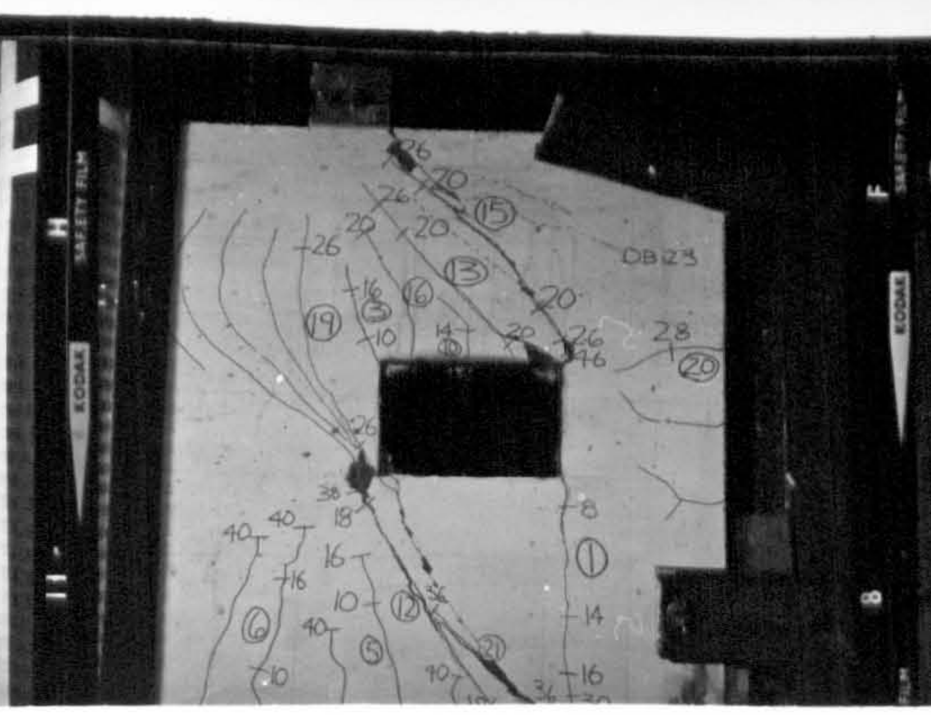

W2-0·3/4

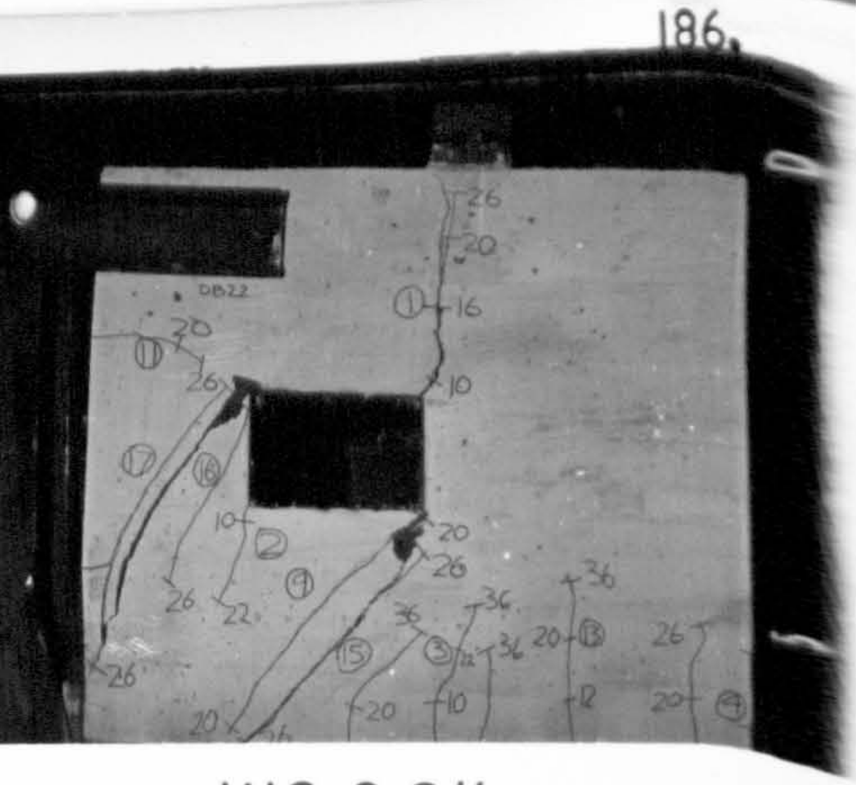

W3-0·3/4

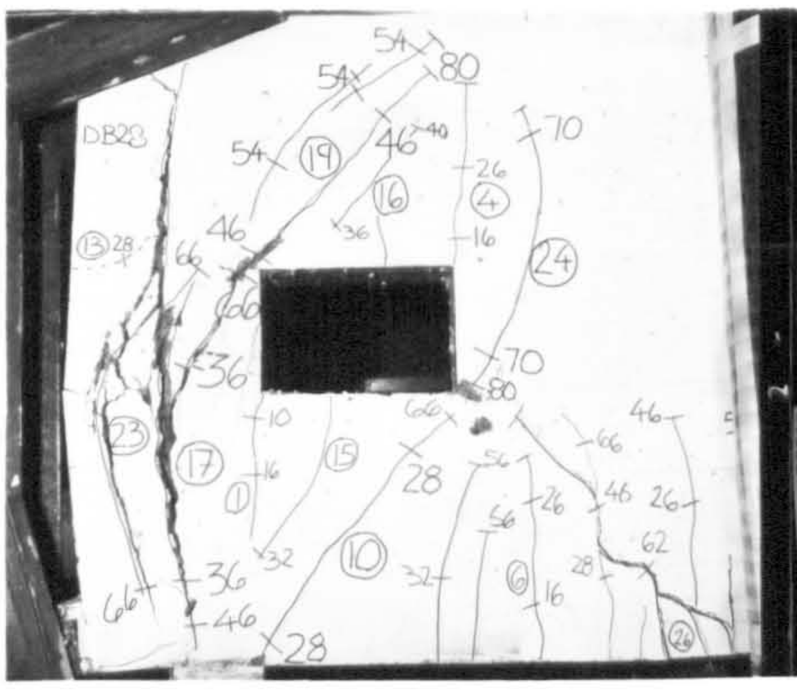

W4-0·3/4

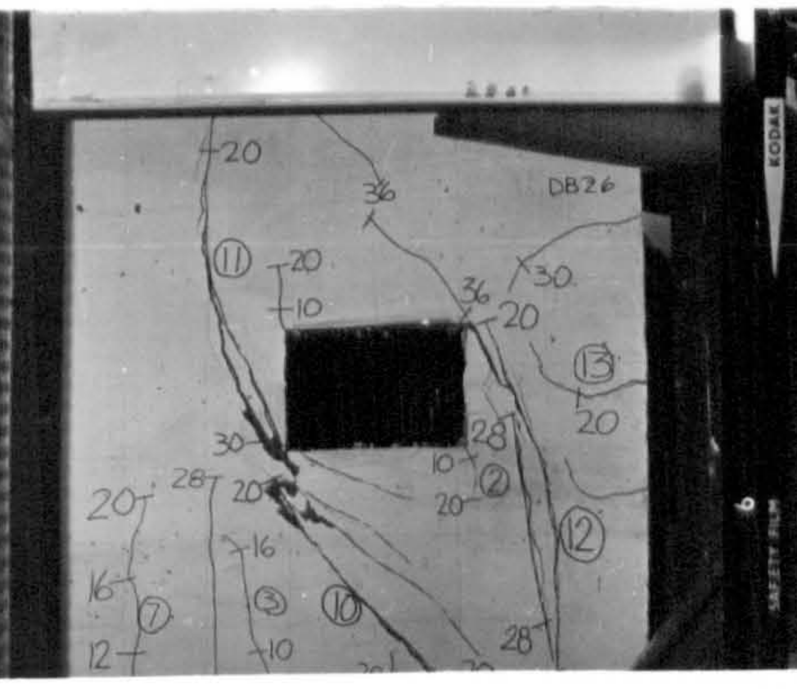

W5-0·3/4

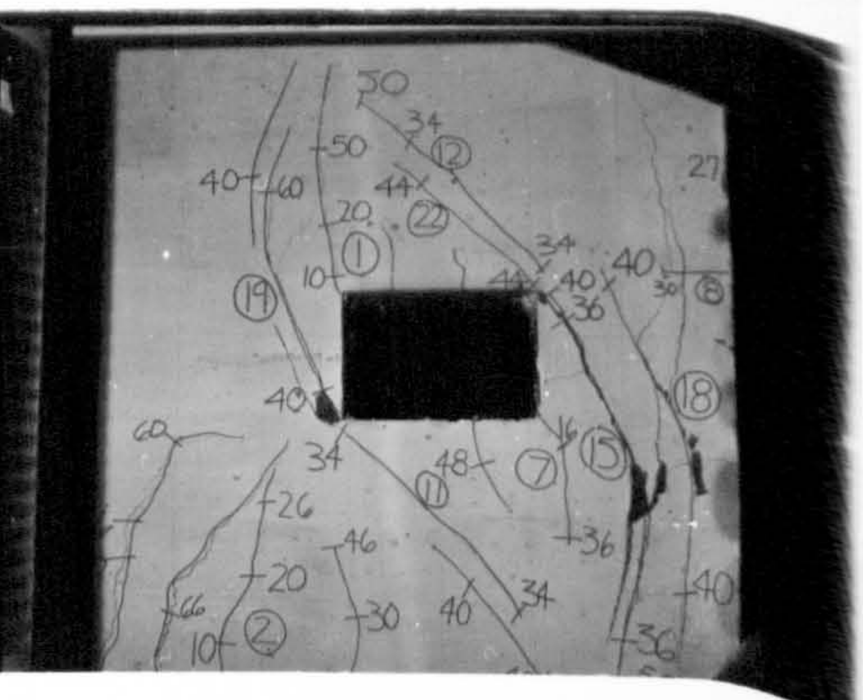

W6-0·3/4

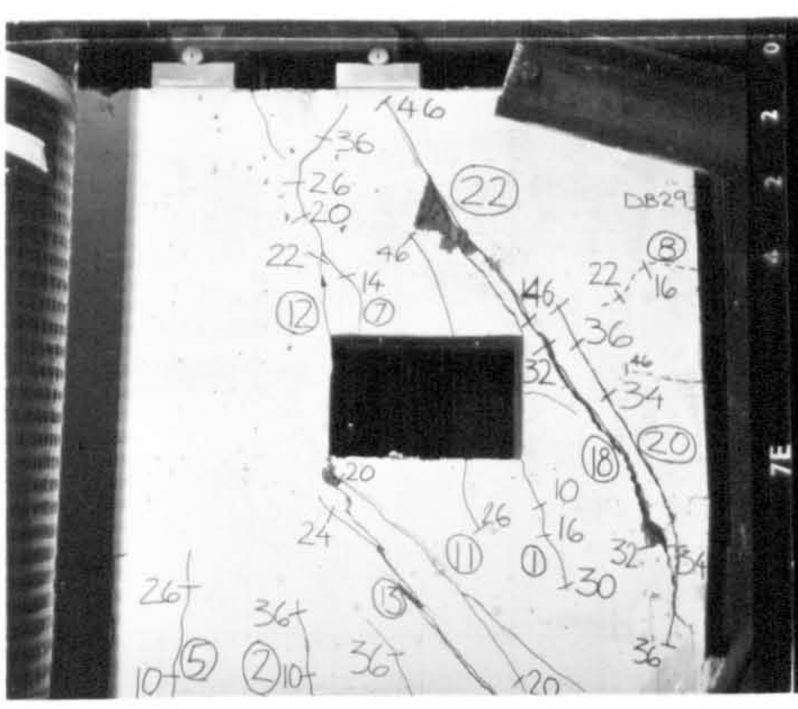

W7-0·3/4

W1(A)

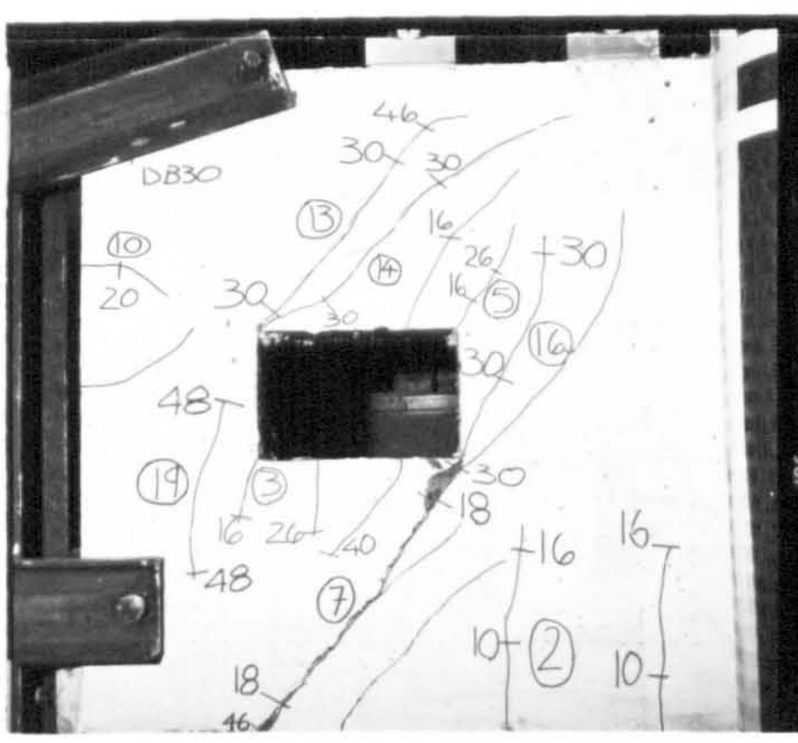

W3(A)

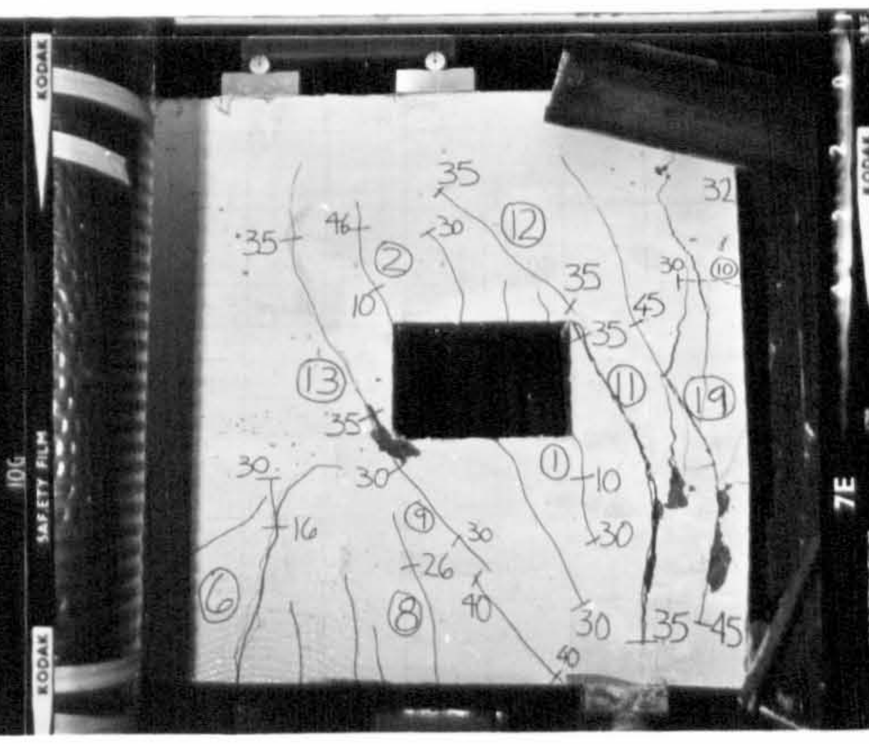

W4(A)

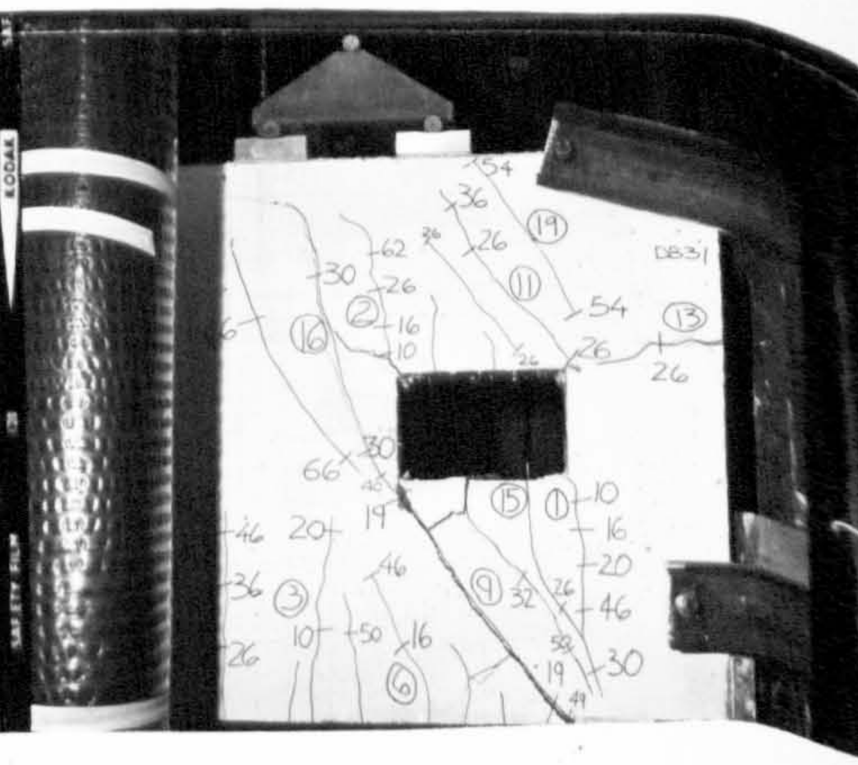

W7(A)

FIG.5.4c TYPICAL CRACK PATTERNS AT FAILURE
- GROUP W BEAMS

(The circled numbers show the sequence in which the cracks were observed; the other numerical figures show the load in 10 kN units, at which the extent of the cracks were as marked. Beam notation as in Table 5.1)

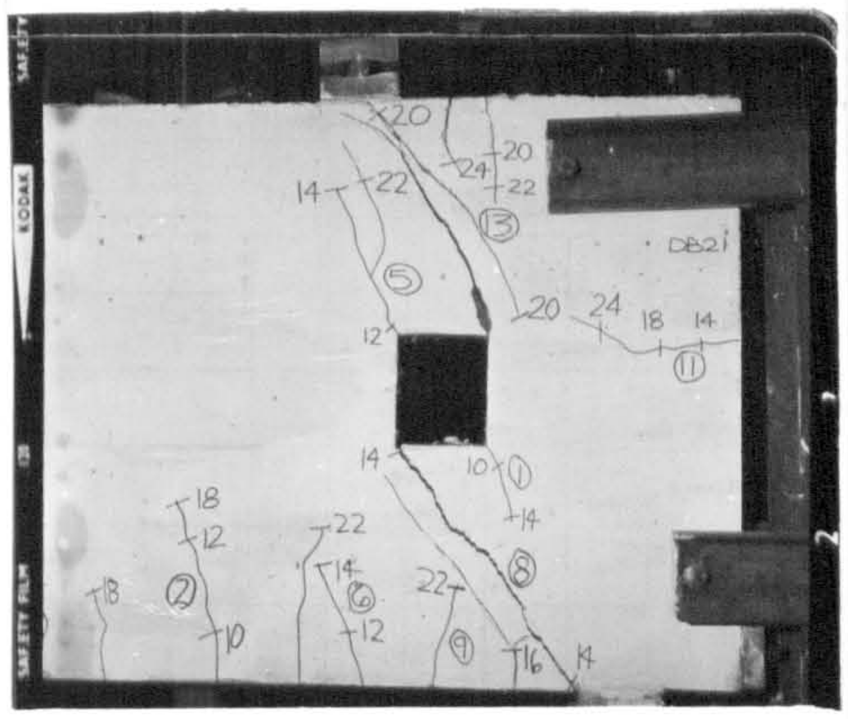

0-0·3/2R

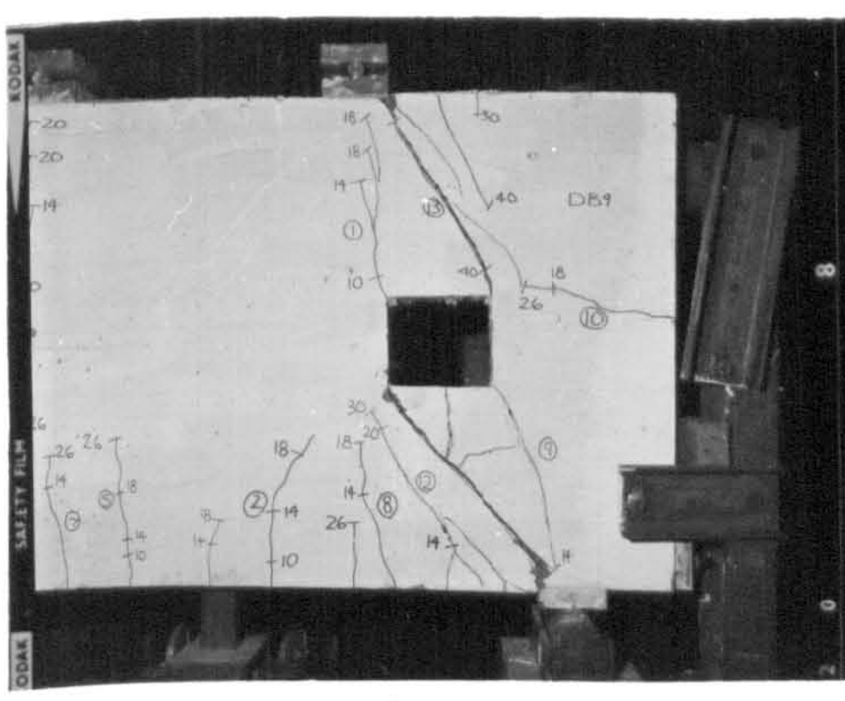

0-0·3/3R

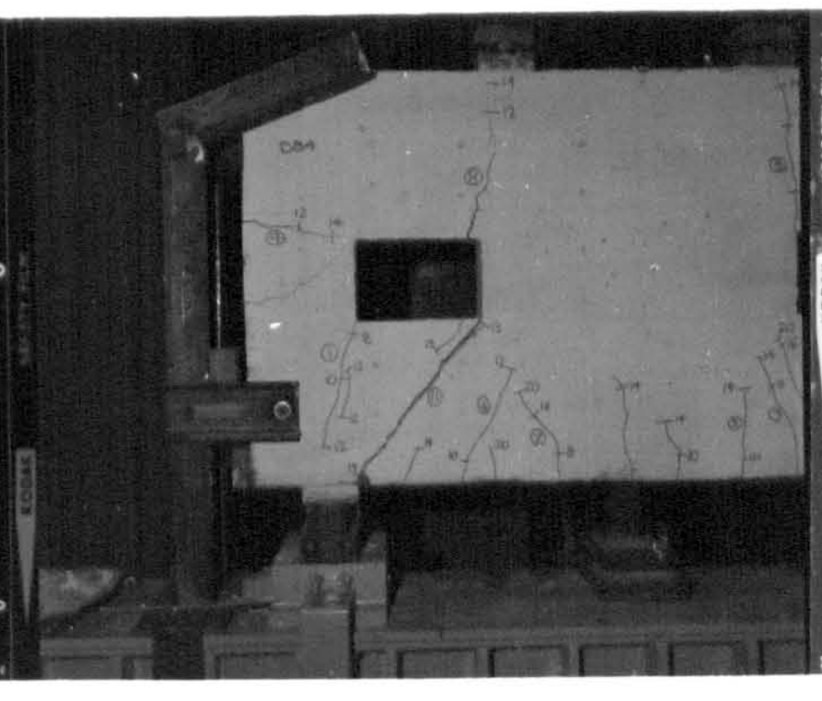

0-0·3/4R

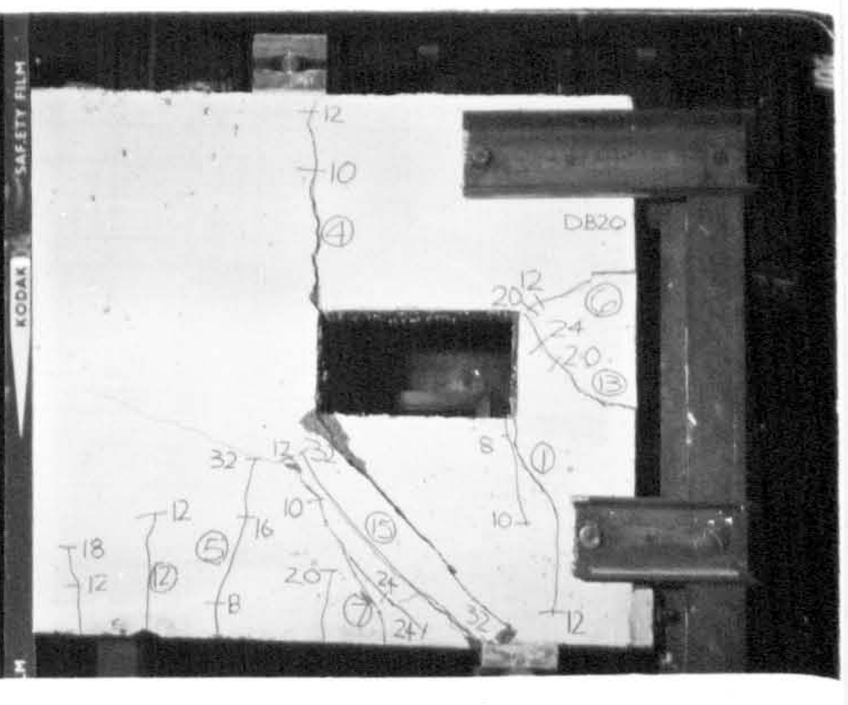

0-0·3/5R

Beam notation as in Table 5.1

(The circled numbers show the sequence in which the cracks were observed; the other figures show the load, in 10 kN units, at which the extent of the cracks were as marked)

FIG.5.4d TYPICAL CRACK PATTERNS AT FAILURE
(continued)

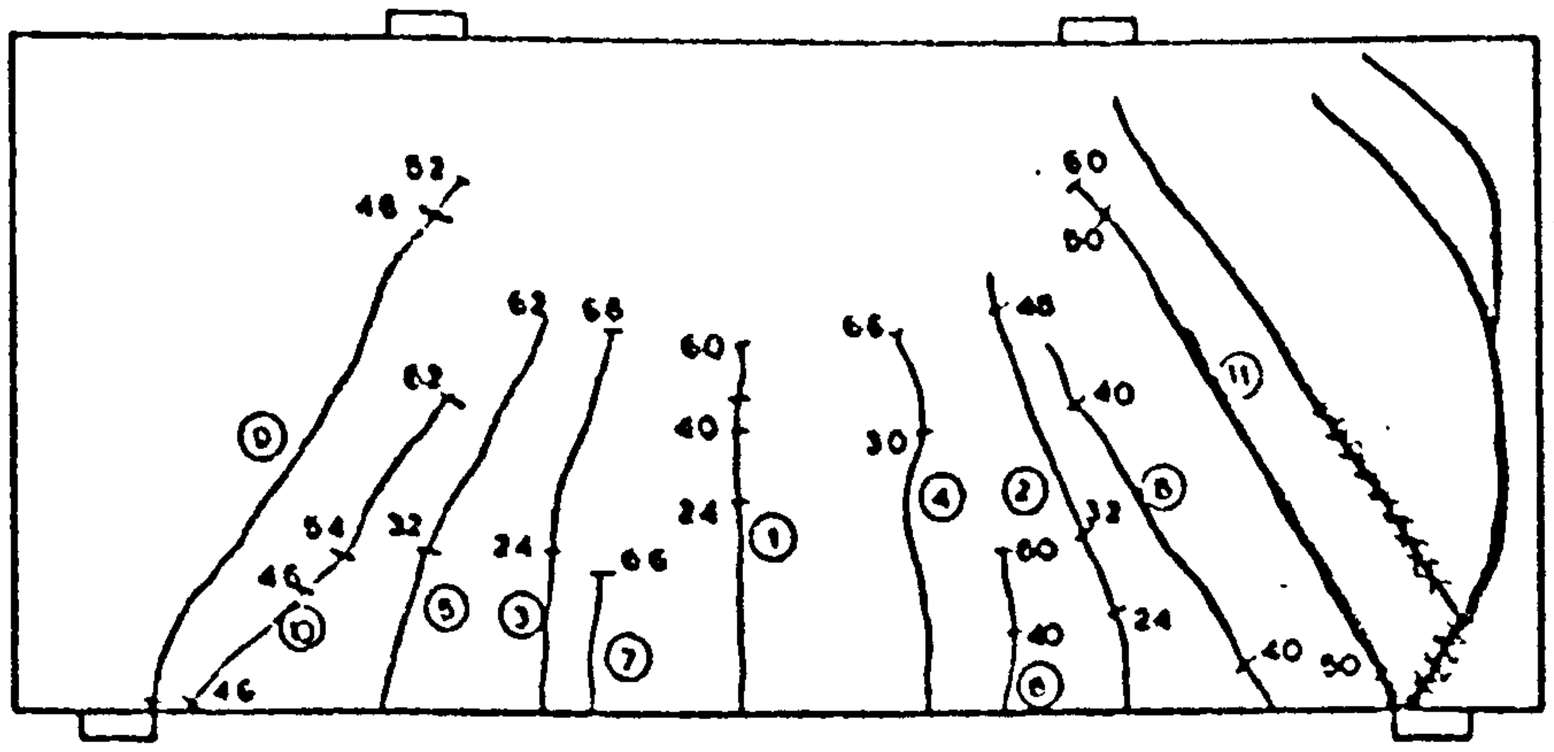

BEAM WM-0.4/0

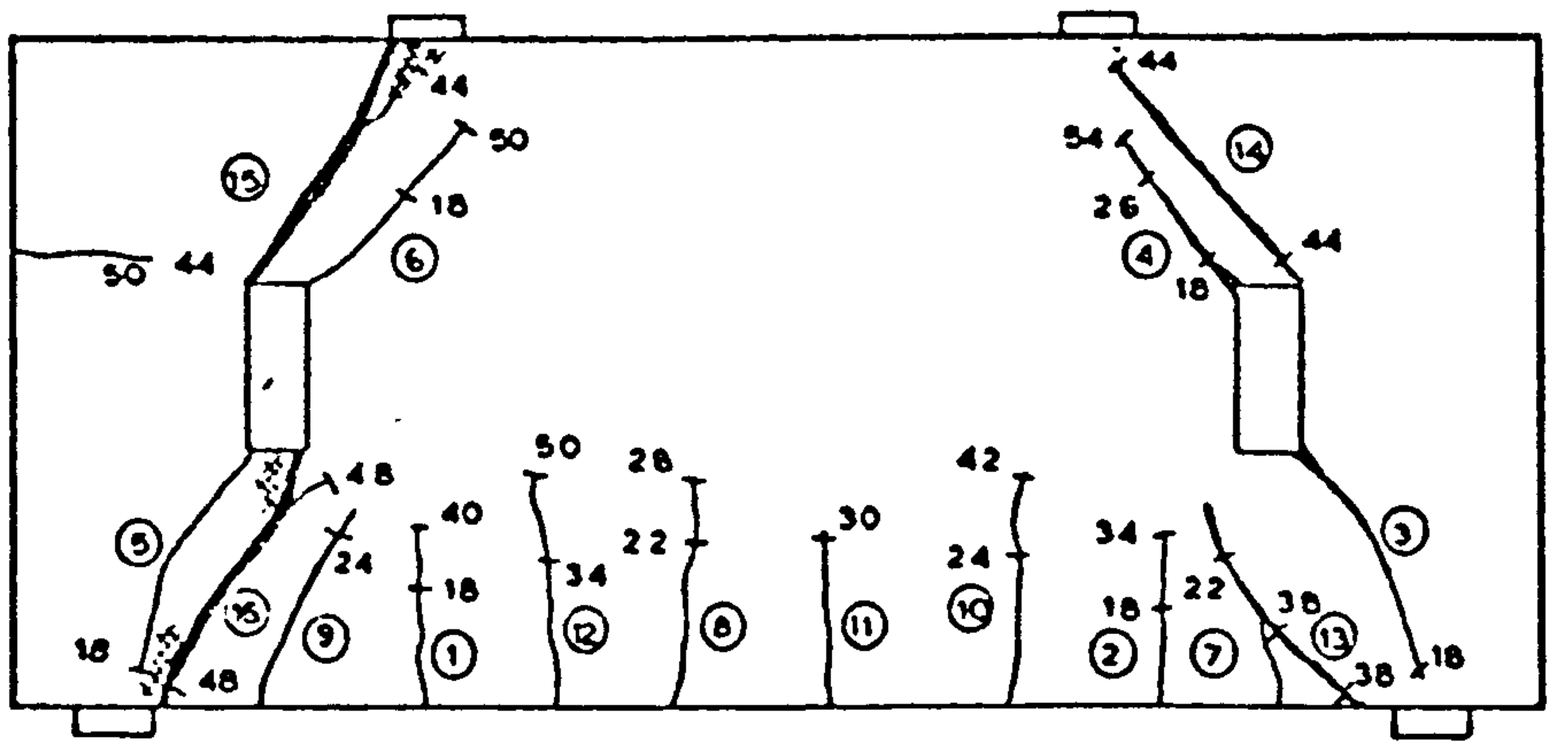

BEAM WM-0.4/18

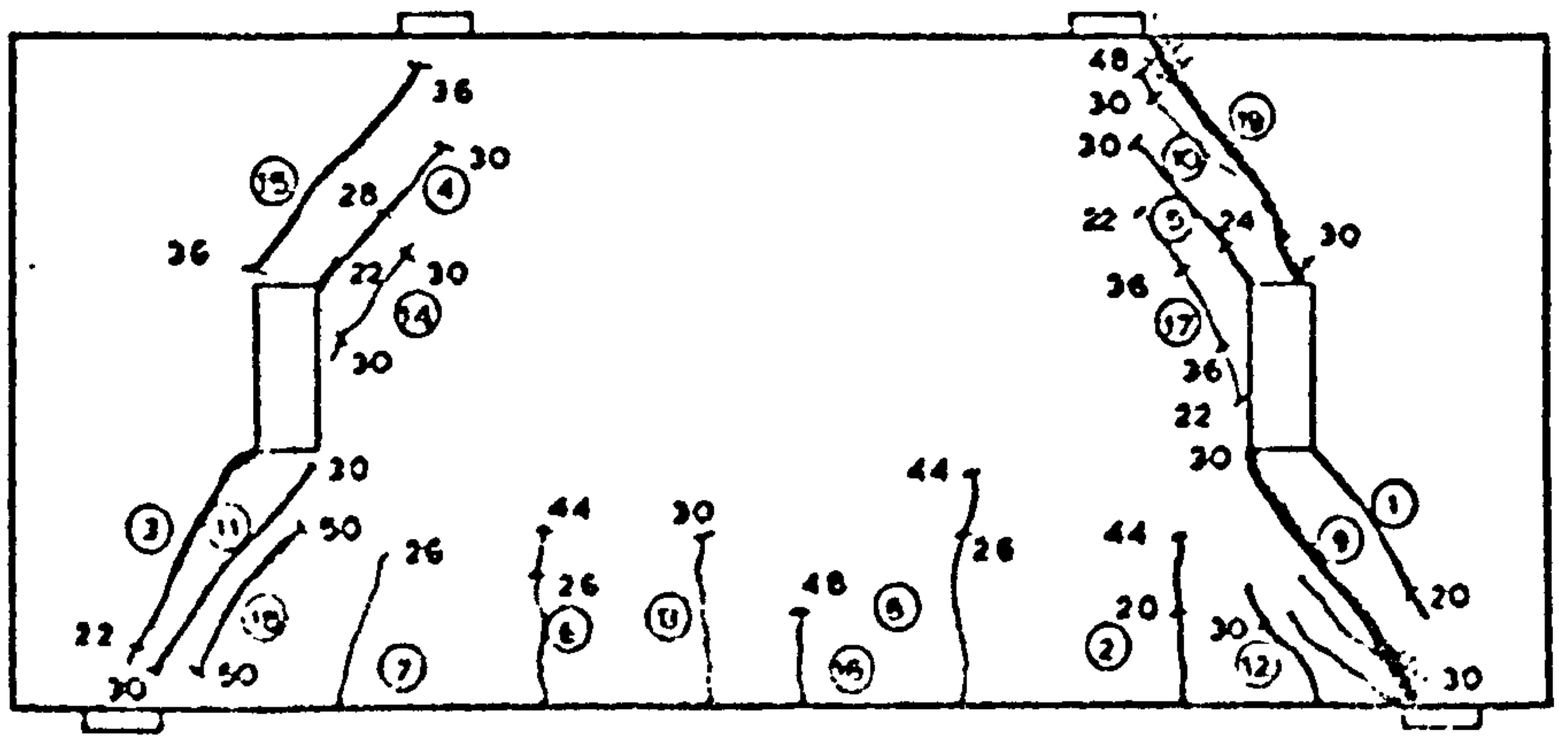

BEAM WM' - 0.4/18

FIG.5.4e TYPICAL CRACK PATTERNS AT FAILURE
(continued)

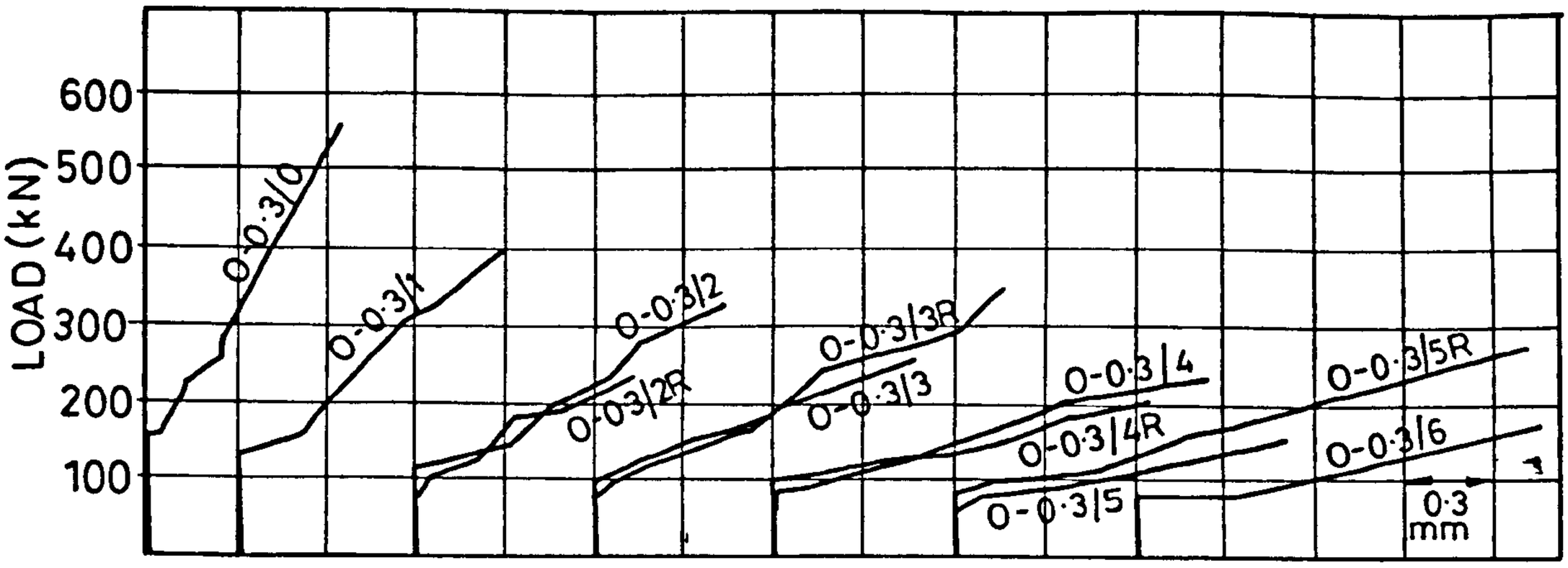

(a) No web steel ; x/D = 0·3; openings 0-6

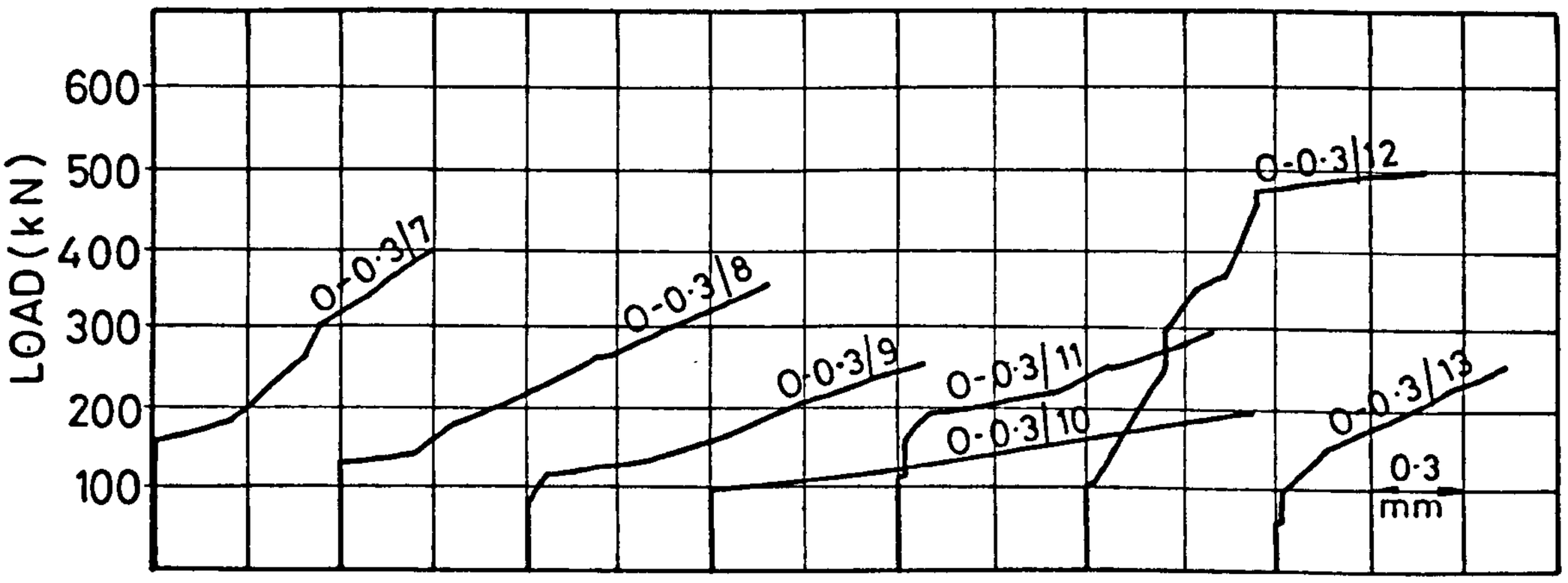

(b) No Web steel; x/D = 0·3; openings 7-13

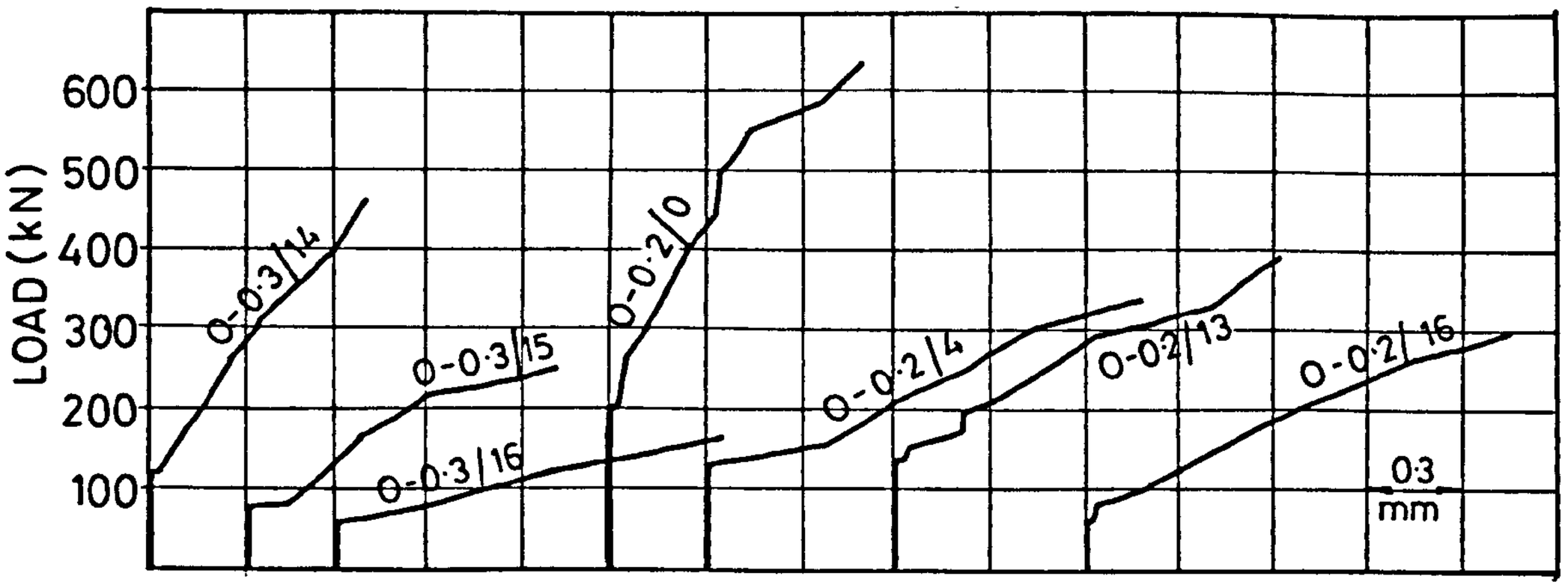

(c) No web steel; x/D = 0·3 or 0·2; opening 0, 4, 13·16

Beam notation as in Table (5.1)

FIG.5.5 MAXIMUM CRACK WIDTHS

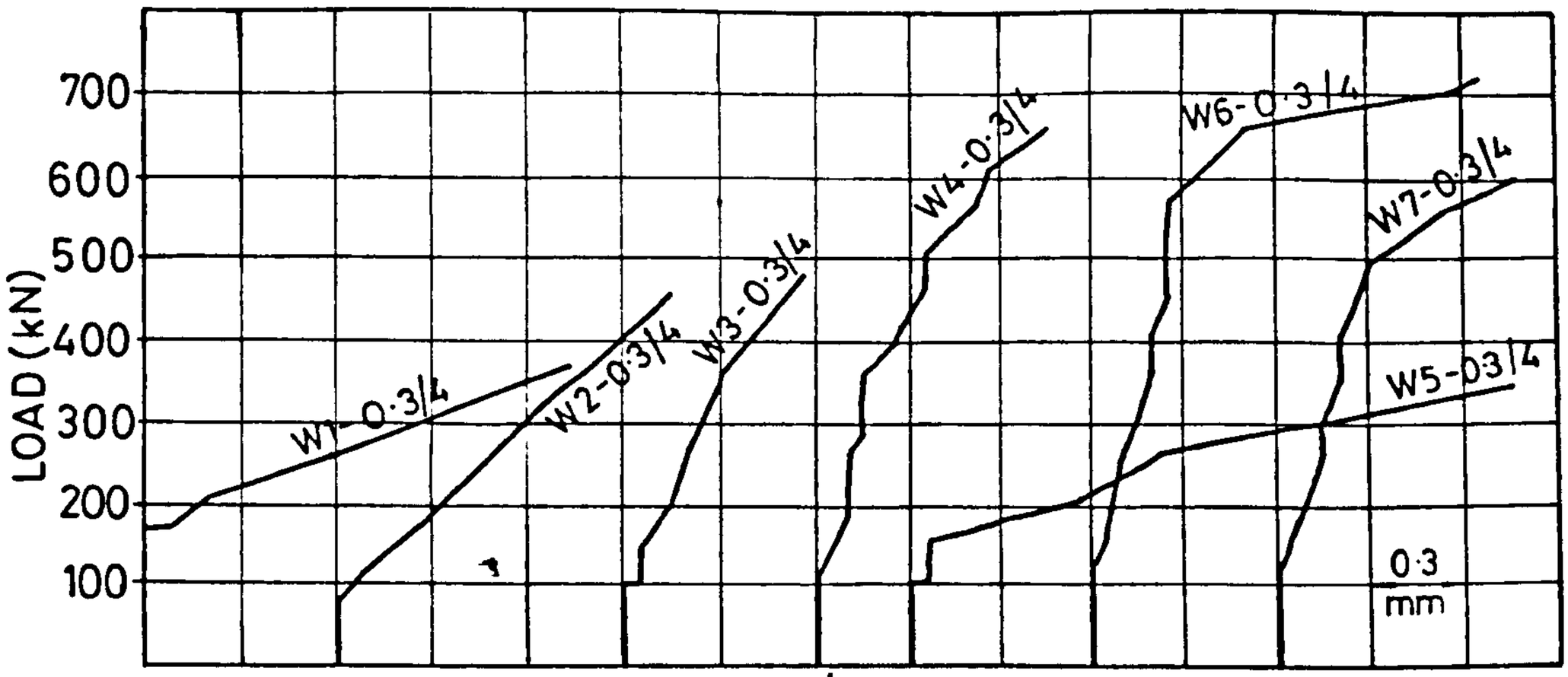

(d) Web steel as in fig 5.1; $^{x}/_{D} = 0{\cdot}3$; opening No. 4

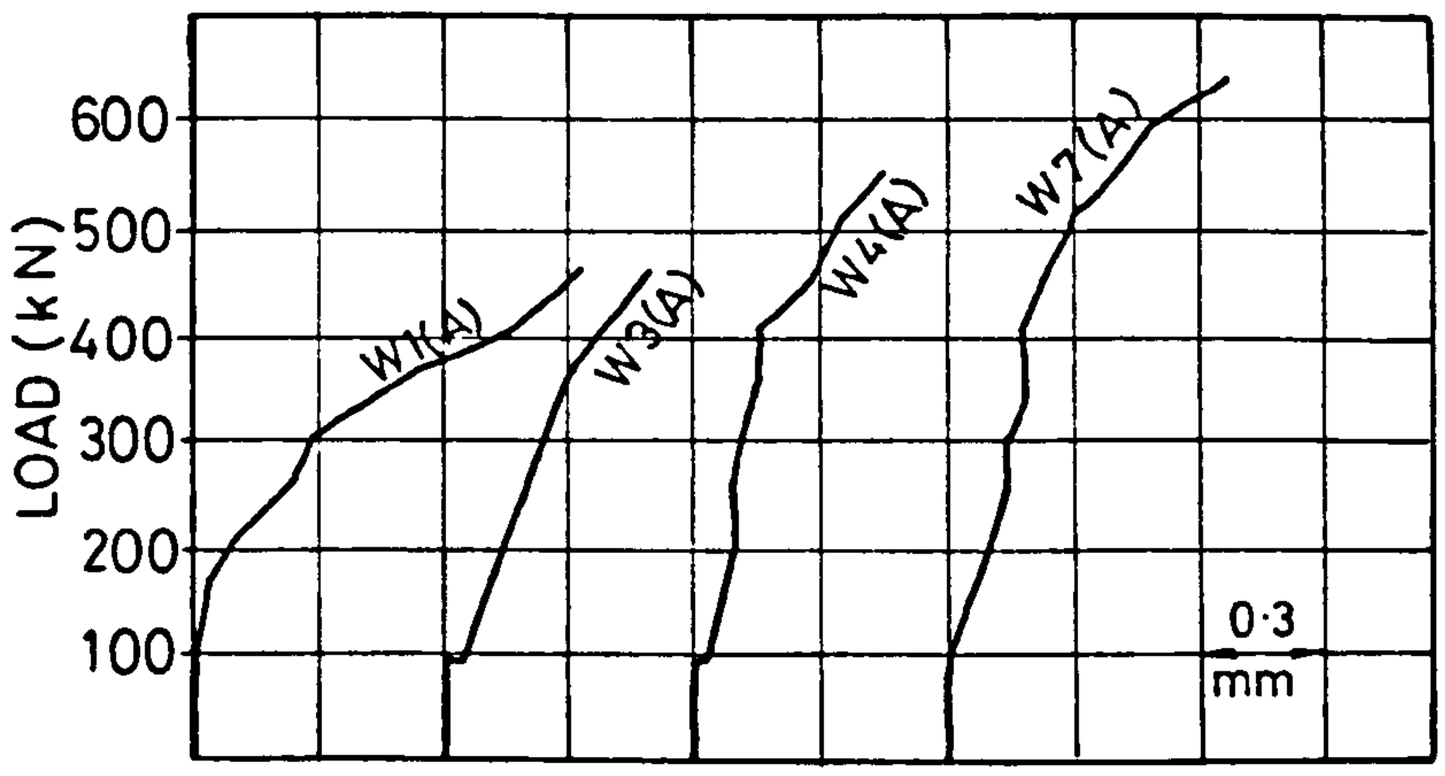

(e) Web steel as in fig 5.1; 4pt. loading; opening No. 4

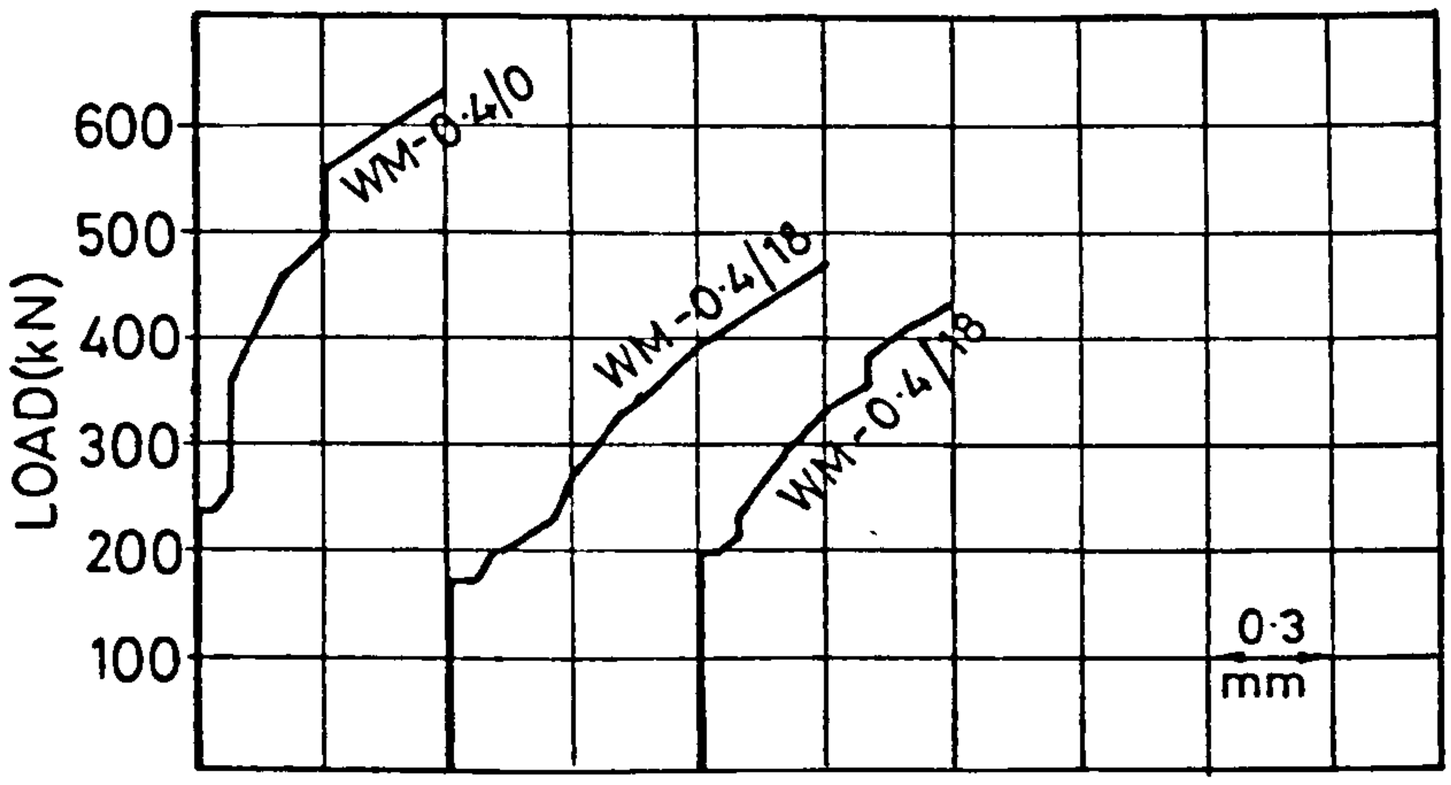

(f) Type WM web steel; $^{x}/_{D} = 0{\cdot}4$; opening No. 18

FIG.5.5 MAXIMUM CRACK WIDTHS (continued)

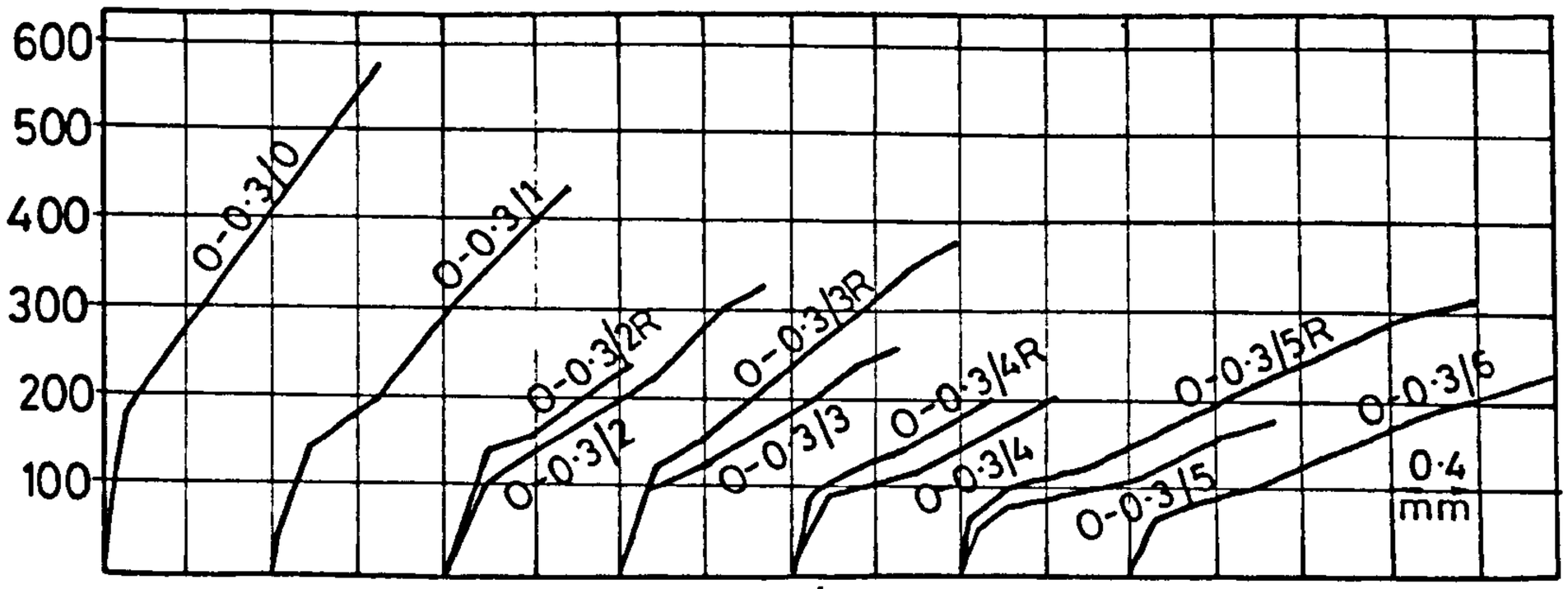

(a) No web steel; $^{x}/_{D} = 0{\cdot}3$; opening 0-6

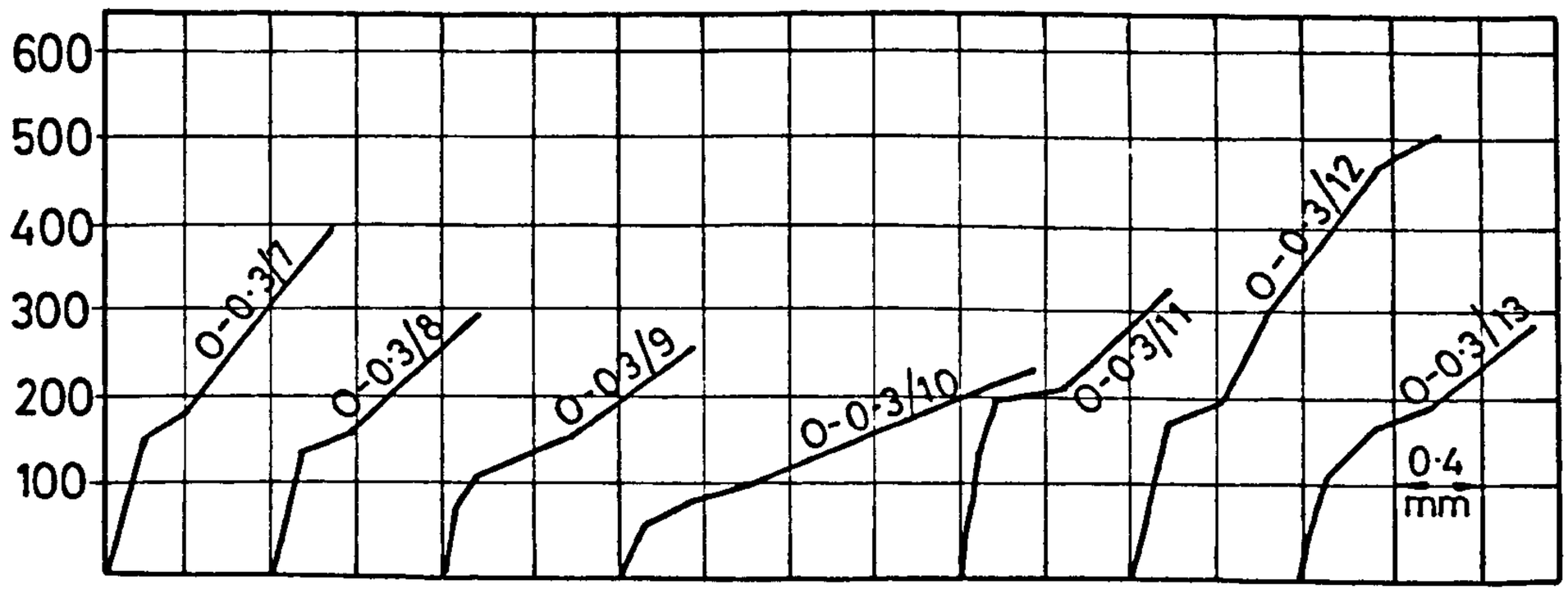

(b) No web steel; $^{x}/_{D} = 0{\cdot}3$; opening 7-13

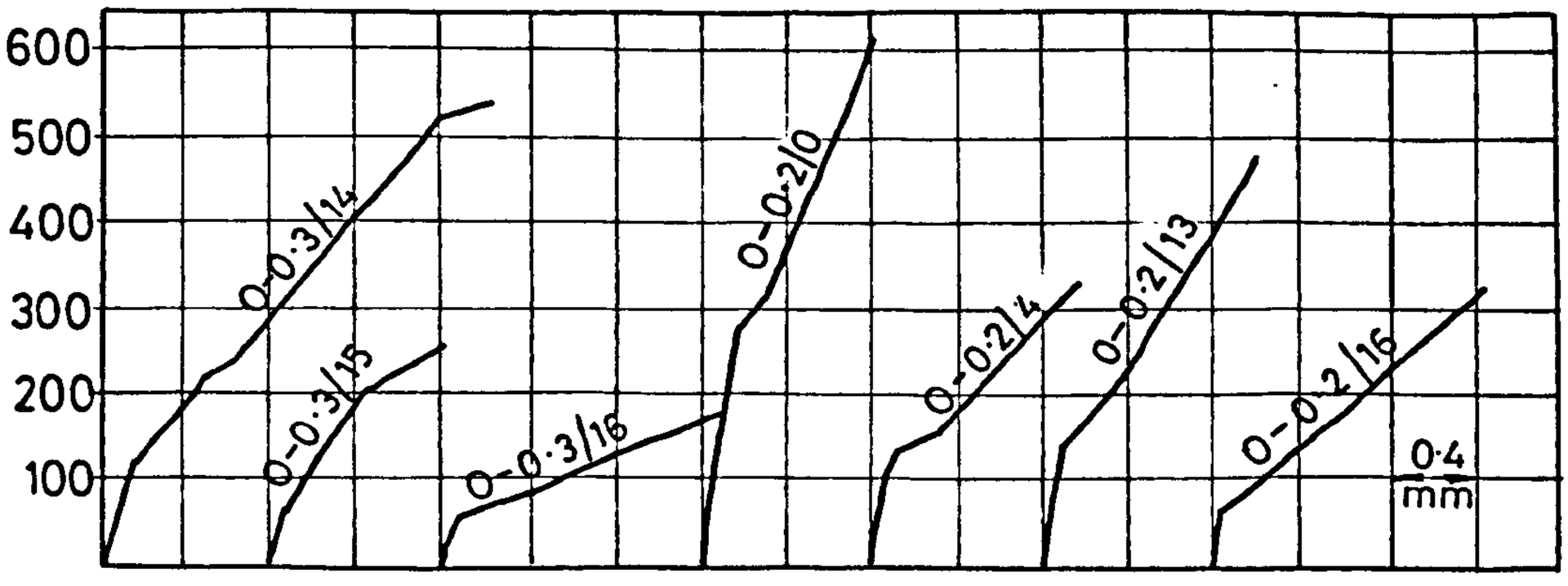

(a) No web steel; $^{x}/_{D} = 0{\cdot}3$ or $0{\cdot}2$; openings 0,4,13-16

Beam notation as in Table 5.1

FIG.5.6 CENTRAL DEFLECTIONS

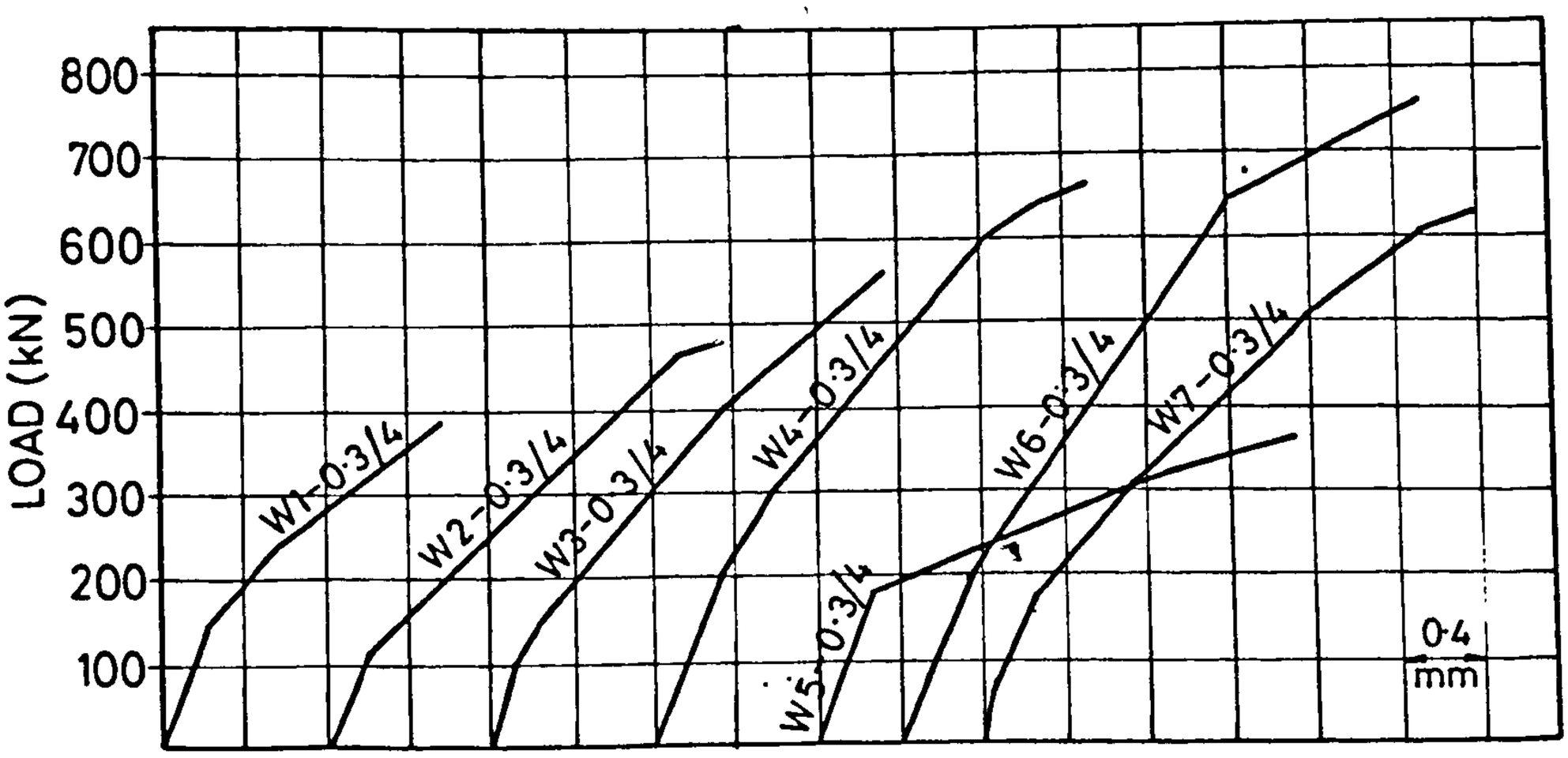

(d) Web steel as in Fig 5.1; x/D = 0·3; opening No.4.

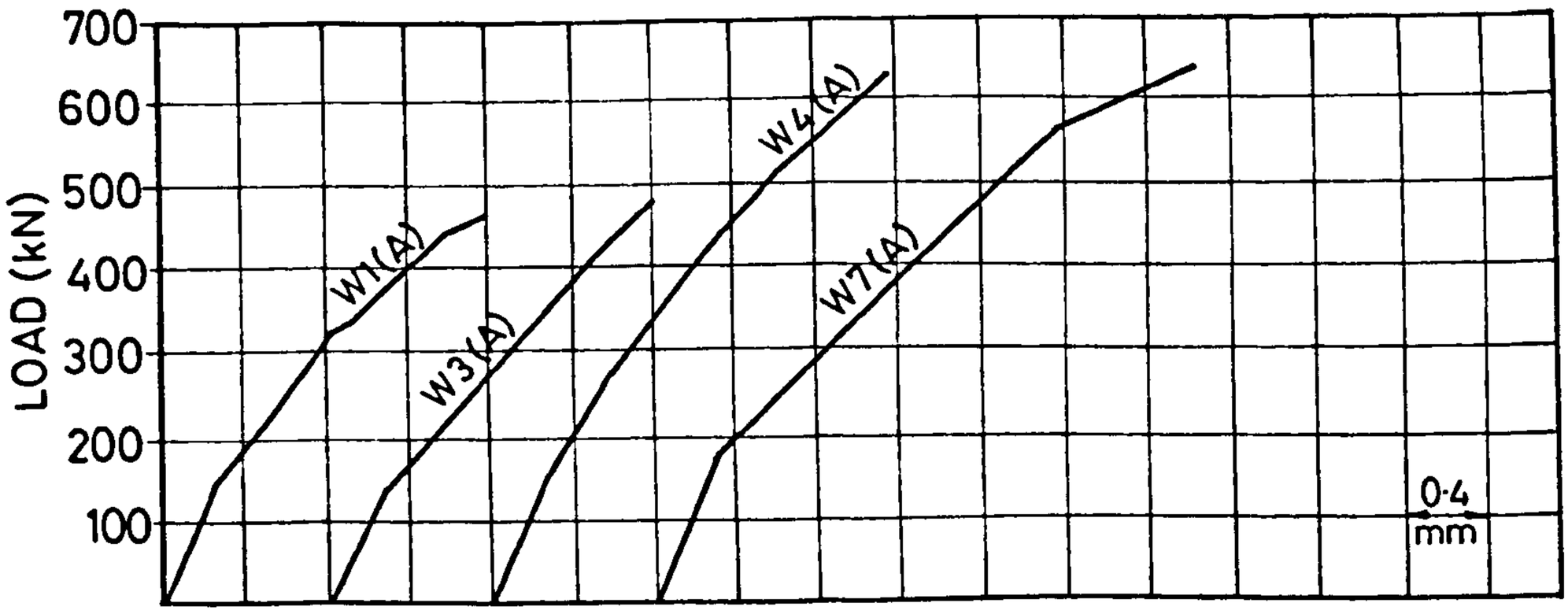

(e) Web steel as in Fig 5.1; 4pt loading; opening No.4.

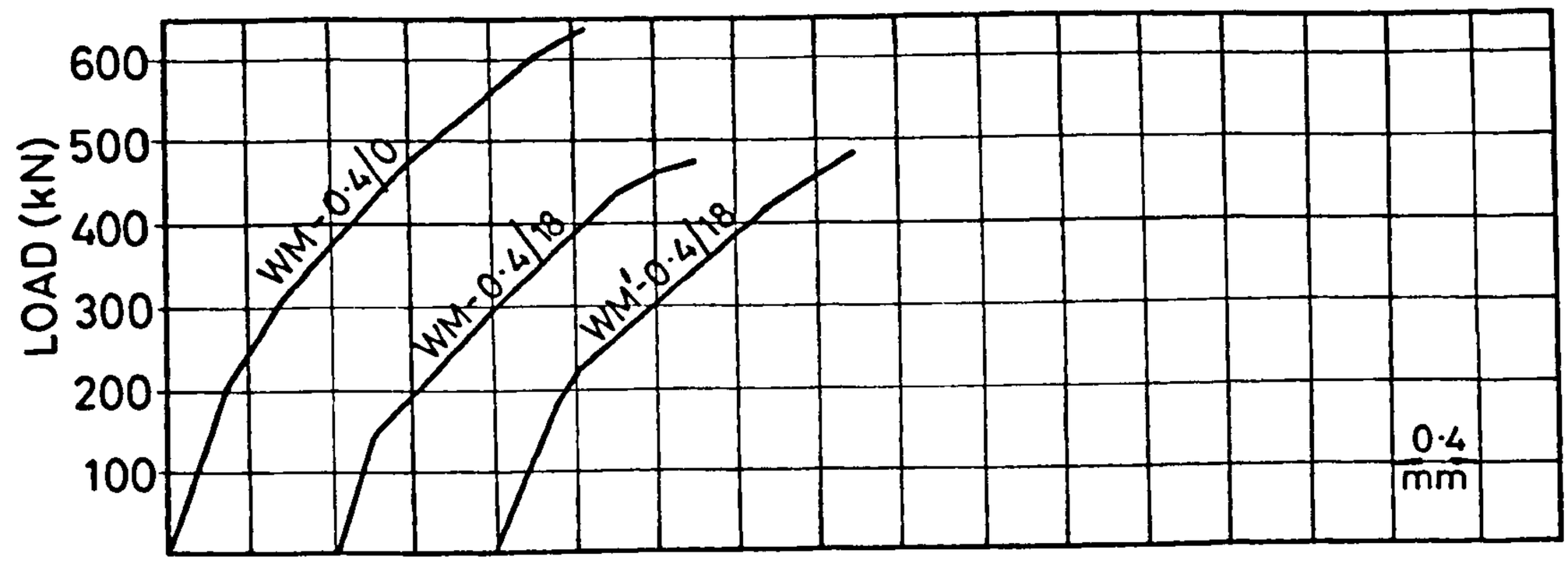

(f) Type WM web steel; x/D = 0·4; opening No.18

FIG.5.6 CENTRAL DEFLECTIONS (continued)

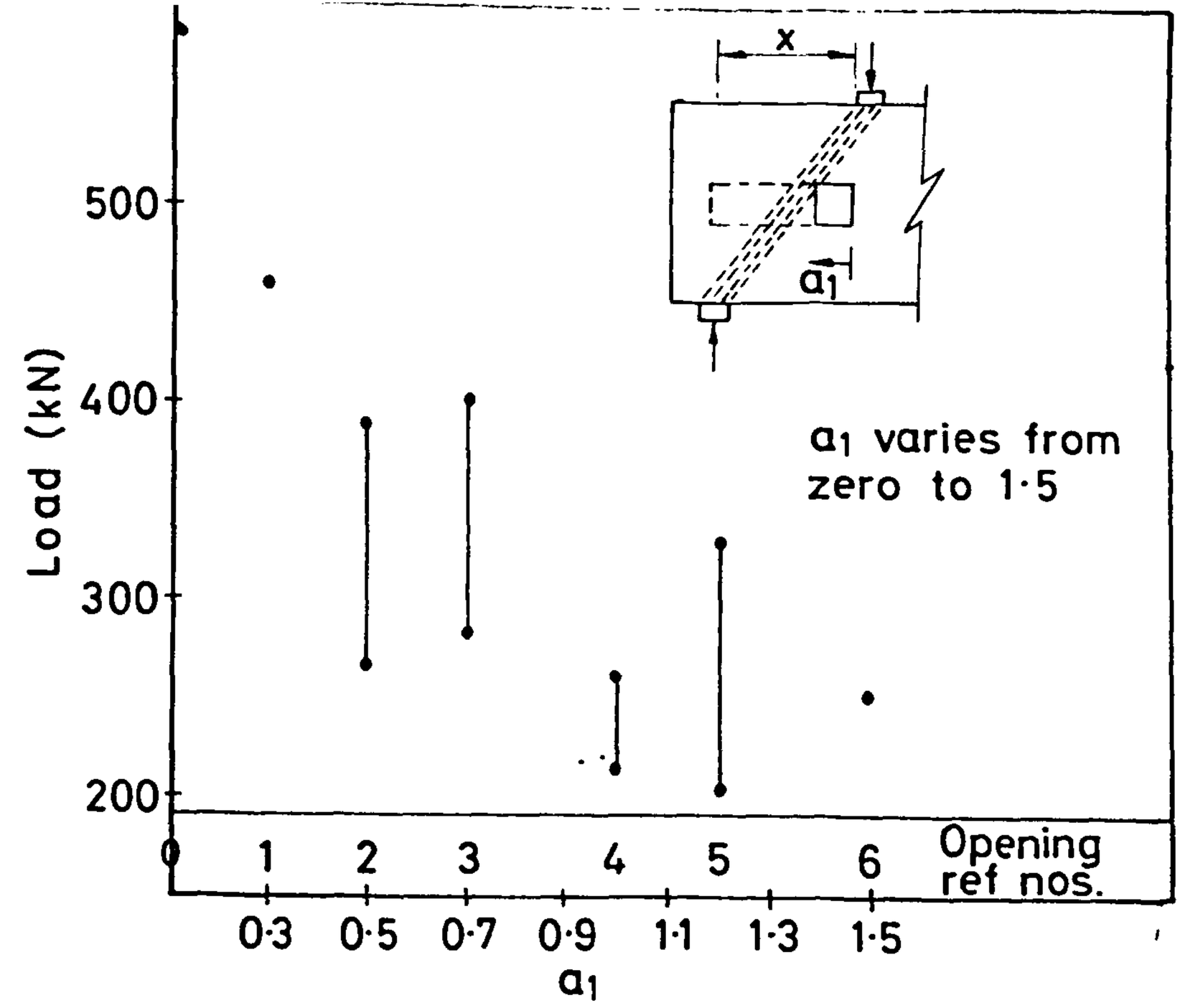

(a) Opening breadth increased towards support (For breadth equal to x, $a_1 = 1$)

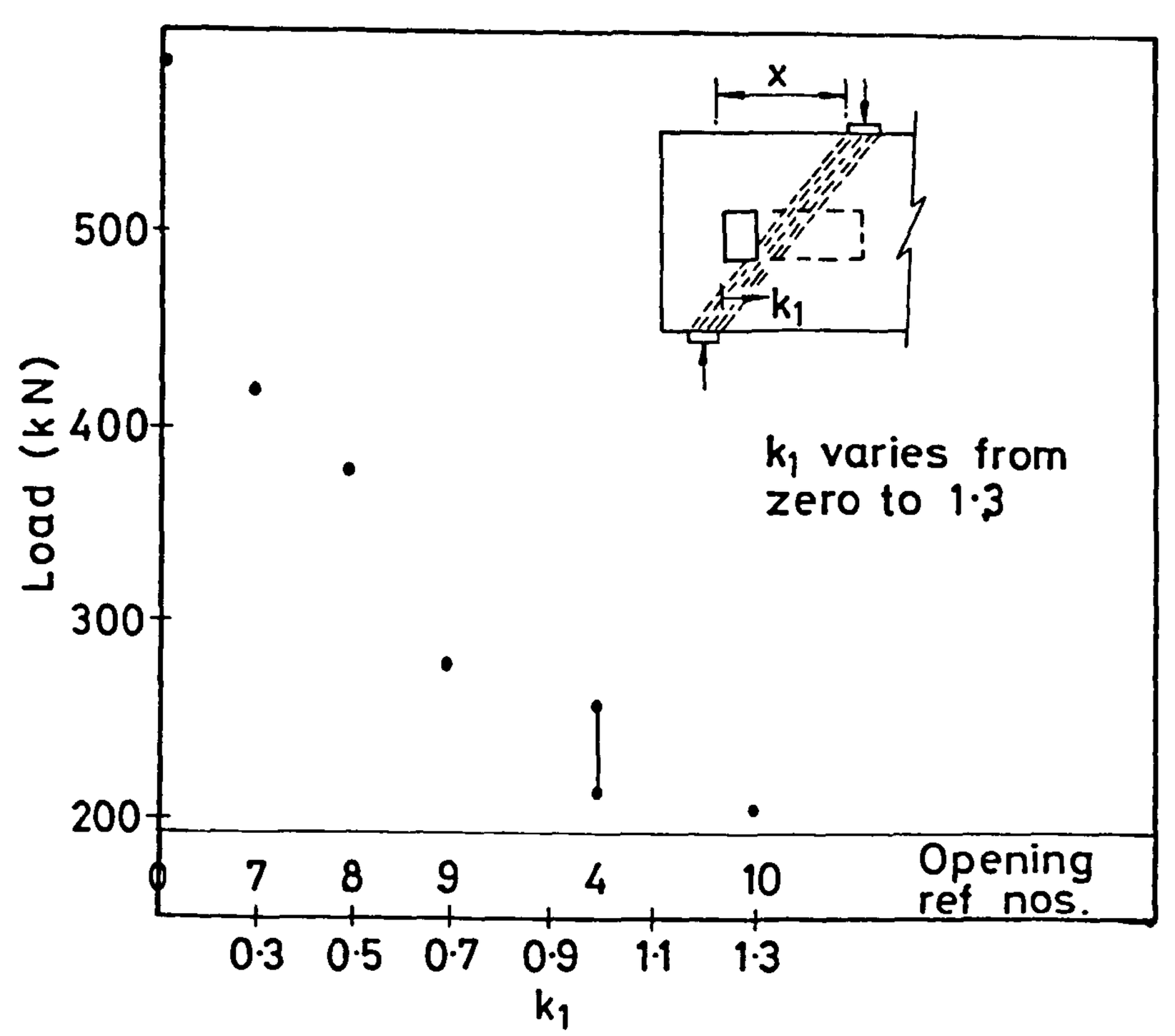

(b) Opening breadth increased towards loading point (For breadth equal to x, $k_1 = 1$)

FIG.5.7 ULTIMATE STRENGTHS OF DEEP BEAMS WITH WEB OPENINGS

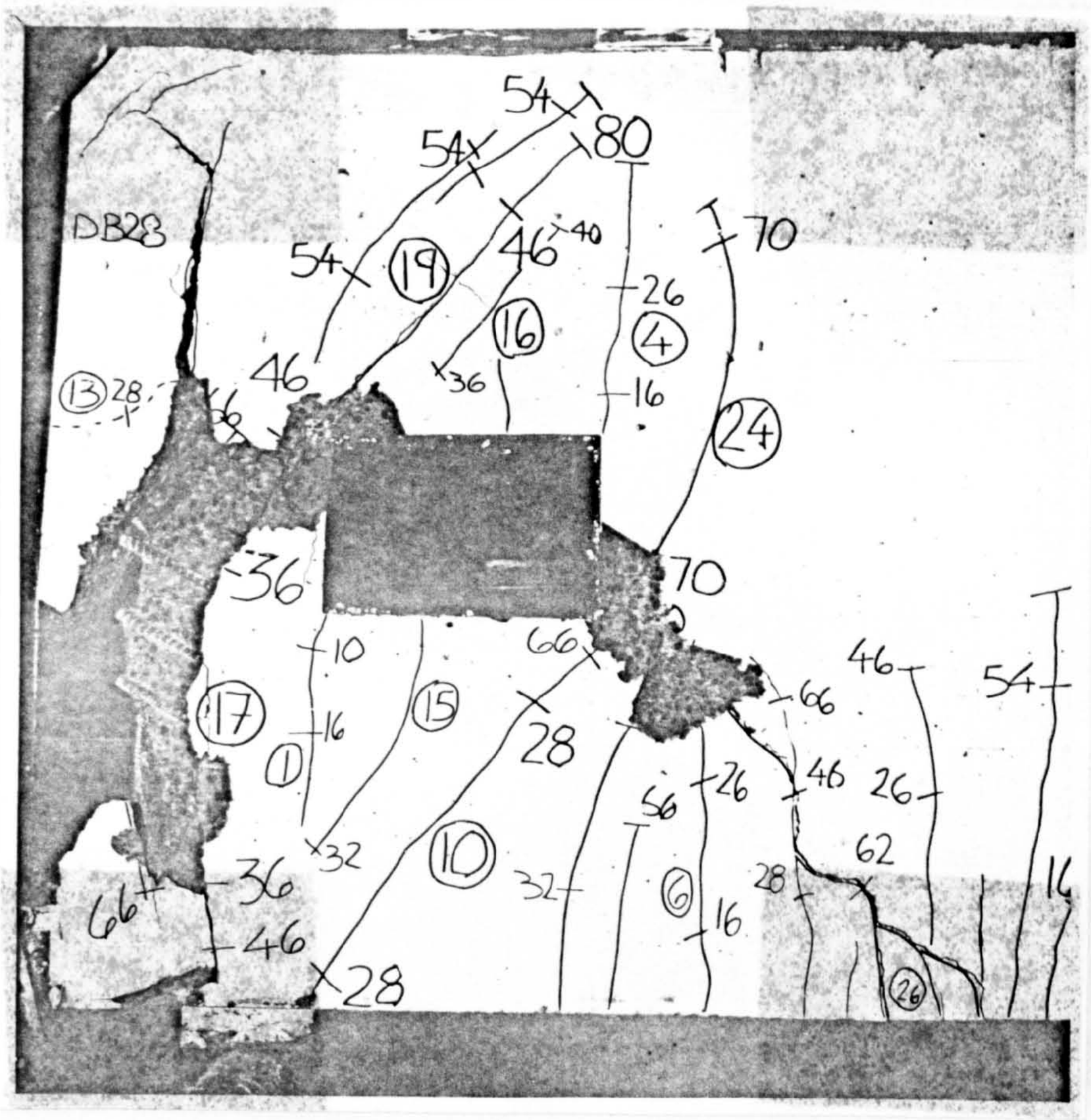

FIG.5.8 BEAM W6-0.3/4 AFTER FAILURE

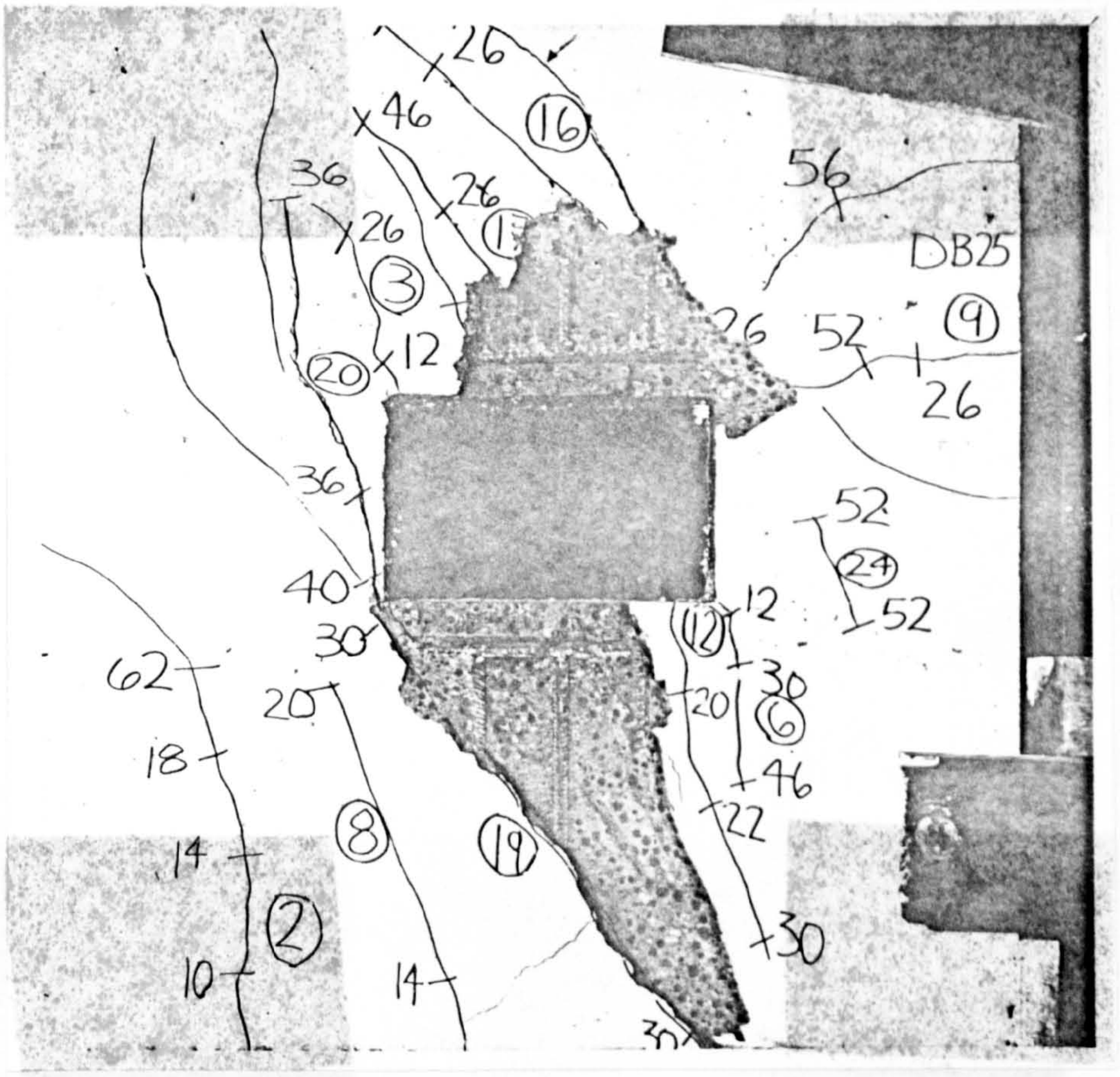

FIG.5.9 BEAM W7-0.3/4 AFTER FAILURE

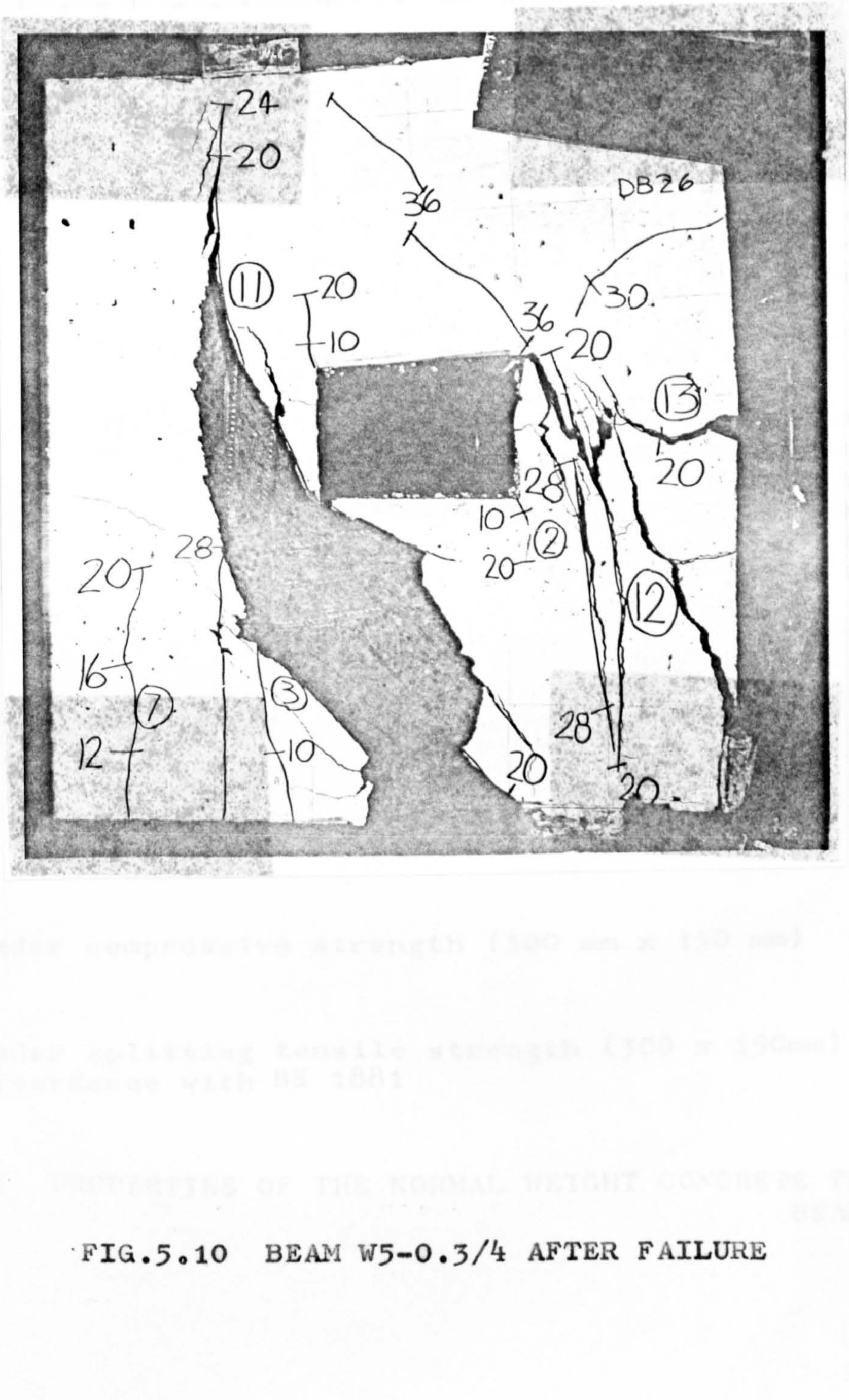

FIG.5.10 BEAM W5-0.3/4 AFTER FAILURE

Beam * Ref. No.	$\frac{L}{D}$	$\frac{x}{D}$	Web opening Ref.No. ++	Web steel		f_{cu} ≠ N/mm^2	f'_c xx N/mm^2	f_t ** N/mm^2
				Type	%			
NO-0.3/0	1.5	0.3	0	0	0	50.4	44.8	3.71
NO-0.3/4	1.5	0.3	4	0	0	57.9	43.7	4.09
NW1-0.3/4	1.5	0.3	4	W1	1.19	51.7	36.8	3.94
NW2-0.3/4	1.5	0.3	4	W2	1.19	51.1	43.4	3.43
NW3-0.3/4	1.5	0.3	4	W3	1.19	60.0	46.2	3.80
NW4-0.3/4	1.5	0.3	4	W4	1.24	45.3	39.5	3.44
NW5-0.3/4	1.5	0.3	4	W5	1.11	50.9	43.5	4.03
NW6-0.3/4	1.5	0.3	4	W6	1.25	56.9	42.7	4.00
NW7-0.3/4	1.5	0.3	4	W7	1.13	53.1	42.9	3.74
NW6A-0.3/0	1.5	0.3	0	W6A	0.65	55.2	40.8	3.58
NW6A-0.3/1	1.5	0.3	1	W6A	0.57	50.2	39.4	3.41
NW6A-0.3/4	1.5	0.3	4	W6A	0.47	52.7	41.2	3.74
NW6A-0.3/17	1.5	0.3	17	W6A	0.49	54.2	40.7	3.60
NW6A-0.3/7	1.5	0.3	7	W6A	0.49	55.0	40.7	3.72
NW6A-0.3/11	1.5	0.3	11	W6A	0.58	51.2	41.7	3.79
NW6A-0.3/15	1.5	0.3	15	W6A	0.61	56.2	40.7	3.92

* Beam notation: The letter N signifies normal weight concrete; a letter O before the hyphen indicates no web reinforcement whilst a letter W indicates the presence of web reinforcement; the x/D ratio is given after the hyphen, followed by the web-opening reference number. Thus NW1-0.3/4 refers to a beam of normal weight concrete with web reinforcement Type W1 (see Fig.6.1), having an x/D ratio of 0.3 and a web opening type 4.

++ Details of web openings are given in Figs.5.2 and 6.2

≠ f_{cu} = cube strength (100 mm)

xx f'_c = cylinder compressive strength (300 mm x 150 mm)

** f_t = cylinder splitting tensile strength (300 x 150mm) - in accordance with BS 1881

TABLE 6.1 PROPERTIES OF THE NORMAL WEIGHT CONCRETE TEST BEAMS.

Beam Ref. No.*	Measured Ult. load W_1 kN
NO-0.3/0	680
NO-0.3/4	240
NW1-0.3/4	420
NW2-0.3/4	580
NW3-0.3/4	620
NW4-0.3/4	780
NW5-0.3/4	370
NW6-0.3/4	1060
NW7-0.3/4	720
NW6A-0.3/0	1215
NW6A-0.3/1	1015
NW6A-0.3/4	620
NW6A-0.3/17	840
NW6A-0.3/7	930
NW6A-0.3/11	880
NW6A-0.3/15	820

*Beam notation as in Table 6.1

TABLE 6.2 MEASURED ULTIMATE LOADS OF THE NORMAL WEIGHT BEAMS.

Beam Ref. No.*	Normal weight concrete‡	Lightweight concrete‡‡	Beam Ref. No.**
NW6-0.3/4	1.56	1.39	W6-0.3/4
NW4-0.3/4	1.15	1.11	W4-0.3/4
NW7-0.3/4	1.06	1.06	W7-0.3/4
NO-0.3/0	1.00	1.00	0-0.3/0
NW3-0.3/4	0.91	0.94	W3-0.3/4
NW2-0.3/4	0.85	0.82	W2-0.3/4
NW1-0.3/4	0.62	0.67	W1-0.3/4
NW5-0.3/4	0.54	0.62	W5-0.3/4
NO-0.3/4	0.35	0.36	O-0.3/4
NW6A-0.3/0	1.79		
NW6A-0.3/1	1.49		
NW6A-0.3/4	0.91		
NW6A-0.3/17	1.24		
NW6A-0.3/7	1.37		
NW6A-0.3/11	1.29		
NW6A-0.3/15	1.21		

*Beam notation as in Table 6.1

**Beam notation as in Table 5.1

‡ Measured ultimate loads ÷ ult.load of Beam NO-0.3/0

‡‡Measured ultimate loads ÷ ult.load of Beam O-0.3/0

TABLE 6.3 COMPARISON OF THE ULTIMATE STRENGTH OF NORMAL WEIGHT AND LIGHTWEIGHT TEST SPECIMENS.

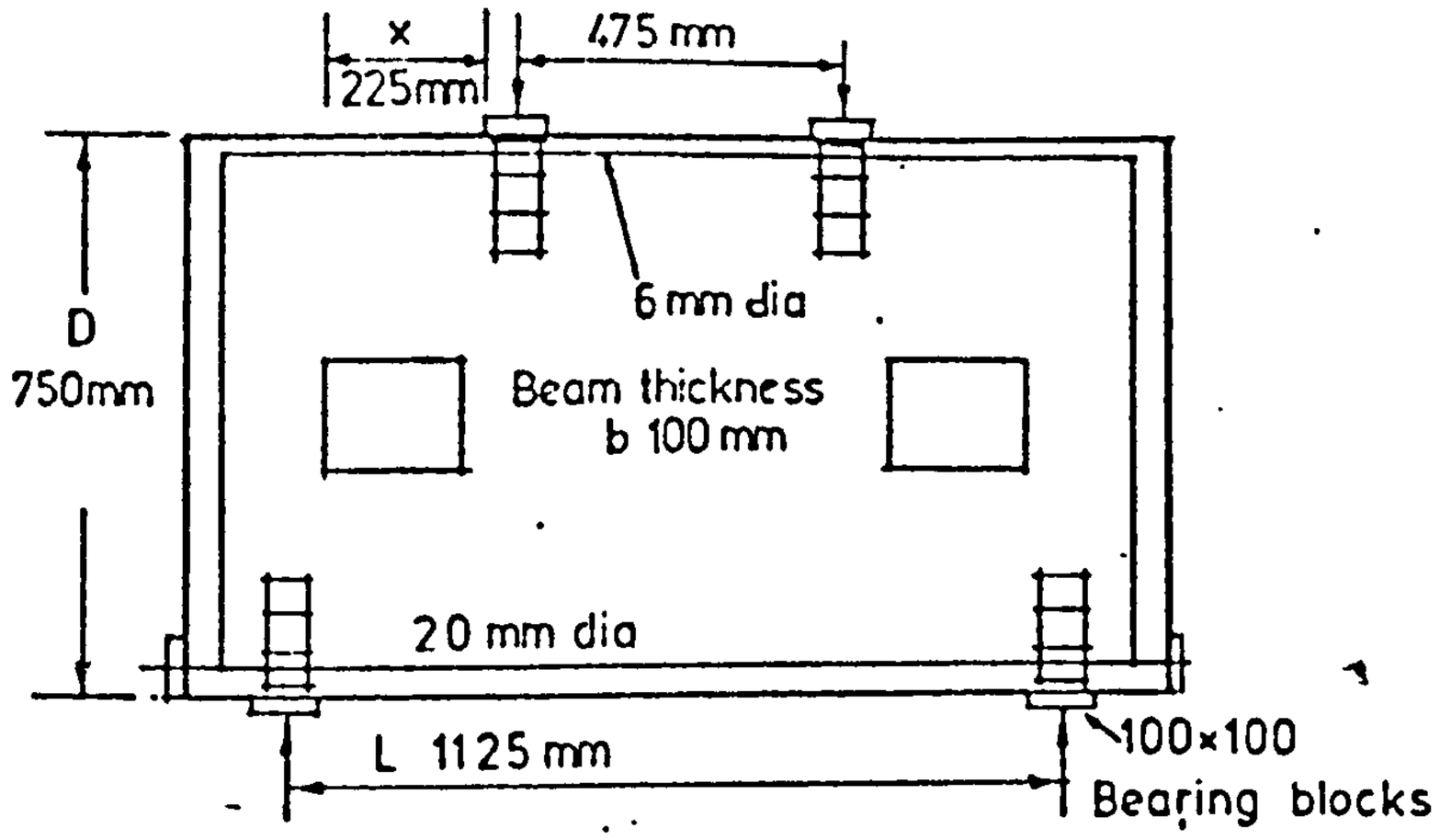

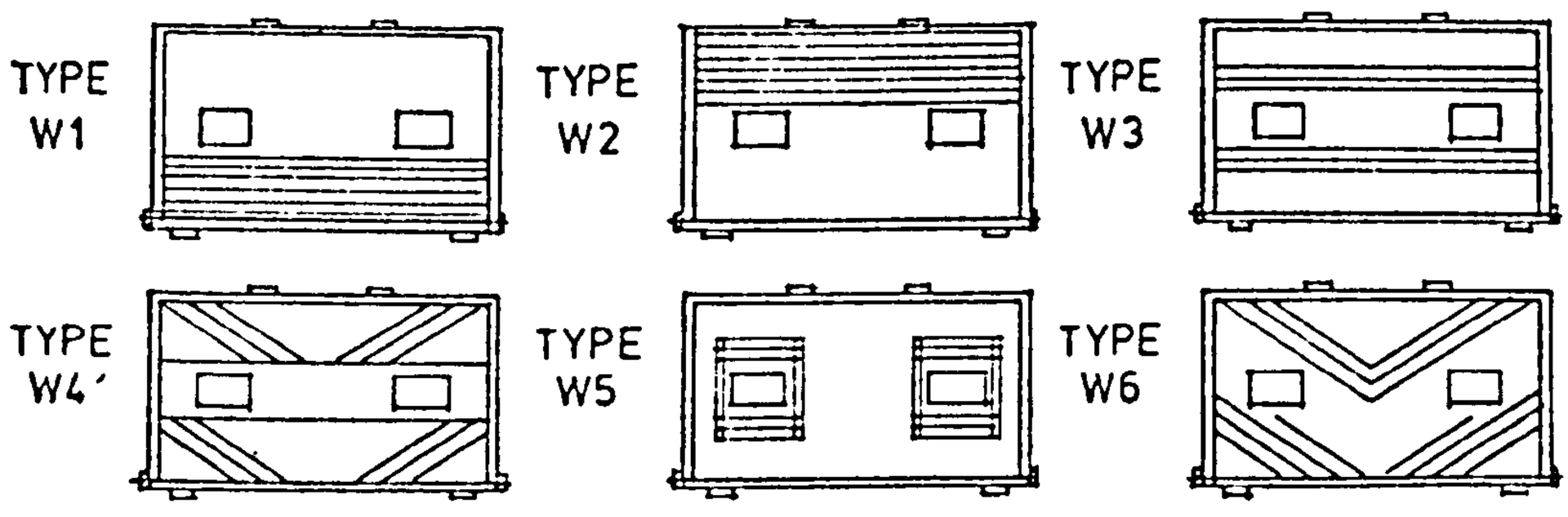

NOTES:

(1) Reinforcement details of Group 0 beams (no web reinforcement) as shown in top diagram above

(2) Web reinforcement Type W1 to W7 consisted of 10 mm diameter stirrups (web steel ratio = 1.13%)

(3) Web reinforcement Type W6A consisted of 6 mm diameter stirrups at 125 mm horizontal spacing. Reinforcement shown in beam without openings (Beam W6A-0.3/0) and typical beam with openings (Beam W6A-0.3/15)

FIG.6.1 DIMENSIONS AND REINFORCEMENT DETAILS OF THE NORMAL WEIGHT CONCRETE BEAMS

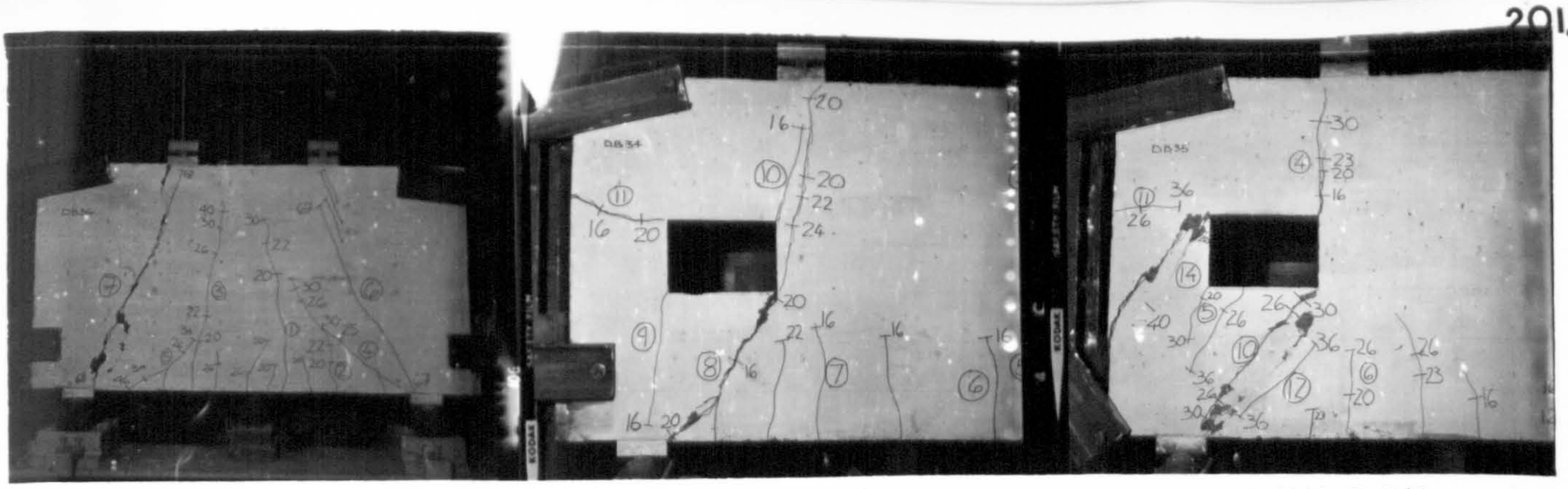

NO-0·3/0 NO-0·3/4 NW1-0·3/4

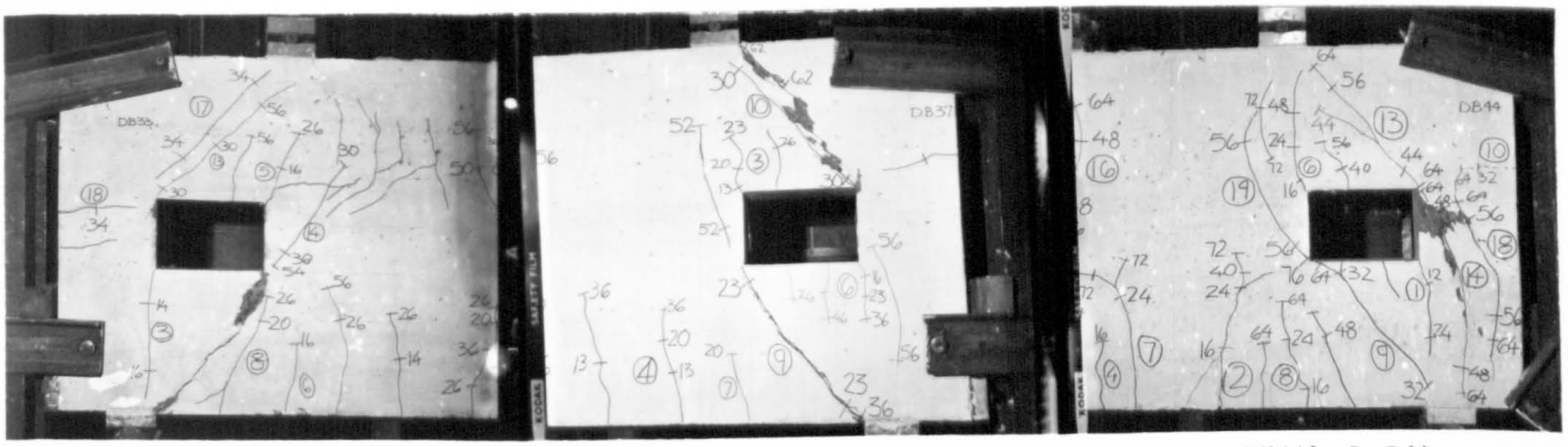

NW2-0·3/4 NW3-0·3/4 NW4-0·3/4

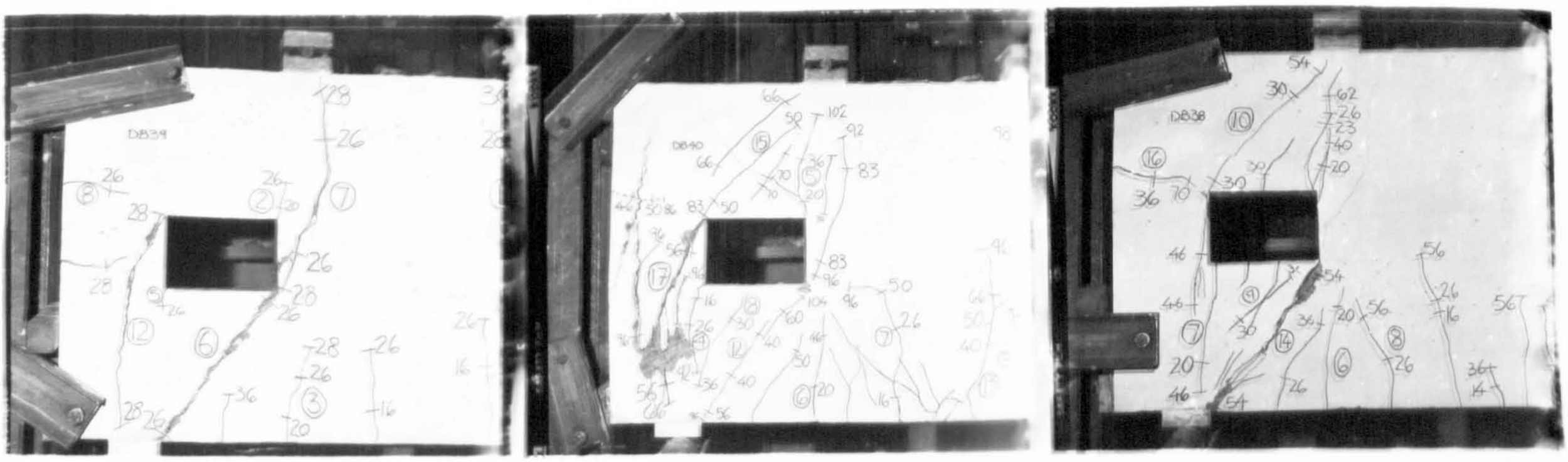

NW5-0·3/4 NW6-0·3/4 NW7-0·3/4

FIG.6.2a CRACK PATTERNS AT FAILURE OF THE NORMAL WEIGHT BEAMS (First nine)

(The circled numbers show the sequence in which the cracks were observed; the other numerical figures show the load, in 10 kN units, at which the extent of the cracks were as marked. Beam notation as in Table 6.1)

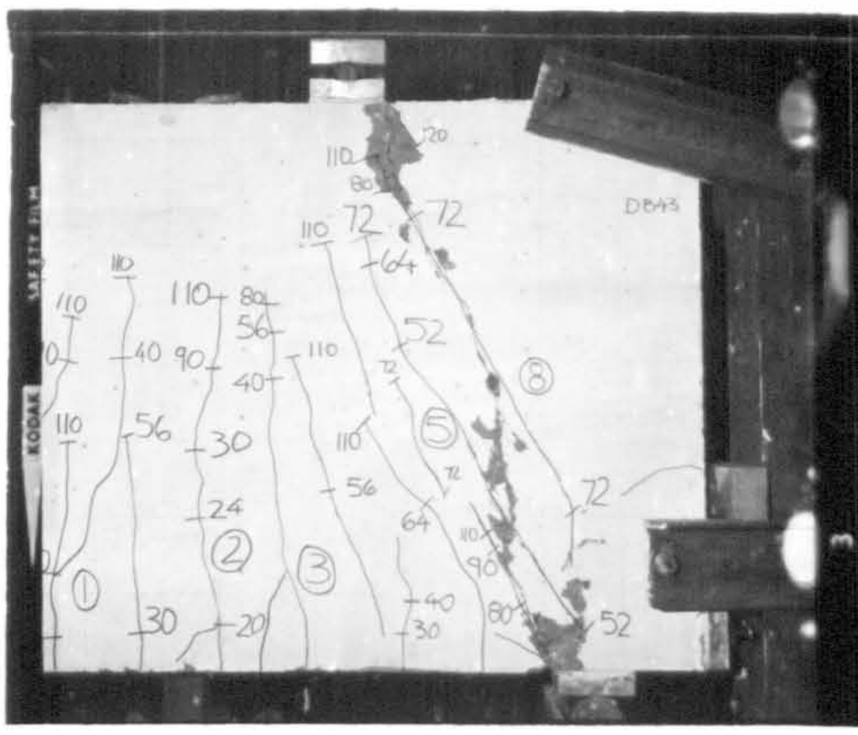

NW6A-0·3/0

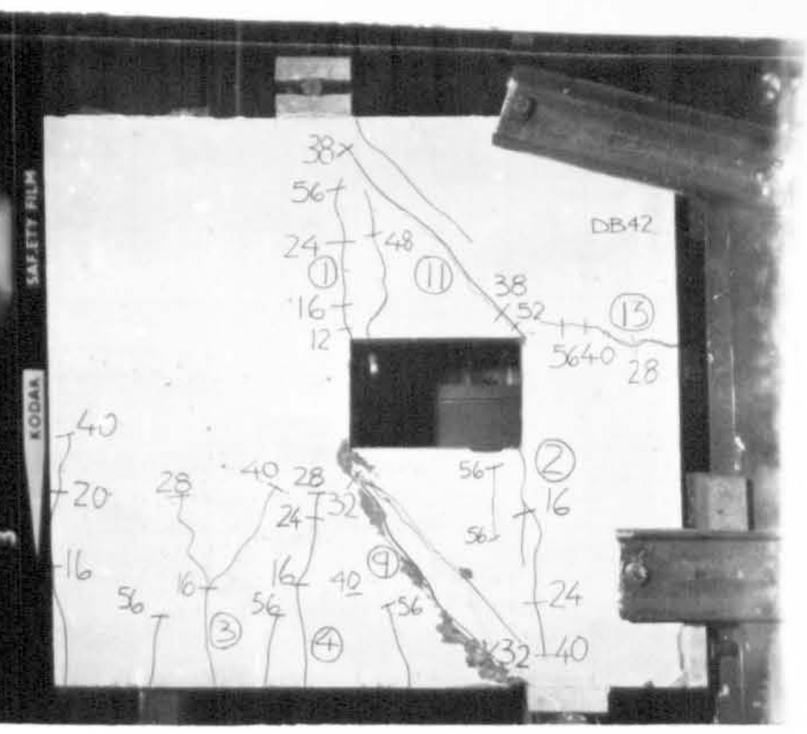

NW6A-0·3/4

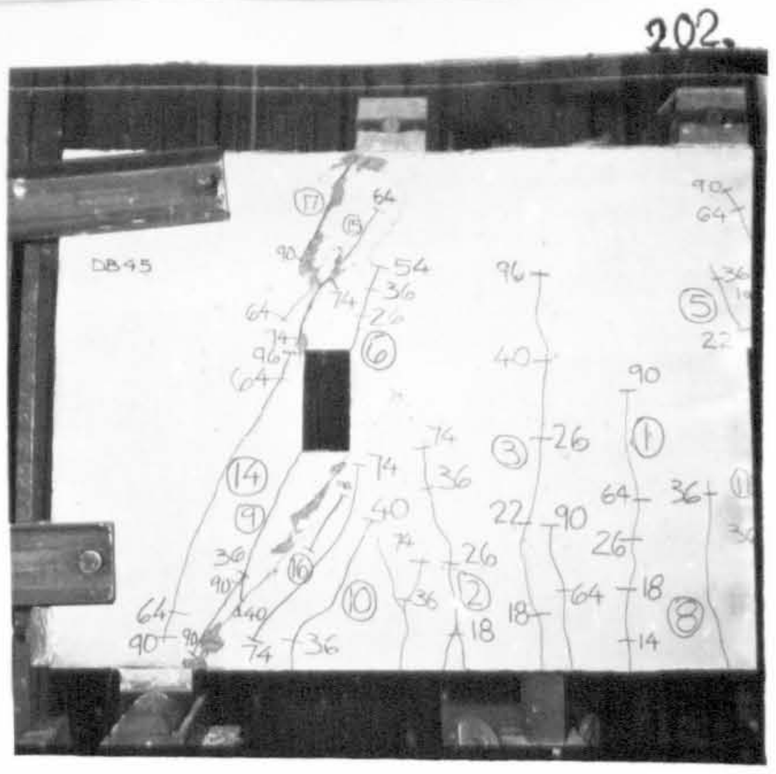

NW6A-0·3/1

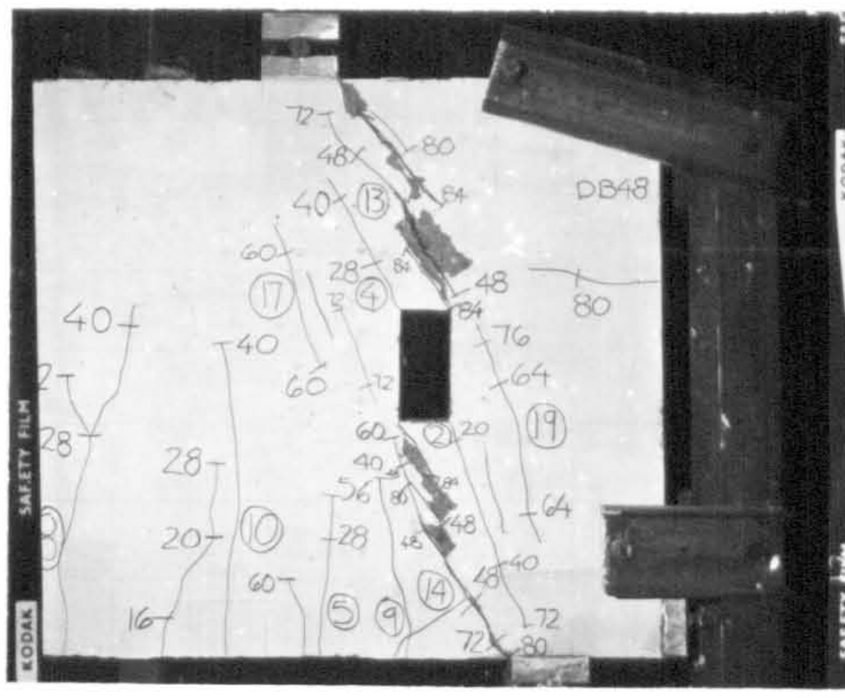

NW6A-0·3/17

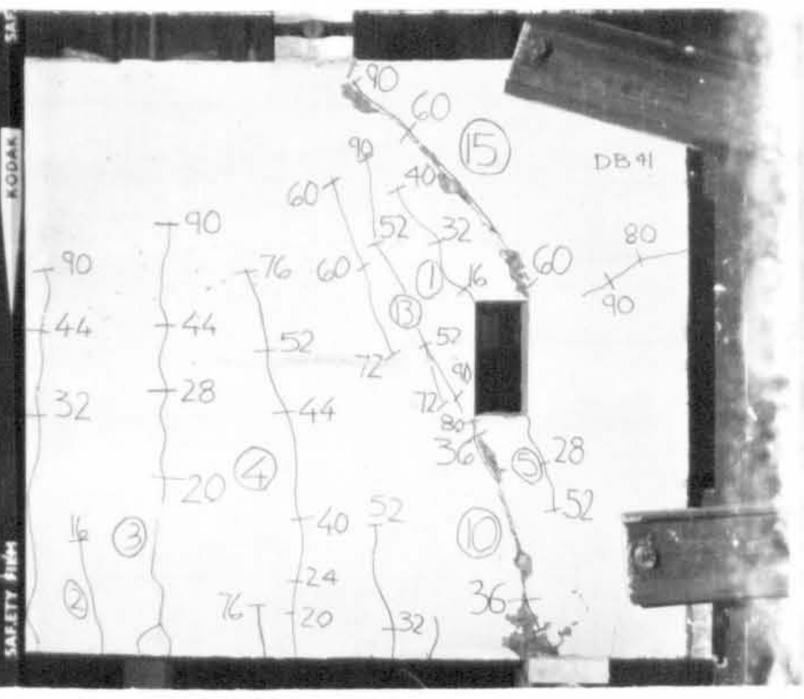

NW6A-0·3/7

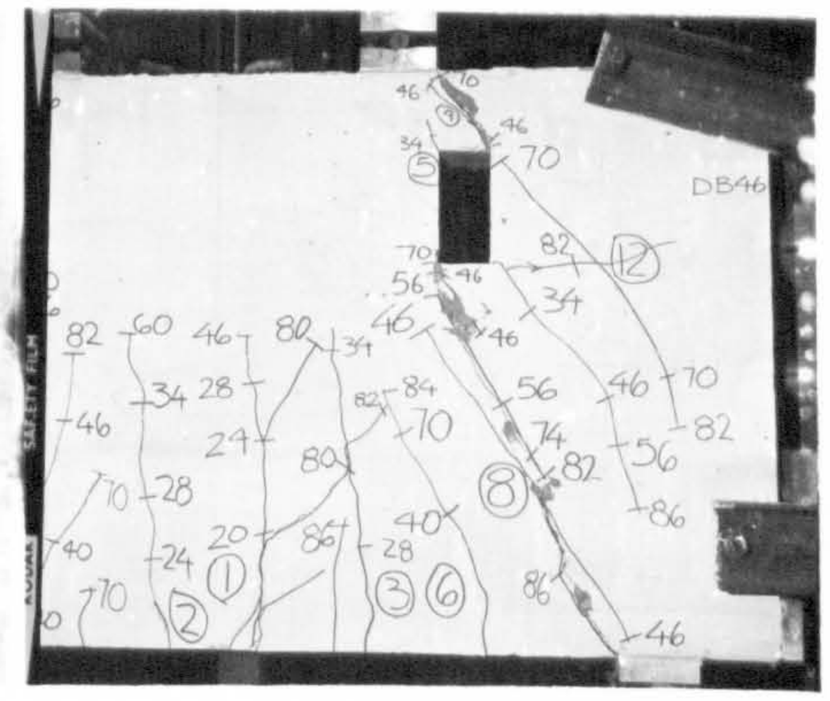

NW6A-0·3/11

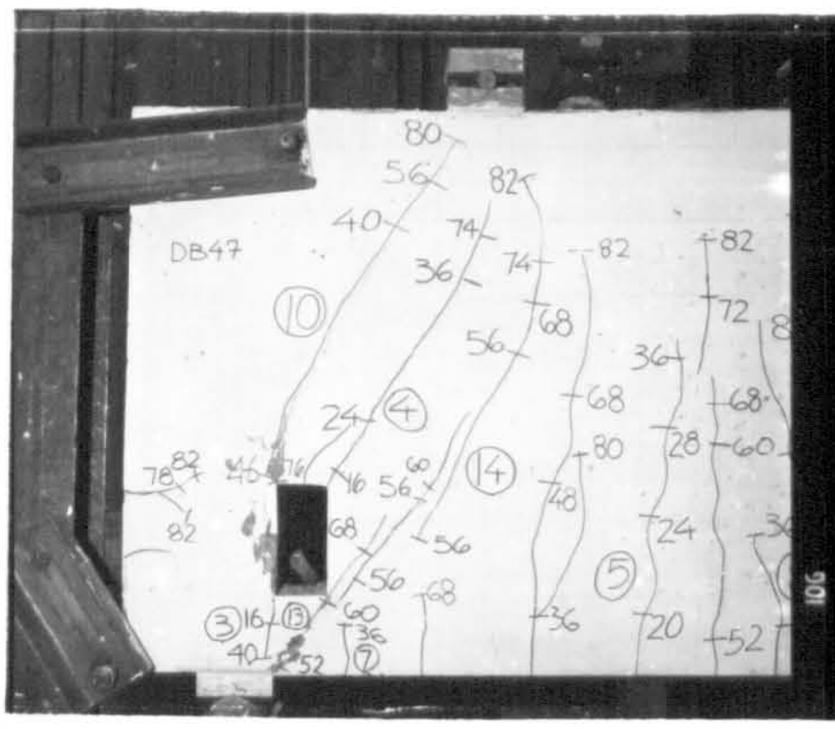

NW6A-0·3/15

FIG.6.2b CRACK PATTERNS AT FAILURE OF THE NORMAL WEIGHT BEAMS (The remaining beams)

(The circled numbers show the sequence in which the cracks were observed; the other numerical figures show the load, in 10 kN units, at which the extent of the cracks were as marked. Beam notation as in Table 6.1)

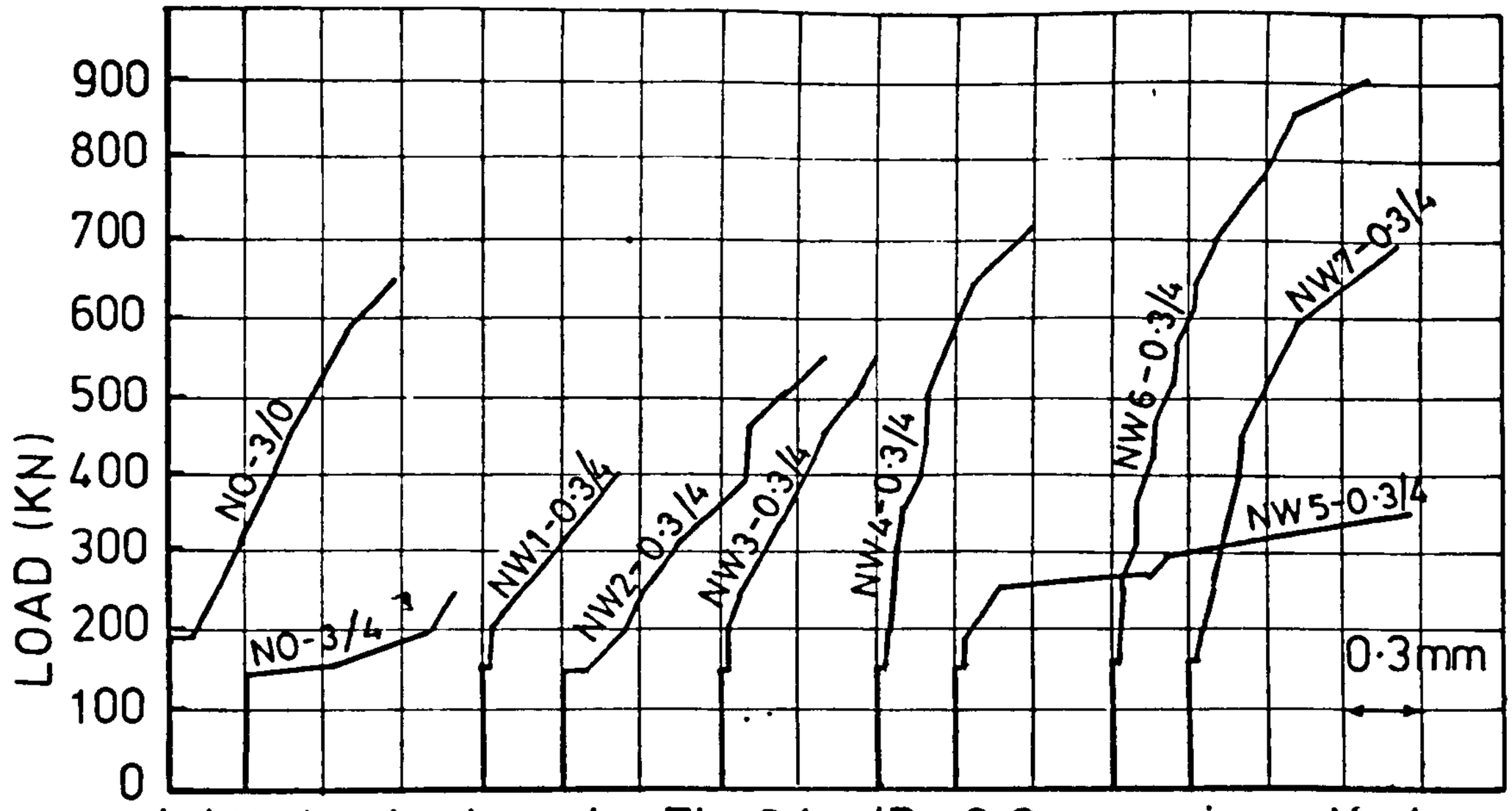

(a) Web steel as in Fig 6.1; x/D = 0·3; opening No 4.

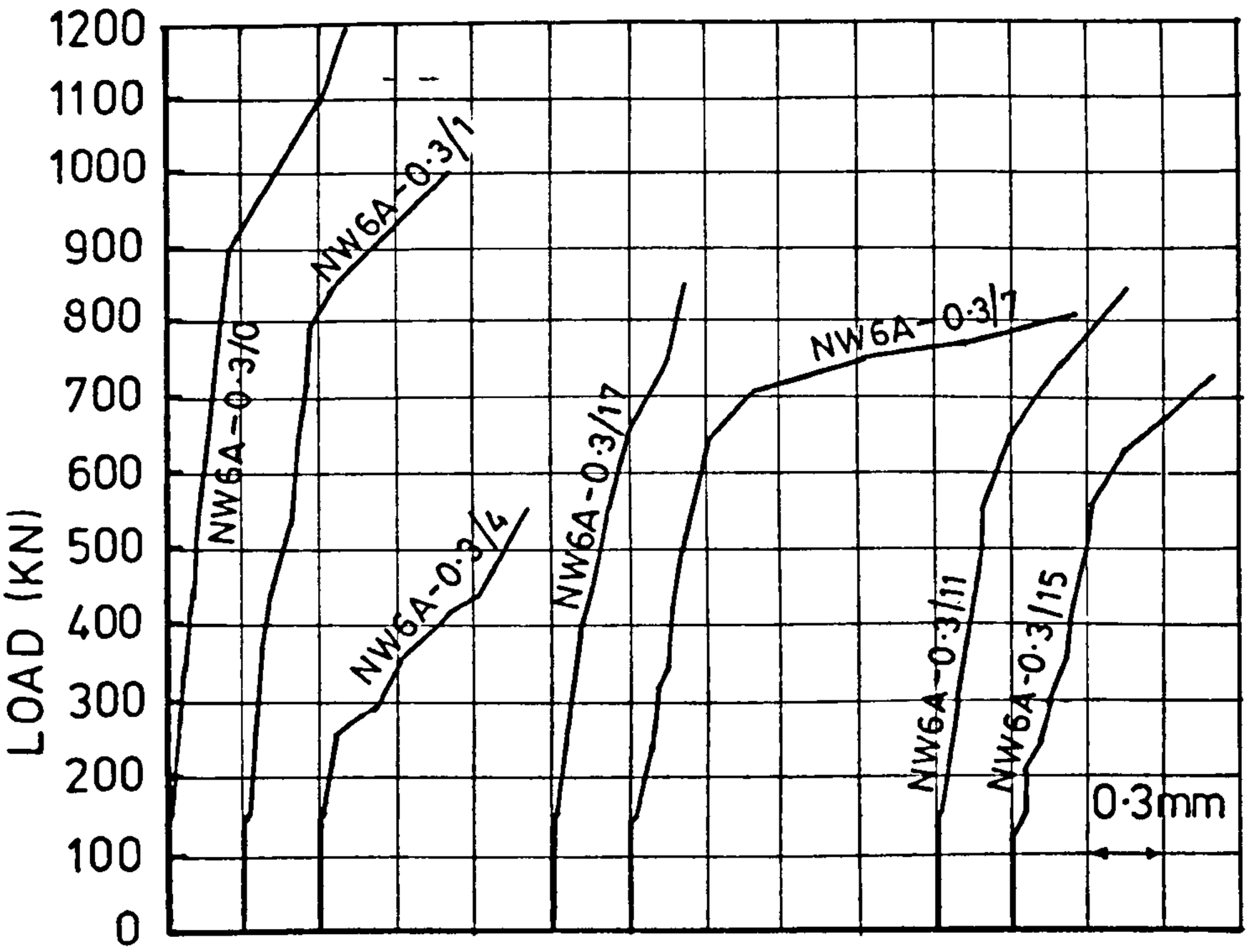

(b) Web steel Type W6A (Fig 6.1); x/D = 0·3; opening varies

Beam notation as in Table 6.1

FIG.6.3 MAXIMUM CRACK WIDTHS

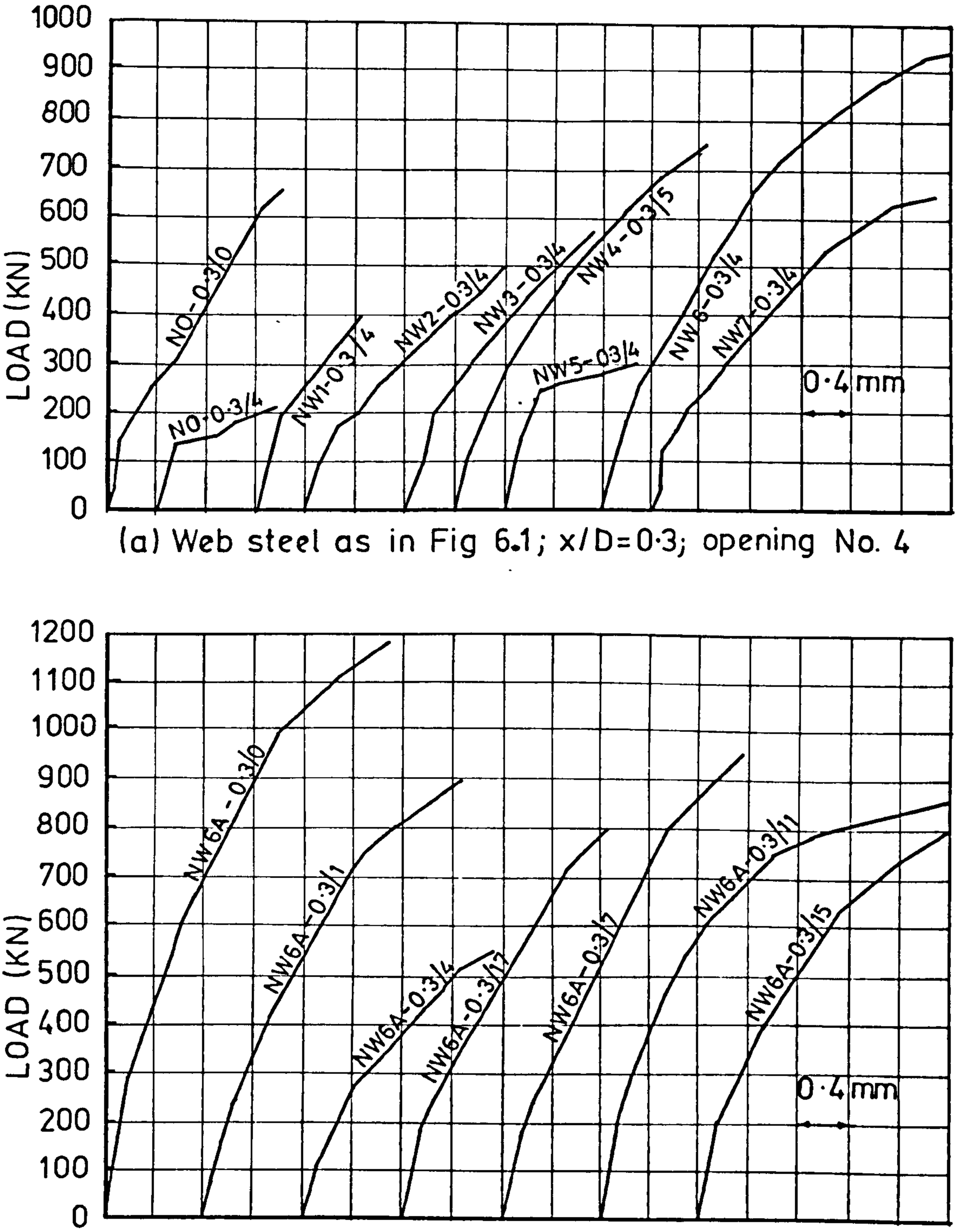

(a) Web steel as in Fig 6.1; x/D=0·3; opening No. 4

(a) Web steel Type W6A (Fig 6.1); x/D=0·3; opening varies

Beam notation as in Table 6.1

FIG.6.4 CENTRAL DEFLECTIONS

Beam Ref. No.*	Ultimate Loads Measured W_1 kN	Computed W_2 kN	$\frac{W_1}{W_2}$
M-0.4/0	660	‡‡695	0.95
M-0.4/1	580	590	0.98
M-0.4/2	360	406	0.88
M-0.4/3	445	231	1.93
M-0.4/4	450	‡270	1.66
M-0.4/5	600	‡‡600	1.00
M-0.4/6	270	102	2.64
M-0.4/8	340	193	1.76
M-0.4/9	240	268	0.89
M-0.4/10	300	‡241	1.25
M-0.4/11	600	‡‡657	0.91
M-0.4/12	520	‡‡653	0.80
M-0.4/13	130	163	0.79
0-0.4/0	660	‡‡590	1.12
0-0.4/2	370	352	1.05
0-0.4/4	340	‡277	1.22
0-0.4/5	540	‡‡550	0.98
0-0.4/6	190	74	2.56
0-0.4/7	420	423	0.99
0-0.25/0	660	‡662	1.00
0-0.25/2	360	441	0.81
0-0.25/4	460	337	1.36
0-0.25/5	560	‡689	0.81
0-0.25/6	280	125	2.23

Continued next page

*Beam notation as in Table 4.1

‡‡Equation (7.1) used for these beams; Eqn.(7.2)used for others.

TABLE 7.1 MEASURED AND COMPUTED ULTIMATE LOADS

Beam Ref. No.*	Ultimate Loads Measured W_1 kN	Computed W_2 kN	$\frac{W_1}{W_2}$
0-0.3/0	595	‡651	0.91
0-0.3/1	460	‡637	0.72
0-0.3/2	390	295	1.32
0-0.3/3	280	275	1.02
0-0.3/4	260	275	0.95
0-0.3/5	200	278	0.72
0-0.3/6	250	287	0.87
0-0.3/7	420	396	1.06
0-0.3/8	380	341	1.11
0-0.3/9	280	325	0.86
0-0.3/10	210	243	0.86
0-0.3/11	360	‡467	0.77
0-0.3/12	560	‡707	0.79
0-0.3/13	300	‡483	0.62
0-0.3/14	560	‡664	0.84
0-0.3/15	260	183	1.42
0-0.3/16	195	48	4.00
0-0.2/0	655	‡720	0.90
0-0.2/4	360	356	1.01
0-0.2/13	500	507	0.99
0-0.2/16	340	92	3.70

Continued next page

*Beam Notation as in Table (5.1)

‡Equation (7.1) used for these beams; equations (7.2) used for the others

TABLE 7.1 Continued.

Beam Ref. No.*	Ultimate Loads Measured W_1 kN	Computed W_2 kN	$\frac{W_1}{W_2}$
0-0.3/2R	260	284	0.92
0-0.3/3R	400	266	1.50
0-0.3/4R	215	294	0.73
0-0.3/5R	330	295	1.12
W1-0.3/4	400	***	
W2-0.3/4	490	***	
W3-0.3/4	560	557	1.01
W4-0.3/4	660	791	0.83
W5-0.3/4	370	***	
W6-0.3/4	825	798	1.03
W7-0.3/4	630	536	1.18
W1(A)	475	***	
W3(A)	500	552	0.91
W4(A)	650	797	0.82
W7(A)	670	542	1.24
WM-0.4/0	660	++667	0.99
WM-0.4/18	500	356	1.4
WM'-0.4/18	500	356	1.4

Continued next page

*Beam notation as in Table (5.2)

‡Equation (7.1) used for these beams; equations (7.2) used for the others.

TABLE 7.1 Continued.

Beam Ref. No.*	Ultimate Loads Measured W_1 kN	Computed W_2 kN	$\frac{W_1}{W_2}$
NO-0.3/0	680	‡861	0.79
NO-0.3/4	240	367	0.65
NW1-0.3/4	420	***	
NW2-0.3/4	580	***	
NW3-0.3/4	620	651	0.95
NW4-0.3/4	780	867	0.90
NW5-0.3/4	370	***	
NW6-0.3/4	1060	907	1.17
NW7-0.3/4	720	591	1.22
NW6A-0.3/0	1215	‡991	1.22
NW6A-0.3/1	1015	‡944	1.07
NW6A-0.3/4	620	542	1.14
NW6A-0.3/17	840	593	1.4
NW6A-0.3/7	930	652	1.4
NW6A-0.3/11	880	845	1.04
NW6A 0.3/15	820	402	2

*Beam notation as in Table (6.2)

‡Equation (7.1) used for these beams; equation (7.2) used for the others.

TABLE 7.1 Continued.

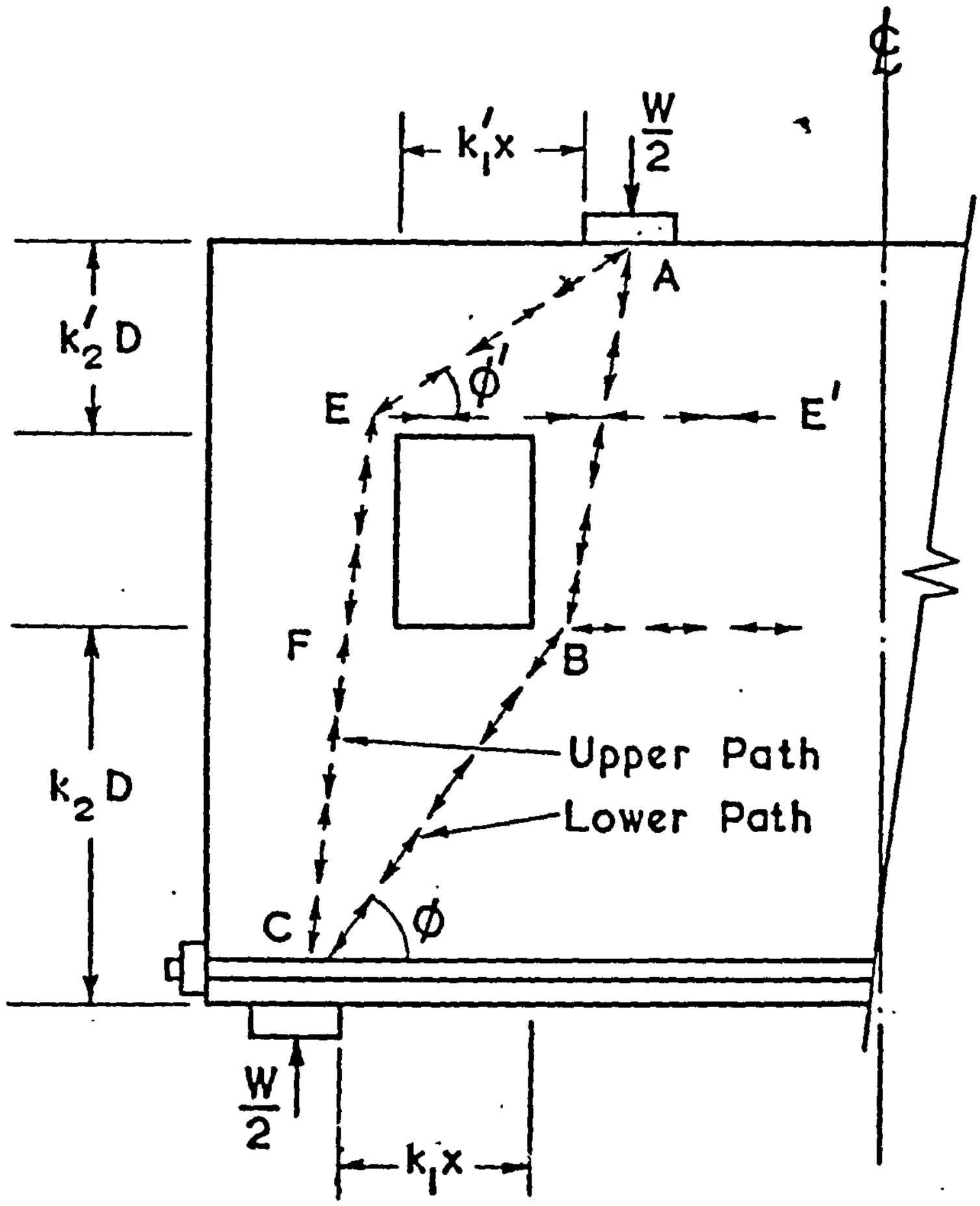

FIG.7.1 THE STRUCTURAL IDEALIZATION

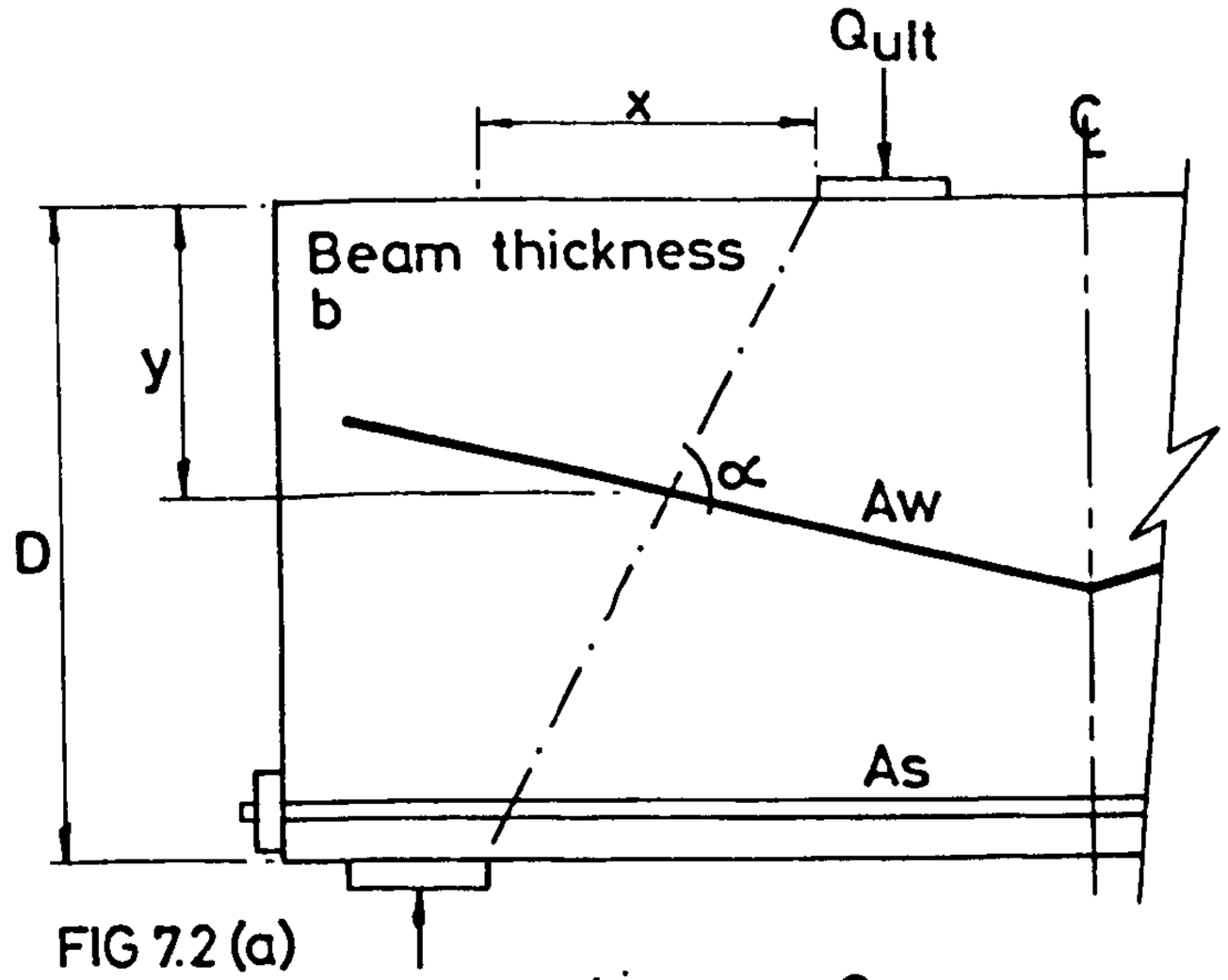

FIG 7.2 (a)

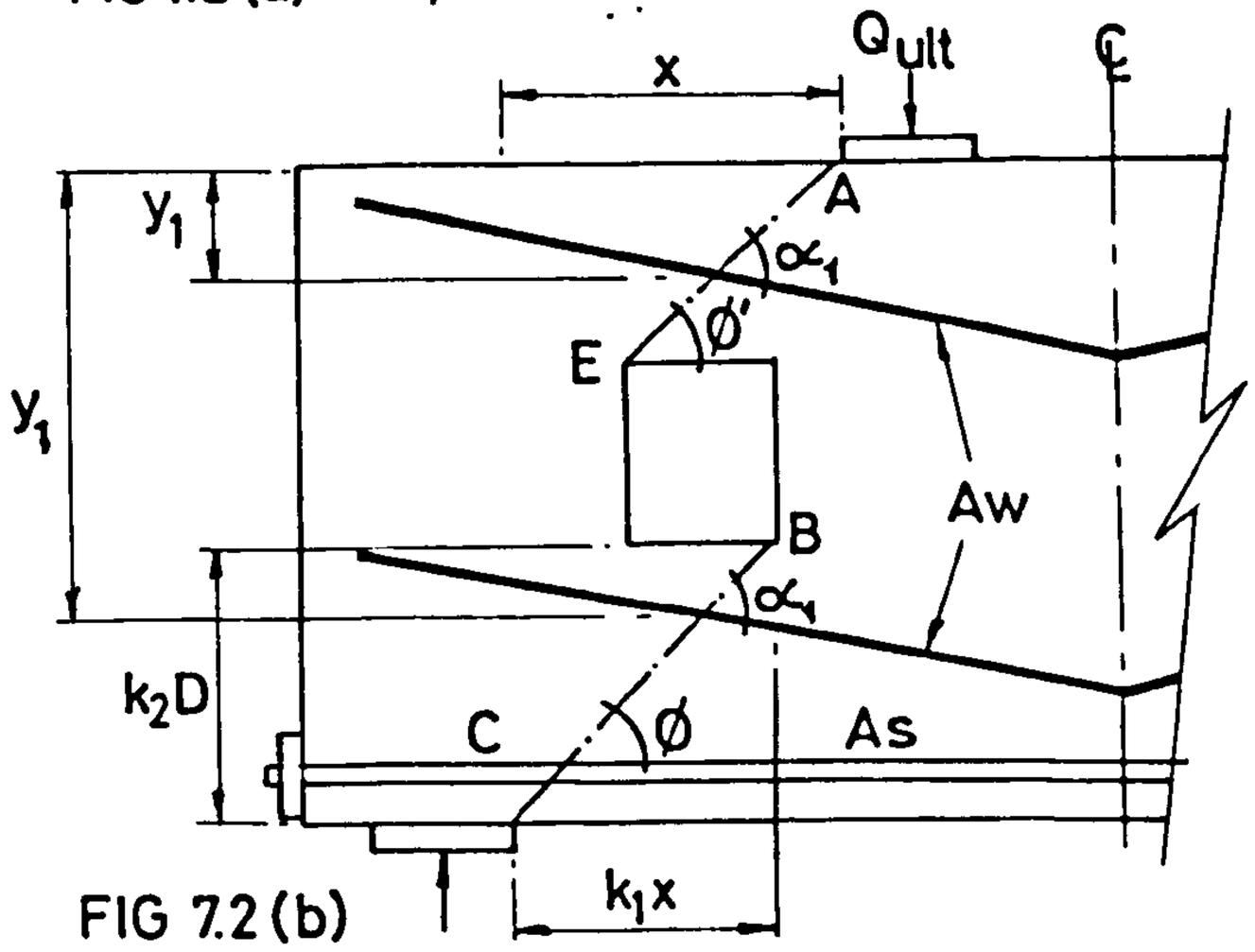

FIG 7.2 (b)

C_1 is an empirical coefficient. For normal weight concrete, $C_1 = 1.4$. For lightweight concrete $C_1 = 1.35$ where the cylinder splitting strength f_t is determined in accordance with ASTM Standard C330; $C_1 = 1.0$ where f_t is determined in accordance with BS 1881

C_2 is an empirical coefficient equal to 300 N/mm^2 and 130 N/mm^2 for deformed bars and plain round bars, respectively

λ is an empirical coefficient equal to 1.0 for main longitudinal bars (A_s) near beam soffit and 1.5 for web reinforcement proper (A_w)

A is equal to the area of the main bars (A_s) or the area of the web bars (A_w) as the case may be

f_t is the cylinder splitting strength of concrete

FIG.7.2 EXPLANATION OF SYMBOLS

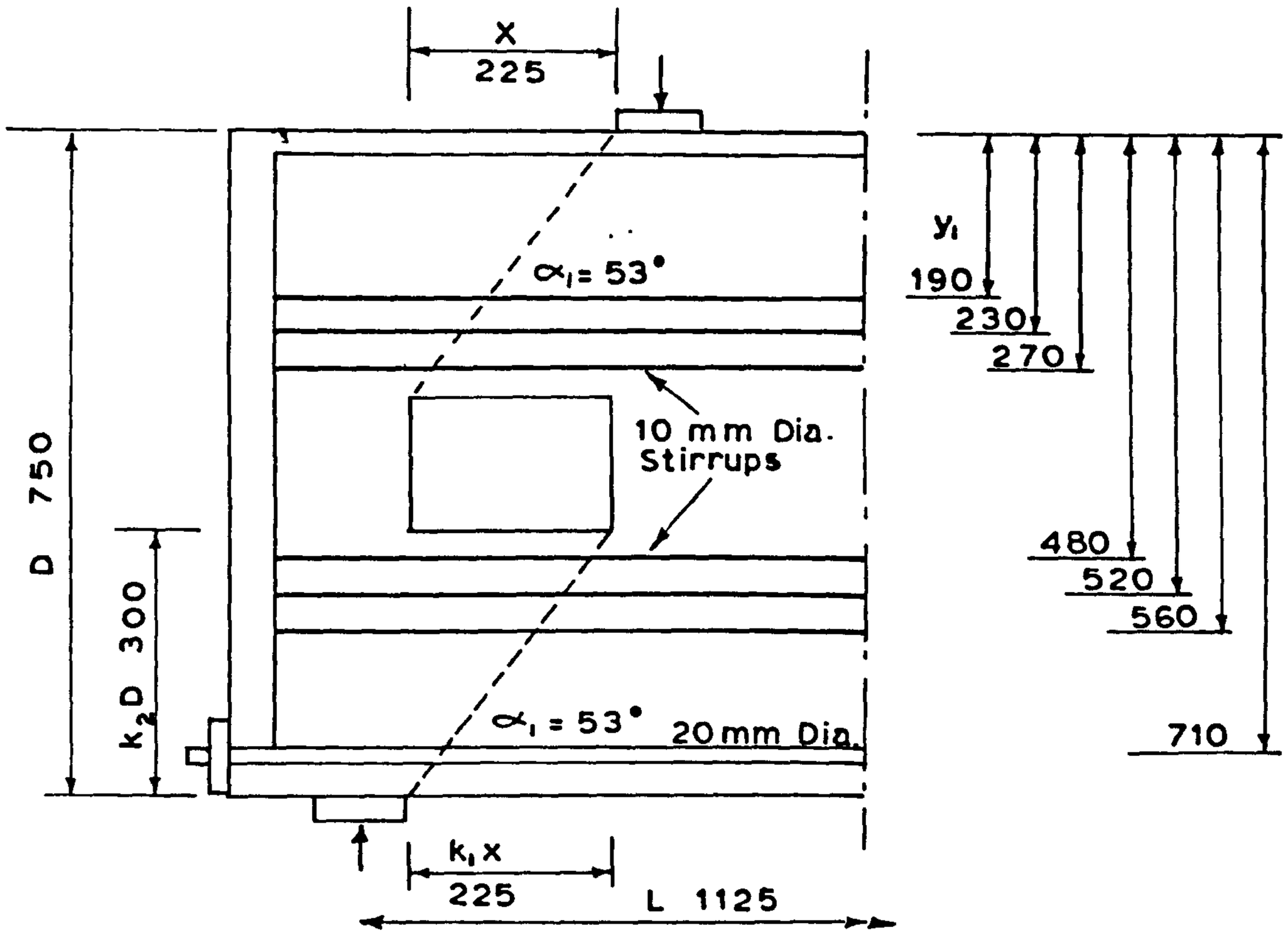

f_t = 2·87 N/mm²

b = 100 mm

All dimensions in mm.

FIG.7.3 PROPERTIES AND DIMENSIONS OF BEAM W3-0.3/4

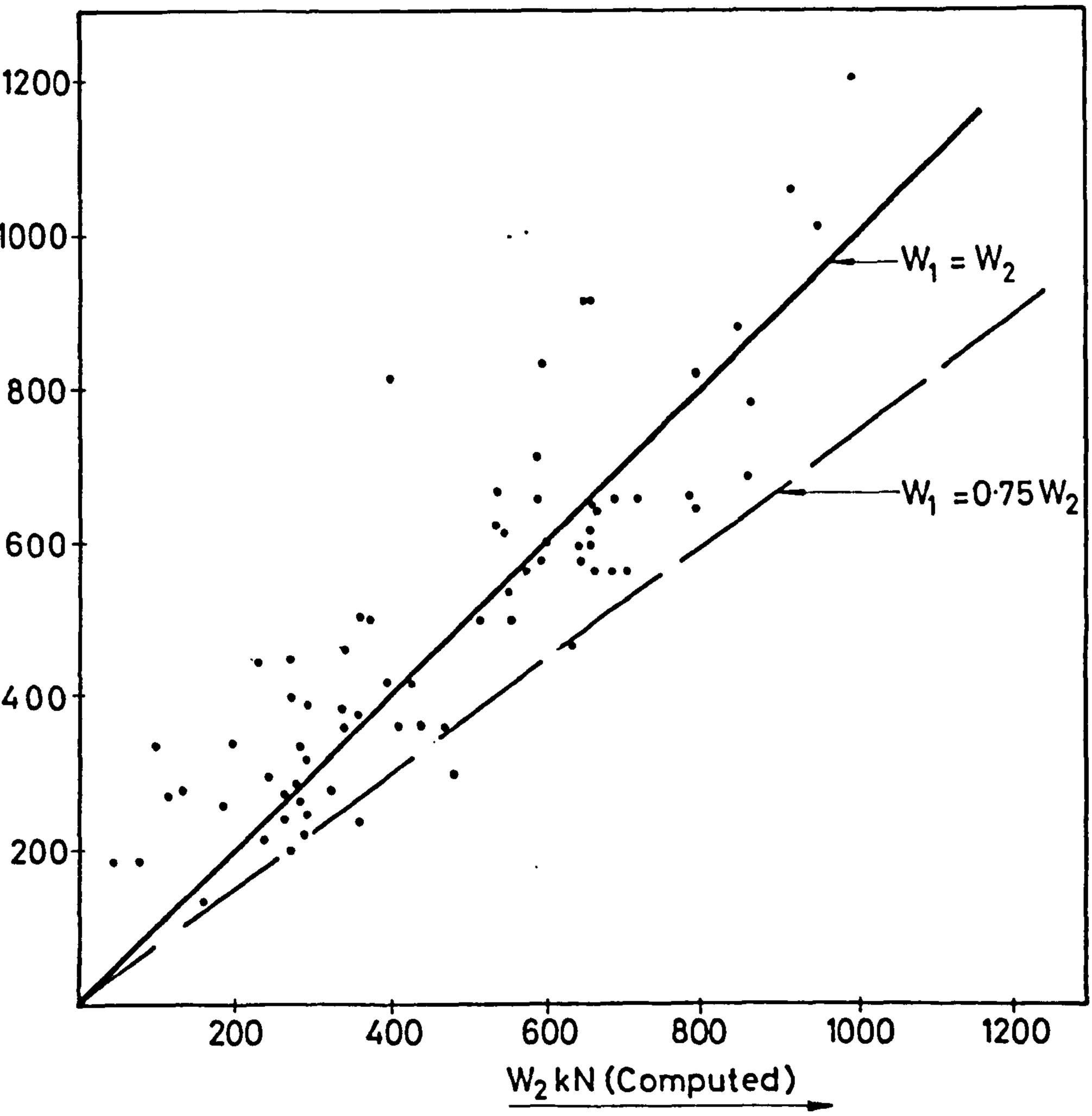

Data taken from Table 7.1

FIG.7.4 COMPARISON OF COMPUTED AND MEASURED ULTIMATE LOADS

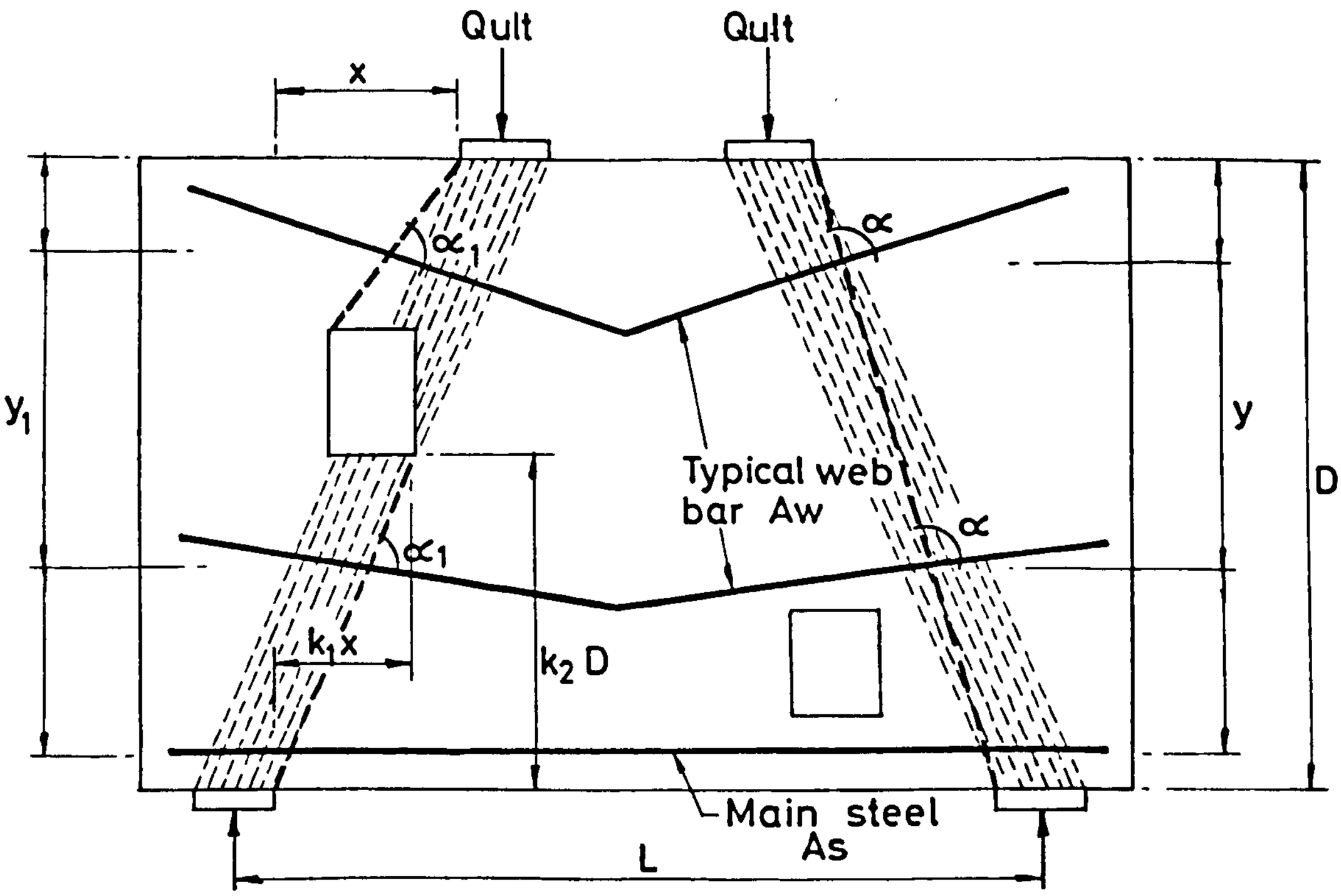

FIG.8.1 DESIGN EQUATIONS: GEOMETRICAL NOTATION

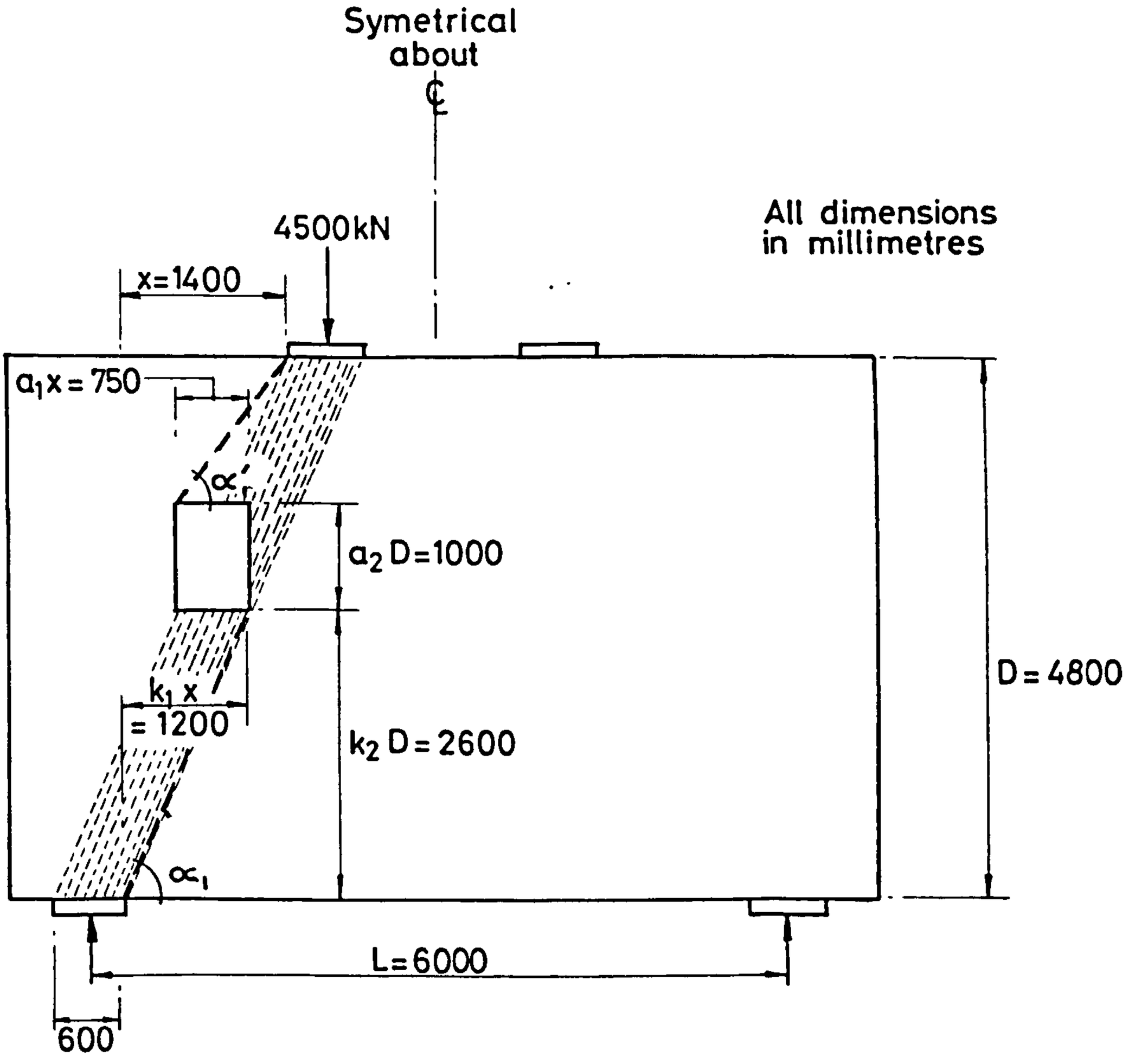

Normal w.t. concrete.
f'c = 22·5 N/mm²
fcu = 30·0 N/mm²
ft = 3·0 N/mm²

Deformed bars
fy = 410·0 N/mm²

FIG.8.2 DESIGN EXAMPLE: GEOMETRY AND LOADING

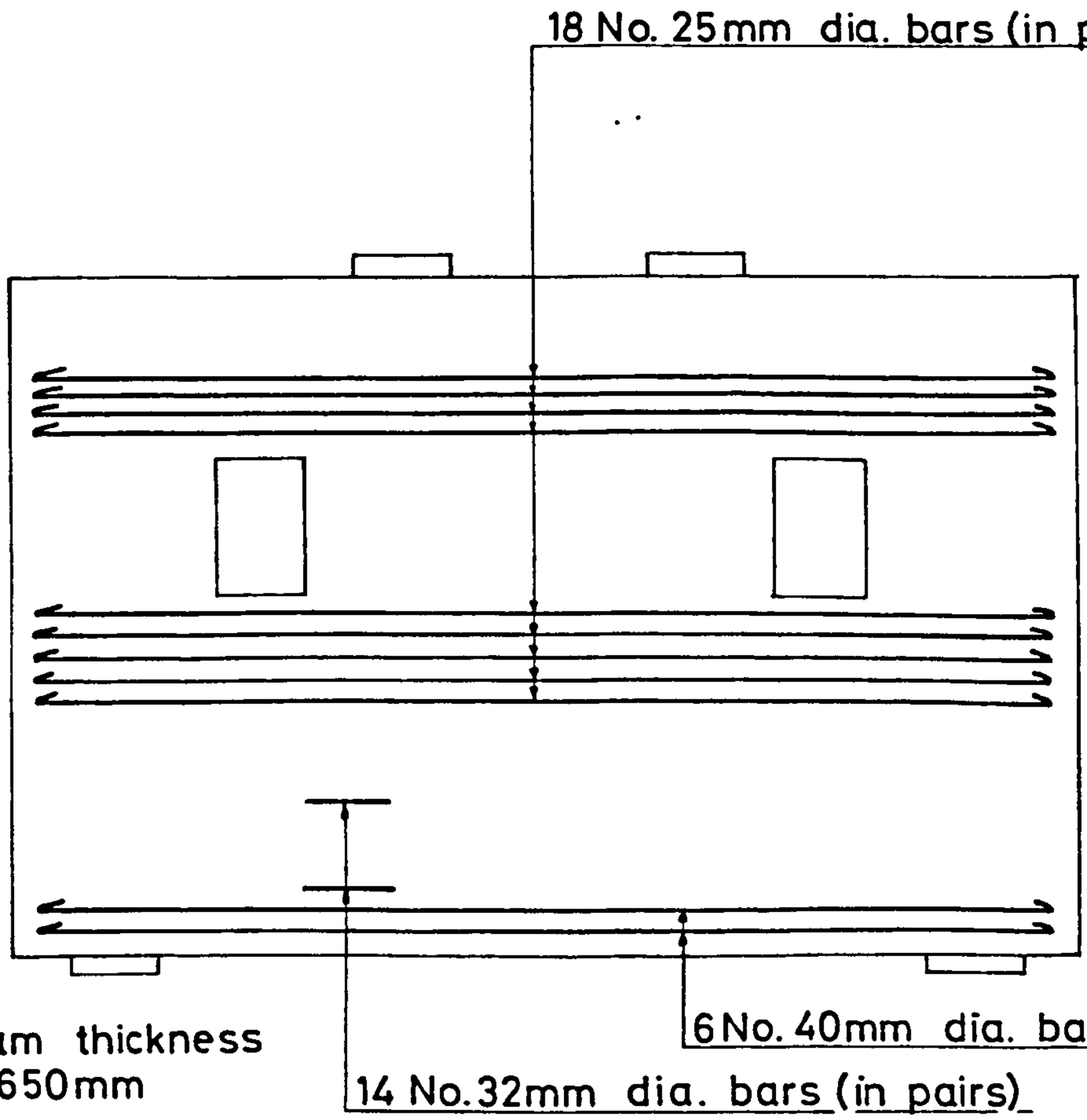

FIG.8.3 DESIGN EXAMPLE: MAIN STEEL AND WEB STEEL DETAILS

Beam Ref. No.*	CEB W_1/W_4	ACI W_1/W_5	PCA W_1 W_6	CIRIA W_1/W_7
M-0.4/0	2.09	1.62	6.2	1.66
0-0.4/0	2.02	2.44	6.1	1.87
0-0.25/0	1.94	2.28	6.0	1.72
0-0.3/0	1.61	2.04	5.1	1.57
0-0.2/0	1.75	2.07	3.7	1.66
WM-0.4/0	3.29	2.13	10.1	1.75
NO-0.3/0	1.52	1.70	4.2	1.41
NW6A-0.3/0	2.98	2.37	7.9	2.24
Average values	2.38	2.08	6.2	1.73

* Beam notation as given in Tables, 4.1,5.1 and 6.1

W_1 is the measured ultimate of the beams as given in Tables 4.2, 5.2 and 6.2

W_4 to W_7 are, respectively, the computed design loads according to the CEB-FIP Recommendations, the ACI Building Code, the PCA Concrete Information ST66 and the CIRIA Guide.

TABLE 9.1 COMPARISON OF COMPUTED DESIGN LOADS

Effective span (l) = l_o + (the lesser of $c_1/2$ or $0.1l_o$)
+ (the lesser of $c_2/2$ or $0.1l_o$)
Active height (h_a) = h when $l > h$
= l when $h > l$

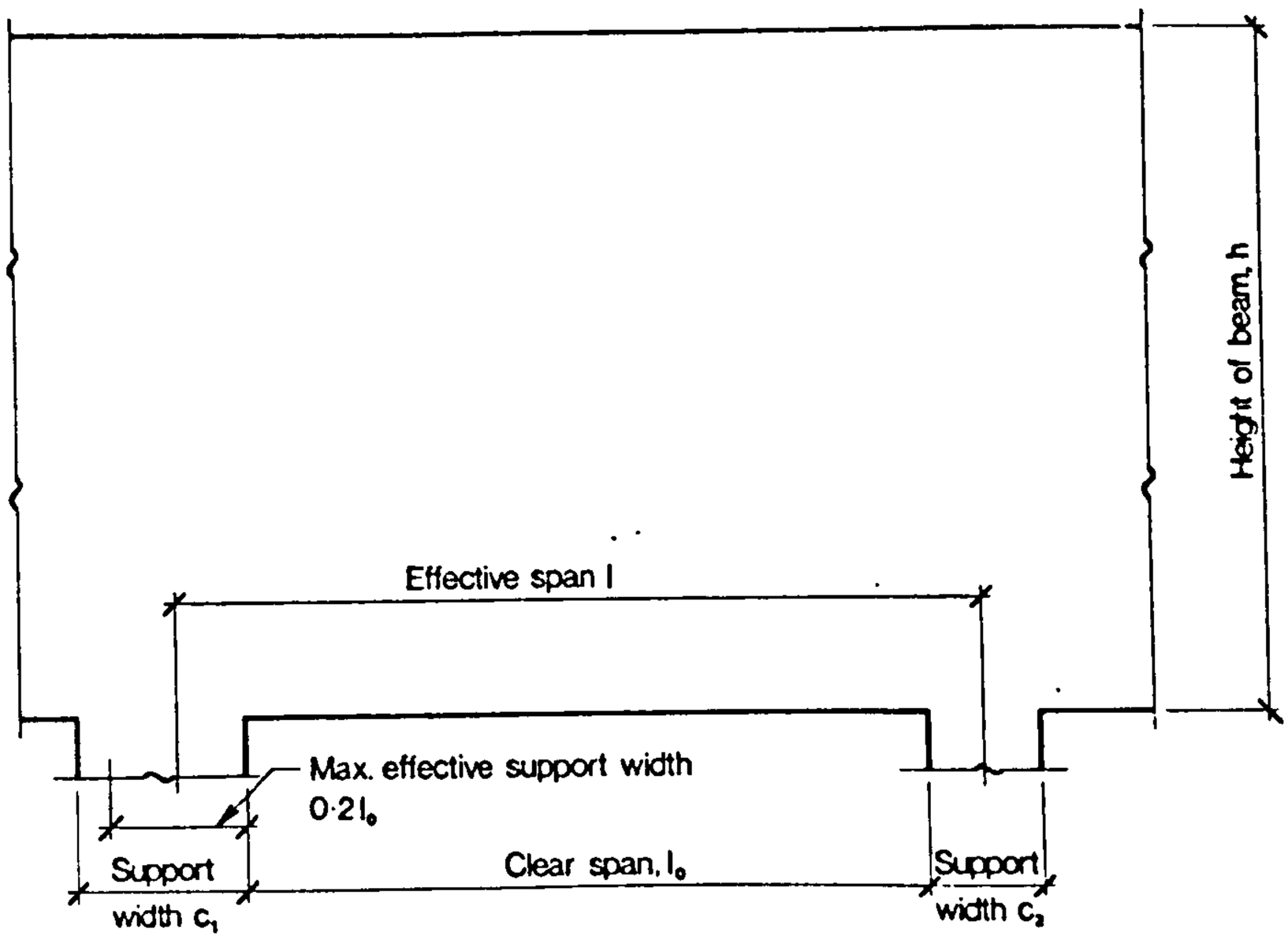

FIG.9.1 BASIC DIMENSIONS OF DEEP BEAMS:CIRIA GUIDE (FIG.5)[9]

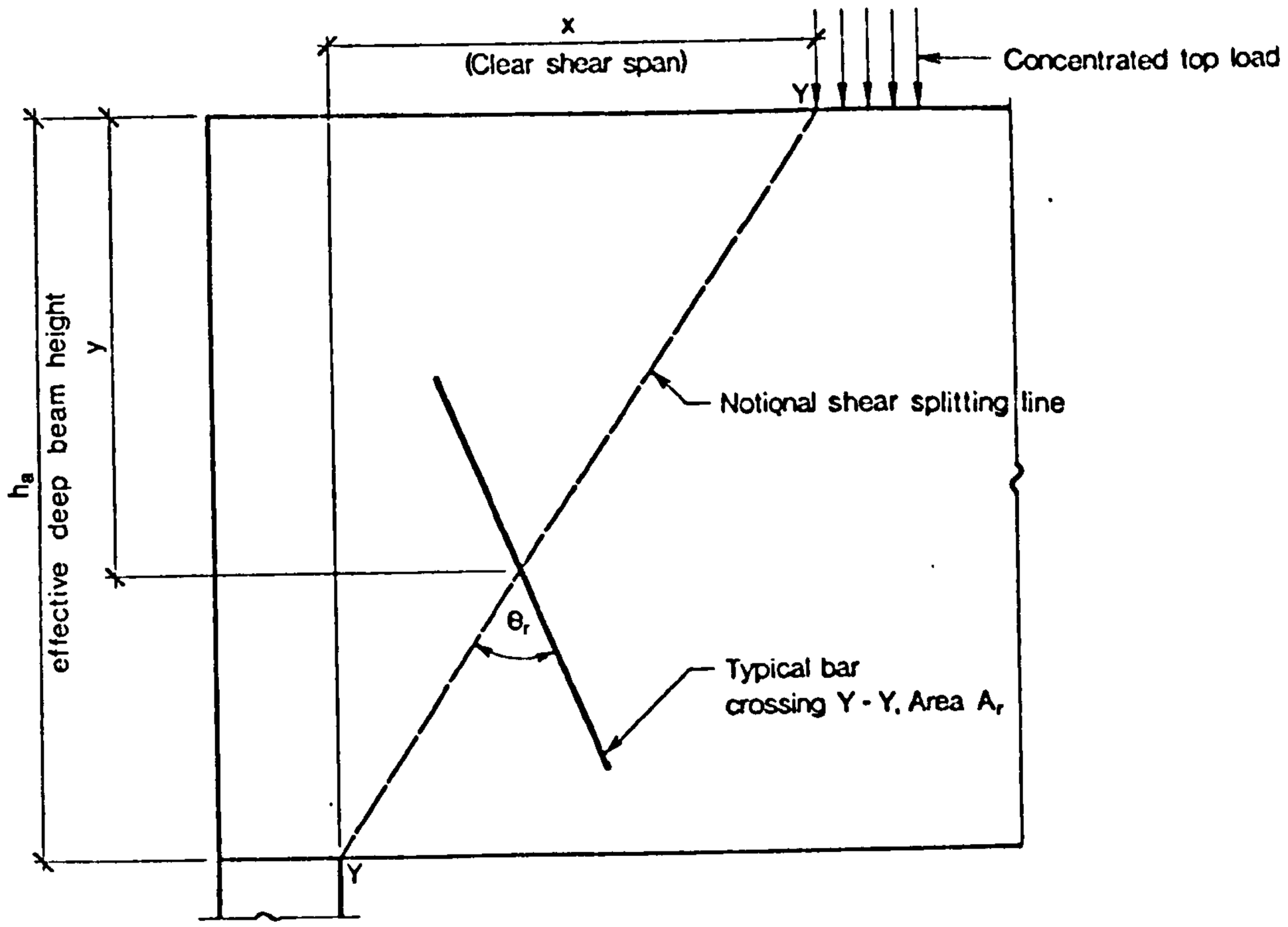

FIG.9.2 MEANING OF SYMBOLS:CIRIA GUIDE (FIG.14)[9]

TABLE 4 *Concrete shear stress parameter,* v_x (N/mm²)

Clear shear span/height (x/h)	Concrete grade (f_{cu})				
	15	20	25	30	40
1.0	2.52	2.91	3.25	3.56	4.11
0.8	2.79	3.22	3.60	3.94	4.55
0.6	3.06	3.53	3.95	4.33	5.00
0.4	3.33	3.85	4.30	4.71	5.44
0.2	3.60	4.16	4.65	5.09	5.88
0	3.87	4.47	5.00	5.48	6.32

TABLE 5 *Maximum shear stress parameter,* v_{max} (N/mm²)

Concrete grade (f_{cu})	v_{max}
15	5.03
20	5.81
25	6.50
30	7.12
40	8.22

TABLE 6 *Main (sagging) steel shear stress parameter,* v_{ms} (N/mm²)

Clear shear span/height (x/h)	% main (sagging) steel (ρ_{ms})				
	0.2	0.4	0.6	0.8	1.0
1.0	0.20	0.39	0.59	0.78	0.98
0.8	0.24	0.48	0.71	0.95	1.19
0.6	0.29	0.57	0.86	1.15	1.43
0.4	0.34	0.67	1.01	1.34	1.68
0.2	0.38	0.75	1.13	1.50	1.88
0	0.39	0.78	1.17	1.56	1.95

TABLE 7 *Horizontal web steel shear parameter,* v_{wh} (N/mm²)

Clear shear span/height (x/h)	% horizontal web reinforcement (ρ_{wh})						
	0.25	0.30	0.35	0.4	0.6	0.8	1.0
1.0	0.12	0.15	0.17	0.20	0.29	0.30	0.40
0.8	0.15	0.18	0.21	0.24	0.36	0.48	0.60
0.6	0.18	0.22	0.25	0.29	0.43	0.57	0.72
0.4	0.21	0.25	0.29	0.34	0.50	0.67	0.84
0.2	0.23	0.28	0.33	0.37	0.56	0.75	0.94
0	0.24	0.29	0.34	0.39	0.59	0.78	0.98

TABLE 8 *Vertical web steel shear parameter,* v_{wv} (N/mm²)

Clear shear span/height (x/h)		% vertical web reinforcement (ρ_{wv})					
	0.15	0.20	0.30	0.40	0.60	0.80	1.0
1.0	0.07	0.10	0.15	0.20	0.29	0.39	0.49
0.8	0.05	0.06	0.09	0.12	0.18	0.24	0.30
0.6	0.02	0.03	0.05	0.06	0.10	0.12	0.16
0.4	0.01	0.01	0.02	0.02	0.03	0.04	0.05
0.2	0.00	0.00	0.00	0.00	0.00	0.01	0.01
0	0.00	0.00	0.00	0.00	0.00	0.00	0.01

FIG.9.3 CIRIA DESIGN TABLES (Nos. 4 to 8)[9]

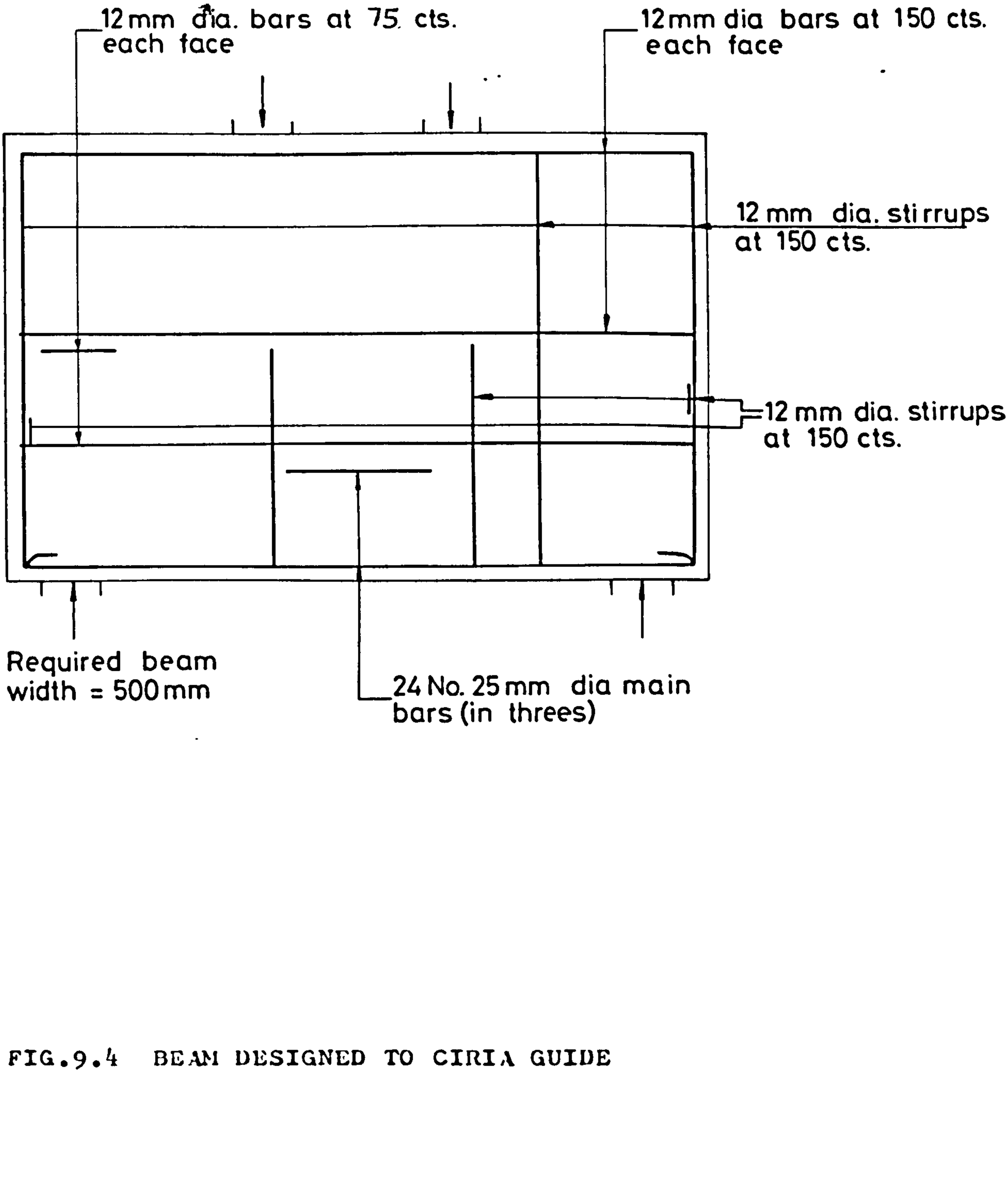

FIG.9.4 BEAM DESIGNED TO CIRIA GUIDE

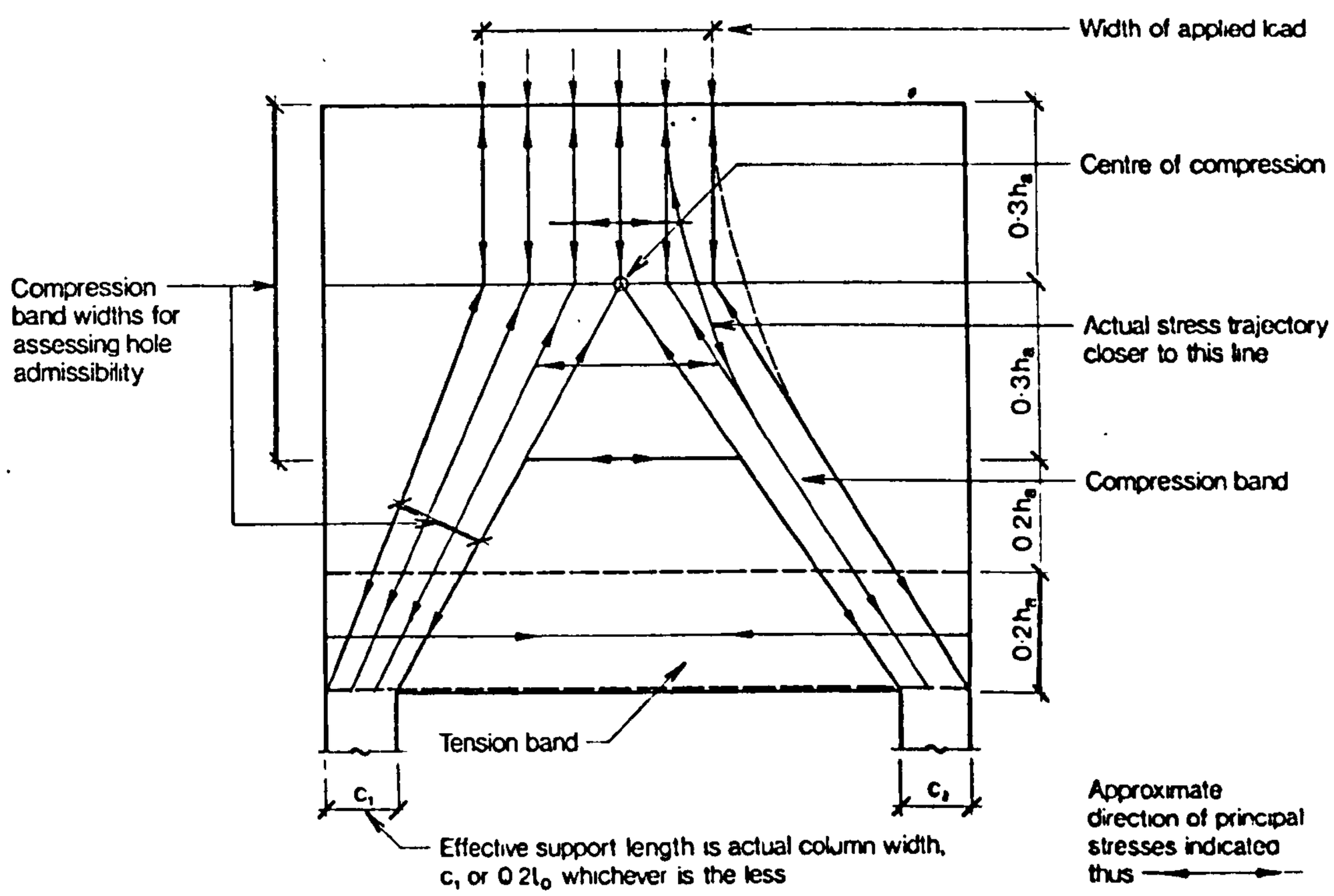

Dimensions of opening ⩾ 0.2 times width of notional force bands given above

FIG.9.5 ASSESSMENT OF HOLE ADMISSIBILITY: CIRIA GUIDE (FIG.19)[9]

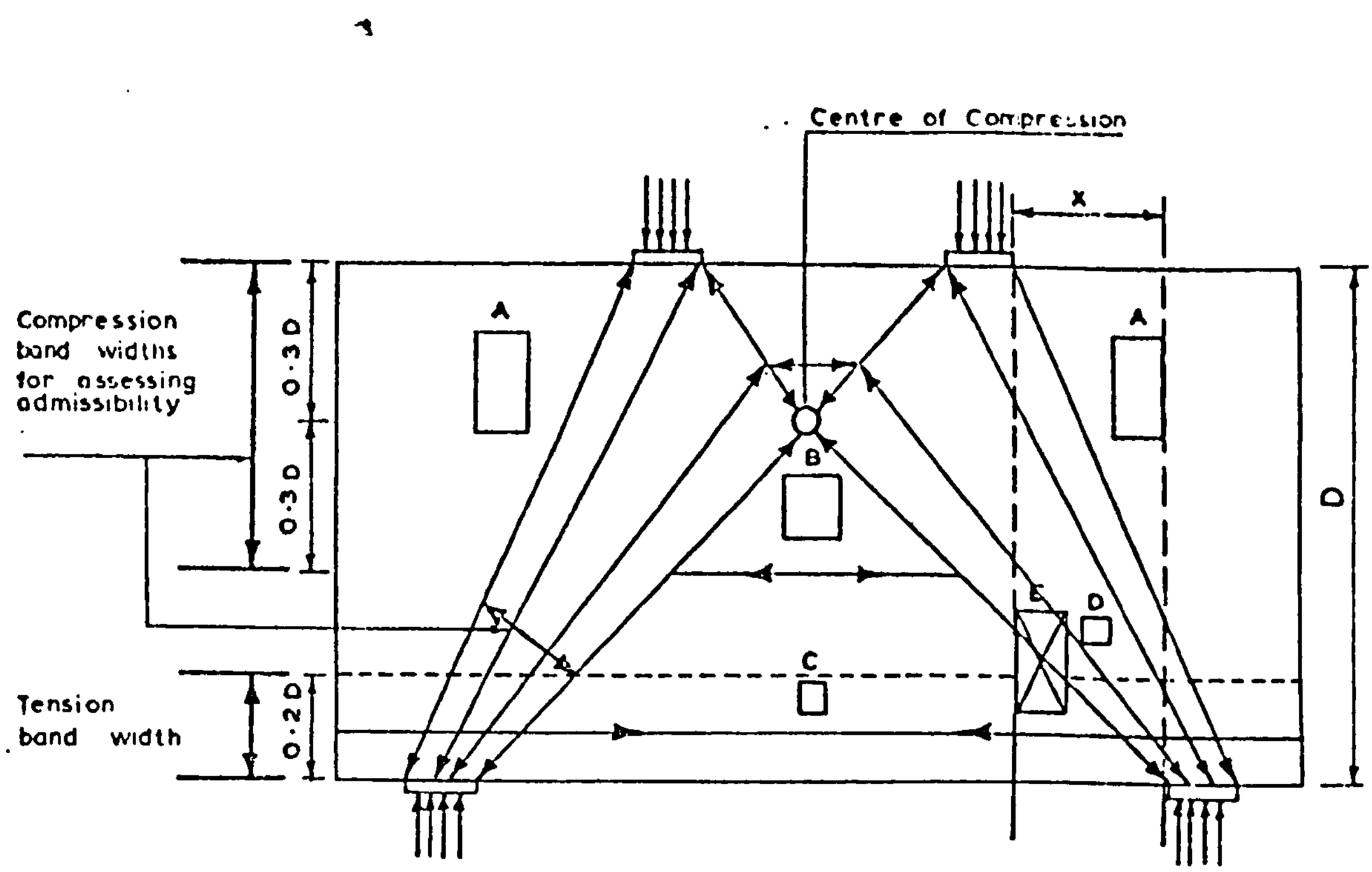

Condition of admissibility:

Dimension of hole $\geq$ 0.2 x width of notional force band under consideration.

Examples:

Hole A - admissible (cf.opening type 11, Fig.5.2 and 5.4)

Holes B,C,D - max. opening sizes admissible for the force bands considered

Hole E - not admissible (cf.opening type 14,Fig.5.2 and 5.4)

FIG.9.6 CIRIA GUIDE'S CONDITION OF ADMISSIBILITY OF HOLES APPLIED TO TEST SPECIMENS

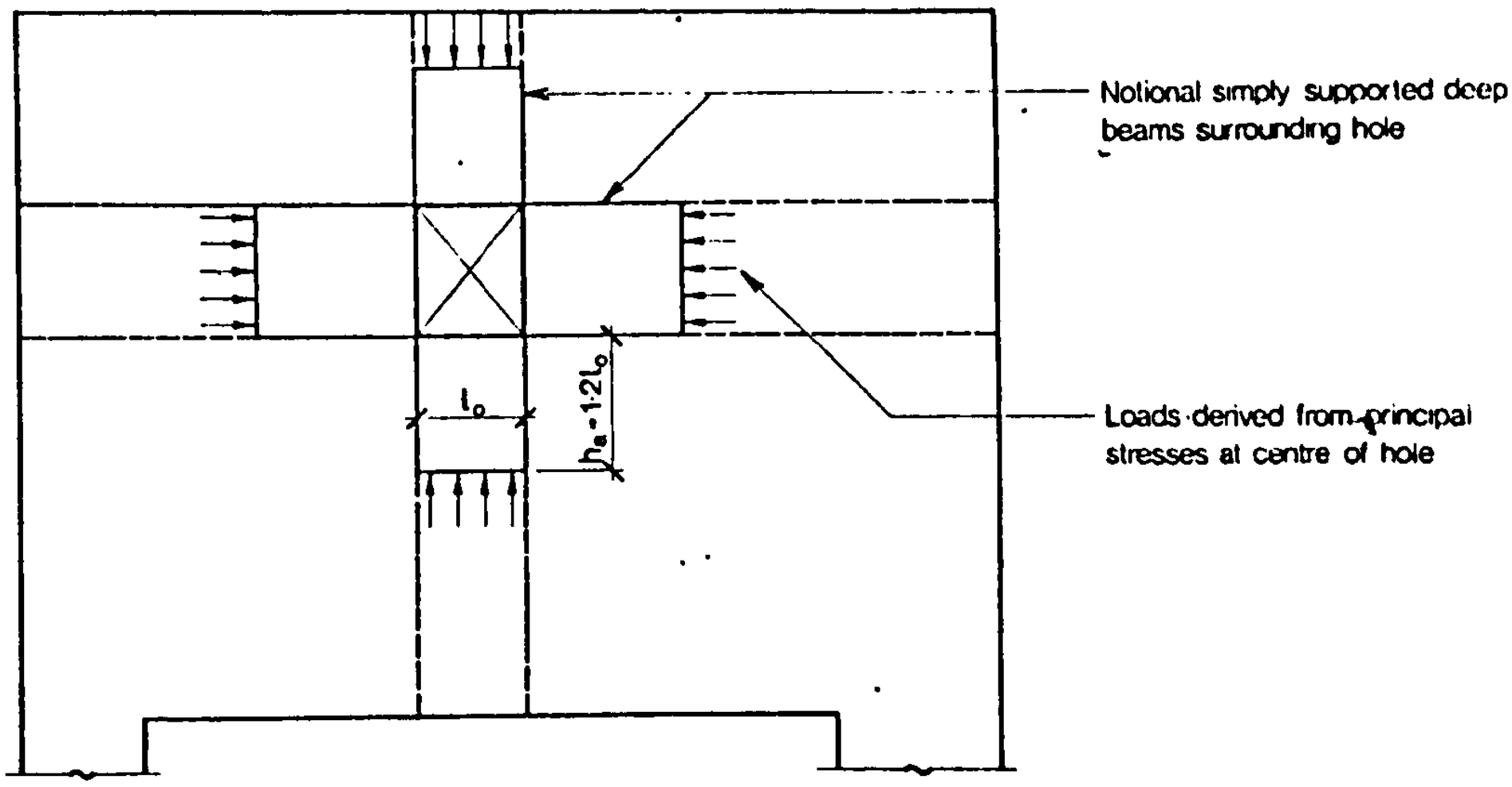

FIG.9.7 SYSTEM OF NOTIONAL DEEP BEAMS AROUND AN OPENING: CIRIA GUIDE (FIG.22)[9]

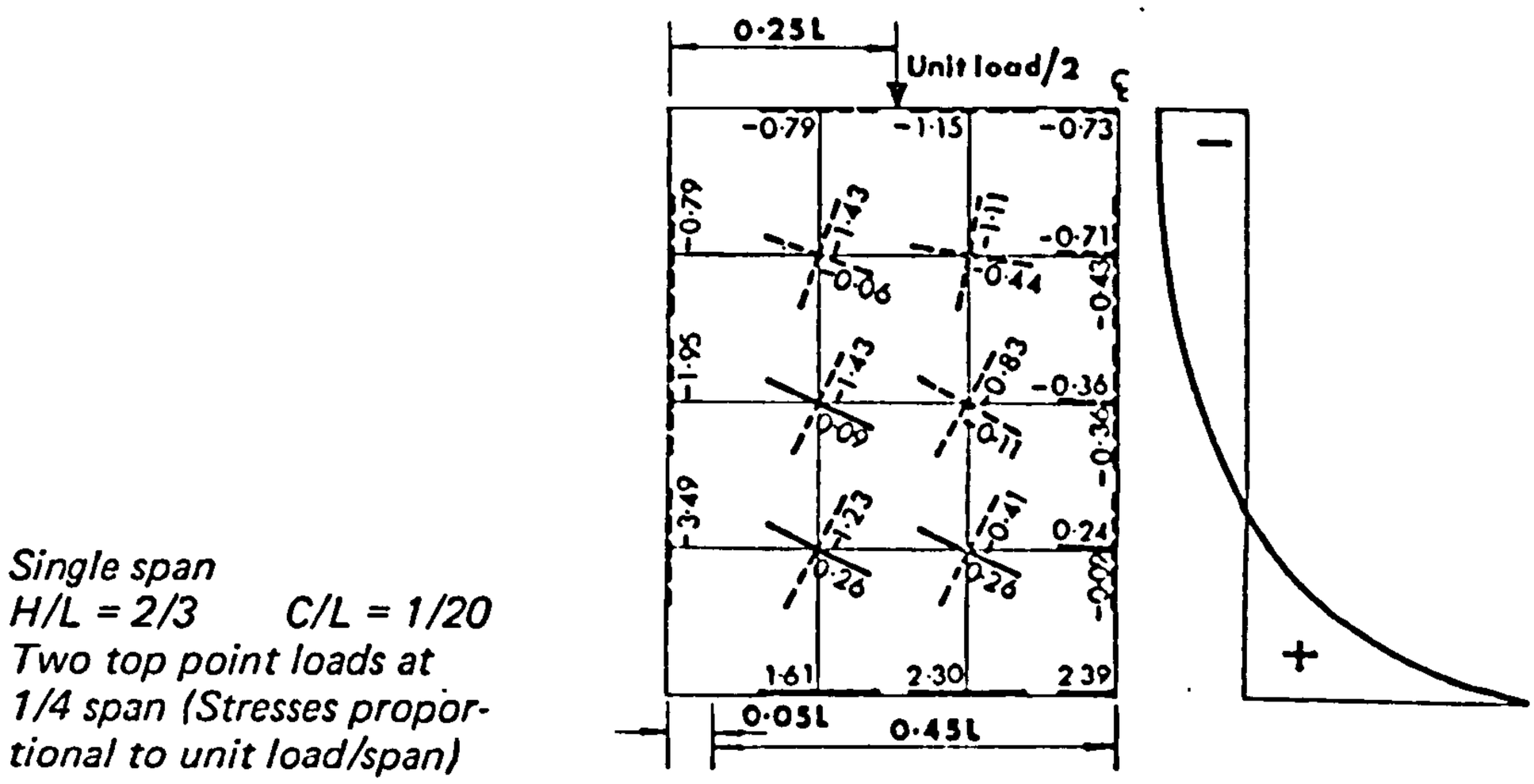

Single span
H/L = 2/3 C/L = 1/20
Two top point loads at 1/4 span (Stresses proportional to unit load/span)

FIG.9.8 TYPICAL PRINCIPAL STRESSES:CIRIA GUIDE (FIG.51)[9]

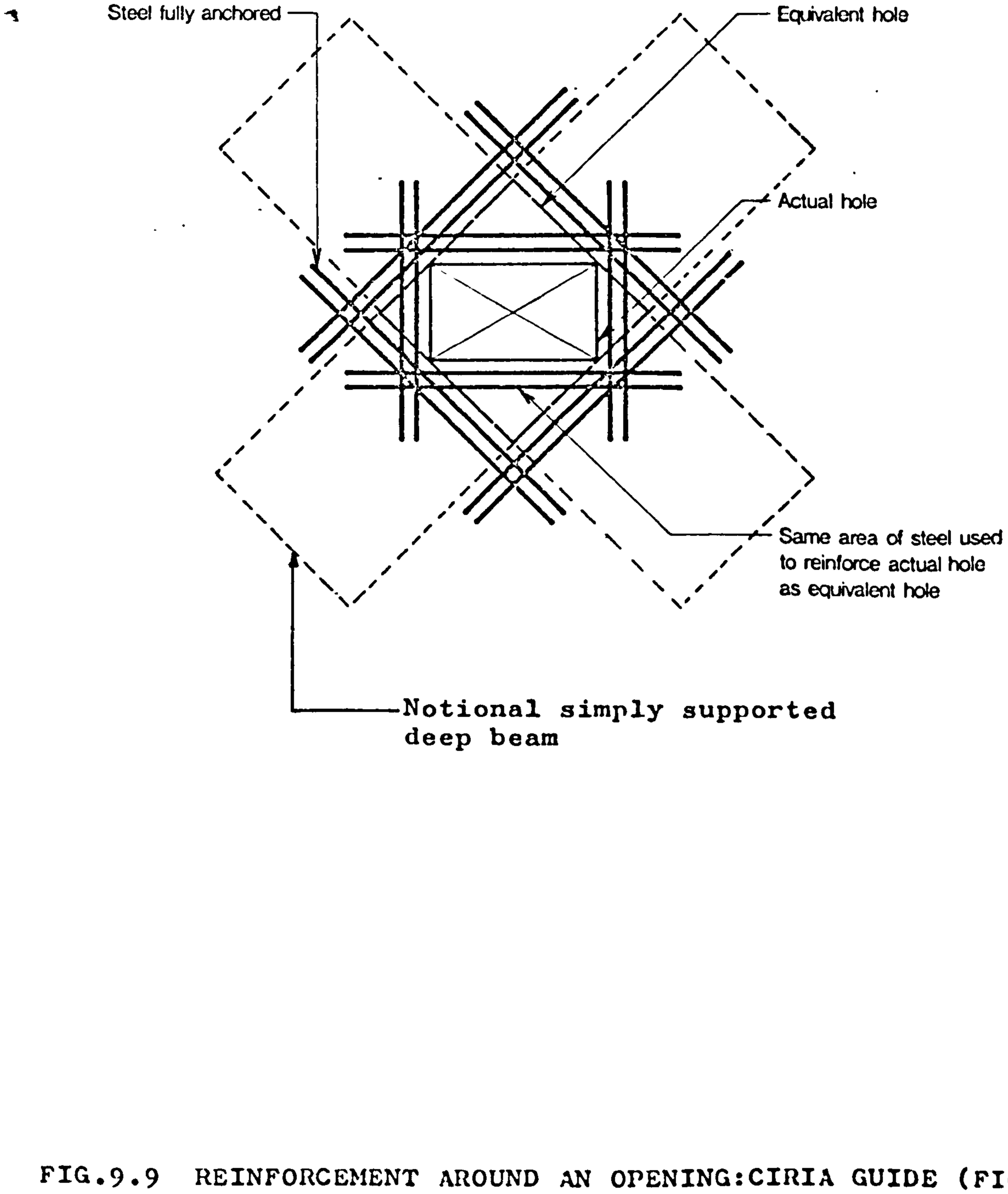

FIG.9.9 REINFORCEMENT AROUND AN OPENING:CIRIA GUIDE (FIG.24)[9]

Beam * Ref.No.	$\frac{L}{D}$	$\frac{x}{D}$	Embedment Length, mm	$f_{cu}^{\neq}$ N/mm^2	$f_c^{'+}$ N/mm^2	f_t^{**} N/mm^2
0-0.3(25+h)	1.25	0.3	200+Std.hook	37.6	31.3	2.53
0-0.3 (25)	1.25	0.3	200	36.2	35.5	2.63
0-0.3 (h)	1.25	0.3	Std. hook	41.2	32.7	2.77
0-0.3 (15)	1.25	0.3	120	36.7	31.5	2.48
0-0.3 (10)	1.25	0.3	80	39.0	32.3	2.83
0-0.3 (0)	1.25	0.3	0	37.2	33.0	3.10
0-0.55(h)	2.0	0.55	Std.hook	39.6	36.7	2.50
0-0.55(10)	2.0	0.55	80	39.8	37.2	2.50
0-0.55(0)	2.0	0.55	0	40.0	37.7	2.45

*Beam notation: The 0 before the hyphen indicates no web reinforcement; the x/D ratio is given after the hyphen, followed by the embedment length in brackets. For example: 0-0.3(10) refers to a beam having an x/D ratio of 0.30 and an embedment length of 10 bar diameters.

$^{\neq}f_{cu}$ = cube strength (100 mm)

$^{+}f_c'$ = cylinder compressive strength (300 mm x 150 mm)

$^{**}f_t$ = cylinder splitting tensile strength (300 mm x 150 mm - in accordance with ASTM C330.

TABLE A1.1 PROPERTIES OF TEST SPECIMENS.

Beam Reference No.*	Measured Ultimate Loads P_{ult} kN	Computed** P_{ult}/P_{flex}
0-0.3(25+h)	320	3.37
0-0.3 (25)	320	3.37
0-0.3 (h)	300	3.16
0-0.3 (15)	320	3.37
0-0.3 (10)	300	3.16
0-0.3 (0)	180	1.89
0-0.55(h)	190	2.52
0-0.55 (10)	190	2.52
0-0.55 (0)	140	1.86

*Beam notation as given in Table A1.1

**Ratio of measured ultimate load (P_{ult}) to computed flexural design load (P_{flex}) using Eqn.(9.1).

TABLE A1.2 ULTIMATE LOADS

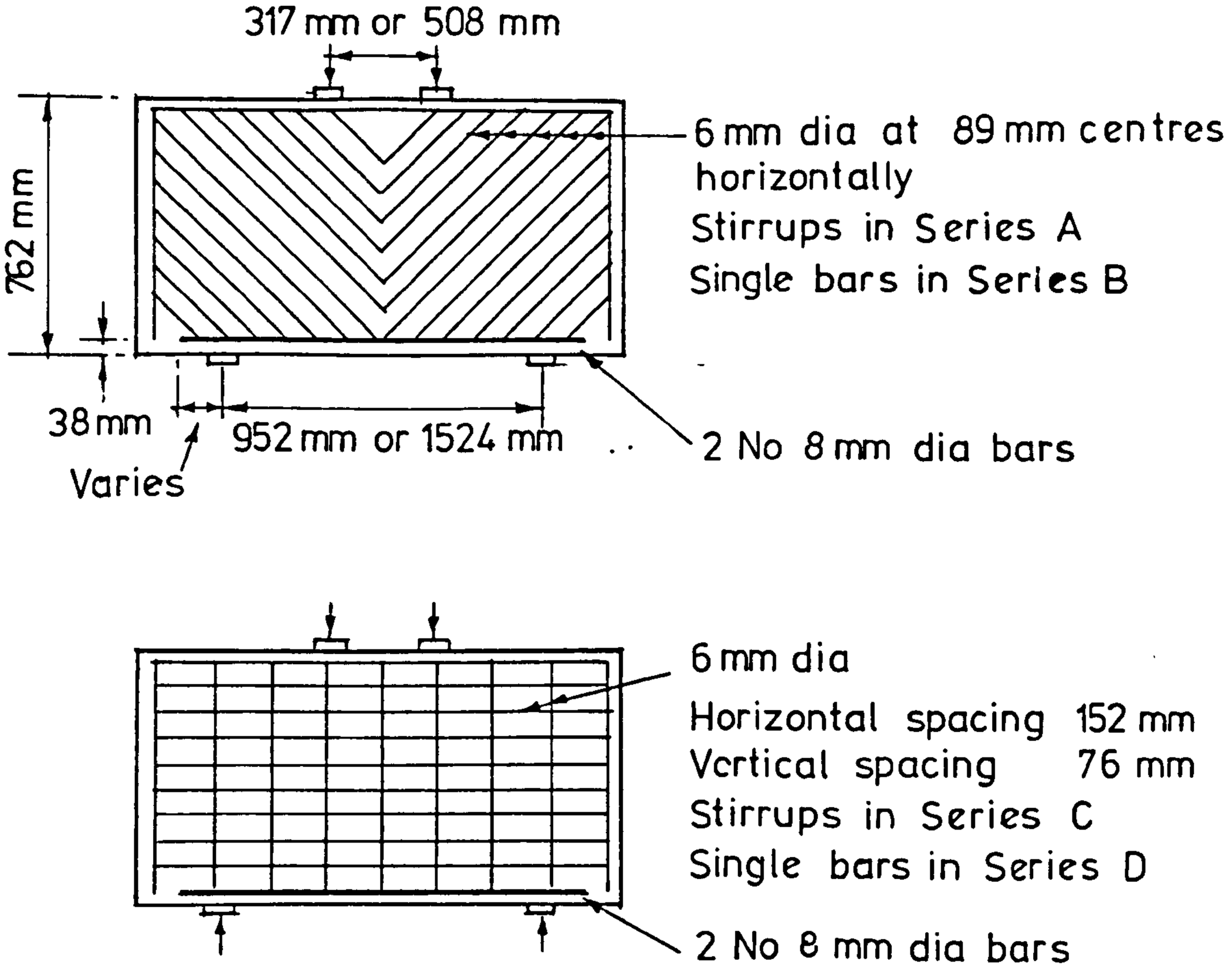

FIG.A1.1 SINGH'S TEST SPECIMENS
(Further details are given in Ref.12)

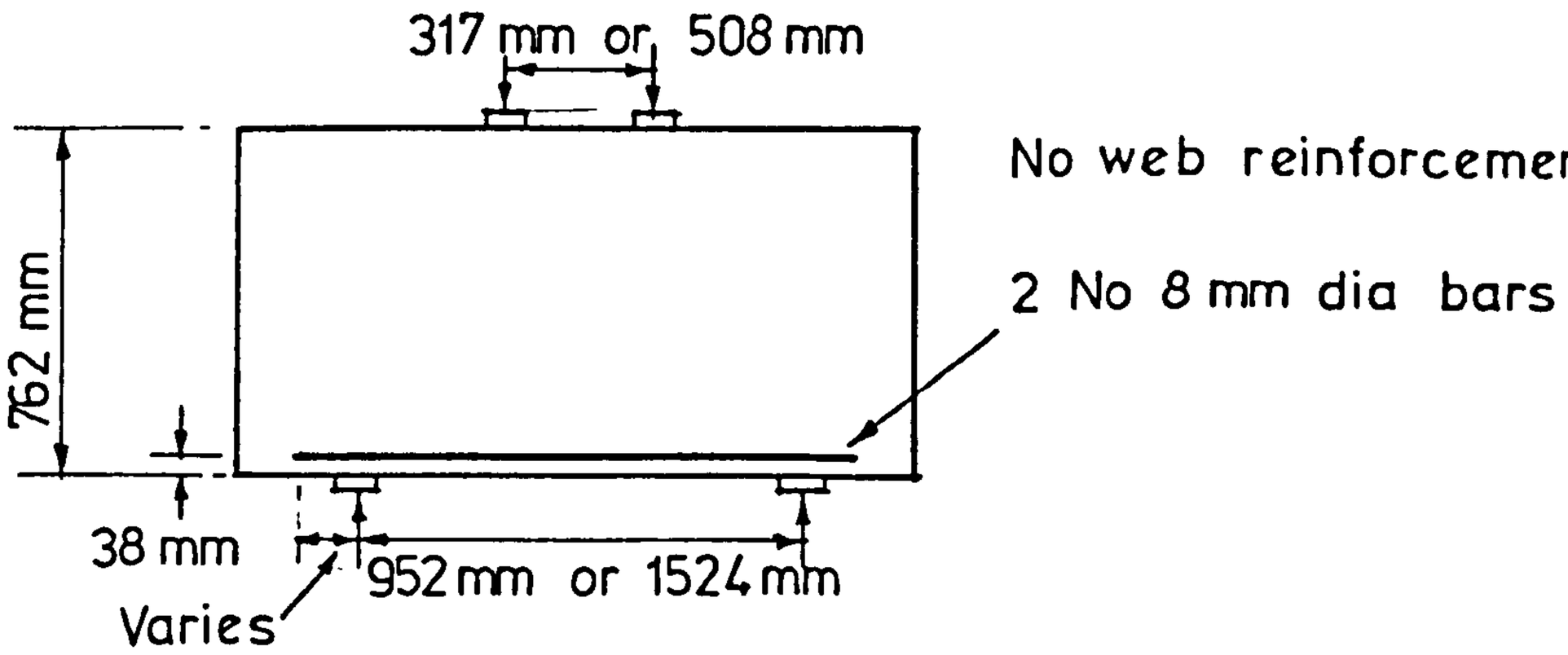

FIG.A1.2 DIMENSIONS AND REINFORCEMENT
DETAILS OF THE PRESENT TEST SPECIMENS

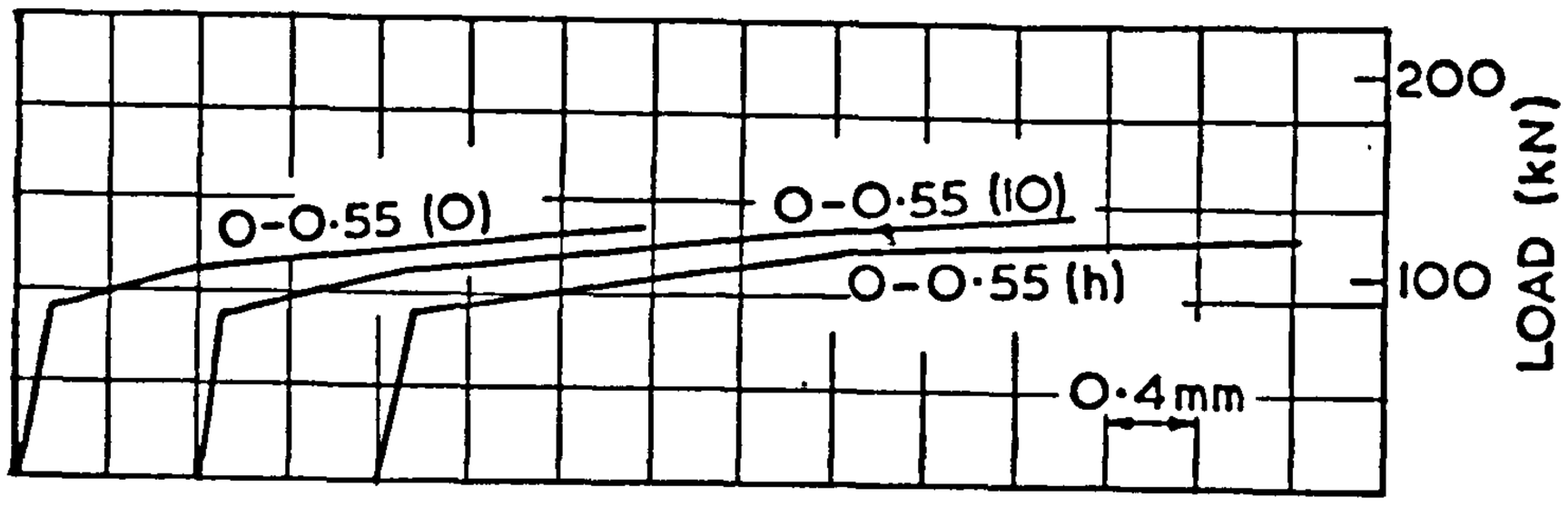

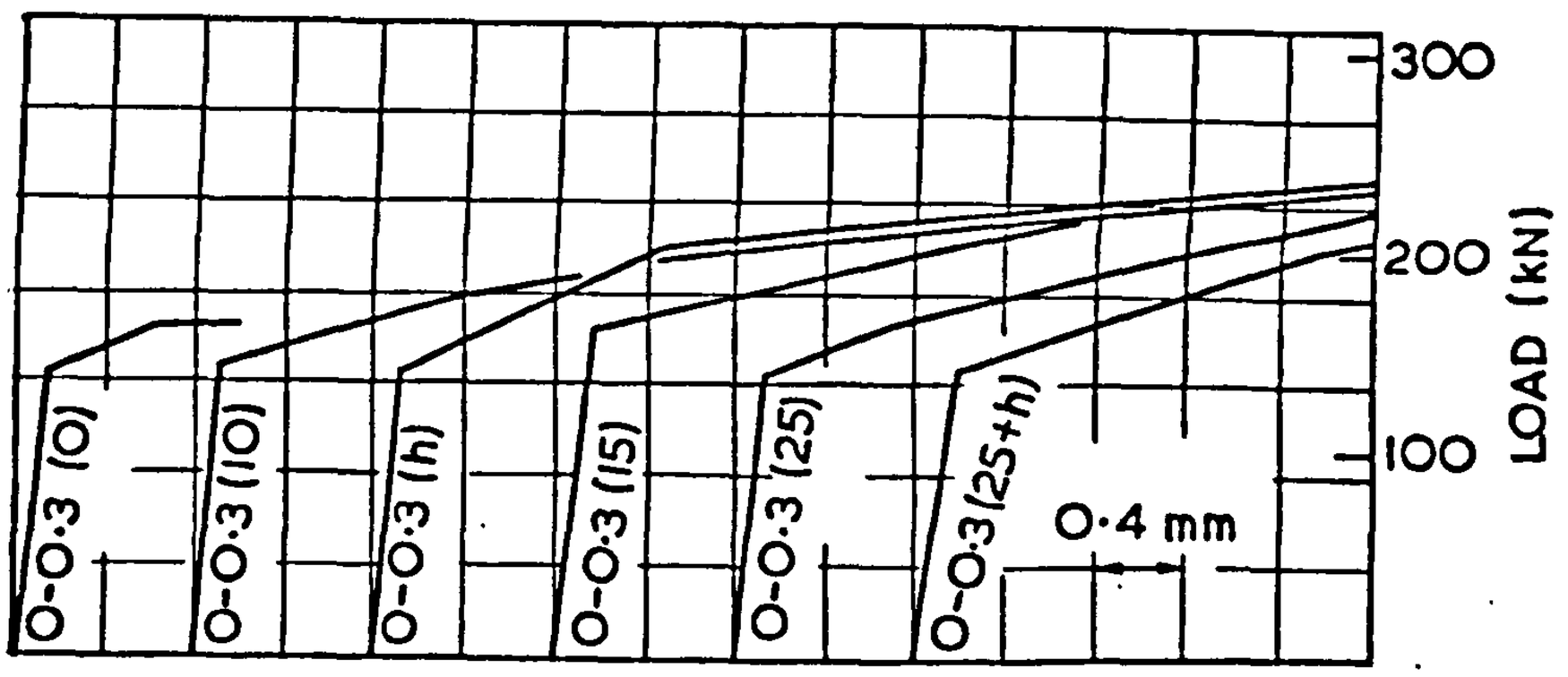

Beam notation as in Table (A1.1)

FIG.A1.3 CENTRAL DEFLECTION CURVES

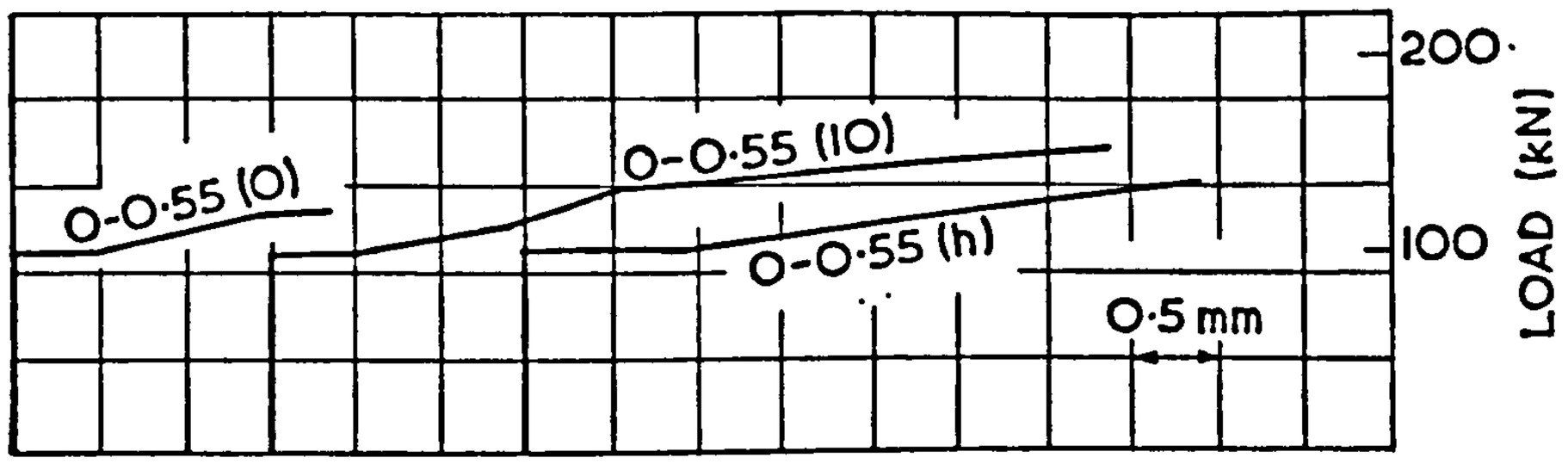

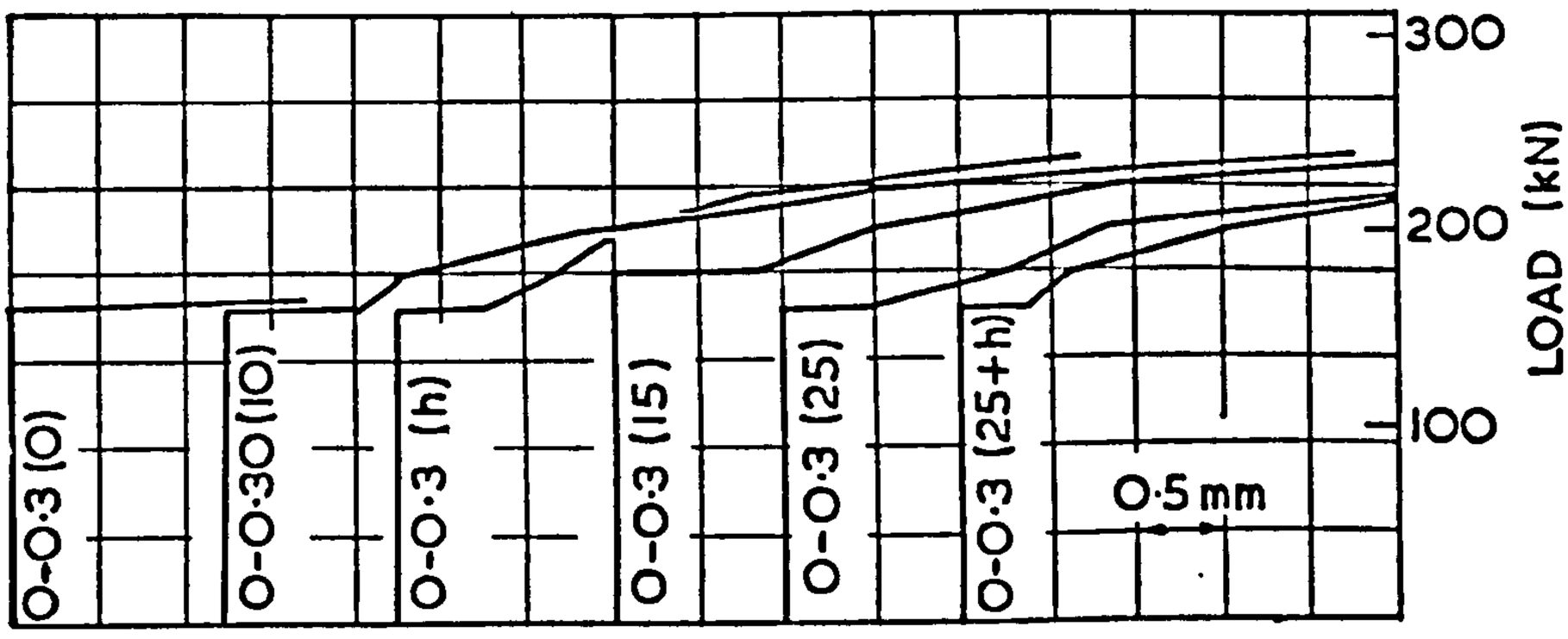

Beam notation as in Table (A1.1)

FIG.A1.4 MAXIMUM CRACK WIDTHS

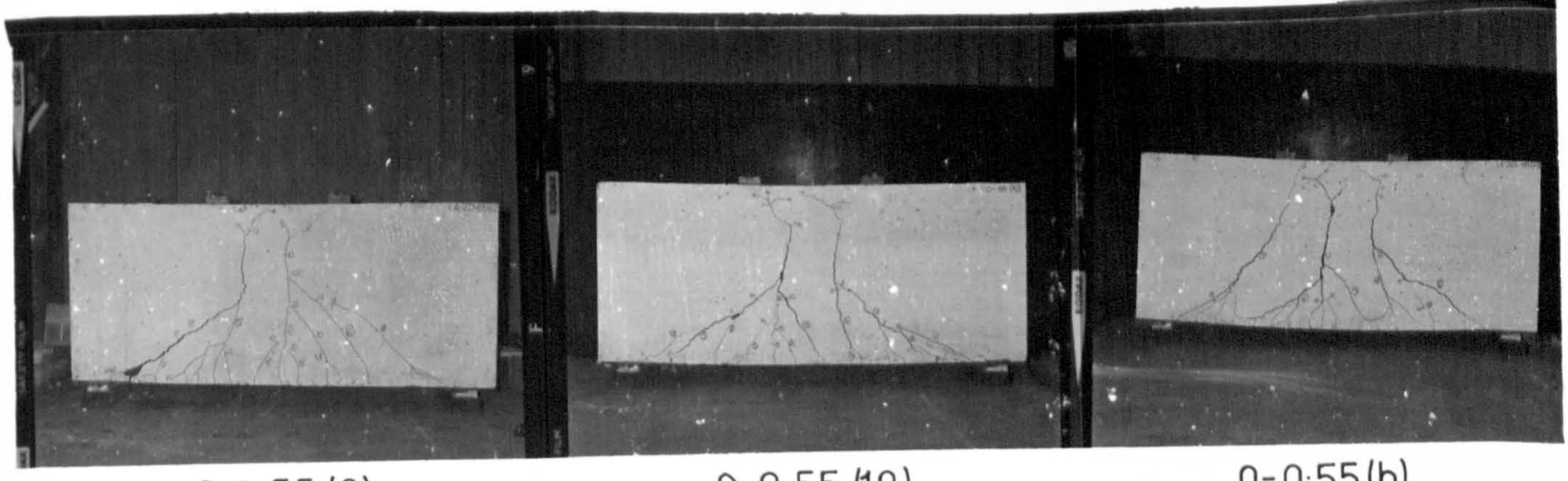

0-0·55 (0) 0-0·55 (10) 0-0·55 (h)

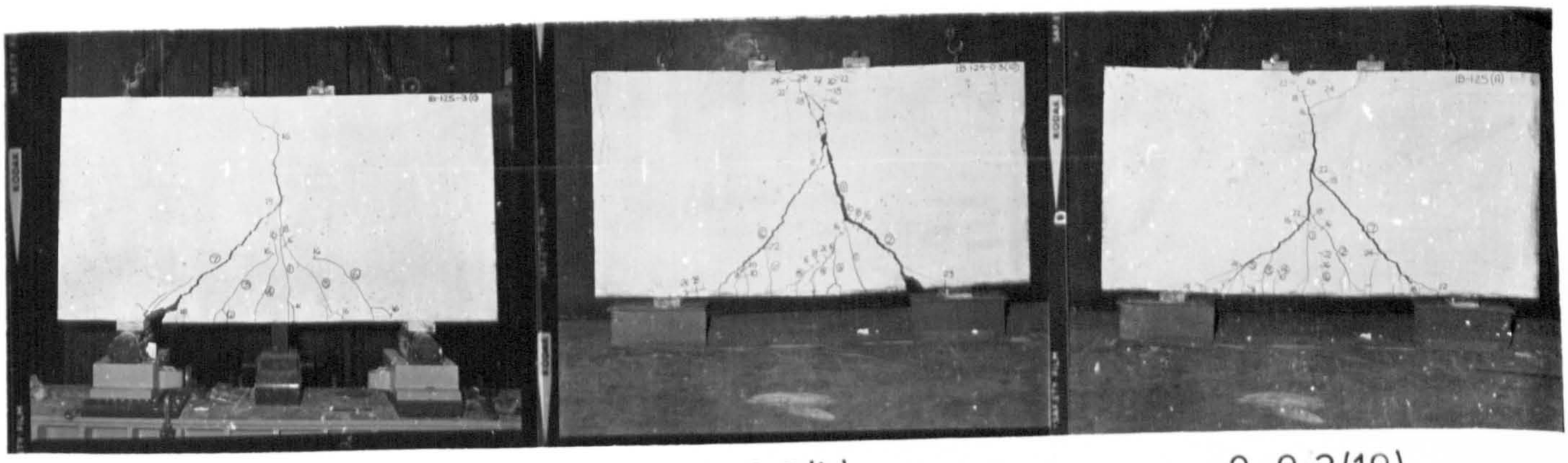

0-0·3 (0) 0-0·3(h) 0-0·3(10)

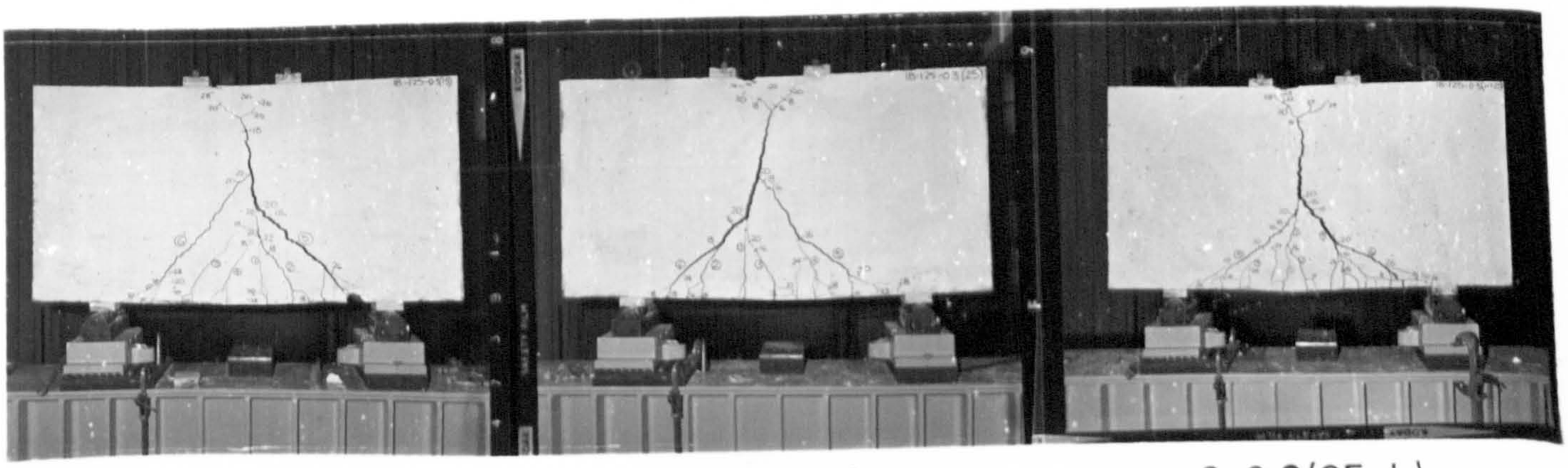

0-0·3(15) 0-0·3 (25) 0-0·3(25+h)

Beam notation as in Table A1.1

The circled numbers show the sequence in which the cracks were observed; the other numerical figures show the load, in 10 kN units, at which the extent of the cracks were as marked.

FIG.A1.5 CRACK PATTERNS AT FAILURE

Beam Ref.No. *	$\frac{L}{D}$	$\frac{x}{D}$	Web steel Type	%	f_{cu} ≠ N/mm^2	f_c' + N/mm^2	f_t ++ N/mm^2	Test age **
A-2/0.4	2	0.4	A	1.2	37.4	29.82	2.44	111
B-2/0.4	2	0.4	B	1.2	45.0	36.26	2.53	149
C-2/0.4	2	0.4	C	1.2	46.6	37.0	2.63	69

* Beam notation: The web reinforcement type (Fig.A2.1) is given before the hyphen; the L/D ratio is given after the hyphen, followed by the x/D ratio.

≠ f_{cu} = cube strength (100 mm) at completion of test.

+ f_c' = cylinder compressive strength (300 mm x 150 mm)

++ f_t = cylinder splitting tensile strength (300 mm x 150 mm) - in accordance with ASTM Standard C330.

** Age in days at completion of test - all beams were cast on the same day and the duration of each test was approximately 41 days.

TABLE A2.1 PROPERTIES OF TEST SPECIMENS

Beam Ref.No.*	Measured ult.load kN	ACI load kN	Diagonal cracking load	Singh's test beams** kN
A-2/0.4	706	283	157	646
B-2/0.4	687	294	216	685
C-2/0.4	726	274	274	724

* Beam notation as in Table A2.1

** Measured ultimate load of Singh's test beams; further details are given in Reference 32.

TABLE A2.2 MEASURED AND COMPUTED LOADS

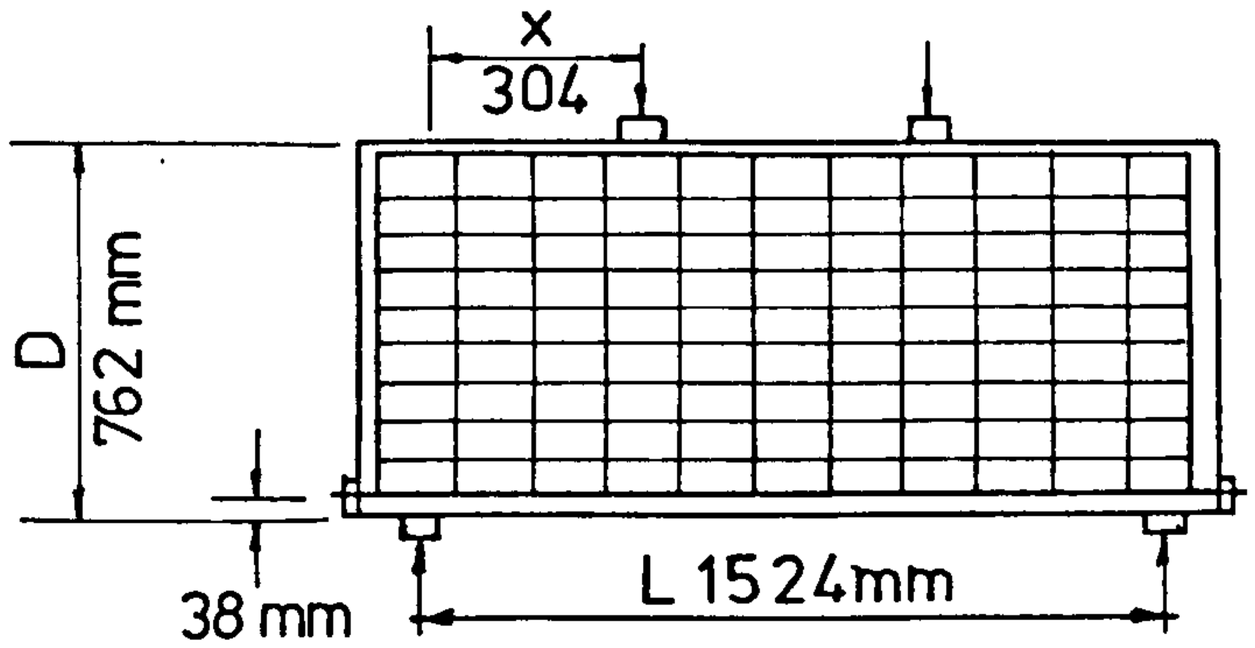

6 mm dia stirrups
Horizontal spacing 152 mm
Vertical spacing 76 mm

TYPE A

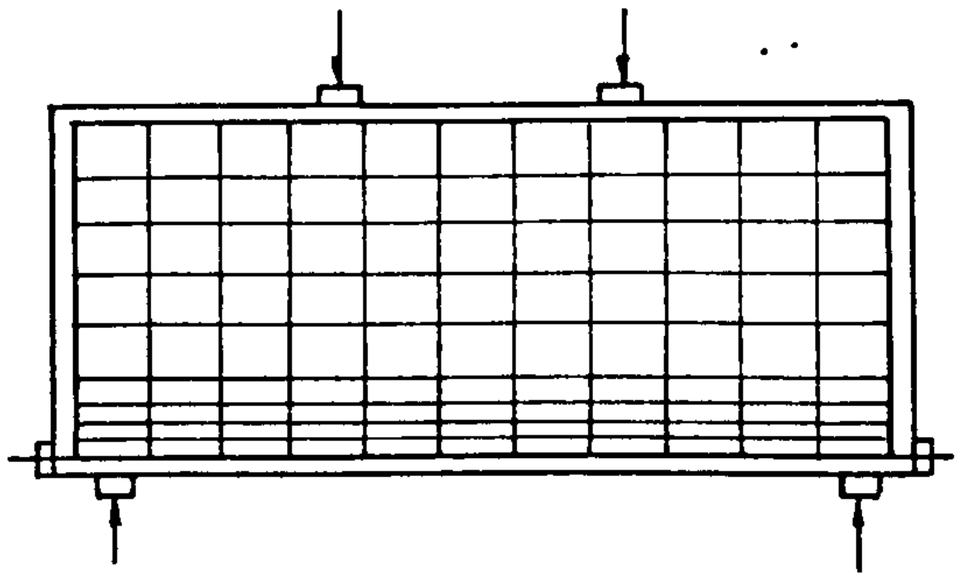

6 mm dia stirrups
Horizontal spacing 152 mm
Vertical spacing 38 mm
and 108 mm

TYPE B

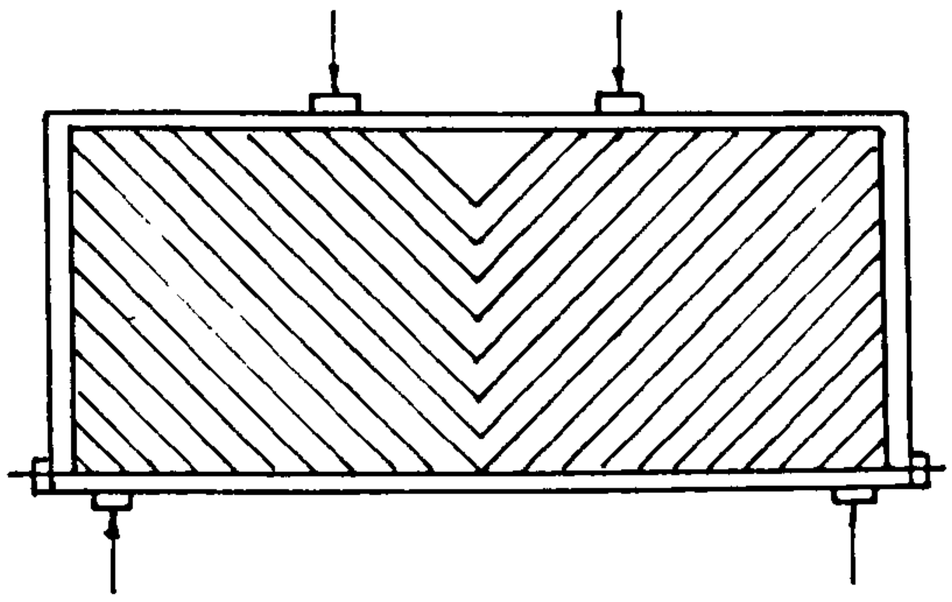

6 mm dia inclined stirrups
45° to horizontal at
76 mm spacing horizontally

TYPE C

FIG. A2.1 GENERAL ARRANGEMENT AND DETAILS OF WEB REINFORCEMENT

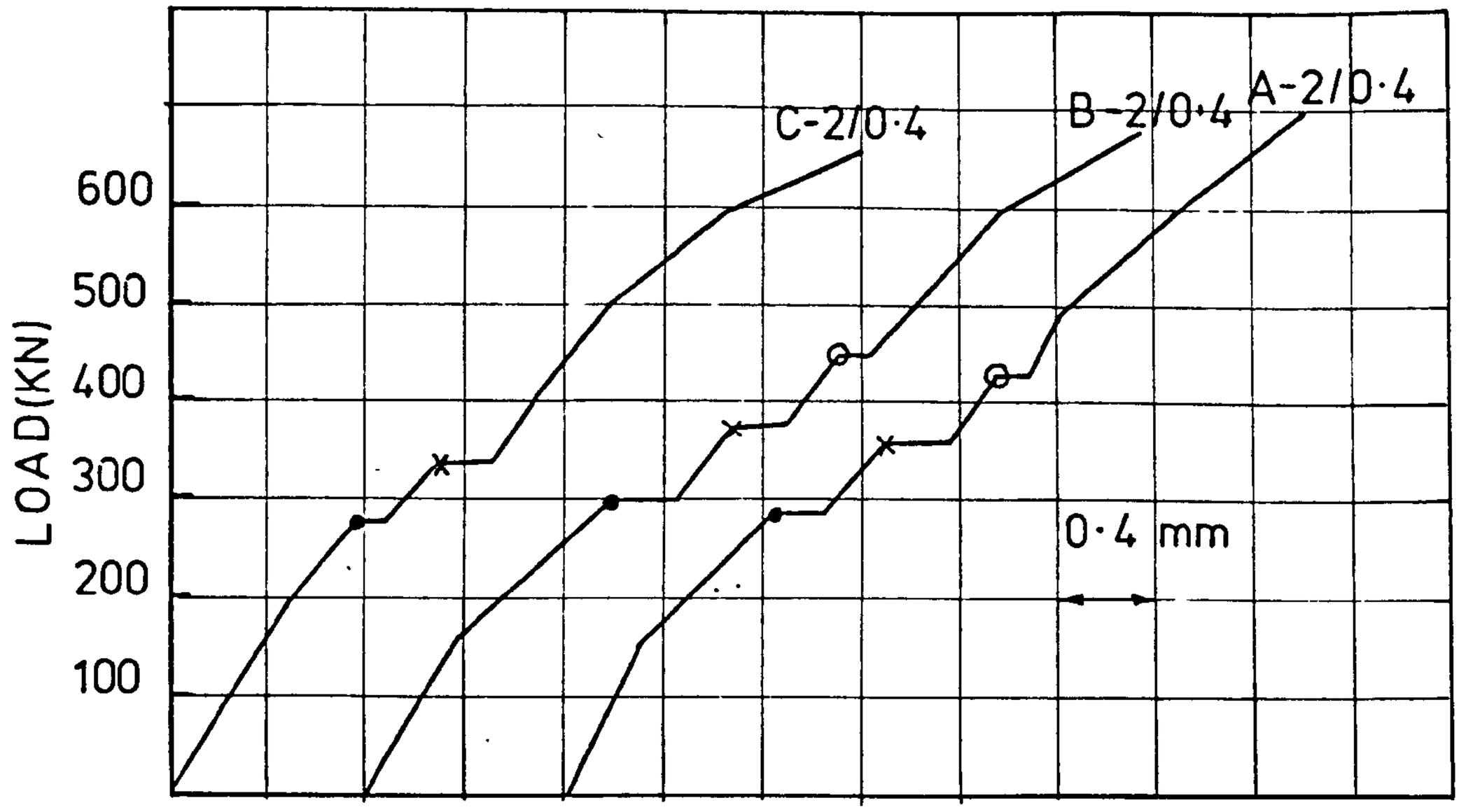

FIG.A2.2 CENTRAL DEFLECTIONS

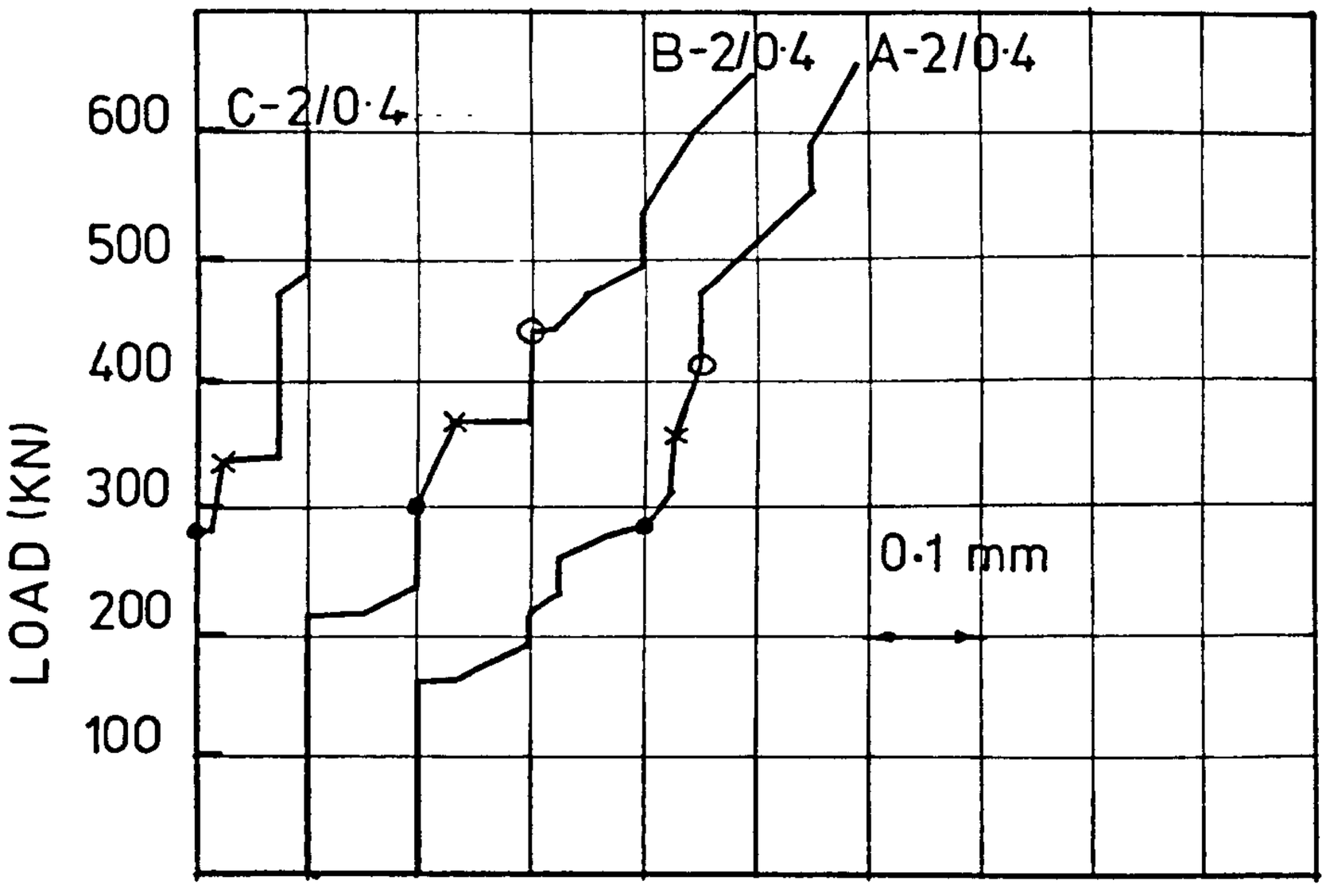

FIG.A2.3 MAXIMUM DIAGONAL CRACK WIDTHS

Beam notation as in Table A2.1

The beginning of Stage 1 cycling is indicated by a dot (.), that of Stage 2 by (x) and that of Stage 3 by (0)

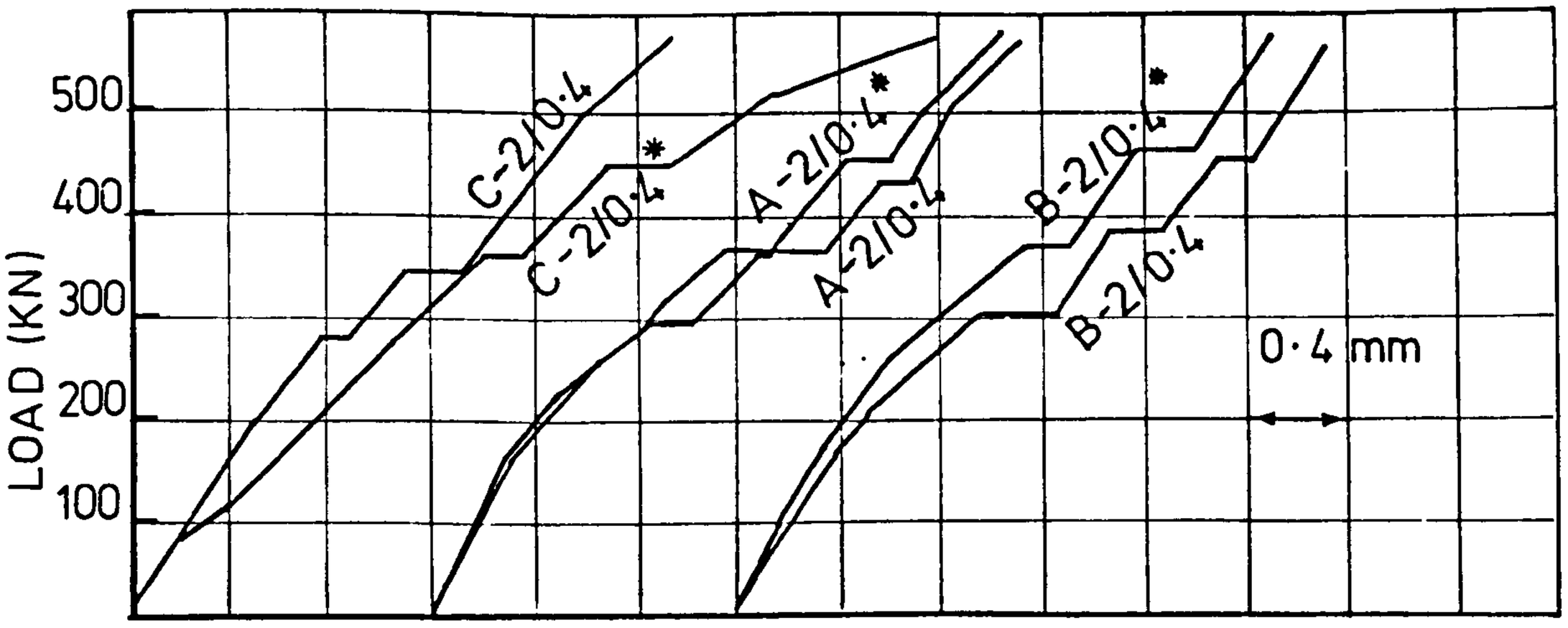

Beam notation as in Table A2.1

Singh's beams are indicated by an asterisk (*); further details are given in Reference 32.

FIG A2.4 COMPARISON OF SINGH'S AND PRESENT TEST RESULTS: CENTRAL DEFLECTIONS

A-2/0·4

C-2/0·4

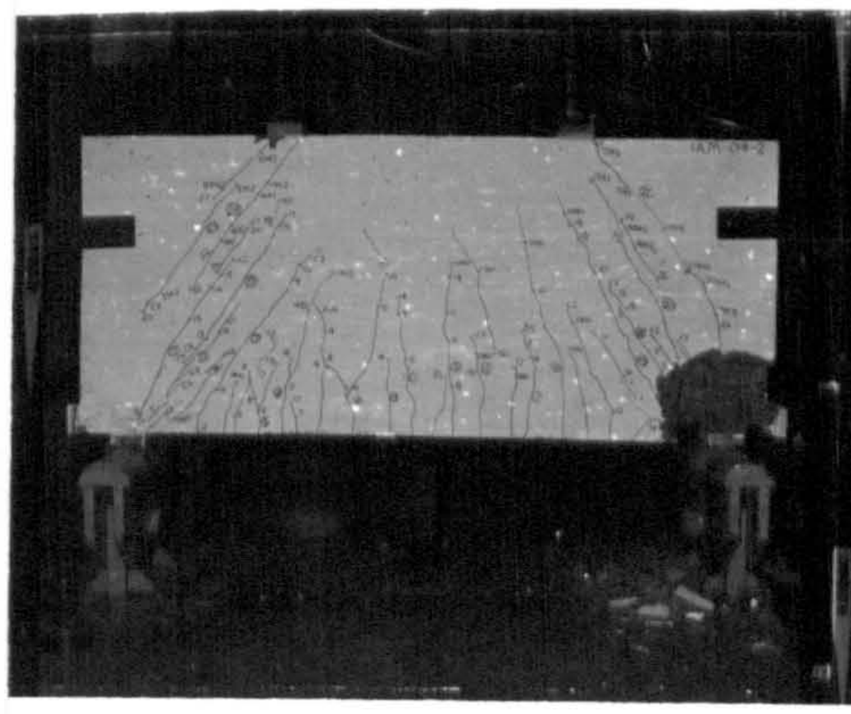

B-2/0·4

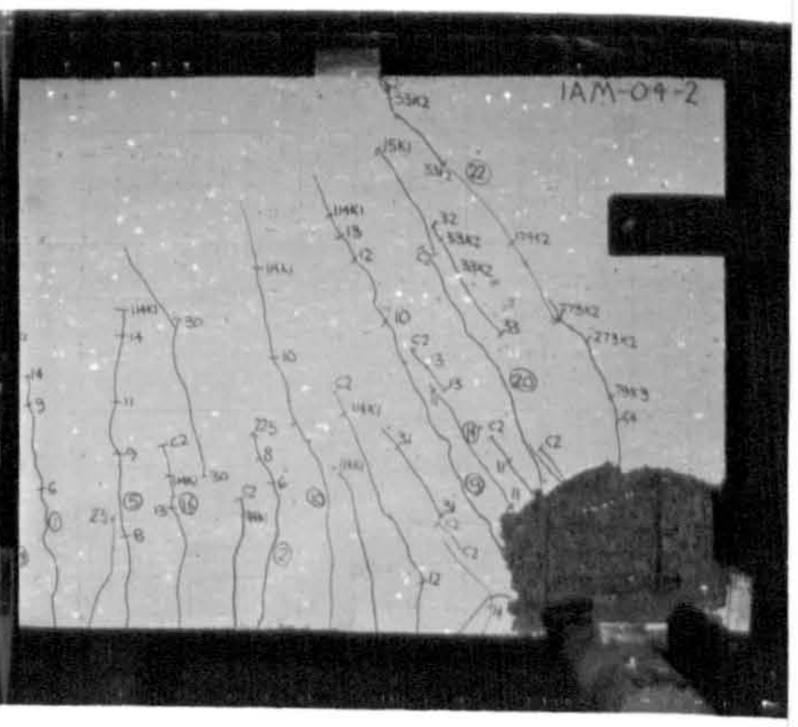

B-2/0·4

Beam notation as in Table A2.1

Numerical figures show the load, in 10 kN units, at which each crack was observed and the extent of the crack at that load, The symbols C1 to C5 indicate the extent of cracking during load cycling as follows:

Beam A - 2/0.4
C1 = 120,000 cycles, Stage 1
C2 = 100,000 cycles, Stage 2
C3 = 200,000 cycles, Stage 2
C4 = 300,000 cycles, Stage 2
C5 = 100,000 cycles, Stage 3

Beam B - 2/0.4
C1 = 120,000 cycles, Stage 1
C2 = 150,000 cycles, Stage 2
C3 = 300,000 cycles, Stage 2
C4 = 100,000 cycles, Stage 3

Beam C = 2/0.4
C1 = 45,000 cycles, Stage 1
C2 = 120,000 cycles, Stage 1
C3 = 11,000 cycles, Stage 2
C4 = 113,000 cycles, Stage 2
C5 = 300,000 cycles, Stage 2

FIG.A2.5 CRACK PATTERNS AT FAILURE